Organophosphorus Chemistry of Camphene

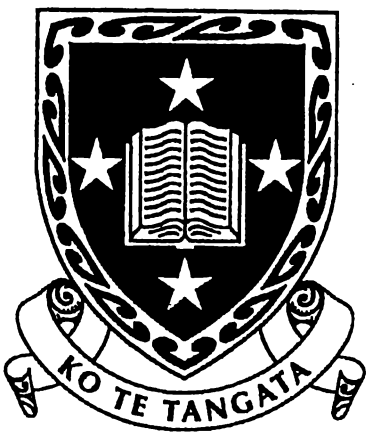

A thesis
submitted in partial fulfilment
of the requirements for the degree
of Doctor of Philosophy in Chemistry
at the University of Waikato

Meto Te Ota Leach

1999

Abstract

Chapter one reviews the literature relating to terpene-phosphorus chemistry. Topics include a summary of the phosphorus chemistry of the monoterpenes and terpenoids camphor, menthol, camphene and pinene. A general discussion on terpene-phosphines and terpene-phosphonates is also included.

Chapter two of this thesis describes the chemistry of the camphene-derived phosphinic acids, 8-camphanylphosphinic acid [$C_{10}H_{17}P(O)(H)(OH)$ **1**] (2,2-dimethylbicyclo[2.2.1] hept-3-ylmethylphosphinic acid) and 8-camphanyl-(phenyl)phosphinic acid [$C_{10}H_{17}P(O)(Ph)(OH)$ **3**], which are formed by the radical-catalysed addition of hypophosphorous acid [H_3PO_2] and phenylphosphinic acid [$PhPO_2H_2$] to camphene. Reaction conditions which optimise the yield of **1** have been investigated along with the detailed characterisation by single crystal X-ray studies, ESMS and one- and two-dimensional NMR studies. The attempted preparation of chiral **1** starting from (R)-(+)-camphene yields only racemic material, the result of the acid-catalysed racemisation of camphene prior to the reaction with H_3PO_2. Methylation of the phosphinic acids **1** and **3** with diazomethane yields the methyl esters **6** [$C_{10}H_{17}P(O)(H)(OMe)$] and **7** [$C_{10}H_{17}P(O)(Ph)(OMe)$]. These methyl esters have been fully characterised by NMR and GCMS. **1** reacts with paraformaldehyde to form the hydroxymethylphosphinic acid **9** [$C_{10}H_{17}P(O)(OH)(CH_2OH)$] and with a formaldehyde/dimethylamine mixture to form **10** [$(C_{10}H_{17}P(O)(OH)\text{-}(CH_2NHMe_2))Cl$]. The oxidative chlorination of **1** and **3** with thionyl chloride [using a pyridine catalyst] yields the acid chlorides **11** [$C_{10}H_{17}P(O)Cl_2$] and **12** [$C_{10}H_{17}P(O)(Ph)Cl$].

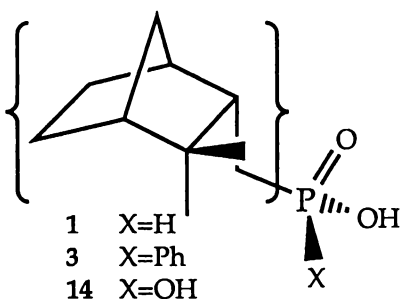

1 X=H
3 X=Ph
14 X=OH

{ } = $C_{10}H_{17}$

The reaction of **1** with calcium nitrate and excess urea (for pH control) for 5 days yields polymeric calcium salt **13** [$(Ca(C_{10}H_{17}PO_2H)_2(C_{10}H_{17}PO_2H_2)$-

$(H_2O))_n$] on the basis of a single crystal X-ray study. The dominance of the bulky camphanyl groups, which form a coherent, essentially 'close-packed' hydrocarbon sheath around the central hydrophilic inorganic Ca/O/P core give the appearance of individual chains resembling 'insulated wire'.

Chapter three describes the synthesis and subsequent derivatisation of the camphene-derived phosphonic acid **14** [$C_{10}H_{17}P(O)(OH)_2$]. The formation of **14** *via* both the oxidation of **1** and the hydrolysis of **11** [$C_{10}H_{17}P(O)Cl_2$] (in mild conditions), are investigated. **14** is characterised in detail by single crystal X-ray studies and one- and two-dimensional NMR studies. The treatment of **14** with diazomethane yields the methyl ester **15** [$C_{10}H_{17}P(O)(OMe)_2$].

Also included in Chapter 3 is the reaction of an excess of silver oxide with equimolar quantities of the platinum dichloride complexes *cis*-[$PtCl_2L_2$] [L=PPh_3, $PPhMe_2$; L_2=DPPE] {DPPE=1,2-bis(diphenylphosphane)ethane} and

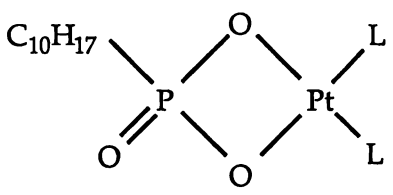

14. The Pt(II) complexes **16**, **17** and **18**, [Pt{OP(O)($C_{10}H_{17}$)O(L)$_2$} L=PPh_3, $PPhMe_2$; L_2=DPPE], which are formed in moderate yields, are characterised in detail by ^{31}P, ^{1}H and ^{13}C NMR spectroscopy. The analogous palladium chemistry of **14** is non-selective, forming a large number of unidentifiable products.

Chapter four describes the formation of the phosphines **20** [$C_{10}H_{17}PH_2$], **23** [$C_{10}H_{17}P(CH_2OH)_2$] and their derivatives. The reaction of phosphonic dichloride **11** [$C_{10}H_{17}P(O)Cl_2$] with lithium aluminium hydride does not afford the free phosphine but a metal-phosphine adduct of 8-camphanylphosphine. However when **1** is heated to 140°C under vacuum [0.5 mm Hg] **1** disproportionates to yield 8-camphanylphosphine **20** [$C_{10}H_{17}PH_2$] which, when treated with aqueous hydrochloric acid/formaldehyde, affords an air-stable tris(hydroxymethyl)phosphonium chloride **22** [($C_{10}H_{17}P(CH_2OH)_3$)Cl]. **22** is the first tris(hydroxymethyl)phosphonium salt to date to be subjected to a crystallographic study.

The treatment of **22** with equimolar amounts of either potassium hydroxide or triethylamine affords the bis(hydroxymethyl)phosphine **23** [$C_{10}H_{17}P(CH_2OH)_2$]. The subsequent addition of an excess of sulfur or selenium yields the phosphine sulfide **24** [$C_{10}H_{17}P(S)(CH_2OH)_2$] and the phosphine selenide **25** [$C_{10}H_{17}P(Se)(CH_2OH)_2$]. The controlled oxidation of **23** with hydrogen peroxide gives the bis(hydroxymethyl)phosphine oxide **26** [$C_{10}H_{17}P(O)(CH_2OH)_2$].

The treatment of **23** with $CODPtCl_2$ {COD = 1, 5 cyclooctadiene} directly precipitates the platinum dichloride complex **27** [$(C_{10}H_{17}P(CH_2OH)_2)_2PtCl_2$] while the gold(I) chloride complex **28** [$C_{10}H_{17}P(CH_2OH)_2AuCl$] is precipitated by the action of tetrahydrothiophene gold(I) chloride upon **23**. Hydroxymethylphosphine **23** and its derivatives **[24-28]** have been fully characterised by NMR spectroscopy and ESMS.

Included in Chapter four is an investigation of the gas phase decomposition of **20** by Berrigan and Russell at Auckland University. Aided by the use of I.R. Laser Powered Homogeneous Pyrolysis, results indicate that phosphine is firstly eliminated followed by the rearrangement and decomposition of camphene through two distinct pathways.

Chapter five describes the formation of uranyl nitrate complexes of the camphene-derived phosphorylic ligands **15, 7** and **29** [the synthesis of **29** [$C_{10}H_{17}P(O)Ph_2$] is also described therein]. The spontaneous evaporation of methanolic solutions containing uranyl(VI) nitrate and these monodentate ligands yield the uranyl(VI) nitrate complexes $UO_2(NO_3)_2L_2$ [**30** L= $C_{10}H_{17}P(O)(OMe)_2$], [**31** L= $C_{10}H_{17}P(O)(Ph)(OMe)$] and [**32** L= $C_{10}H_{17}P(O)Ph_2$]. The uranyl(VI) nitrate complex $[UO_2(NO_3)_2\{C_{10}H_{17}P(O)(OMe)_2\}_2]$ (**30**) has been subjected to a single crystal X-ray study. The structure determination was not straightforward, largely as a result of the combination of a dominant scattering atom (uranium) and substantial disorder of the camphanyl groups.

Acknowledgments

I would like to thank those who contributed to my research. The Chemistry technicians in particular Amu Upreti, for her advice on life and amusing stories on what happens at home with her children, Annie Baker, Janine Sims for help with GCMS and Brett Loper for computer help. To Greg Olsen, Scott McEndoe and Allen Oliver thanks for making life in the lab more enjoyable. Many thanks to all the chemistry staff, in particular Prof. Brian Nicholson for XRD assistance, Dr Ralph Thompson for his NMR advice and genuine concern for a problem and Dr Michelle Princep for optical rotation measurements.

A special thanks to my supervisors, Dr Bill Henderson and Prof. Alistair Wilkins. Thank you Bill for the support and dedication you showed to my topic of study.

To my Whanau, in particular my Mum, for support and encouragement throughout my academic career. To my Dad, thanks for your love and caring. Thanks to Richard and Franqui, George and Jackie, John, Alma, Cheyenne and baby Meto, Darren and Michael for support over the years. To Kirsty's parents, Allen and Barbara Walker, thanks for your encouragement and financial support over the years.

I would like to acknowledge the financial assistance from the following organisations: Waikato University, DSIR, MEF, Mangatu Blocks and Tahora.

Finally I would like to thank the two most important people in my life. Thanks to my God and King who sacrificed his Son, the **Lord Jesus Christ**, so that we may have life, life everlasting. Praise be to the King of Kings.

I thank God for Kirsty, my wife, who has been there to comfort me in times of trouble, to weep with in times of sorrow, to laugh with in times of joy. My most precious treasure on the earth, thanks for making my life complete.

Table of Contents

	page
Abstract	ii
Acknowledgments	v
Table of Contents	vi
List of Schemes	xiv
List of Figures	xix
List of Equations	xxii
List of Tables	xxii
Abbreviations	xxv

Chapter One: Terpene-phosphorus chemistry

1.1	Introduction	1
1.2	Menthyl-phosphorus chemistry	2
1.3	Camphor-phosphorus chemistry	4
1.4	Terpene-phosphonate chemistry	7
1.5	Terpene-phosphine chemistry	9
1.6	Pinene- and camphene-phosphorus chemistry	
	1.6.1 Pinene	13
	1.6.2 Camphene	13
References		17

Chapter Two: Synthesis and characterisation of camphene-derived phosphinic acids

2.1 The radical-catalysed addition of phosphinic acids to alkenes

2.1.1 Introduction. 19

2.1.2 Results and discussion 21

2.1.3 X-ray crystal structure of **1** 25

2.1.4 Electrospray mass spectrometric analysis of camphene-derived phosphinic acids 29

2.1.5 Detailed NMR analyses of 8-camhanylphosphinic acid (**1**) and 8-camphanyl(phenyl)phosphinic acid (**3**)

2.1.5.1 General NMR features of the camphanyl region of camphene-derived phosphorus compounds. 31

2.1.5.2 NMR analysis of 8-camphanylphosphinic acid (**1**) 32

2.1.5.3 NMR analysis of 8-camphanyl(phenyl)-phosphinic acid (**3**) 38

2.2 Synthesis and characterisation of phosphinic acid esters

2.2.1 Introduction 41

2.2.2 Results and discussion 42

2.2.3 Gas chromatography mass spectrometric analysis of the 8-camphanylphosphinic acid methyl esters 45

2.2.4 NMR analysis of methyl 8-camphanyl(phenyl)-phosphinate (**7**) 47

2.3 Synthesis and characterisation of some 8-camphanyl-phosphinic acid derivatives

2.3.1 Introduction 53

2.3.2 Results and discussion 54

2.3.3 Electrospray mass spectrometric analysis of camphene-derived phosphinic acids **9** and **10** 57

2.3.4 NMR analysis of 8-camphanylphosphinic acid derivatives

2.3.4.1 NMR analysis of 8-camphanylphosphonic dichloride (**11**) 58

2.3.4.2 NMR analysis of **9** and **10** 60

2.4 Synthesis and characterisation of polymeric calcium 8-camphanylphosphinate (**13**)

2.4.1 Introduction 63

2.4.2 Results and discussion 65

2.4.3 X-ray crystal structure of polymeric calcium phosphinate (**13**) 66

2.5 Experimental

2.5.1 Synthesis of 8-camphanylphosphinic acid (**1**). 70

2.5.2 Synthesis of 8-camphanyl(phenyl)phosphinic acid (**3**) 71

2.5.3 Synthesis of methyl 8-camphanylphosphinate (**6**) 73

2.5.4 Synthesis of methyl 8-camphanyl(phenyl) phosphinate (**7**) 74

2.5.5 Synthesis of hydroxymethyl 8-camphanylphosphinic acid (**9**) 75

2.5.6 Synthesis of 8-camphanyl-N, N-dimethylmethylamino phosphinic acid hydrochloride (**10**) 76

2.5.7 Synthesis of 8-camphanylphosphonic dichloride (**11**) 77

2.5.8 Synthesis of 8-camphanyl(phenyl)phosphinic chloride (**12**) 78

2.5.9 Synthesis of polymeric calcium phosphinate (**13**) 78

References 80

Chapter Three: Synthesis and chemistry of 8-camphanyl-phosphonic acid and derivatives

3.1 Synthesis and characterisation of 8-camphanylphosphonic acid (**14**)

3.1.1 Introduction 84

3.1.2 Results and discussion 85

3.1.3 X-ray crystal structure of 8-camphanylphosphonic acid (**14**) 87

3.1.4 NMR analysis of 8-camphanylphosphonic acid (**14**) 93

3.2 Synthesis and characterisation of the dimethyl 8-camphanyl-phosphonate (**15**)

3.2.1 Results and discussion 97

3.2.2 NMR analysis of dimethyl 8-camphanyl-phosphonate (**15**) 98

3.3 A comparison of NMR data of the organophosphorus acids **1** and **14** with dimethyl 8-camphanylphosphonate (**15**) 101

3.4 Synthesis and characterisation of platinum complexes derived from 8-camphanylphosphonic acid

3.4.1 Introduction 103

3.4.2 Results and discussion

3.4.2.1 Synthesis of the 8-camphanylphosphonic acid-derived platinacycles **16, 17** and **18** 105

3.4.2.2 Attempted synthesis of the 8-camphanylphosphonic acid-derived palladinacycles 107

3.4.2.3 Attempted synthesis of the 8-camphanylphosphinic acid-derived platinacycles 107

3.4.3 Spectroscopic characterisation of **16, 17** and **18**

3.4.3.1 NMR analysis of $[Pt\{OP(O)(C_{10}H_{17})O\}(PPh_3)_2]$ (**16**) 109

3.4.3.2 NMR analysis of $[Pt\{OP(O)(C_{10}H_{17})O\}(PPhMe_2)_2]$ (**17**) 115

3.4.3.3 NMR analysis of [Pt{OP(O)($C_{10}H_{17}$)O}(DPPE)] (**18**) 118

3.4.4 A comparison of the NMR data of the platinacyclic complexes **16, 17, 18**

3.4.4.1 A comparison of ^{31}P NMR of **16, 17** and **18** 120

3.4.4.2 A comparison of ^{1}H and ^{13}C NMR of **16, 17** and **18** 122

3.4.5 Electrospray mass spectrometric analysis of **16, 17** and **18** 125

3.5 Experimental

3.5.1 Synthesis of 8-camphanylphosphonic acid (**14**) by direct oxidation using SO_2 127

3.5.2 Synthesis of 8-camphanylphosphonic acid (**14**) by direct oxidation using $Cu(NO_3)_2$ 129

3.5.3 Synthesis of 8-camphanylphosphonic acid (**14**) by hydrolysis of **11** 129

3.5.4 Synthesis of dimethyl 8-camphanylphosphonate (**15**) 130

3.5.5 Synthesis of [Pt{OP(O)($C_{10}H_{17}$)O}(PPh_3)$_2$] (**16**) 131

3.5.6 Synthesis of [Pt{OP(O)($C_{10}H_{17}$)O}($PPhMe_2$)$_2$] (**17**) 132

3.5.7 Synthesis of [Pt{OP(O)($C_{10}H_{17}$)O}(DPPE)] (**18**) 133

3.5.8 Attempted synthesis of [Pt{OP(O)($C_{10}H_{17}$)O}(PPh_3)$_2$] 134

3.5.9 Attempted synthesis of [Pt{OP(O)($C_{10}H_{17}$)O}(COD)] 134

3.5.10 Attempted synthesis of [Pd{OP(O)($C_{10}H_{17}$)O}(PPh_3)$_2$] 135

References 136

Chapter Four: Syntheses and characterisation of camphene-derived phosphines and their derivatives

4.1 Introduction. 139

4.2 Synthesis and characterisation of 8-camphanylphosphine

4.2.1 Introduction 142

4.2.2 Results and discussion 143

4.2.3 NMR analysis of 8-camphanylphosphine (**20**) 146

4.3 The gas phase decomposition of 8-camphanylphosphine 150

4.4 Synthesis and characterisation of 8-camphanyltris-(hydroxymethyl) phosphonium chloride (**22**)

4.4.1 Introduction 152

4.4.2 Results and discussion 152

4.4.3 X-ray crystal structure of 8-camphanyl tris(hydroxy-methyl)phosphonium chloride (**22**) 153

4.4.4 Spectroscopic analyses of 8-camphanyl tris(hydroxy-methyl)phosphonium chloride (**22**)

4.4.4.1 NMR analysis 156

4.4.4.2 Electrospray mass spectrometric analysis 158

4.5 Synthesis and characterisation of 8-camphanyl bis(hydroxy-methyl)phosphine (**23**) and derivatives

4.5.1 Introduction 159

4.5.2 Results and discussion 161

4.5.3 Spectroscopic analyses of camphene-derived hydroxymethylphosphines and their derivatives 163

4.5.3.1 NMR analysis of 8-camphanyl bis(hydroxy-methyl)phosphine (**23**) 164

4.5.3.2 NMR analysis of 8-camphanyl bis(hydroxy-methyl)phosphine sulphide (**24**), selenide (**25**) and oxide (**26**) 164

4.5.3.3 Electrospray mass spectrometric analysis of camphene-derived phosphine derivatives 167

4.6 Synthesis and characterisation of metal complexes of 8-camphanyl bis(hydroxymethyl)phosphine (**23**)

4.6.1 Introduction 170

4.6.2 Results and discussion 170

4.6.3 Spectroscopic analysis of the metal complexes of 8-camphanyl bis(hydroxymethyl)phosphine (**23**)

4.6.3.1 NMR analysis 173

4.6.3.2 Electrospray mass spectrometric analysis 173

4.7 Comparison of NMR data of camphene-derived phosphines and their derivatives

4.7.1 Comparison of ^{31}P NMR data of camphene-derived phosphines and their derivatives 176

4.7.2 Comparison of ^{1}H and ^{13}C NMR data of camphene -derived phosphines and their derivatives 176

4.8 Experimental

4.8.1 Synthesis of 8-camphanylphosphine **19** *via* $LiAlH_4$ route. 181

4.8.2 Synthesis of 8-camphanylphosphine **20** *via* disproportionation of **1** 182

4.8.3 Synthesis of 8-camphanylphosphine oxide **21** *via* air oxidation 182

4.8.4 Synthesis of tris(hydroxymethyl)camphanyl-phosphonium chloride (**22**) 183

4.8.5 Synthesis of bis(hydroxymethyl)camphanyl-phosphine (**23**)*via* use of NaOH. 185

4.8.6 Synthesis of bis(hydroxymethyl)camphanyl-phosphine (**23**) *via* use of Et_3N 186

4.8.7 Air oxidation of bis(hydroxymethyl)camphanyl-phosphine 186

4.8.8 Synthesis of 8-camphanyl bis(hydroxymethyl)camphanyl-phosphine sulfide (**24**) 187

4.8.9 Synthesis of 8-camphanylphosphine selanide (**25**) 188

4.8.10 Synthesis of bis(hydroxymethyl)camphanyl-phosphine oxide (**26**) 189

4.8.11 Synthesis of bis(hydroxymethyl)camphanyl platinum dichloride (**27**) 189

4.8.12 Synthesis of bis(hydroxymethyl)camphanyl gold chloride (**28**) 190

References 192

Chapter Five: Uranyl nitrate complexes of camphene-derived phosphorylic compounds.

5.1 Introduction 196

5.2 Synthesis and characterisation of 8-camphanyl-diphenylphosphine oxide (**29**)

5.2.1 Introduction 197

5.2.2 Results and discussion 198

5.2.3 Characterisation of 8-camphanyldiphenyl-phosphine oxide (**29**) 199

5.3 Synthesis and characterisation of camphanyl-derived uranyl(VI) nitrate complexes **30, 31** and **32**

5.3.1 Introduction 201

5.3.2 Results and discussion 202

5.3.3 X-ray crystal structure of uranyl(VI) nitrate complex **30** 203

5.3.4 Vibrational spectroscopic analysis of the uranyl nitrate complex **30** 208

5.4 Experimental

5.4.1 Synthesis of 8-camphanyldiphenylphosphine oxide (**29**) 210

5.4.2 Synthesis of $UO_2(NO_3)_2(C_{10}H_{17}PO(OMe)_2)_2$ (**30**) 211

5.4.3 Synthesis of $UO_2(NO_3)_2(C_{10}H_{17}PO(OMe)(Ph))_2$ (**31**) 212

5.4.4 Synthesis of $UO_2(NO_3)_2(C_{10}H_{17}POPh_2)_2$ (**32**) 212

References 213

Appendix I: Nomenclature of phosphorus compounds 215

Appendix II: Instrumental Techniques 217

Appendix III

AIII.1 Complete bond lengths, bond angles, and thermal and positional parameters for **1** 220

AIII.2 Complete bond lengths, bond angles, and thermal and positional parameters for **13** 224

AIII.3 Complete bond lengths, bond angles, and thermal and positional parameters for **14** 233

AIII.4 Complete bond lengths, bond angles, and thermal and positional parameters for **22** 237

AIII.5 Complete bond lengths, bond angles, and thermal and positional parameters for **30** 241

Appendix IV: List of publications 246

Appendix V: Methods of identification of products from the gas phase decomposition of **20** 247

List of schemes

Scheme		Page
1.1	Reaction sequences of organophosphorus derivatives containing the menthyl group.	3
1.2:	Reaction schemes of menthyl-derived phosphorus compounds.	3
1.3	Reactions of (+)-9-bromocamphor.	4
1.4	The proposed mechanism for the formation of a 4-oxatricyclo[4.3.0.0] nonane skeleton.	5
1.5	Reactions of 8,10-dibromocamphor.	5
1.6	Reactions of (+)-8-bromocamphor.	5

1.7	General reaction scheme for the synthesis of β -keto phosphonates using α-bromo ketones.	6
1.8	Reaction of bromocamphor with lithium $LiN(SiMe_3)_2$, *tert*-BuLi and $(EtO)_2P(O)Cl$.	6
1.9	Synthesis of (-)-camphorphosphinoylimine.	6
1.10	Reaction of menthol and borneol with phenylphosphonic anhydride.	8
1.11	Reaction of aliphatic terpenic alcohols with phenylphosphonic anhydride.	8
1.12	Reaction of alpha-, beta-unsaturated monoterpenic ketones with the sodium salt of diethylphosphite.	9
1.13	Formation of diphenylvinylphosphines by the reaction of optically active terpene alcohols with vinyl derivatives and $SiHCl_3$.	10
1.14	Formation of β-(amino)ethylphosphines.	10
1.15	Preparation of β-hydroxyphosphines by an epoxide-opening reaction.	10
1.16	Reaction of commercial mixtures of limonene oxide with $LiPPh_2$.	11
1.17	Reaction of β-pinene oxide with $LiPPh_2$.	11
1.18	Preparation of diphenylalkylphosphine-borane complexes using zinc organometallics.	12
1.19	Chiral diphosphines prepared from β-pinene- and (+)-longifolene-derived zinc reagents.	12
1.20	Reaction of α-pinene with the PCl_2Me-$AlCl_3$ complex.	13
1.21	The treatment of camphene with diethyl hydrogen phosphite $[(EtO)_2P(O)H]$ under free radical conditions.	14
1.22	Reaction of camphene with the PCl_2Me-$AlCl_3$ complex.	14
1.23	The formation and subsequent oxidation of **1** to **14**.	15
2.1	(i) The addition of hypophosphorous acid $[H_3PO_2]$ to alkenes (ii) The addition of a second alkene molecule to phosphinic acid.	19

2.2	The radical-catalysed addition of H_3PO_2 to simple alkenes.	20
2.3	The modes of radical addition to an unsaturated bond.	20
2.4	The radical-catalysed addition of hypophosphorous acid to camphene.	21
2.5	The synthesis of **1** by the radical-catalysed addition of hypophosphorous acid to camphene	22
2.6	Possible modes of radical attack of camphene.	23
2.7	The Nametkin-type rearrangement of camphene.	24
2.8	The Wagner-Meerwein 2, 6-hydride shift of camphene.	24
2.9	The radical-catalysed addition of phenylphosphinic acid [PhP(O)(OH)(H)] to camphene.	25
2.10	Esterification of phosphinic acids with a trialkyl phosphite.	41
2.11	Acid-catalysed esterification of phosphinic acids.	41
2.12	Esterification of phosphinic acids with diazomethane.	41
2.13	The esterification of camphene-derived phosphinic acids **1** and **3** with diazomethane.	42
2.14	Interconversion of 8-camphanylphosphinic acid (**1**) and its methyl ester methyl 8-camphanylphosphinate (**6**).	43
2.15	Tautomerism of methyl 8-camphanylphosphinate (**6**) by hydride transfer.	43
2.16	The methyl esters **6a** and **7a**, formed by the methylation of **1a** and **3a**.	44
2.17	The methylation of di(8-camphanyl)phosphinic acid (**2**).	44
2.18	The acid-catalysed addition of formaldehyde to phosphinic acids to give hydroxymethylphosphinic acids.	53
2.19	Addition products formed by the reaction of phosphorous acids with Schiff's bases [formed *in situ* from HCOH and R_2NH].	53
2.20	Chlorination of phosphonates with thionyl chloride [$SOCl_2$].	54
2.21	The acid-catalysed addition of HCOH and HCOH/Me_2NH to **1**.	55

2.22	The pyridine-catalysed chlorination of **1** and **3** with $SOCl_2$.	56
2.23	The precipitation of metal phosphinates from the phosphinic acid and metal salt.	63
2.24	The schematic formation of divalent metal phosphinates by the slow hydrolysis of urea.	64
2.25	The synthesis of polymeric calcium phosphinate.	65
3.1	The oxidation of phosphinic [RPO_2H_2] to phosphonic acid [RPO_3H_2] {R=alkyl group}.	84
3.2	The hydrolysis of phosphonic dichloride to phosphonic acid.	85
3.3	The oxidation of **1** to 8-camphanylphosphonic acid (**14**) using either (i) SO_2 or (ii) $Cu(NO_3)_2$.	86
3.4	The synthesis of phosphonic acid **14** by the hydrolysis of 8-camphanylphosphonic dichloride (**11**).	86
3.5	The methylation of **14** with an excess of diazomethane.	97
3.6	The hydrolysis of dimethyl 8-camphanylphosphonate (**15**) in air.	98
3.7	The methylation of the minor addition product **14a** with diazomethane.	98
3.8	The synthesis of four-membered platinacycles using silver(I) oxide as a base and halide-abstracting agent.	104
3.9	General reaction scheme for the synthesis of four-membered phosphonic acid-derived platinacycles using silver(I) oxide as a base and halide-abstracting agent.	104
3.10	The synthesis of 8-camphanylphosphonic acid-derived platinacycles **16, 17** and **18** using silver(I) oxide as a base and a halide-abstracting agent.	106
3.11	The attempted synthesis of the di(8-camphanyl)-phosphinic acid-derived platinum(II) complex.	108
4.1	The disproportionation of phosphinic acids.	142
4.2	The reduction of phosphorus compounds with $LiAlH_4$.	143
4.3	The reduction of 8-camphanylphosphonic dichloride (**11**) with lithium aluminium hydride [$LiAlH_4$].	144

4.4	The thermal reduction of 8-camphanyl-phosphinic acid (**1**).	145
4.5	The oxidation of phosphine **20** to the phosphine oxide **21**.	146
4.6	Proposed pathways to the gas phase decomposition of 8-camphanylphosphine (**20**).	151
4.7	The synthesis of bis(hydroxymethyl)phosphonium salt by treatment of primary phosphine with HCl/HCOH.	152
4.8	The synthesis of the phosphonium salt **22** by addition of excess HCl/HCOH to the primary phosphine 8-camphanylphosphine (**20**).	153
4.9	A summary of some reactions of tris(hydroxymethyl)phosphine.	160
4.10	Synthesis of hydroxymethylphosphine **23** by treatment of **22** with potassium hydroxide or Et_3N.	161
4.11	Synthesis of formaldehyde adducts of 8-camphanyl bis(hydroxymethyl)phosphine (**23**).	162
4.12	The synthesis of the phosphine sulfide **24** and selenide **25**.	162
4.13	The oxidation of **23** to the hydroxymethylphosphine oxide **26**.	163
4.14	The synthesis of the platinum dichloride complex **27**.	171
4.15	The synthesis of the gold(I) chloride complex **28**.	172
5.1	The synthesis of phosphine oxides by the treatment of a phosphonic dichloride [$RP(O)Cl_2$] with a Grignard reagent [R'-MgCl].	197
5.2	The synthesis of 8-camphanyldiphenylphosphine oxide (**29**).	198
5.3	Synthesis of uranyl(VI) nitrate complexes of the type $UO_2(NO_3)_2(L)_2$.	201
5.4	The synthesis of camphanyl-derived uranyl(VI) nitrate complexes **29**, **30** and **31**.	202

List of Figures

Figure		Page
1.1	Structures of naturally-occurring monoterpenes.	1
1.2	Menthyl-derived phosphorus compounds.	2
1.3	The molybdenum complex $MoO_2Cl_2\{OC_{10}H_{15}PO(OEt)_2$ containing the β-ketophosphonate derived from camphor.	7
1.4	The phosphonic acids formed by the reaction of camphene with phosphorus pentachloride [PCl_5].	14
2.1	The molecular structure of **1**, together with the atom numbering scheme.	26
2.2	The negative-ion electrospray mass spectra of (a) **3** at 45 V, (b) **1** at 45 V.	30
2.3	Atom numbering scheme for camphanyl-phosphorus derivatives.	31
2.4	The ^{13}C-^{1}H correlated NMR spectrum of 8-camphanyl-phosphinic acid (**1**), recorded in $CDCl_3$ at 300 MHz.	35
2.5	COSY45 spectrum of 8-camphanylphosphinic acid (**1**), recorded in $CDCl_3$ at 300 MHz.	37
2.6	(i) total ion chromatogram of **6** from 4 to 9 min. (ii) mass spectrum of major product methyl 8-camphanylphosphinate (**6**) eluting at 5.92 min. (iii) mass spectrum of minor addition product **6a** eluting at 5.74 min. (iv) mass spectrum of methyl 8-camphanyl(phenyl)phosphinate (**7**).	46
2.7	The ^{13}C-^{1}H correlated NMR spectrum of the camphanyl moiety of methyl 8-camphanyl(phenyl)phosphinate isomers (**7**), recorded in $CDCl_3$ at 300 MHz.	49
2.8	The COSY45 spectrum of the camphanyl moiety of methyl 8-camphanyl(phenyl)phosphinate (**7**) recorded in $CDCl_3$ at 300 MHz.	52
2.9	Coordination geometry about the calcium atoms in the polymeric chain of **13**, showing the alternating four- and eight-membered rings and the atom numbering scheme.	67
2.10	Space-filling representation of the polymeric chain, with calcium, phosphorus and oxygen atoms of the central	

	hydrophilic core shown by the smaller black circles, and the carbon atoms of the camphanyl group by the larger open circles.	68
3.1	Molecular structure of 8-camphanylphosphonic acid (**14**) together with the atom numbering scheme.	88
3.2	Stereo view of the $CH_2P(O)(OH)_2$ core in which three molecules are linked in a ring by O(3)-H(130)...O(2) hydrogen bonding. These trimers are linked together by six O(1)-H(110)...O(2) bonds.	91
3.3	Stereo view of the core of two $CH_2P(O)(OH)_2$ hexamers which stack upon each other giving a discontinuous hydrophilic central core.	91
3.4	Stereoview of the unit cell depicting the bulky camphanyl groups that surround the central core.	92
3.5	COSY45 spectrum of 8-camphanylphosphonic acid (**14**) recorded in $CDCl_3$ at 300MHz.	96
3.6	The phenyl and methyl phosphonic acid-derived platinacycles.	105
3.7	The ^{31}P NMR spectrum of **16**, recorded in $CDCl_3$ at 36 MHz.	110
3.8	NOE difference spectra of **16** recorded in $CDCl_3$ at 300 MHz. (a) ^1H NMR spectrum of **16** (b) Irradiation of H_4 (δ 2.29) (c) Irradiation of Me' (δ 0.95) (d) Irradiation of $H_{7'/1}$ (δ 1.05) (e) Irradiation of $H_{5'}$ (δ 0.83).	114
3.9	The ^{31}P NMR spectrum of **17**, recorded in $CDCl_3$ at 36MHz.	117
3.10	Positive-ion electrospray mass spectrum of **16** in 1:1 $MeCN/H_2O$ at a cone voltage of 20 V. The insert shows observed (LHS) and calculated (RHS) isotope distribution pattern of $[M+H]^+$ at *m/z* 936.	126
4.1	Apparatus designed to facilitate both the disproportionation of phosphinic acid **1** and the distillation of the primary phosphine **20**.	145
4.2	The P-H region of the ^1H NMR spectrum of **20** displaying (a) the highly coupled PH_2 signals (b) the result of irradiating the signals assigned to $H_{8'/8''}$ [δ 1.49].	149

4.3	(a) Molecular structure of 8-camphanyl tris(hydroxy-methyl)phosphonium chloride (**21**), together with the atom numbering scheme (b) stereoview of the cell packing diagram of **22** .	155
4.4	(a) Electrospray mass spectrum of $C_{10}H_{17}P(S)(CH_2OH)_2$ (**24**) in 1:1 H_2O/CH_3CN [containing $AgNO_3$] at a cone voltage of 20 V. (b) observed [LHS] and calculated [RHS] isotope patterns of peak at *m/z* 412. (c) observed [LHS] and calculated [RHS] isotope patterns of peak at *m/z* 633.	169
4.5	The ^{31}P NMR spectrum of the platinum dichloride complex **27** at 121.51 MHz.	171
4.6	Positive-ion electrospray mass spectrum of the gold(I) chloride complex **28** recorded in 1:1 H_2O/MeCN at a cone voltage of 50V.	174
4.7	Observed (LHS) and calculated (RHS) isotope patterns for the gold(I)-phosphine adducts (a) $[M+Au]^+$ at *m/z* 427. (b) $[M+Au+CH_3CN]^+$ at *m/z* 468. (c) $[2M+Au]^+$ at *m/z* 657. (d) $[2M+2Au+Cl]^+$ at *m/z* 889.	175
5.1	Positive-ion electrospray mass spectrum of **29** in 1:1 MeCN/H_2O [containing KCl] at 80 V.	200
5.2	The molecular structure of the camphene-derived phosphorylic compounds **7**, **15** and **29**.	202
5.3	Molecular structure of the "*cis*-isomer" of **30**, together with the atom numbering scheme and selected bond lengths (Å)	204
5.4	Molecular structure of the *trans*-isomer of **30**, together with the atom numbering scheme and selected bond lengths (Å)	207

List of Equations

Equation		page
4.1	Synthesis of hydroxymethylphosphines by the treatment of a phosphonium salt with potassium hydroxide.	159
4.2	Synthesis of hydroxymethylphosphine oxides by treatment of a phosphonium salt with an excess of potassium hydroxide.	159
4.3	General reaction scheme for the synthesis of gold(I) complexes containing donor phosphorus ligands.	172

List of Tables

Table		page
2.1	Bond lengths (Å) and selected bond angles (°) of 8-camphanylphosphinic acid (**1**).	26
2.2	A comparison of bond lengths and dihedral angles of **1** determined by X-ray crystallography and calculated by molecular modelling.	27
2.3	Summary of the ^{1}H and ^{13}C NMR data [δ in $CDCl_3$] for 8-camphanylphosphinic acid (**1**).	33
2.4	NOE's observed for the protons of **1**.	36
2.5	A comparison of the ^{1}H and ^{13}C NMR data [δ in $CDCl_3$] of **3** and **1**.	38
2.6	NOE's observed for the protons of **3**.	40
2.7	A comparison of ^{1}H NMR data [δ in $CDCl_3$] of the isomers of **7** with their parent acid **3**.	47
2.8	A comparison of the ^{13}C NMR data [δ in $CDCl_3$] of the isomers of **7** with their parent acid **3**.	48
2.9	NOE's observed for the protons of **7**.	51
2.10	A comparison of electrospray mass spectral data of **9** and **10** collected in positive and negative ion modes.	57
2.11	A comparison of the ^{1}H NMR data [δ in $CDCl_3$] of the camphanyl moieties of **11** and **1**.	58

2.12	A comparison of the ^{13}C NMR data (δ in $CDCl_3$) of **11** with **1**.	59
2.13	A comparison of the ^{13}C NMR chemical shifts [75 MHz] of 8-camphanylphosphinic acid (**1**) and derivatives **9** and **10** .	61
2.14	One-bond phosphorus-to-carbon coupling constants of **1, 9** and **10**.	62
2.15	Selected bond lengths (Å) and angles (°) of **13**.	67
3.1	Bond lengths (Å) and selected bond angles (°) of 8-camphanylphosphonic acid (**14**).	88
3.2	A comparison of selected bond lengths (Å) and torsion angles (°) of the phosphinic acid **1** and phosphonic acid **14**.	89
3.3	A comparison of bond lengths (Å) and bond angles (°) of **14** with 1-amino-2-phenylethyl)phosphonic acid monohydrate [$PhCH_2CH(NH_2)$-PO_3H_2] and 3-amino-3-phosphono-propionic acid [$HC(NH_2)(CH_2COOH)$-PO_3H_2].	90
3.4	Summary of the ^1H and ^{13}C NMR data [δ in CD_3OD] for 8-camphanylphosphonic acid (**14**).	93
3.5	NOE's observed for the protons of **14**.	95
3.6	Summary of the ^1H and ^{13}C NMR data [δ in $CDCl_3$] for dimethyl 8-camphanylphosphonate (**15**).	99
3.7	NOE's observed for protons of **15**.	100
3.8	A comparison of the ^1H NMR data [300 MHz] of organo-phosphorus acids **1** and **14** with dimethyl 8-camphanylphosphonate (**15**).	101
3.9	A comparison of the ^{13}C NMR data [75 MHz] of organo-phosphorus acids **1** and **14** with dimethyl 8-camphanylphosphonate (**15**).	102
3.10	NOE's observed for protons of **16**.	112
3.11	^1H and ^{13}C NMR data [δ in $CDCl_3$] of **17**.	116
3.12	^1H and ^{13}C NMR data [δ in $CDCl_3$] of **18**.	119
3.13	^{31}P NMR data of platinacycles **16, 17** and **18**.	120
3.14	^1H NMR data of platinacyclic complexes **16, 17** and **18**.	123

3.15	^{13}C NMR data of the camphanyl moiety of platinacyclic complexes **16, 17** and **18.**	124
4.1	A comparison of the ^{1}H NMR [δ in $CDCl_3$] and ^{13}C NMR [δ in $CDCl_3$] data of phosphinic acid **1** and primary phosphine **20.**	147
4.2	Bond lengths (Å) and angles (°) of 8-camphanyl tris-(hydroxymethyl)phosphonium chloride (**22**) associated with interionic H-bonding interactions.	154
4.3	A comparison of selected bond lengths of **22** with the analogous bond lengths of $[Ph_2P(CH_2OH)_2]Cl$.	156
4.4	^{1}H NMR [δ in $CDCl_3$] and ^{13}C NMR[δ in $CDCl_3$] data of **22.**	158
4.5	Electrospray mass spectral data of 8-camphanyl tris(hydroxy-methyl)phosphonium chloride (**22**) in 1:1 H_2O/CH_3CN.	158
4.6	A comparison of the $^{1}J_{\mathbf{P\text{-}C(8)}}$ and $^{1}J_{\mathbf{P\text{-}CH_2OH}}$ coupling constants of the phosphine **23,** phosphine sulfide **24,** selenide **25** and oxide **26** with phosphonium salt **22.**	166
4.7	Electrospray mass spectral data of camphene-derived hydroxymethylphosphine derivatives in 1:1 $MeCN/H_2O$.	167
4.8	Electrospray mass spectral data of the gold(I) chloride complex **28** recorded in 1:1 H_2O/MeCN at a cone voltage of 50V.	174
4.9	^{1}H NMR data of camphene-derived phosphines and their derivatives.	179
4.10	^{13}C NMR data of camphene-derived phosphines and their derivatives.	180
5.1	Vibrational spectroscopic data for ligand **15** and the uranyl(VI) nitrate complex **30.**	209

Abbreviations

The following abbreviations have been used in this thesis:

Ar	Aryl
Bu	butyl
CD	circular dichroism
δ	chemical shift (ppm) [NMR]
J	coupling constant in Hertz [NMR]
COD	1,5-cyclooctadiene
DMSO	dimethylsulfoxide
d	doublet (NMR)
ESMS	electrospray mass spectrometry
Et	ethyl
GCMS	gas chromatography mass spectrometry
I.R	Infrared
m.p.	melting point
m	meta
m	multiplet
Me	methyl
NMR	nuclear magnetic resonance
NOE	nuclear overhauser effect
ORD	optical rotatory dispersion
o	ortho
p	para
Ph	phenyl
s	singlet (NMR)
υ	stretching frequency (I.R)
THF	tetrahydrofuran
t	triplet (NMR)
XRD	X-ray diffraction

Chapter One

Terpene-phosphorus chemistry

1.1 *Introduction*

In the strictest sense, terpenes are the volatile aromatic hydrocarbons of the empirical formula $C_{10}H_{16}$. In a wider sense the term includes sesquiterpenes, $C_{15}H_{24}$, diterpenes, $C_{20}H_{32}$, and higher polymers. In a still looser sense the term includes various oxygen-containing compounds derived from the terpene hydrocarbons, such as alcohols, ketones and camphors. Terpenes are readily obtained from many varieties of vegetable life[1]. Their highly characteristic and usually pleasant odours means terpenes, natural and synthetic, are readily employed in the perfumery industry as important constituents of most odorants[1]. Many of them, for example the constituents of eucalyptus oils [menthol and camphor], and limonene, which has been shown to prevent carcinogen-induced mammary cancer[2], are of pharmaceutical importance.

Monoterpenes are also an attractive source of chirality, since they occur naturally in high enantiomeric purities and are inexpensive. A range of chiral auxiliaries have been derived from monoterpenes[3] and their oxygenated congeners, such as camphor (see Figure 1.1). Although the steric bulk of terpenes is advantageous, the lack of appropriate functional groups may possibly be the reason why only two monoterpenes have been used extensively for types of chiral auxiliaries: camphor, where additional functional groups must be introduced, and menthol, where the hydroxy group is replaced in order to obtain suitable ligands. Both terpenes are the starting point for several families of highly effective ligands. Their chemistry relevant to this thesis is discussed in detail in sections 1.2 and 1.3.

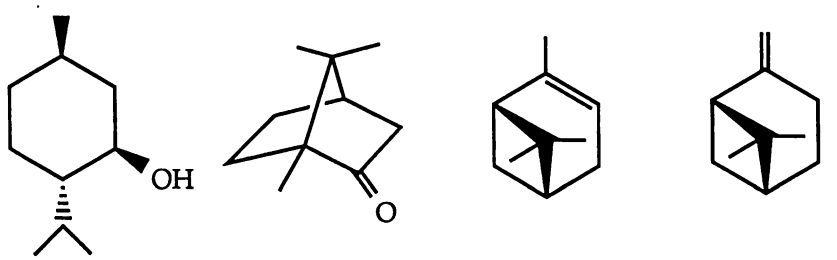

menthol camphor α-pinene β-pinene

Figure 1.1: Structures of naturally-occurring monoterpenes.

The best-studied terpene-based chiral reagents are the versatile organoboranes developed by Brown over the last two decades[4]. Of the five reagents which are extensively used in asymmetric reduction the pinene-derived borane diisopinocampheylchloroborane [DIP-Chloride™] has proved to be a good chiral auxiliary.

Somewhat surprisingly, relatively little work has been carried out on organophosphorus derivatives of terpenes, and much of this work has been largely restricted to menthyl-phosphorus compounds. A review of the chemistry of terpene-containing organophosphorus compounds is presented within this chapter.

1.2 *Menthyl-phosphorus chemistry*

The organophosphorus chemistry of the chiral menthyl group [refer to Figure 1.1] is by far the most extensive of the monoterpenes. The structural diversity of menthyl-containing phosphorus compounds is clearly illustrated in Figure 1.2 where a series of tri- and tetra-coordinate phosphorus compounds have been synthesised[5].

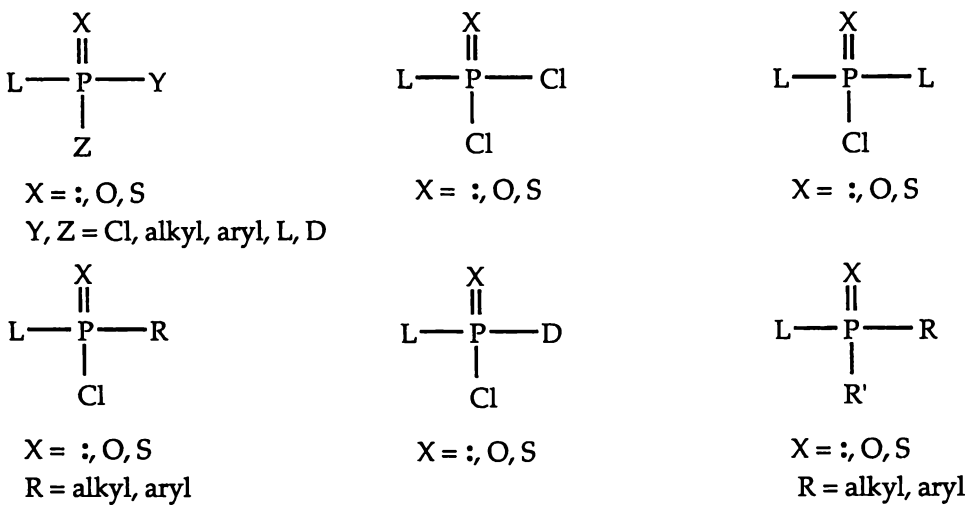

: = lone pair of electrons
L = (-)-menthyl group
D = (+)-menthyl group

Figure 1.2: Menthyl-derived phosphorus compounds.

Outlined in Schemes 1.1 and 1.2 are the elaborate reaction sequences and equations employed to synthesise (-)-menthylphosphonic acid[6], a phosphonic acid [R-P(O)(OH)$_2$] containing the bulky chiral menthyl group. This is particularly relevant to the research discussed within chapter three of

this thesis where the synthesis and derivatisation of the analogous camphene-derived phosphonic acid, 8-camphanylphosphonic acid, is investigated.

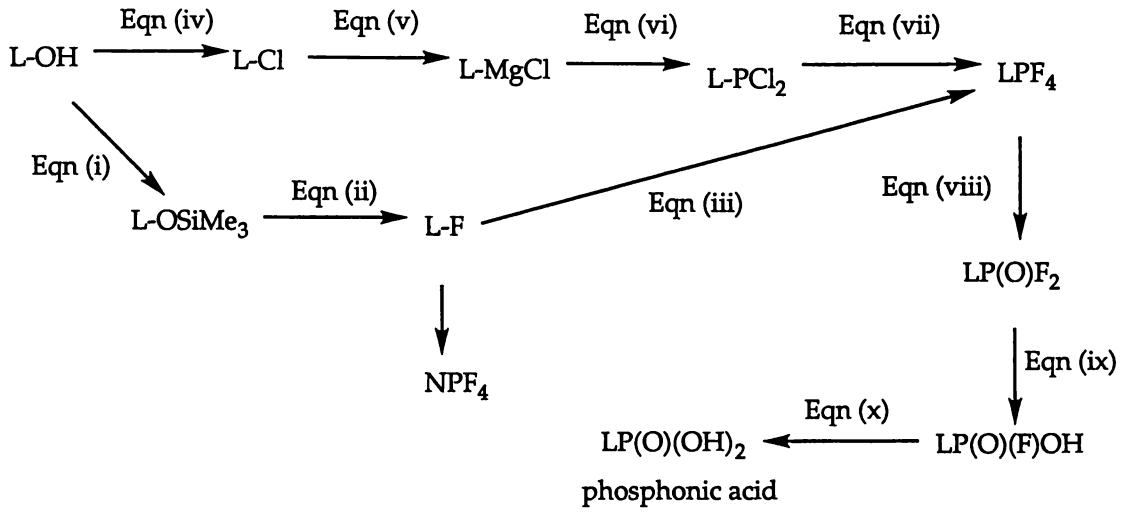

Scheme 1.1: Reaction sequences of organophosphorus derivatives containing the menthyl group. Refer to Scheme 1.2 for reaction equation details.

(i) L-OH + Me_3SiCl ⟶ L-$OSiMe_3$

(ii) L-$OSiMe_3$ + $C_6H_5PF_4$ ⟶ L-F

(iii) L-F + PF_3 + cat.$C_6H_5PF_4$ ⟶ L-PF_4 (+NPF_4)

(iv) L-OH + $ZnCl_2$ $\xrightarrow{\text{conc HCl}}$ L-Cl

(v) L-Cl + Mg turnings ⟶ L-MgCl

(vi) L-MgCl + PCl_3 ⟶ L-PCl_2 + $MgCl_2$

(vii) 3LPCl_2 + 4AsF_3 ⟶ 3LPF_4 + 2As + 2$AsCl_3$

(viii) two possible routes

[a] LPF_4 + $[Me_3Si]_2O$ ⟶ L$P(O)F_2$ + 2Me_3SiF

[b] LPF_4 + H_2O ⟶ L$P(O)F_2$ + 2HF

(ix) L$P(O)F_2$ + H_2O ⟶ L$P(O)(F)OH$ + HF

(x) L$P(O)(F)OH$ + H_2O ⟶ L$P(O)(OH)_2$ + HF

phosphonic acid

Scheme 1.2: Reaction schemes of menthyl-derived phosphorus compounds. Refer to scheme 1.1 for details of reaction sequences.

The coordination of dimenthylphosphine [HPL_2 where L= menthyl group], which is synthesised by the reduction of chlorodimenthylphosphine [L_2PCl] with $LiAlH_4$, with $[(\eta^5\text{-}C_5H_5)Fe(CO)_2]_2$ has been studied[7]. Results

indicate that the hydrido-phosphido-bridged complex [$(\eta^5\text{-}C_5H_5)_2Fe_2(\mu\text{-}H)(\mu\text{-}PL_2)(CO)_2$ where L= menthyl group] is formed.

1.3 *Camphor-phosphorus chemistry*

As mentioned previously in section 1.1, the need to introduce functional groups in addition to the keto group already present in camphor has been pivotal in the development of camphor-based compounds. It is now well known that camphor can be stereospecifically transformed into a wide variety of its derivatives. One such example is the well established mono- and di-bromocamphor family of compounds. The following examples are those which incorporate the use of bromocamphor derivatives to obtain organophosphorus compounds containing the camphor moiety.

The reactions of (+)-8- and (+)-9-bromocamphors with some nucleophiles have been studied[8]. The reaction of (+)-9-bromocamphor with Ph_2PLi proceeds under mild conditions and yields, after hydrolysis, 9-diphenylphosphanylcamphor (see Scheme 1.3). The subsequent oxidation of 9-diphenylphosphanylcamphor to a phosphine oxide allows the conversion, by reduction with $LiAlH_4$, of the keto group to the hydroxy group.

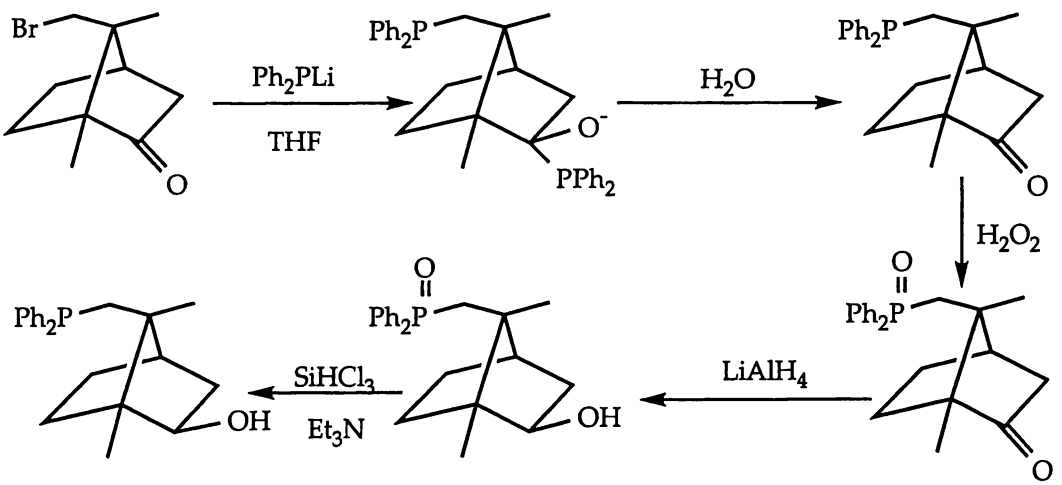

Scheme 1.3: Reactions of (+)-9-bromocamphor.

The reaction of (+)-8-bromocamphor with Ph_2PLi followed by oxidation gives compounds containing a 4-oxatricyclo[4.3.0.0] nonane skeleton. The proposed mechanism for this reaction is given in Scheme 1.4. Analogously, reaction of Ph_2Li with 8,10-dibromocamphor, Scheme 1.5, yields a functionalised tricyclic diphosphine.

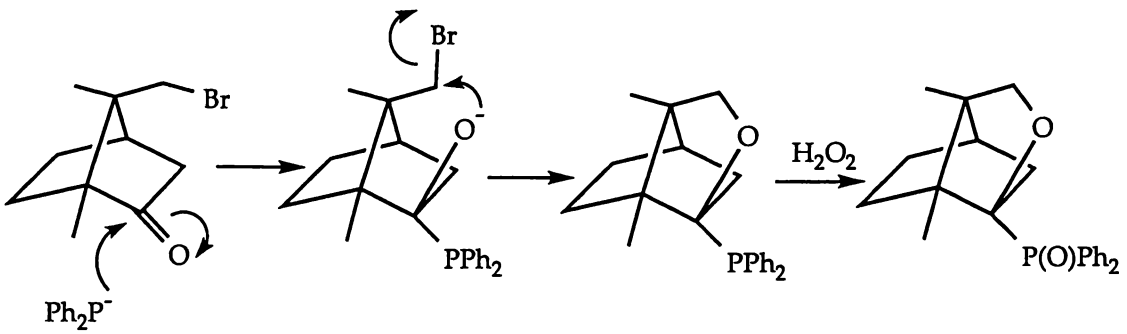

Scheme 1.4: The proposed mechanism for the formation of a 4-oxatricyclo[4.3.0.0] nonane skeleton.

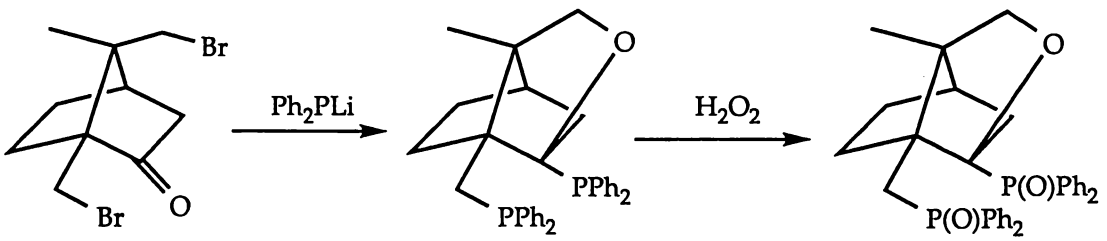

Scheme 1.5: Reactions of 8,10-dibromocamphor.

The reaction of (+)-8-bromocamphor in which the carbonyl group has been protected by the formation of the ethylene ketal, with Ph_2Li is outlined in Scheme 1.6. The subsequent reduction of the P=O bond followed by hydrolysis affords 8-diphenylphosphanylcamphor.

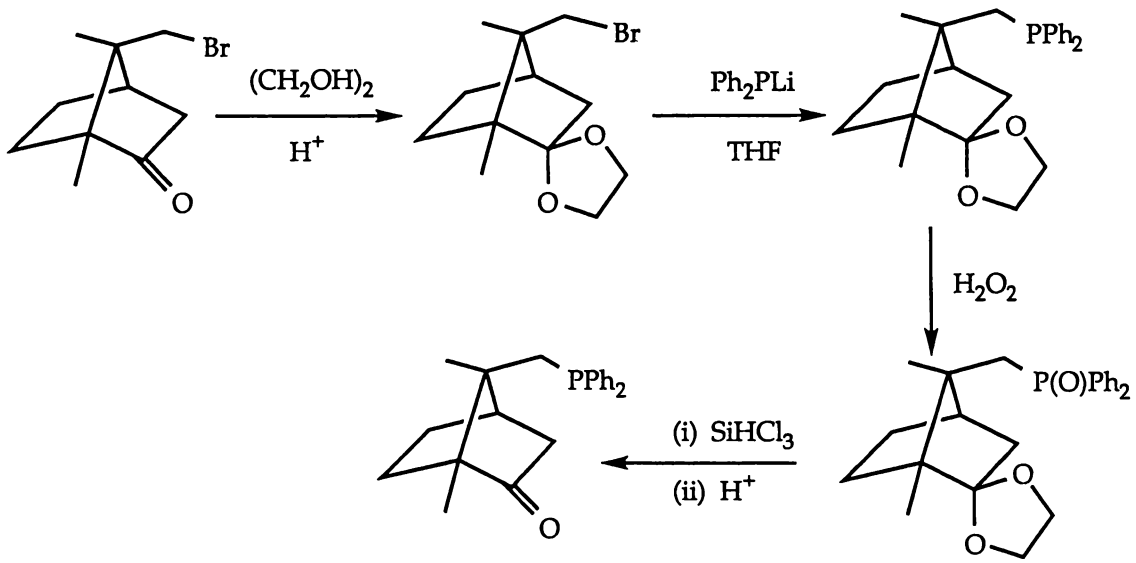

Scheme 1.6: Reactions of (+)-8-bromocamphor.

Scheme 1.7 describes the general route in which α-bromo ketones react with lithium hexamethyldisilazide [$LiN(SiMe_3)_2$] and *tert*-BuLi to produce a dilithiated species which, in turn, reacts with electrophiles such as a dialkyl chlorophosphate [$(EtO)_2P(O)Cl$] to afford β-keto phosphonates.

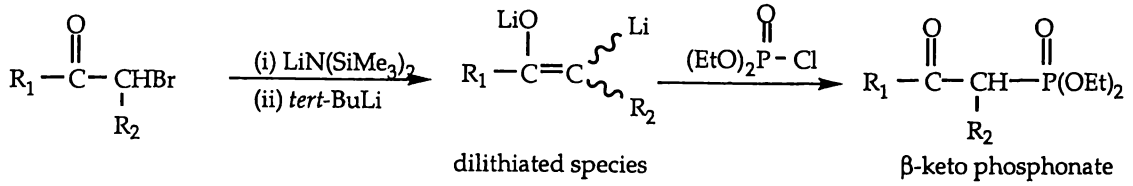

Scheme 1.7: General reaction scheme for the synthesis of β-keto phosphonates using α-bromo ketones.

Similarly the treatment of α-bromocamphor with $LiN(SiMe_3)_2$, *tert*-BuLi and $(EtO)_2P(O)Cl$[9], Scheme 1.8, affords the β-keto phosphonate 3-(diethylphosphonyl)camphor.

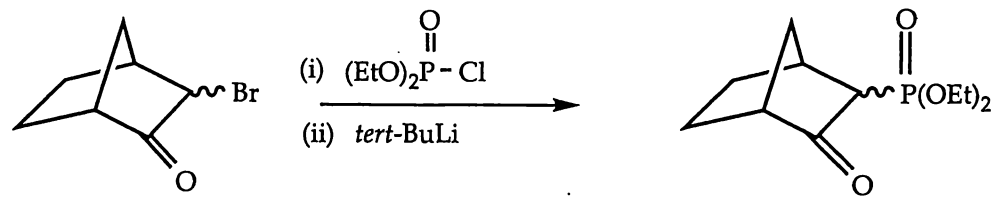

Scheme 1.8: Reaction of bromocamphor with lithium $LiN(SiMe_3)_2$, *tert*-BuLi and $(EtO)_2P(O)Cl$.

Reactions involving the keto group present in camphor have been investigated. One such example is the use of phosphinic amides which react with the keto group of camphor to afford imines. Thus the reaction of (+)-camphor with diphenylphosphinic amide in toluene heated at reflux in the presence of titanium tetrachloride and triethylamine affords (-)-camphorphosphinoylimine in moderate yield[10] (see Scheme 1.9).

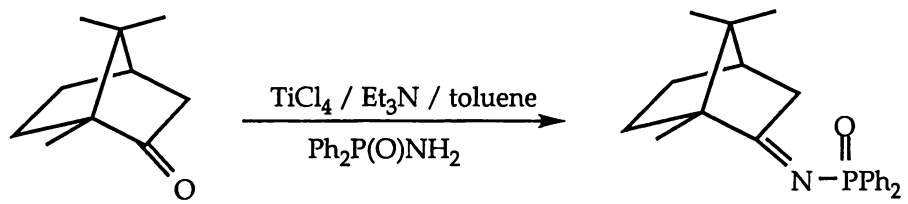

Scheme 1.9: Synthesis of (-)-camphorphosphinoylimine.

The coordination chemistry of camphor-containing ligands to metal centres has also been studied. The molybdenum complex $MoO_2Cl_2\{OC_{10}H_{15}P(O)(OEt)_2$ containing the β-ketophosphonate derived from camphor, Figure 1.3, is a highly active and regioselective catalyst for the epoxidation of certain alkenes using *tert*-butyl hydroperoxide as oxidant[11].

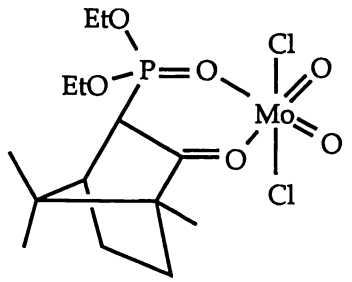

Figure 1.3: The molybdenum complex $MoO_2Cl_2\{OC_{10}H_{15}PO(OEt)_2$ containing the β-ketophosphonate derived from camphor.

The mixed monoazines of the type $H_2C{=}N\text{-}N{=}C_{10}H_{16}$ [$C_{10}H_{16}$ is a (1R)-(+)-camphor residue (L^1)] or α-diazines $C_{10}H_{16}{=}N\text{-}N\text{-}CH\text{-}CH{=}N\text{-}N{=}C_{10}H_{16}$ [$C_{10}H_{16}$ is a (1R)-(+)-camphor residue (L^2)] or α-2-pyridyl diazines $C_{10}H_{16}{=}N\text{-}N{=}CHC_5H_4N$ [$C_{10}H_{16}$ is a (1R)-(+)-camphor residue (L^3)] react with $[Pd_2Cl_4(PR_3)_2]$ to give the palladium complexes $[Pd_2Cl_4(PR_3)L^n]$ [n=1, R_3=Me_2Ph or $Me_2(C_6H_4OMe\text{-}4)$; n=2, R_3=Me_2Ph; n=3, R_3=$Bu^n{}_3$] in which the ligands are monodentate, or $[\{Pd_2Cl_4(PR_3)_2\ L^n\}]$ (L^n=L^2, L^3; R_3=Me_2Ph), in which the ligands are bidentate[12].

1.4 Terpene-phosphonate chemistry

Unlike the alkyl- and aryl-based phosphonate/phosphinate chemistry [consult chapters 2 and 3], the study of terpene-based phosphon(in)ates has attracted little interest. Surprisingly there has also been little interest in the coordination chemistry of terpene-phosphonates to metal centres. This is in contrast to its alkyl- and aryl-based counterpart where the coordination chemistry to metal centres is extensive[13]. Thus the terpene-phosphon(in)ate chemistry which is outlined below is somewhat dated and sparse.

The phenylphosphonic monoesters of menthol and borneol are prepared by reaction of phenylphosphonic anhydride with menthol and borneol in the presence of a tertiary base [pyridine][14] (see Scheme 1.10).

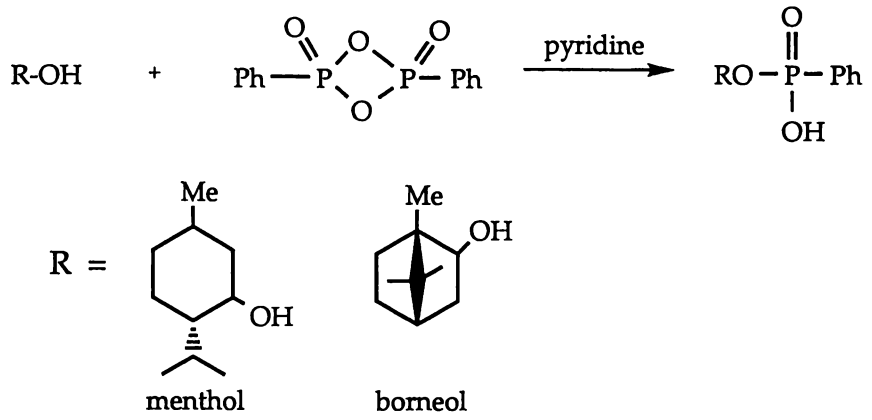

Scheme 1.10: Reaction of menthol and borneol with phenylphosphonic anhydride.

The reaction of the aliphatic terpenic alcohols nerol [trans-3,7-dimethyl-2,6-octadien-1-ol], geraniol [cis-3,7-dimethyl-2,6-octadien-1-ol], farnesol [3,7,11-trimethyldodeca-trans-2-trans-6,10-trien-1-ol], linalool [3,7-dimethyl-1,6-octadien-1-ol] and nerolidol [3,7,11-trimethyldodeca-1,6,10-trien-3-ol] with phenylphosphonic anhydride [in the presence of triethylamine] also yields the corresponding phenylphosphonic monoesters[15] (see Scheme 1.11).

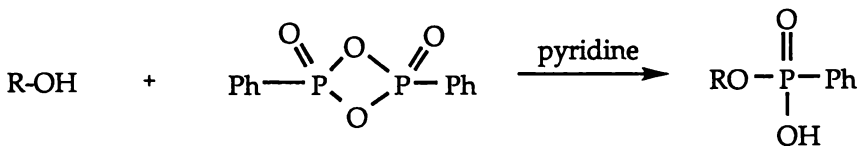

R = farnesol, nerol, geraniol, nerolidol, linalool

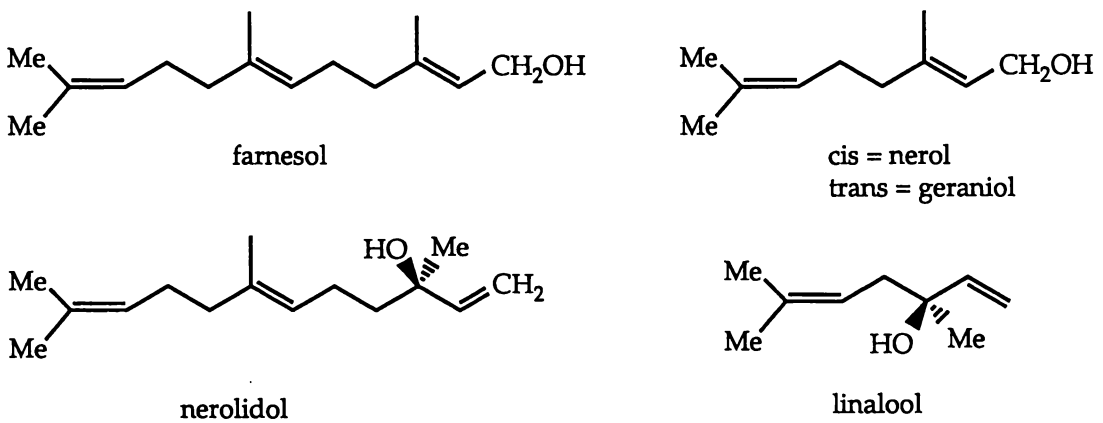

Scheme 1.11: Reaction of aliphatic terpenic alcohols with phenylphosphonic anhydride.

The reaction of the alpha-, beta-unsaturated monoterpenic ketones carvone [5-isopropenyl-2-methyl-2-cyclohexenone] and pinocarvone with the sodium salt of diethylphosphite in diethylphosphite media results in the

regioselective addition to the conjugated carbon-carbon double bond and formation of the corresponding oxophosphonates[16] (Scheme 1.12).

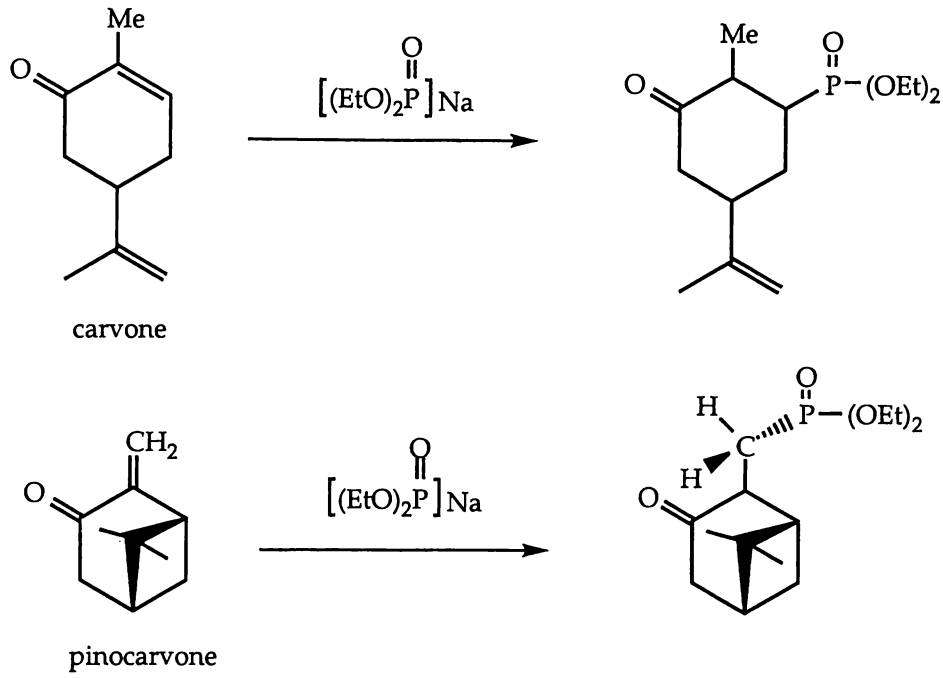

Scheme 1.12: Reaction of alpha-, beta-unsaturated monoterpenic ketones with the sodium salt of diethylphosphite.

Unlike the alkyl- and aryl-based phosphonates which are often employed in industrial solvent extraction [hydrometallurgical] processes [consult chapter 5], the terpene-based phosphonates have, to date, little or no industrial applications.

1.5 Terpene-phosphine chemistry

The extensive volume of chemistry that exists within the general class of phosphines is summarised in chapter 4. Included in this general class is the synthesis of chiral phosphines and the applications of metal phosphine derivatives in asymmetric catalysis. Monoterpenes are ideal chiral auxiliaries since they occur naturally in high enantiomeric purities and are inexpensive. However, as with most other areas involving organophosphorus chemistry of terpenes, the study of phosphines derived from terpenes is limited. Their chemistry is summarised below.

Michael-type addition of optically active terpene alcohols (-)-borneol, (-)-menthol and (-)-myrtanol to vinylphosphine derivatives afford β-alkoxy ethyldiphenylphosphine oxides which in turn react with $SiHCl_3$ affording diphenylvinylphosphines with chiral terpene groups[17] (see Scheme 1.13).

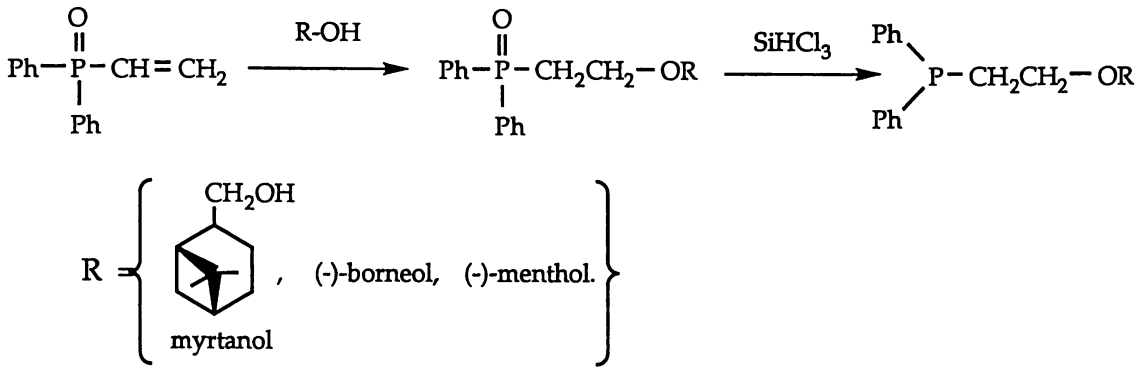

Scheme 1.13: Formation of diphenylvinylphosphines by the reaction of optically active terpene alcohols with vinyl derivatives and $SiHCl_3$.

Similarly, the Michael-type addition of (-)-N-ethyl-N-[3-pinanmethyl]amine to vinyl derivatives affords β-(amino)ethylphosphines[18] (see Scheme 1.14).

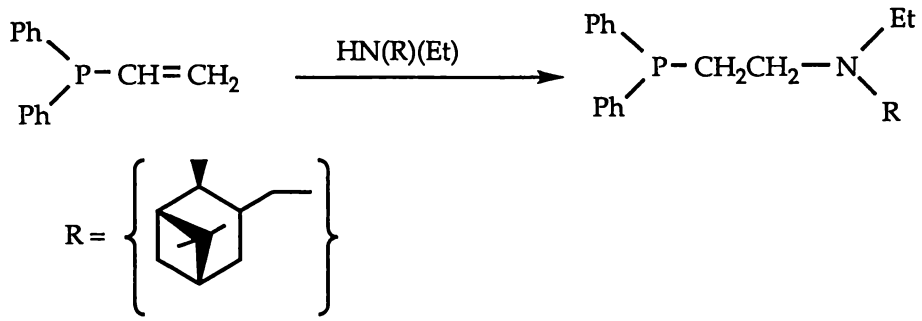

Scheme 1.14: Formation of β-(amino)ethylphosphines.

The preparation of β-hydroxyphosphines has been achieved in high yield by the reaction of $HPPh_2$ or $LiPPh_2$ with the oxides of limonene and pinene. The general reaction equation, Scheme 1.15, is highly selective and involves an epoxide-opening reaction.

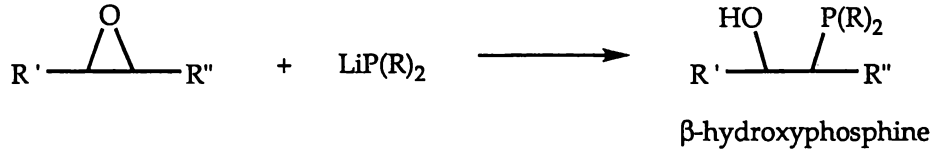

Scheme 1.15: Preparation of β-hydroxyphosphines by an epoxide-opening reaction.

The reactions with the oxides are very regioselective, giving only one of the possible isomers. Cis- and trans-limonene oxides react with $LiPPh_2$ at -78°C giving trans-phosphino derivatives from commercial mixtures of limonene oxide[19] (see Scheme 1.16). It is worth noting that the equivalent

reaction with the cis isomer at -10°C does not afford a single isomer. Instead an oil containing two cis-isomers is obtained.

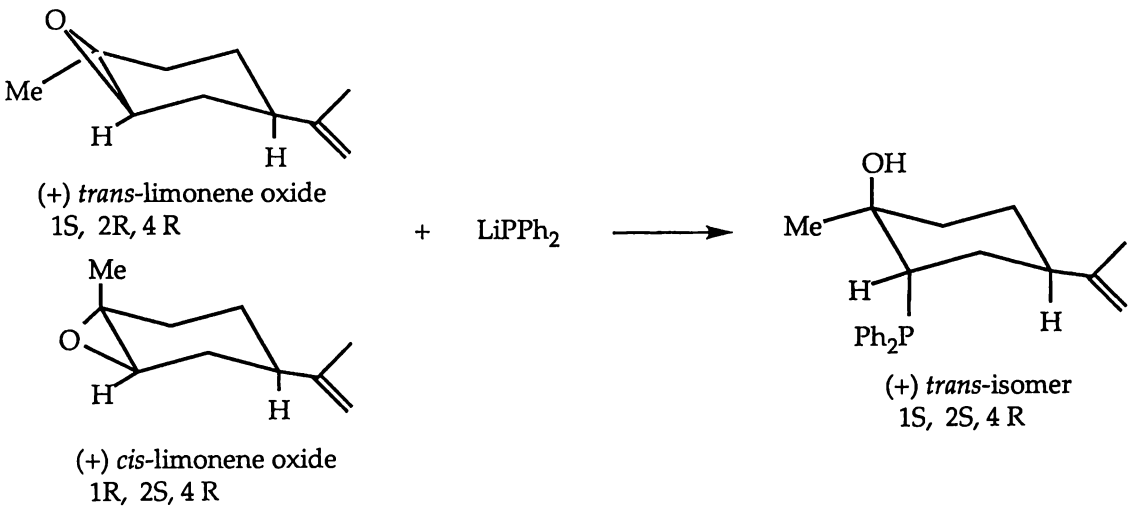

Scheme 1.16: Reaction of commercial mixtures of limonene oxide with $LiPPh_2$.

The sterically-crowded pinene oxides show different reactivity toward the diphenylphosphide ion. Although (-)-α-pinene does not react with $LiPPh_2$, (+)-β-pinene oxide gave selectivity with the phosphine that corresponds to attack at the less hindered carbon being formed (Scheme 1.17).

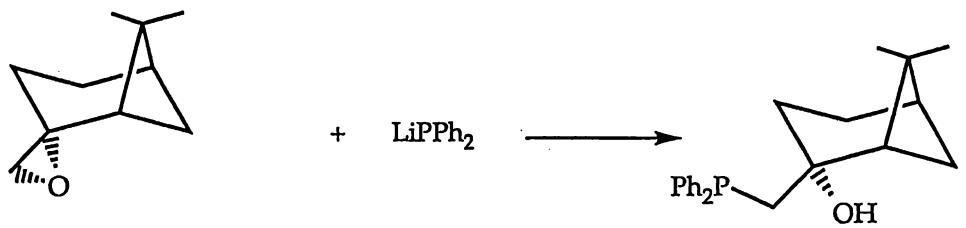

Scheme 1.17: Reaction of β-pinene oxide with $LiPPh_2$.

The reaction of the chiral terpene-derived organozinc iodides RZnI [R=camphene, 2-methylenebornane] and R_2Zn [R=formylpinane] with Ph_2PCl, Scheme 1.18, afford the diphenylalkylphosphine-borane complexes in high yield.

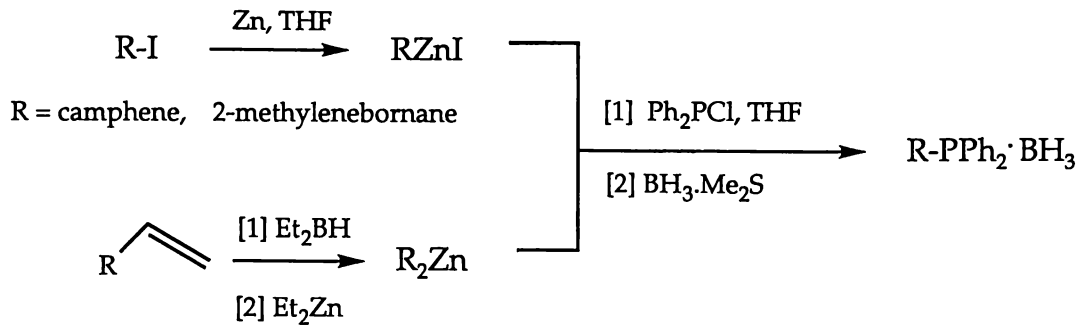

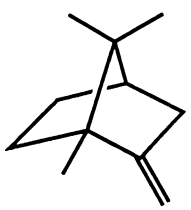

2-methylenebornane

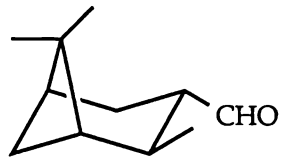

formylpinane

Scheme 1.18: Preparation of diphenylalkylphosphine-borane complexes using zinc organometallics.

The β-pinene- and (+)-longifolene-derived zinc reagents [R_2Zn], when treated with 1,2-bis(dichlorophosphino)ethane and 1,2-bis(dichlorophosphino)butane, afford the diphosphines[20] outlined in Scheme 1.19.

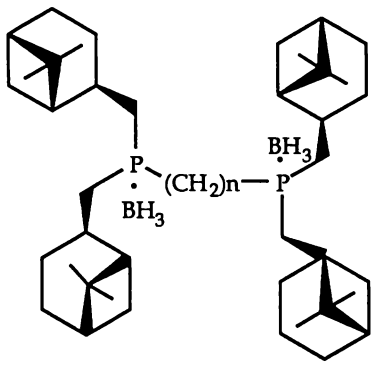

n=2 or 4

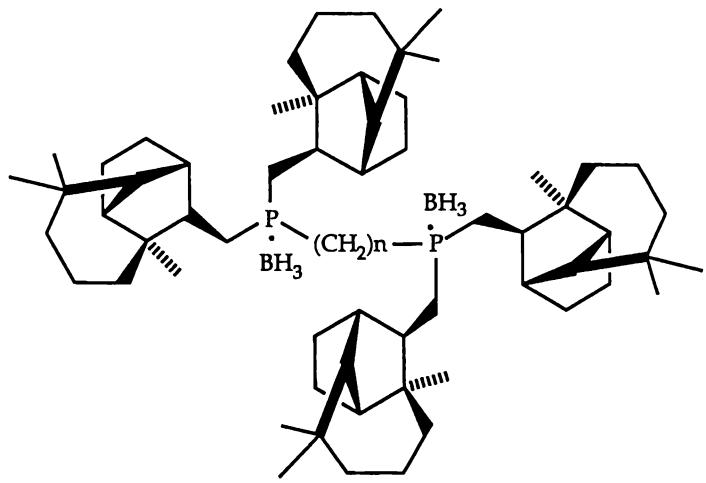

Scheme 1.19: Chiral diphosphines prepared from β-pinene- and (+)-longifolene-derived zinc reagents.

1.6 Pinene- and camphene-phosphorus chemistry

1.6.1 Pinene

The reaction of α-pinene with PCl_2Me-$AlCl_3$ complex yields a bridged bicyclic phosphetane[21]. The major product arises from the primary adduct **A** (see Scheme 1.20) by double bond formation with the opening of the cyclobutane ring, rather than its enlargement by a 1,2-carbon migration, which is commonly observed.

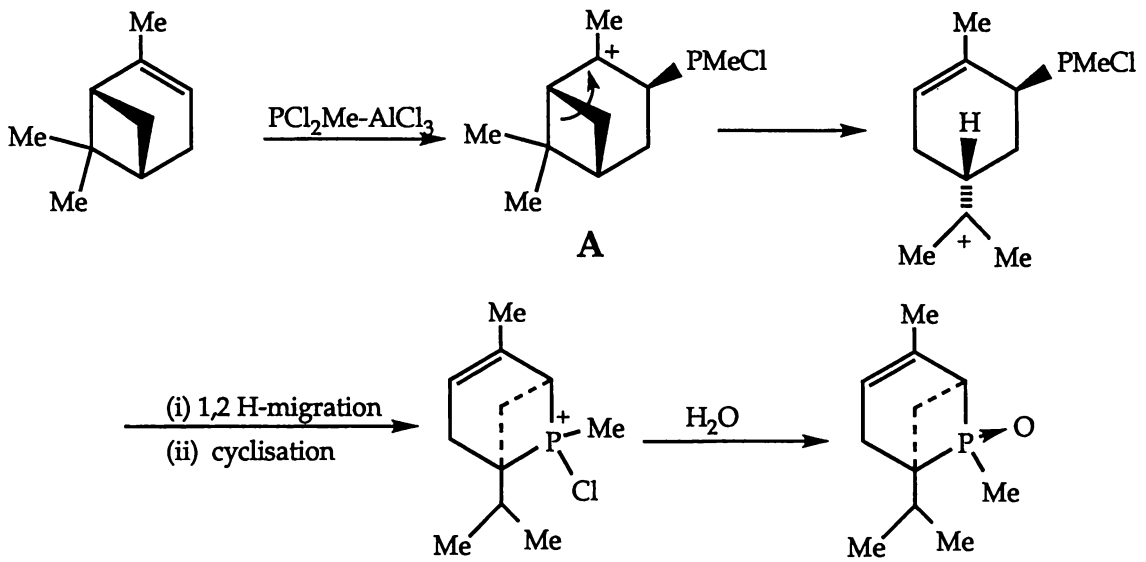

Scheme 1.20: Reaction of α-pinene with the PCl_2Me-$AlCl_3$ complex.

1.6.2 Camphene

Marsh and Gardner's original work in the 1890's, involved the moderate heating of an excess of phosphorus pentachloride with camphene[22]. The subsequent addition of water results in the formation of two phosphonic acids, α– and β-camphenylphosphonic acid (Figure 1.4), which are separable as only one of the two acids readily dissolves in ether. Various metal salts of these acids were also synthesised and characterised by elemental analysis[22]. An improved procedure for the synthesis of α– and β-camphenylphosphonic acid, involving the moderate heating of a benzene solution of phosphorus pentachloride with camphene, was subsequently developed[23].

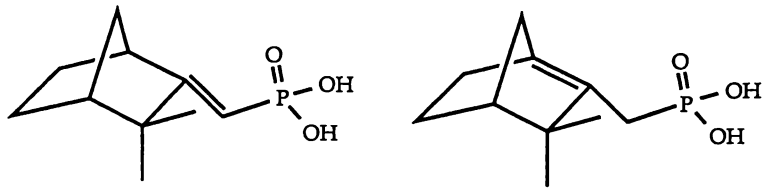

α-camphenylphosphonic acid β-camphenylphosphonic acid

Figure 1.4: The phosphonic acids formed by the reaction of camphene with phosphorus pentachloride [PCl_5].

Kenney *et al* in 1973 reported the reaction of camphene with diethyl hydrogen phosphite under free radical conditions. As illustrated in Scheme 1.21, a mixture of two isomers, *exo-* and *endo*-isocamphanylphosphonate, are formed in a 1:3 ratio[24]. The *endo-* isomer is isolated in about 90% purity by preparative gas chromatography.

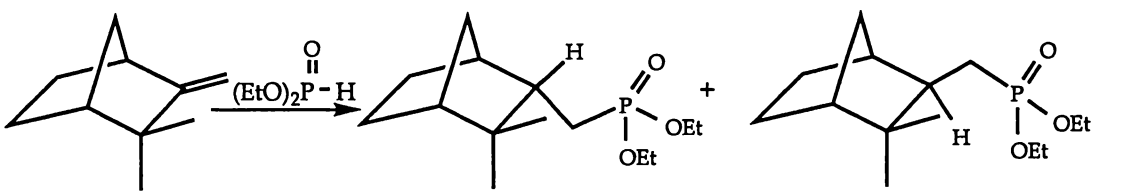

camphene *endo*-isocamphanylphosphonate *exo*-isocamphanylphosphonate

Scheme 1.21: The treatment of camphene with diethyl hydrogen phosphite [$(EtO)_2P(O)H$] under free radical conditions.

Vilkas *et al* in 1979 reported the reaction of the PCl_2Me-$AlCl_3$ complex with camphene[25]. The formation of a compound with a phosphetane ring was observed and was thought to arise from the Nametkin methyl 1,2-shift (see Scheme 1.22).

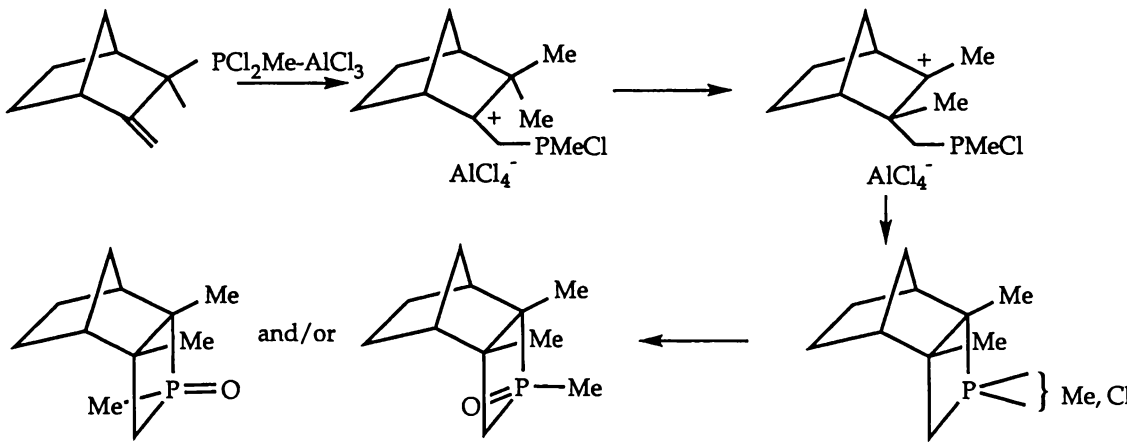

Scheme 1.22: Reaction of camphene with the PCl_2Me-$AlCl_3$ complex.

The next reported publication some 20 years later was by Henderson and co-workers at Albright and Wilson Ltd in the U.K.. Here the radical-catalysed addition of hypophosphorous acid to camphene [2,2-dimethyl-bicyclo-3-methyl-[2.2.1]-heptane] gave 2,2-dimethylbicyclo[2.2.1]hept-3-ylmethylphosphinic acid[26] [hereafter 8-camphanylphosphinic acid] (**1**) which was in turn oxidised with sulfur dioxide to 8-camphanylphosphonic acid (**14**) (Scheme 1.23).

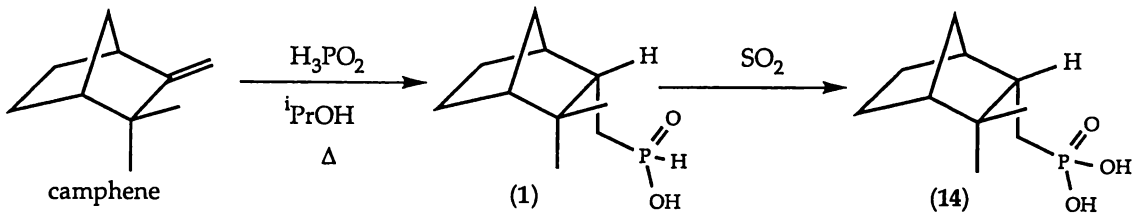

Scheme 1.23: The formation and subsequent oxidation of **1** to **14**.

The Ca, Zn and Al salts of **14** were also synthesised by the addition of the metal salt to **14** which had been previously neutralised with NaOH. The Ca, Zn and Al salts of **14** are found to be effective anticorrosive pigments in paint compositions[27]. Furthermore, the addition of this pigment not only reduces the amount of other anticorrosive pigment required but also enhances the properties of the paint film on the substrate, for example the anticorrosive and adhesive properties. However these terpene-phosphorus acids and their metal salts were not fully characterised.

It is worth noting that the radical-catalysed addition of hypophosphorous acid to camphene had previously been reported in 1960, however it was stated that no reaction had occurred[28]. Within this same publication it was also stated that there was no reaction between camphene and diethyl hydrogen phosphite.

Camphene has numerous attributes. A by-product of the New Zealand forestry industry, camphene is an inexpensive, readily accessible, renewable resource. This means that novel applications derived from research may also be applied in industry. Camphene, being a rigid bicyclic structure, is not expected to undergo skeletal rearrangement (as compared to other terpenic systems, such as those derived from pinene, which are prone to skeletal rearrangement reactions), suggesting that the chemistry will be simpler. Both enantiomeric forms, *1R, 4S*-(+)-camphene and *1S, 4R*-(-)-camphene are also available, allowing exploration of chiral derivatives and their possible applications.

The potential to further develop the chemistry of camphene-phosphorus compounds became apparent. Thus the objective of this thesis

is to further develop the chemistry initiated by Henderson *et al.* That is, to synthesise new camphene-derived phosphorus compounds derived from 8-camphanylphosphinic acid (**1**) and 8-camphanylphosphonic acid (**14**).

References

1 J.L Simonsen in *The Terpenes*, Cambridge University Press, Vol I (1953) to Vol V (1957).

2 M.N. Gould, *J. Cell. Biochem.*, (1995), **22**, 139-144

3 H. Blaser, *Chem. Reviews*, (1992), **92**, 935-952.

4 B.H. Brown, P.V. Ramachandran, *Pure Appl. Chem.*, (1991), **63**, 307.

5 G. Hagele, W. Kuckelhaus, G. Tossing, J. Seega, R. K. Harris, C.J Creswell, P.T. Jageland, *J. Chem. Soc.Dalton Trans..*, (1985), 2803.

6 M. Gruber, R. Schmutzler, M. Ackermann, J. Seega, G. Hagele, *Phosphorus and Sulfur*, (1989), **44**, 109-122.

7 H. Brunner, M. Rotzer, *J. Organometallic Chem.*, (1992), **425**, 119-124.

8 I.V. Komarov, M.V. Gorichko, M.Y. Kornilov, *Tetrahedron: Asymmetry*, (1997), **8**, 435-445.

9 P. Sampson, G.B. Hammond, D.F. Wiemer, *J. Org. Chem.*, (1986), **51**, 4342-4347.

10 W.B. Jennings, C.J. Lovely, *Tetrahedron*, (1991), **47**, 5561-5568.

11 R. Clarke, D. Cole-Hamilton *J. Chem. Soc. Dalton Trans.*, (1993), 1913; R.J. Cross, L.J. Farrugia, P.D. Newman, R.D. Peacock, D. Stirling, *J. Chem. Soc., Dalton Trans.*, (1996), 4149-4150].

12 B.L. Shaw, M. Thornton-Pett, J.D. Vessey, *J. Chem. Soc. Dalton Trans.*, (1995), 1697-1707.

13 G. Cao, V.M. Lynch, L.N. Yacullo, *Chem. Mater.*, (1993), **5**, 1000; G. Cao, T. Mallouk, *Inorg. Chem.*, (1991), **30**, 1434, G. Cao, M.E. Garcia, M. Alcalá, L.F. Burgess, T.E. Mallouk, *J. Am. Chem. Soc.*, (1992), 114, 7574.

14 E. Cherbuliez, B. Baehler, H. Probst, J. Rabinowitz, *Helvetica Chimica Acta*, (1962), **300**, 2656.

15 E. Cherbuliez, G. Weber, A. Yazgi, J. Rabinowitz, *Helvetica Chimica Acta*, (1962), **299**, 2652.

16 V.D. Kolesnik, M.M. Shakirov, A.V. Tkachev, *Mendeleev Comm.*, (1997), **4**, 141-143.

17 Von G. Markl, B. Merkl, *Tetrahedron Letters*, (1981), **45**, 4463-4466.

18 Von G. Markl, B. Merkl, *Tetrahedron Letters*, (1981), **45**, 4459-4462.

19 G. Muller, D. Sainz, *J. Organometallic Chem.*, (1995), **495**, 103-111.

20 F. Langer, K. Puntener, R. Sturmer, P. Knochel, *Tetrahedron: Asymmetry*, (1997), **8**, 715-738.

21 E.Vilkas, M. Vilkas, D. Joniaux, *J.Chem. Soc., Chem. Comm.*, (1978), 125-127.

22 J. E. Marsh, J. A. Gardner, *J . Am. Chem. Soc.*, (1894), 35.

23 V. Chavane, *Ann. Chim.*, (1949), **4**, 365.

24 R. L. Kenney, G. S. Fisher, *J. Org. Chem.* , (1974), **39**, 682.

25 E.Vilkas, M. Vilkas, J. Sainton, B. Meunier, C. Pascard, *J. Chem. Soc., Perkin I*, (1979), 2136-2140.

26 U.K. Patent, Albright and Wilson Ltd, GB 2268178 A, (1994).

27 U.K. Patent, Albright and Wilson Ltd, GB 2279953 A, (1995).

28 G. Quesnel, M. De Botton, A. Chambolle, R. Dulou, *Compt. Rend.*, (1960), **251**, 1074.

Chapter Two

Synthesis and characterisation of camphene-derived phosphinic acids

2.1 The radical-catalysed addition of phosphinic acids to alkenes

2.1.1 Introduction

The radical-catalysed addition of hypophosphorous acid [H_3PO_2] to simple alkenes to form phosphinic acids is well documented in the literature[1]. The general equation for this reaction is illustrated in Scheme 2.1, equation (i). Where the alkene used is not bulky the reaction can proceed further with the addition of a second alkene molecule [equation (ii)]. The product in this case is a dialkylphosphinic acid.

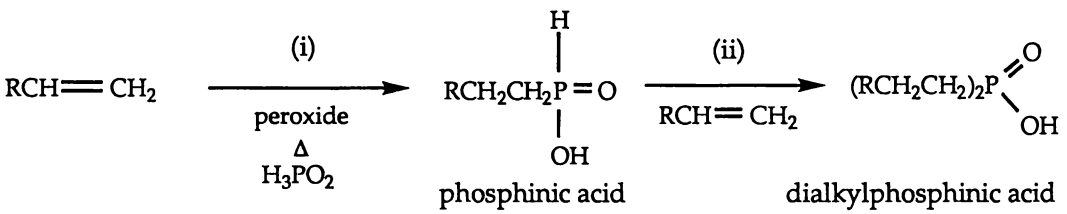

Scheme 2.1: (i) The addition of hypophosphorous acid [H_3PO_2] to alkenes (ii) The addition of a second alkene molecule to phosphinic acid.

Research in this area has involved the use of numerous catalysts such as peroxides, peracids, azo compounds and ferrous sulphate[2]. Solvents used also vary significantly, from water, hydrocarbons, ethers, ketones to alcohols[2].

The proposed mechanism for the addition of hypophosphorous acid to alkenes is illustrated in Scheme 2.2 and involves the generation of a hypophosphorous acid-derived radical, **X**, which attacks an unsaturated bond. The new radical, **Y**, then reacts with another hypophosphorous acid molecule to generate another radical X^2.

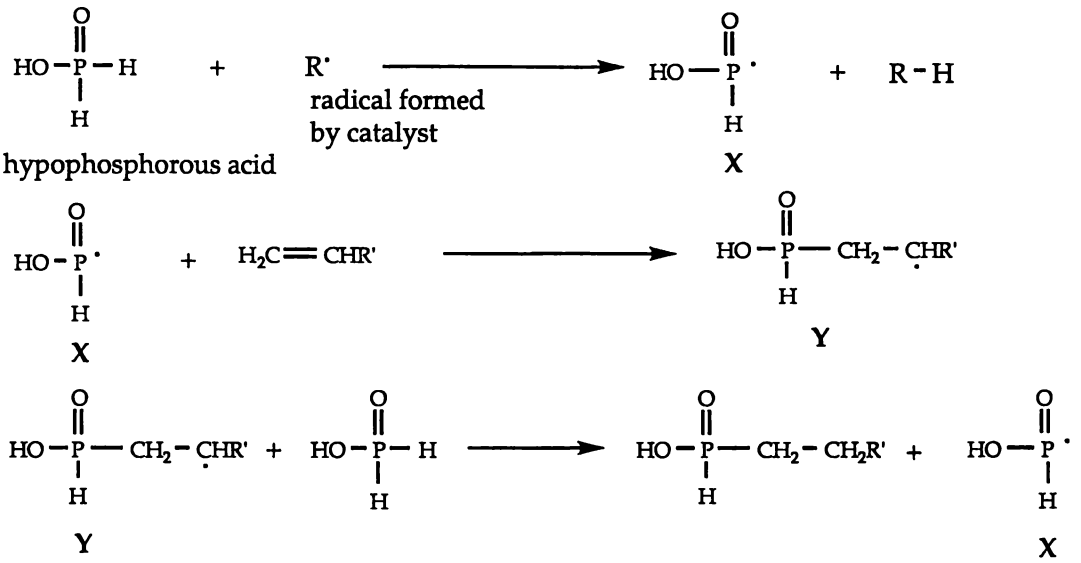

Scheme 2.2: The radical-catalysed addition of H_3PO_2 to simple alkenes.

As illustrated in Scheme 2.3, there are two possible modes of radical attack, the first of which produces radical intermediate Y, by attack at position 1 and the second of which produces radical intermediate Z, by attack at position 2. The protonation of Y and Z by a second hypophosphorous acid molecule produces the major and minor addition products Y' and Z' respectively. The minor addition product Z' is expected to exist only in trace amounts as the radical attack at position 2 is more sterically restricted than the attack at position 1.

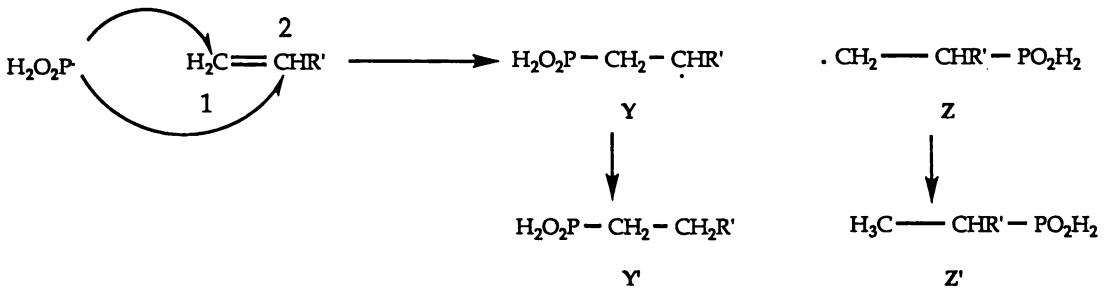

Scheme 2.3: The modes of radical addition to an unsaturated bond.

Although the radical-catalysed addition of hypophosphorous acid to alkenes is well documented, the equivalent chemistry involving terpenes is limited to two reports. The first report stated that no reaction occurs between hypophosphorus acid and camphene[3]. However an investigation by Henderson[4] *et al* [see chapter 1, section 1.6] revealed that this was not the case. The radical-catalysed addition of hypophosphorus acid to camphene affords the camphene-derived phosphinic acid **1** (Scheme 2.4). However the phosphinic acid **1** was not fully characterised.

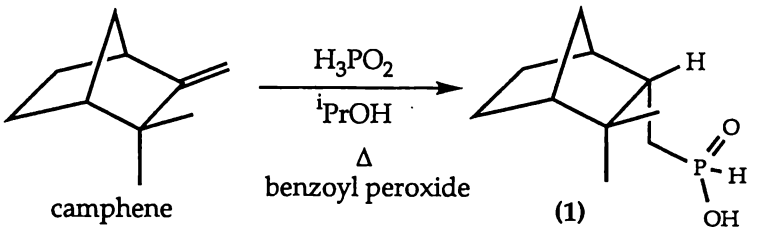

camphene (1)

Scheme 2.4: The radical-catalysed addition of hypophosphorous acid to camphene.

Thus the objectives of chapter two were as follows:

(i) to identify suitable reaction and work-up conditions so as to optimise the yields of 8-camphanylphosphinic acid.

(ii) to fully characterise 8-camphanylphosphinic acid.

(iii) to synthesise and characterise new camphene-derived phosphinic acids.

(iv) to synthesise and characterise new camphene-phosphorus derivatives.

2.1.2 Results and discussion

The general synthetic route to camphene-derived phosphinic acids involves the reaction of camphene and the phosphinic acid in isopropanol heated at reflux for 6-14 h. During this time a catalyst, benzoyl peroxide, which has a half-life of approximately 10 h at 73°C, is added sparingly until reaction is seen to be complete by ^{31}P NMR. The crude product is extracted

into sodium hydroxide and washed with dichloromethane. The aqueous extract is acidified, extracted into an organic phase and evaporated to dryness to give a white crystalline solid. Hence, using the catalyst benzoyl peroxide, the radical-catalysed addition of hypophosphorous acid [H_3PO_2] to the terpene camphene in isopropanol heated at reflux, Scheme 2.5, gives 8-camphanylphosphinic acid (**1**). Formed quantitatively, **1** is a white crystalline solid most soluble in organic solvents such as dichloromethane and chloroform. Analytical data collected for **1** are consistent with its formulated structure. Detailed characterisation of **1** by X-ray crystallography, ESMS and NMR spectroscopy are presented in sections 2.1.3, 2.1.4 and 2.1.5 respectively.

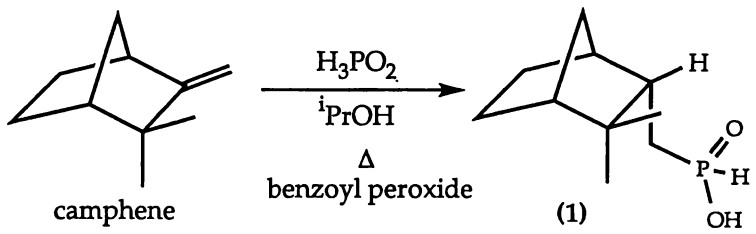

Scheme 2.5: The synthesis of **1**[ψ] by the radical-catalysed addition of hypophosphorous acid [H_3PO_2] to camphene.

When low hypophosphorous acid to camphene ratios are employed, e.g. a 1 to 1 mole ratio, the crude product from this preparation is always found to contain a small amount of a compound tentatively identified as di(8-camphanyl)phosphinic acid (**2**), which is difficult to remove by recrystallisation. Thus the proton-coupled ^{31}P NMR spectrum of the crude isolated reaction product shows a single, slightly broadened peak at δ 58.0, which is consistent with the range in which phosphinic acids appear (δ 50-60), in addition to the expected doublet [$^1J_{P\text{-}H}$ 556.7] for **1** at δ 38.8.

When the reaction between camphene and hypophosphorous acid is conducted using an excess [>3 mole equivalent] of the latter reagent no di(8-

---

[ψ] Due to rapid inter- and intramolecular proton exchange, the hydroxy group and oxygen atom of the phosphinic acid **1** are rendered equivalent in solution. Although the phosphorus centre is therefore not asymmetric it is illustrated structurally as being asymmetric for simplicity.

camphanyl)phosphinic acid (**2**) is observed, simplifying purification of the product. Reaction time and purity is optimised by using a 3.5 to 1 mole ratio of hypophosphorous acid to camphene. Attempts to prepare pure **2** using higher camphene to hypophosphorous acid ratios, higher reaction temperatures [aqueous dioxane heated at reflux], prolonged reaction times, or increased quantities of benzoyl peroxide initator does not lead to an increased amount of **2** being formed[5].

Experimental yields suggest that of the two possible modes of radical attack available (see Scheme 2.6), attack of the least sterically hindered site of camphene, which affords **1**, is preferred. The phosphinic acid, **1a**, which arises from the radical attack of the more sterically hindered site of camphene [refer to section 2.1.1 for details], is not obtained in any appreciable quantities.

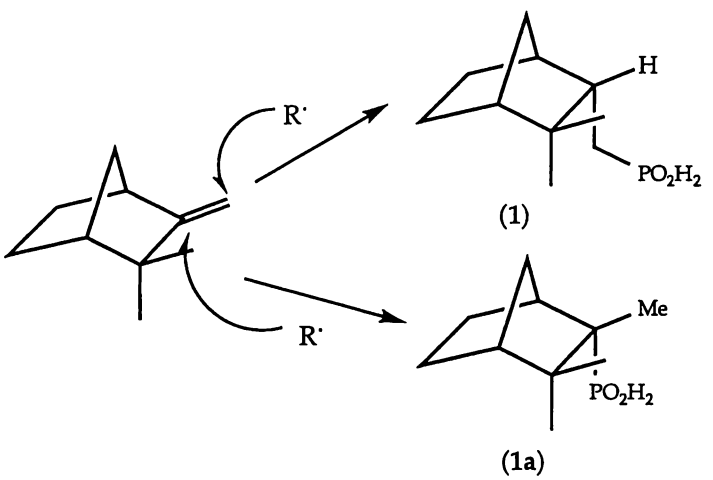

Scheme 2.6: Possible modes of radical attack of camphene.

The attempted preparation of chiral **1** starting from (R)-(+)-camphene yielded only racemic material. This is expected to be the result of acid-catalysed racemisation of the camphene, which has been extensively studied by Vaughan *et al*, [6-9] prior to reaction with the H_3PO_2. The estimated extent of participation of four distinctive pathways has been identified[8]. Two of these are Nametkin-type rearrangements[7] in which an acid catalyst induces migration of the *endo*- or *exo*-methyl groups. The remaining methyl group then loses a proton to produce the enantiomer of the original camphene [Scheme 2.7]. The two other pathways are the Wagner-Meerwein 2,6-

hydride shift[6], Scheme 2.8, and the mechanism involving tricyclene formation[7].

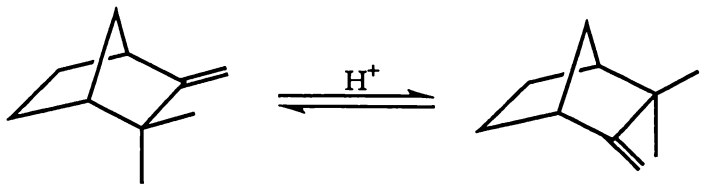

Scheme 2.7: The Nametkin-type rearrangement of camphene.

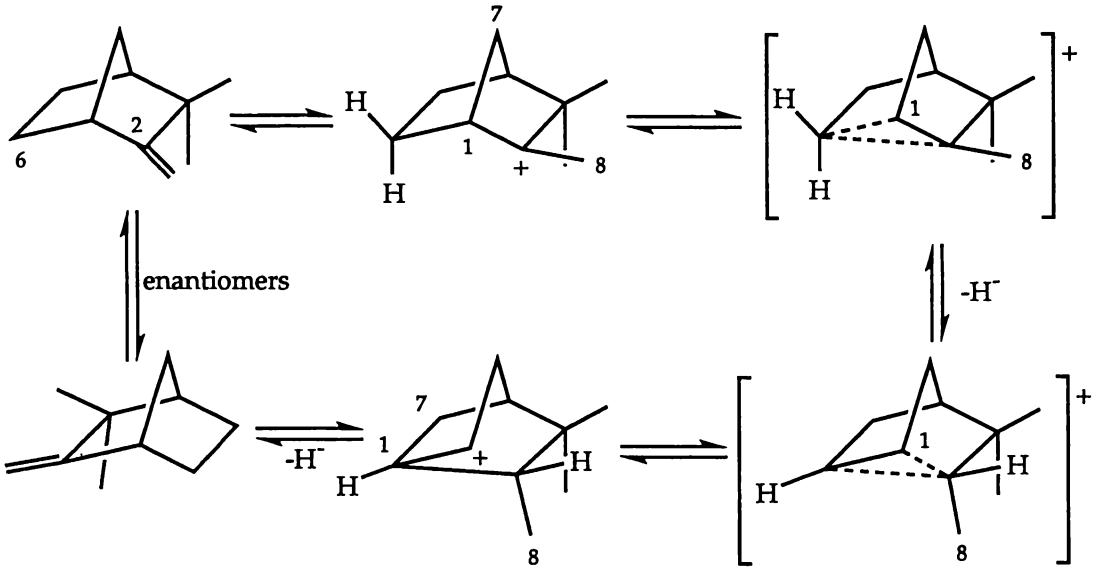

Scheme 2.8: The Wagner-Meerwein 2, 6-hydride shift of camphene.

The most significant pathways to the racemisation of camphene are the *exo*-methyl migration and 2,6-hydride shift. The racemisation of camphene *via* tricyclene formation and *endo*-methyl migration are almost negligible.

An investigation of the radical-catalysed addition of phenylphosphinic acid ($PhPO_2H_2$) to camphene was also undertaken. Hence the reaction of phenylphosphinic acid with camphene, Scheme 2.9, affords 8-camphanyl(phenyl)phosphinic acid (**3**) [^{31}P-{H} NMR δ 47.1, s] in high yield. With the exception of the use of an excess of camphene, which is employed to optimise the yield of the product, the reaction and workup are as described for **1**. Like **1**, phosphinic acid **3** is a white crystalline solid, most soluble in organic solvents such as dichloromethane and chloroform.

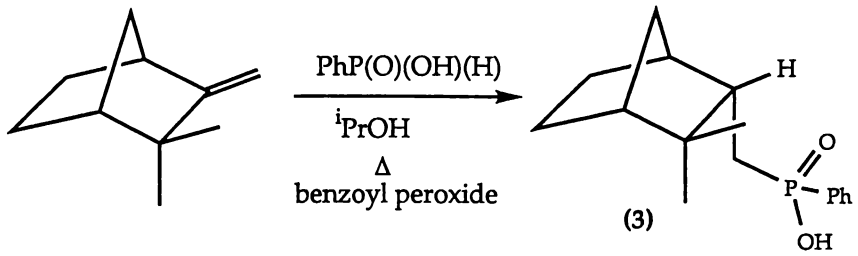

Scheme 2.9: The radical-catalysed addition of phenylphosphinic acid [PhP(O)(OH)(H)] to camphene.

Elemental microanalytical data collected for **3** are consistent with its formulated structure. Detailed characterisation of **3** by ESMS and NMR spectroscopy is presented in sections 2.1.4 and 2.1.5 respectively.

2.1.3 X-ray crystal structure of 8-camphanylphosphinic acid (1)

A single crystal X-ray diffraction study has been carried out on 8-camphanylphosphinic acid (**1**) (Dr M. Sabat, University of Virginia, Charlottesville, Virginia, U.S.A.). Full details of the X-ray structure determination for **1** are presented in Appendix III, along with the tables of final positional parameters and bond angles. The molecular structure is shown in Figure 2.1, together with the atom numbering scheme. Selected bond lengths and angles are also included in Table 2.1. The structure confirms the formulation of the compound as 8-camphanylphosphinic acid, containing an *endo* $-CH_2PO_2H_2$ group. The structure reveals the presence of strongly hydrogen-bonded dimers in the crystal, as is commonly observed for organophosphorus and carboxylic acids of this general type, both in solution and in the solid state[10, 11].

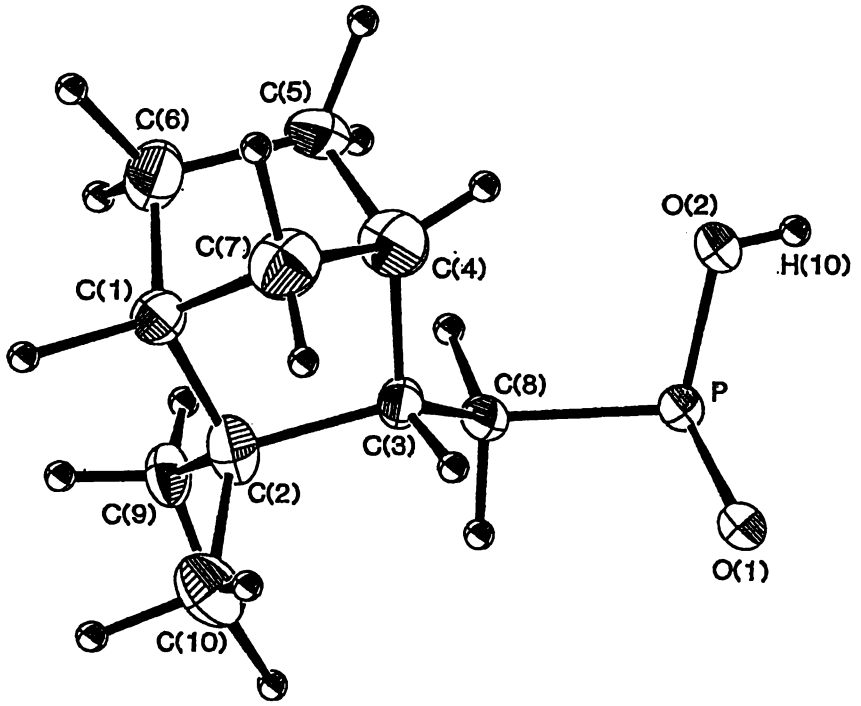

Figure 2.1: The molecular structure of **1**, together with the atom numbering scheme.

P-O(1)	1.486(4)	C(3)-C(4)	1.545(9)
P-O(2)	1.540(5)	C(3)-C(2)	1.565(8)
P-C(8)	1.785(6)	C(3)-C(8)	1.537(8)
C(1)-C(2)	1.541(8)	C(4)-C(5)	1.53(1)
C(1)-C(7)	1.59(1)	C(4)-C(7)	1.49(1)
C(2)-C(9)	1.536(8)	C(5)-C(6)	1.53(1)
C(2)-C(10)	1.497(9)	C(6)-C(1)	1.546(9)
O(1)-P-O(2)	115.0(2)	O(2)-P-C(8)	106.2(2)
O(1)-P-C(8)	113.2(2)		

Table 2.1: Bond lengths (Å) and selected bond angles (°) of 8-camphanyl-phosphinic acid (**1**). Estimated standard deviations are in parentheses.

There is a marked asymmetry in the bond distances to the bridgehead carbon C(7), with C(1)-C(7) [1.59(1) Å] being significantly longer than C(4)-C(7)

[1.49(1) Å]. This is not observed for the related compound 2,2-dimethyl-bicyclo-3-methyl[2.2.1]heptane-1-carboxylic acid [(-)-camphene-8-carboxylic acid][12], where the C(1)-C(7) and C(4)-C(7) bond distances are 1.517(11) Å and 1.518(9) Å respectively. While the *exo*-methyl group of **1** adopts an ideal position, with a C(8)-C(3)-C(2)-C(10) torsion angle of 109.3(7)°, there is a twist of -11.3(7)° in the C(8)-C(3)-C(2)-C(9) torsion angle of the *endo*-methyl group. This is due to the presence of an adjacent $-CH_2PO_2H_2$ group in an *endo* position. A similar distortion is also seen in (-)-camphene-8-carboxylic acid where the dihedral angles involving the two methyl groups at C(2) are unequal, and differ from the idealised 60° value; the angle C(8)-C(3)-C(2)-C(10) is 65.1° while C(8)-C(3)-C(2)-C(9) is 55.7°.

Molecular modelling studies of **1** were also carried out on an Iris Indigo computer [Silicon Graphics] using Macromodel version 4.5 [Chemistry Department, Columbia University, New York, NY]. The global energy minimisation of the structure of **1** was assumed to be that depicted by X-ray crystallography. The local energy minima of the structure of **1** was then calculated using supplied MM2* force fields, the results of which are given in Table 2.2. This minimised energy structure shows that although the C(8)-C(3)-C(2)-C(9) and C(8)-C(3)-C(2)-C(10) dihedral angles are consistent with crystallographic studies, the asymmetry in the bridgehead is not. This suggests that the bridgehead distortion observed in crystallographic studies is a result of intermolecular contacts and not intramolecular contacts. All other bond parameters calculated by molecular studies were consistent with those found by crystallographic studies.

	Bond length (Å)		Dihedral angle (°)	
	C(1)-C(7)	C(4)-C(7)	C(8)-C(3)-C(2)-C(9)	C(8)-C(3)-C(2)-C(10)
X-ray crystallography	1.59(1)	1.49(1)	-11.3(7)°	109.3(7)°
Molecular modelling	1.53	1.55	-11.7°	109.1°

Table 2.2: A comparison of bond lengths and dihedral angles of **1** determined by X-ray crystallography and calculated by molecular modelling.

There are no other extraordinary features regarding the structure of **1**. With the exception of the C(2)-C(3) and C(3)-C(4) bonds, all other C-C distances for **1**, which lie between 1.54(18) and 1.497(9) Å, are comparable with that of (-)-camphene-8-carboxylic acid [1.566(9)-1.532(11) Å]. A comparison of the C(2)-C(3) and C(3)-C(4) bond lengths of **1** and (-)-camphene-8-carboxylic acid shows that the difference between these bonds is crystallographically significant. However this anomaly is consistent with the difference in bond lengths that exists between the sp^3-sp^3 hybrid C(2)-C(3) and C(3)-C(4) bonds of **1**, and the sp^3-sp^2 hybrid C(2)-C(3) and C(3)-C(4) bonds of (-)-camphene-8-carboxylic acid[13]. The P-C(8), P=O and P-OH bond distances are 1.785(6), 1.486(4) and 1.540(5) Å respectively and are comparable with R-$(CH_2)_2$P(Me)(O)OH [R=C(NH_3)(COOH)Cl] which has P-C, P=O and P-OH bond distances of 1.786(3), 1.494(2) and 1.560(2) Å respectively[14]. Examination of the O-P-O and O-P-C bond angles of **1** [Table 2.1] shows that the coordination about the P is somewhat distorted from tetrahedral. A similar distortion is seen in other phosphinic acids, for example $(Me_3C)_2$P(O)OH where the O-P-O, C-P-C and average O-P-C bond angles are equal to 114.3, 115.4 and 106.8° respectively[10, 12]. Like $(Me_3C)_2$P(O)OH, the observed distortion in **1** is expected to result from the greater repulsive effect of the bulky group.

The adopted position of the $CH_2PO_2H_2$ group is expected to be the result of steric effects, that is, the bridgehead [C(7)] and the $CH_2PO_2H_2$ group are located on opposite sides of the ring to minimise steric congestion.

2.1.4 Electrospray mass spectrometric analysis of camphene-derived phosphinic acids

Characterisation of the new organophosphorus acids **1** and **3** is also aided by electrospray mass spectrometry [ESMS]. This technique is well suited to the analysis of these involatile acids as derivatisation is not required to obtain mass spectra [*c.f.* GCMS where the acid is first treated with diazomethane before analysis; refer to section 2.2.3 for more detail]. ESMS is a soft chemical ionisation technique, the result of the minimal energy requirements to transfer pre-existing ions from solution to the gas phase. This softer mode of ion formation[15] results in the minimal fragmentation of species [*c.f.* other "harder techniques" such as fast atom bombardment (FAB)] which in turn results in a more intense parent ion. As the polarity of the potential [*i.e.* cone voltage] is reversible, both positively and negatively charged species are able to be routinely analysed. This includes species such as the positively charged phosphonium ion[16], borane salts[17], ionic inorganic and organometallic compounds[18] and phosphorus acids[19]. As the cone voltage is also variable, the extent of fragmentation can also be altered. This enables both an enhanced parent ion detection method as well as the ability to structurally analyse fragmented species.

The relative ease with which acids deprotonate to give a negatively charged ion means that the negative ion mode is ideally suited to the characterisation of the new organophosphorus acids. As shown in Figure 2.2, both **1** and **3** give very simple spectra in negative ion mode when pyridine is added to convert the acid into its phosphinate anion. Varying the cone voltage [15 to 100V] has little effect on the complexity of the spectra and illustrates the stability of the phosphinate anion.

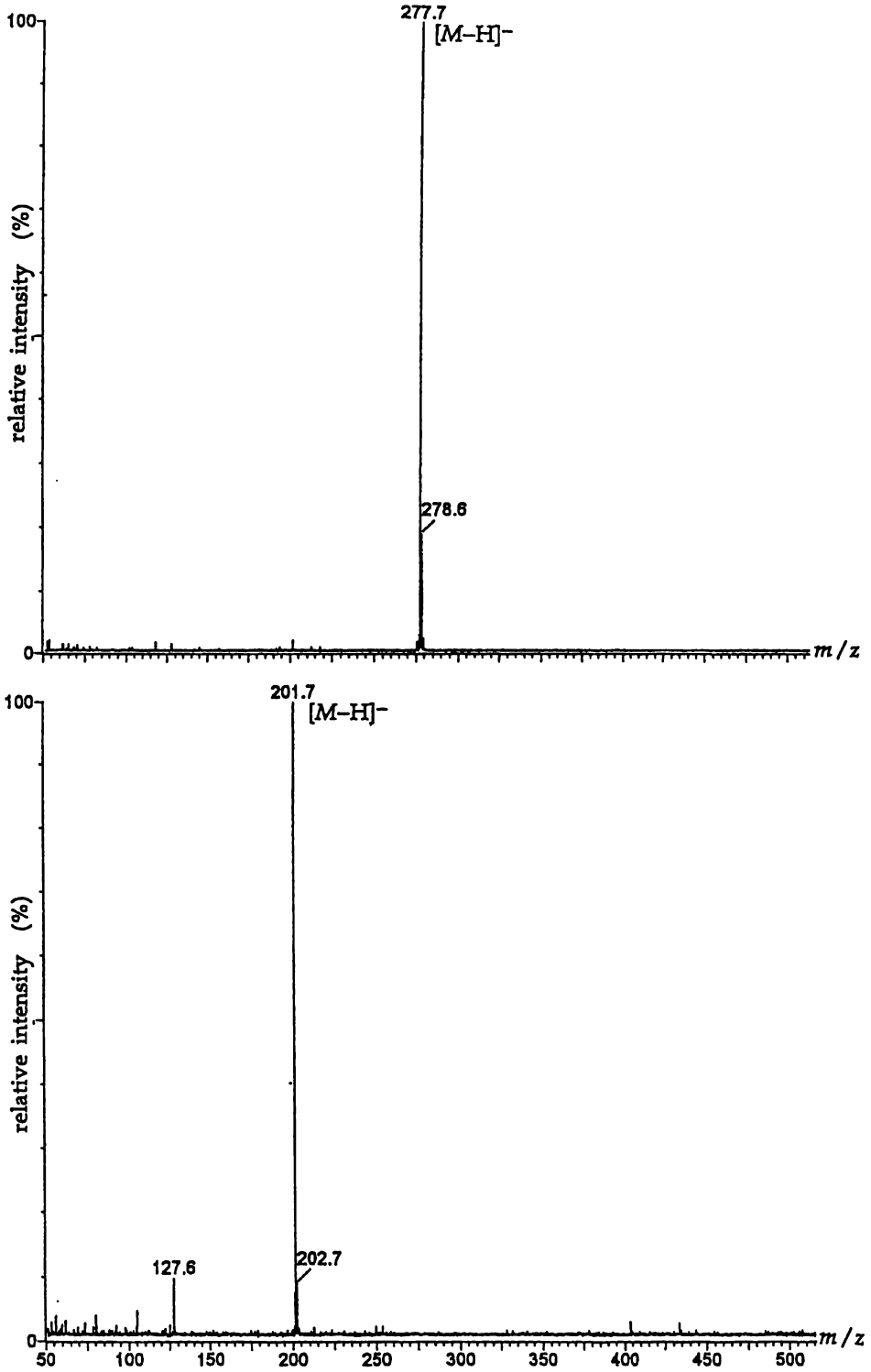

Figure 2.2: The negative-ion electrospray mass spectra of (a) **3** at 45 V, (b) **1** at 45 V.

2.1.5 NMR analyses of 8-camphanylphosphinic acid (1) and 8-camphanyl(phenyl)phosphinic acid (3)

2.1.5.1 General NMR features of the camphanyl region of camphene-derived phosphorus compounds

The structure of the camphanyl moiety deduced by NMR spectroscopy is consistent with that determined by X-ray crystallography. The general atom numbering scheme for the camphanyl fragment is shown in Figure 2.3, while full NMR data are given in the experimental section.

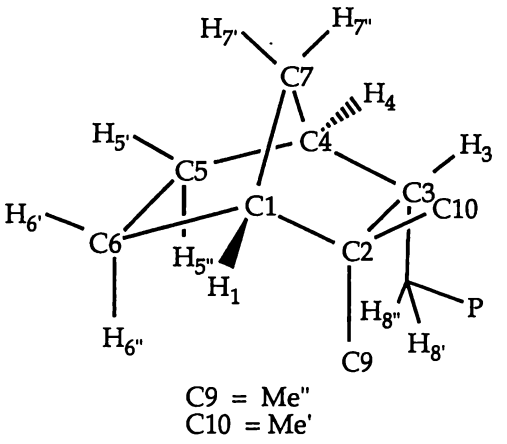

Figure 2.3: Atom numbering scheme for camphanyl-phosphorus derivatives.

With the exception of the resonance belonging to H_4 the ^1H NMR spectra [300 MHz] of camphanyl-phosphorus compounds in chloroform [δ 2.35 to 0.60] are generally complicated by overlapping signals. As the resonance belonging to H_4 [δ 2.35 to 2.00] is well separated from other resonances [δ 1.95 to 0.60], identification of many of the H_4 cross peaks is possible in the COSY45 spectrum. These include correlation peaks arising from coupling between H_4 and H_3, H_1, $H_{7"}$, $H_{5'}$ and $H_{7'}$.

Many of the proton resonances are readily identified in 1-D ^1H NMR spectra by their distinctive multiplets. $H_{7"}$ and $H_{7'}$ are in most cases

distinguishable by their doublet type patterns [$^2J_{H\text{-}C\text{-}H}$ 9.9-12.0 Hz]. The H_3 and H_1 resonances are distinguishable as the former gave broad, highly coupled multiplets while the latter gave broad singlets. Although these general features are easily observed, the low field resolution of the 1-D ^1H NMR spectra coupled with the natural line broadening of signals meant that, in most cases, the exact multiplicity of these resonances are not resolved. This is particularly applicable to the resonances associated with H_4 and H_1 where broad singlets are obtained.

The *endo*-protons $H_{7''}$ and $H_{6''}$ are found to be at a higher chemical shift relative to their *exo*- counterparts $H_{7'}$ and $H_{6'}$. This also applies to the protons $H_{5''}$ and $H_{5'}$ when distinction between resonances is possible.

2.1.5.2 *NMR analysis of 8-camphanylphosphinic acid (1)*

One- and two-dimensional NMR studies were carried out on 8-camphanylphosphinic acid (**1**). A summary of the ^1H and ^{13}C NMR data of **1** is presented in Table 2.3. Unlike the discrepancies found in the ^1H NMR assignment of the terpene β-pinene[20], which have been only recently rectified (1994)[21], no discrepancies exist in the NMR assignment of **1**.

The ^{31}P NMR shift of 8-camphanylphosphinic acid (**1**) [$C_{10}H_{17}P(O)(OH)(H)$] [δ 38.8] is similar to that of dimethylphosphinic acid [$Me_2P(O)(OH)$] (δ 49.4)[22]. The observed $^1J_{P\text{-}H}$ coupling [556.7 Hz] is consistent with those reported for phosphinic acids, which range from 400-850 Hz[23].

Atom	^{13}C NMR	^{1}H NMR	Assignment
PH	-	7.06, dt	PH
C(4)	42.1, d, $^{3}J_{P\text{-}C\text{-}C\text{-}C}$ = 6.2 Hz	2.26, br, s	H_4
C(3)	43.4, d, $^{2}J_{P\text{-}C\text{-}C}$ = 1.5 Hz	1.79, m	H_3
C(2)	37.5, d, $^{3}J_{P\text{-}C\text{-}C\text{-}C}$ = 12.2 Hz		
C(1)	48.4	1.75, s	H_1
C(8)	26.6, d, $^{1}J_{P\text{-}C}$ = 93.5 Hz	1.75, m, 1.71, m	$H_{8'/8''}$
C(7)	37.6	1.64, m	$H_{7''}$
		1.18, dt	$H_{7'}$
C(6)	24.6	1.53, m	$H_{6''}$
		1.24, m	$H_{6'}$
C(5)	20.2	1.29, m	$H_{5''/5'}$
C(10)	31.8	0.95, s	Me'
C(9)	21.1	0.78, s	Me''

Table 2.3: Summary of the ^{1}H and ^{13}C NMR data [δ in $CDCl_3$] for 8-camphanylphosphinic acid (**1**).
Refer to atom numbering scheme given in Figure 2.3

The ^{13}C NMR spectrum of **1** comprised ten resonances, consisting of two methyl signals, three methine signals, four methylene signals and one quaternary signal [refer to the ^{13}C NMR spectrum given in Figure 2.4]. The quaternary carbon C(2) is assigned by the absence of the signal [δ 37.5] in the DEPT experiment. The methylene signal which exhibited a large $^{1}J_{P\text{-}C}$ coupling [93.5 Hz] is assigned to C(8). Lesser two- or three-bond, carbon-to-phosphorus couplings are observed for the quaternary C(2) resonance and for the C(3) [δ 43.4] and C(4) [δ 42.1] methine resonances [J 12.2, 1.5 and 6.2 Hz respectively]. The comparatively small coupling exhibited by C(3) [1.5 Hz] is consistent with the well-documented tendency for $^{3}J_{P\text{-}C\text{-}C\text{-}C}$ couplings to be greater than $^{2}J_{P\text{-}C\text{-}C}$ couplings[24]. The remaining methine is assigned to C(1). Since this carbon is separated from the phosphorus atom by four bonds, a carbon-to-phosphorus coupling is not expected.

In the ^{13}C-^{1}H correlated NMR spectrum of **1**, Figure 2.4, the cross peaks relating to the ^{13}C NMR signals of C(8), C(3), C(4) and C(1) identified the corresponding resonances belonging to $H_{8'/8''}$, H_3, H_4 and H_1 [δ 1.71-1.75, 1.79 and 2.26 respectively]. The inverse mode HMBC NMR spectrum of **1** included correlations between the protons of the Me'' group [δ 0.78] and C(1), C(2), C(3) and C(10) [δ 48.1, 37.5, 43.4 and 31.9 respectively] and the protons of the Me' group [δ 0.95] and C(1), C(2), C(3) and C(9) [δ 48.1, 37.5, 43.4 and 22.1 respectively].

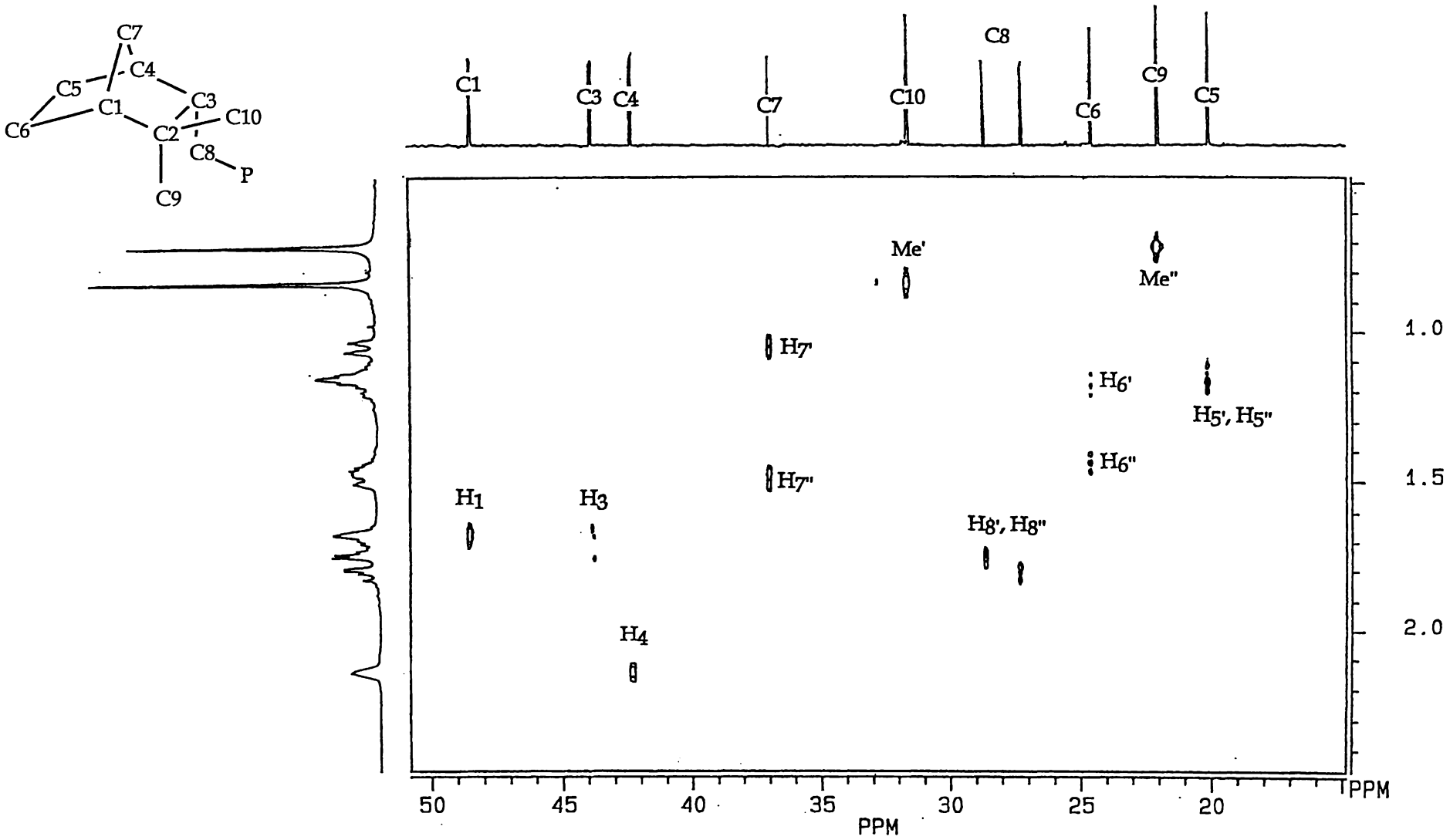

Figure 2.4: The ^{13}C-^{1}H correlated NMR spectrum of 8-camphanylphosphinic acid (**1**), recorded in $CDCl_3$ at 300 MHz.

The COSY45 spectrum of **1**, Figure 2.5, included correlation peaks arising from coupling between H_1 and H_4 (2), $H_{7'}$ (10), $H_{7''}$ (8), and the overlapping $H_{5'}$ and/or $H_{5''}$ and $H_{6'}$ (9) multiplets respectively, and between H_4 and H_3 (1), H_1 (2), $H_{7''}$ (3), $H_{5'}$ and/or $H_{5''}$ (4), and $H_{7'}$ (5). Correlations attributable to a strong ^5J coupling between the Me'' and $H_{7'}$ (15), a weak ^4J coupling between H_3 and $H_{5'}$ (7) and a strong ^4J coupling between H_1 and $H_{5''}$ (12) are also observed. All other cross peaks are as expected and are included in Figure 2.5 along with a complete ^{1}H-NMR spectral assignment of **1**.

^{1}H-NMR assignments are supported by NOE-difference experiments, the results of which are included in Table 2.4. Particularly diagnostic are the NOE's observed from Me' to $H_{7''}$ and to H_3 [but not significantly from Me' to $H_{8'/8''}$ indicating that $H_{7''}$ and H_3 are on the same side of the molecule, confirming the *endo* disposition of the -$CH_2PO_2H_2$ group]. Recognition of the $H_{5'}$, $H_{5''}$, $H_{6'}$, $H_{6''}$, $H_{7'}$ and $H_{7''}$ resonances, as revealed by crosspeaks in the COSY45 and enhancements observed in the NOE-difference spectra, identified the C(5), C(6) and C(7) methylene carbon resonances, *via* correlation peaks observed in the ^{13}C-^{1}H correlated NMR spectrum of **1**.

Irradiated hydrogen	*Enhanced signal (%)*
PH	H_4 (0.6), H_3 (0.5), $H_{8',8''}$ (0.8)
H_4 (δ 2.26)	H_3 (1.6), $H_{7''}$ (1.2), $H_{5''}$ (x) and $H_{5'}$ (y), x+y = 1.9, $H_{7'}$ (1.8), PH (0.5)
H_3 (δ 1.79)	H_4 (0.9)
H_1 (δ 1.70)	$H_{6''}$ (0.7), $H_{6'}$ (1.1), $H_{7'}$ (1.1), Me' (0.4), Me''(0.3)
$H_{6''}$ (δ 1.53)	$H_{5'}$ and/or $H_{5''}$ (x) and $H_{6'}$ (y), x+y = 8.1
$H_{7'}$ (δ 1.18)	H_4 (2.3), $H_{7''}$ (8.9)
Me' (δ 0.95)	H_3 (3.9), H_1 (2.3), $H_{7''}$ (3.4), Me'' (0.9)
Me'' (δ 0.78)	PH (0.6), H_1 (1.7), $H_{8',8''}$ (9.2), $H_{6''}$ (6.8), Me' (1.5)

Table 2.4: NOE's observed for the protons of **1** [% enhancements are given in brackets].

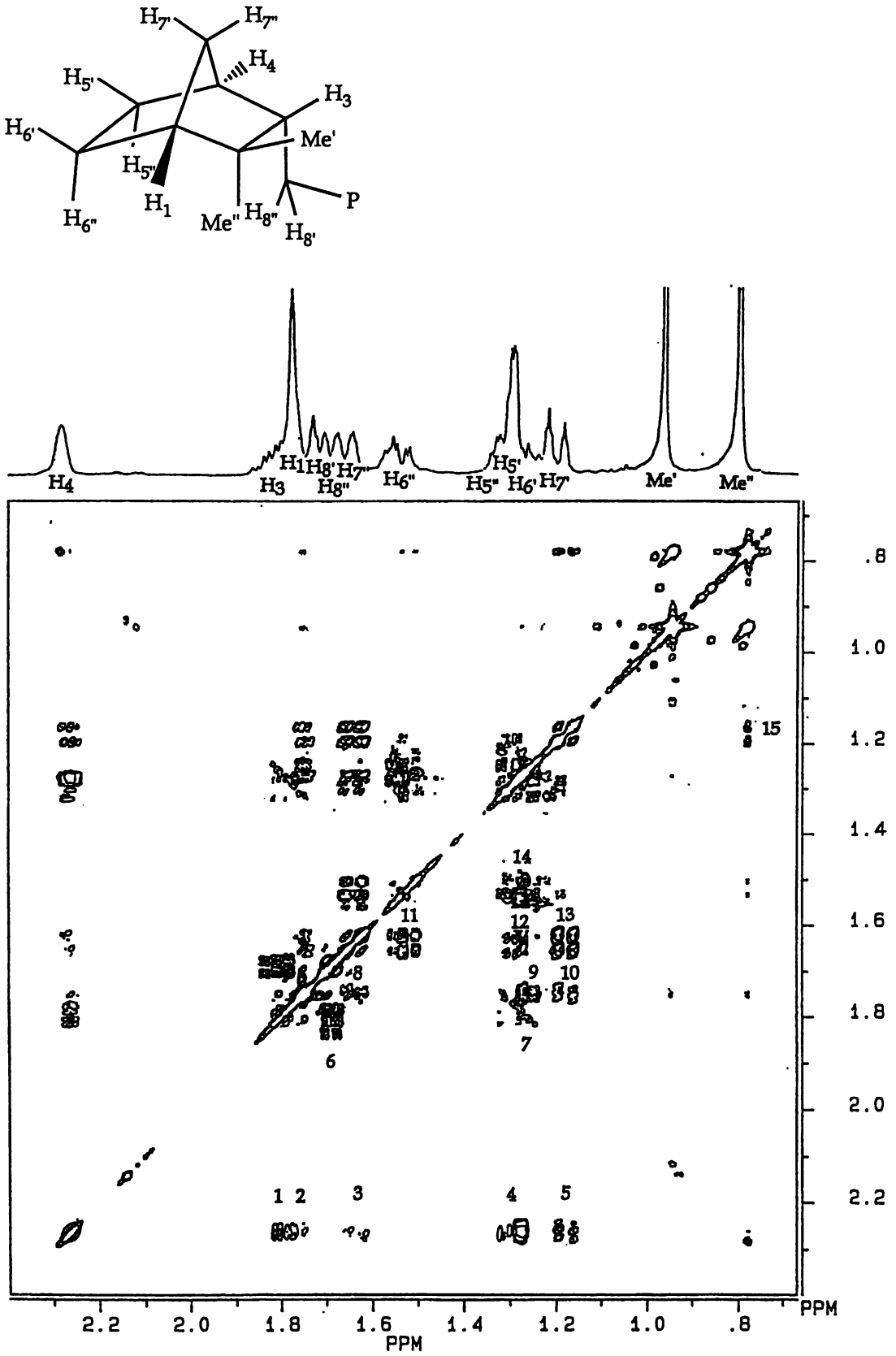

Figure 2.5: COSY45 spectrum of 8-camphanylphosphinic acid (1), recorded in $CDCl_3$ at 300 MHz.

Crosspeaks 1:H_4/H_3 2:H_4/H_1 3:$H_4/H_{7"}$ 4:$H_4/H_{5'}$ and/or $H_1/H_{5"}$ 5:$H_4/H_{7'}$ 6:$H_3/H_{8',8"}$ 7:$H_3/H_{5'}$ 8:$H_1/H_{7"}$ 9:$H_1/H_{6'}$ and/or $H_1/H_{5'}$ 10: $H_1/H_{7'}$ 11: $H_{7"}/H_{6"}$ 12:$H_1/H_{5"}$ 13: $H_{7"}/H_{7'}$ 14: $H_{6"}/H_{5'}$ and/or $H_{6"}/H_{5"}$, $H_{6"}/H_{6'}$ 15: $H_{7'}/Me"$

2.1.5.3 *NMR analysis of 8-camphanyl(phenyl)phosphinic acid (3)*

One- and two-dimensional NMR studies were undertaken to fully assign the ^{1}H and ^{13}C NMR spectra of 8-camphanyl(phenyl)phosphinic acid (**3**). A summary of the ^{1}H and ^{13}C NMR data are presented in Table 2.5.

Assignment	^{13}C NMR	^{1}H NMR	Assignment
C(4)	42.8, d, $^{3}J_{P\text{-}C\text{-}C\text{-}C}$ = 4.4 Hz	2.14, br, s	H_4
	[42.1, d, $^{3}J_{P\text{-}C\text{-}C\text{-}C}$ = 6.2 Hz]	[2.26, br, s]	
C(3)	43.8, d, $^{2}J_{P\text{-}C\text{-}C}$ = 3.2 Hz	1.75, m	H_3
	[43.4, d, $^{2}J_{P\text{-}C\text{-}C}$ = 1.5 Hz]	[1.79, m]	
C(2)	37.5, d, $^{3}J_{P\text{-}C\text{-}C\text{-}C}$ = 11.9 Hz	-	-
	[37.5, d, $^{3}J_{P\text{-}C\text{-}C\text{-}C}$ = 12.2 Hz]		
C(1)	48.5	1.67, m	H_1
	[48.4]	[1.75, m]	
C(8)	27.9, d, $^{1}J_{P\text{-}C}$ = 101.1 Hz	1.79, m, 1.76, m	$H_{8'/8''}$
	[26.6, d, $^{1}J_{P\text{-}C}$ = 93.5 Hz]	[1.75, m, 1.71, m]	
C(7)	37.0	1.49, d, ^{2}J 10.6 Hz	$H_{7''}$
		1.05, d, ^{2}J 10.6 Hz	$H_{7'}$
	[37.6]	[1.64, d, ^{2}J 10.6 Hz]*	
		[1.18, dt, ^{2}J 10.6 Hz]	
C(6)	24.6	1.49, m, 1.23, m	$H_{6''/6'}$
	[24.6]	[1.53, m, 1.43, m]	
C(5)	20.0	1.18, m, 1.16, m	$H_{5''/5'}$
	[21.0]	[1.29, m, 1.29, m]	
C(10)	31.6	0.83, s	Me'
	[31.8]	[0.95, s]	
C(9)	22.0	0.71, s	Me"
	[21.1]	[0.74, s]	

Table 2.5: A comparison of the ^{1}H and ^{13}C NMR data [δ in $CDCl_3$] of **3** and **1**.

* denotes an unresolved resonance. [ ] represents the equivalent ^{13}C NMR data obtained for 8-camphanyl-phosphinic acid (**1**).

both the *ortho* [δ 7.74-7.70] and *para* [δ 7.40-7.36] proton resonances whereas irradiation of the *ortho* proton [δ 7.74-7.70] gives only an enhanced *meta* proton signal [δ 7.46-7.43].

Irradiated hydrogen	*Enhanced signal (%)*
H_4 (δ 2.14)	H_3 (3.4), $H_{7''}$ (2.1), $H_{5'}$ (x), $H_{7'}$ (y), x + y = 8.0, Ph (1.7)
$H_{7''/6''}$ (δ 1.5)	H_4 (0.9), H_3 (1.7), $H_{6'}$ (10), $H_{7'}$ (7.5), Me'(1.6), Me'' (1.9)
Me'' (δ 0.71)	Me' (0.6), $H_{6''}$ (3.2), $H_{8'/8''}$ (x), H_1 (y), x + y = 3.9
Me' (δ 0.83)	Me'' (0.5), $H_{7''}$ (1.6), H_3 (x), H_1 (y), x + y = 3.7
$H_{7'}$ (δ 1.03)	H_4 (4.0), H_1 (2.9), $H_{7''}$ (21.5)
$H_{5''/5'/6'}$ (δ 1.16)	H_4 (2.26), $H_{8'/8''}$ (x), H_1 (y), x + y = 4.0, $H_{6''}$ (10.4)
$H_{3,1}$ (δ 1.67)	H_4 (1.1), $H_{7''}$ (2.2), $H_{6'}$ (1.4), $H_{7'}$ (1.3), Me' (2.5) Me'' (0.6)
$H_{8'/8''}$ (δ 1.79)	H_4 (1.5), $H_{5''}$ (3.0), Me' (1.2), Me'' (3.4)
para-Ph (δ 7.37)	*meta*-Ph (2.2)
meta-Ph (δ 7.46)	[Ph; *ortho*-Ph (3.5), *para*-Ph (7.0)]
ortho-Ph (δ 7.72)	*meta*-Ph (11.9)

Table 2.6: NOE's observed for the protons of **3** [% enhancements are given in brackets].

A comparison of the ^{1}H- and ^{13}C-NMR data of **1** and **3**, Table 2.5, shows that the chemical shifts only vary slightly between analagous resonances. The multiplicity between analogous resonances are also seen to be identical.

2.2 *Synthesis and characterisation of 8-camphanyl phosphinic acid esters*

2.2.1 *Introduction*

The esterification of phosphinic acids [RP(O)(H)(OH)] to their corresponding phosphinic acid esters [RP(O)(H)(OR')], which are more commonly known as phosphinates, is well documented in the literature. Esterifying agents used include trialkyl phosphite (Scheme 2.10), epoxides and dialkyl sulfates[25].

$$R_2PO_2H + (R'O)_3P \longrightarrow R_2P(O)(OR) + (R'O)_2P(O)H$$

Scheme 2.10: Esterification of phosphinic acids with a trialkyl phosphite.

The acid-catalysed esterification of phosphinic acids, illustrated in Scheme 2.11, also gives high yields of the phosphinic acid esters provided the by-product water is removed by azeotropic distillation[26].

$$RPH(O)(OH) + R'OH \longrightarrow RPH(O)(OR') + H_2O$$

Scheme 2.11: Acid-catalysed esterification of phosphinic acids.

Diazomethane is another convenient and well known laboratory reagent for the small scale conversions of acids to their methyl esters (Scheme 2.12).

$$RPH(O)(OH) + CH_2N_2 \longrightarrow RPH(O)(OCH_3) + N_2$$

Scheme 2.12: Esterification of phosphinic acids with diazomethane.

The phosphinic acids **1** and **3** are ideal precursors in the synthesis of new camphene-derived phosphinic acid esters Thus an investigation into their reactivity, particularly relating to their esterification, was undertaken.

2.2.2 Results and discussion

The treatment of phosphinic acids **1** and **3** with an excess of a diethyl ether solution of diazomethane affords the methyl esters methyl 8-camphanylphosphinate (**6**) and methyl 8-camphanyl(phenyl)phosphinate (**7**), Scheme 2.13. Formed quantitatively, both **6** and **7** are colourless oils.

With the substitution of the methoxy group for the hydroxy group in **1** and **3**, the proton transfer present in the free acids [refer to section 2.1.2] does not exist in the methyl esters, thus producing in each case an asymmetric phosphorus centre. As a result of these additional chiral centres which combine with the chiral camphanyl moiety [refer to chapter 1, section 1.6], the methyl esters **6** and **7** exist as diastereoisomers. The GCMS data [refer to section 2.2.3 for more detail], ^{31}P and ^{13}C NMR data [refer to section 2.2.4 for more detail] are consistent with the existence of these diastereoisomers.

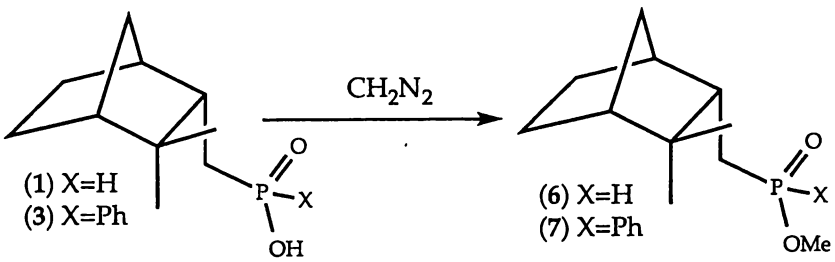

Scheme 2.13: The esterification of camphene-derived phosphinic acids **1** and **3** with diazomethane.

Not unlike carboxylic acid esters, phosphinic acid ester **6** readily hydrolyses over 24 h in air to form the parent acid **1** (Scheme 2.14). In contrast to **6**, phosphinate **7** was found to be stable with respect to atmospheric hydrolysis.

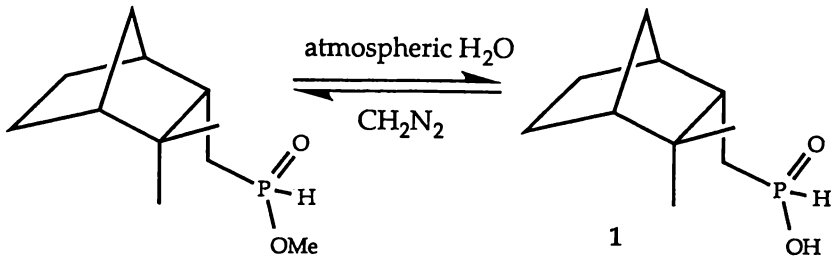

Scheme 2.14: Interconversion of 8-camphanylphosphinic acid (**1**) and its methyl ester methyl 8-camphanylphosphinate (**6**).

The greater stability of **7** [*c.f.* **6**] to nucleophilic attack of a hydroxy group is expected to be due to the steric and electronic effects of the phenyl ring. Another possible factor which may influence the greater stability of the ester **7** [*c.f.* **6**] may be the ability of **6** to undergo tautomerism, a rearrangement observed for phosphorus compounds (Scheme 2.15)[26].

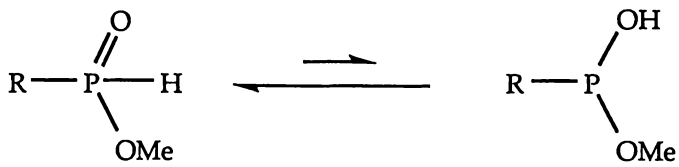

Scheme 2.15: Tautomerism of methyl 8-camphanylphosphinate (**6**) by hydride transfer.

The less sterically congested tautomer may be more inclined to nucleophilic attack by water as compared to the phenyl analogue **7** where this type of rearrangement is less likely to occur. It is worth noting that kinetic studies of phenylphosphinic acid established that the tricoordinate tautomeric form exists in low concentration. The tautomeric form of the methyl ester **7** is also expected to exist in similar concentrations. Despite several attempts to purify methyl ester **6** by vacuum distillation, a sample of suitable purity for elemental analysis was not obtainable.

The methyl esters **6a** and **7a**, which are formed by the treatment of the phosphinic acids **1a** and **3a** [refer to section 2.1.2 for details on synthesis] with diazomethane (Scheme 2.16), are detected in trace amounts by GCMS [refer to section 2.2.3 for detailed discussion]. Like their parent acids the methyl esters **6a** and **7a** are expected to have to adopt the *endo*-$CH_2P(O)(OMe)X$ [where X = H or P] position. This is the least sterically congested isomer, as

the bridgehead and $CH_2P(O)(OMe)X$ [where X = H or Ph] group are on opposite sides of the ring [*c.f.* the *exo*-$CH_2P(O)(OMe)X$ conformer].

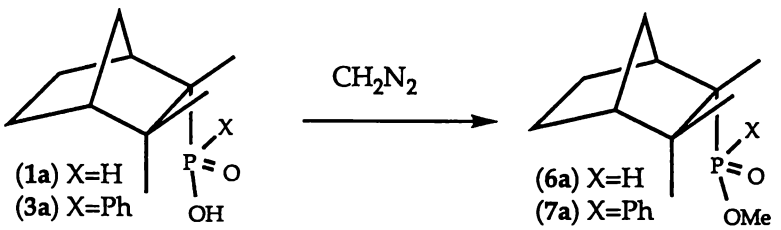

Scheme 2.16: The methyl esters **6a** and **7a**, formed by the methylation of **1a** and **3a**.

The ester methyl di(8-camphanyl)phosphinate (**8**), which is formed by the methylation of di(8-camphanyl)phosphinic acid (**2**) with diazomethane is also detected by GCMS [refer to section 2.2.3 for characterisation], thus reaffirming the tentative assignment of **2** previously postulated in section 2.1.2. (see Scheme 2.17).

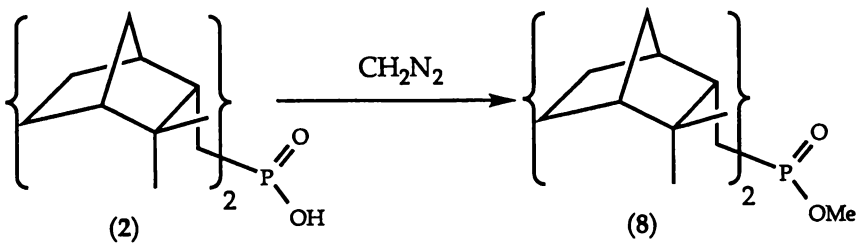

Scheme 2.17: The methylation of di(8-camphanyl)phosphinic acid (**2**).

2.2.3 Gas chromatography mass spectrometric analysis of the 8-camphanylphosphinic acid methyl esters

Characterisation of the new organophosphorus esters **6**, **7** and **8** is aided by gas chromatography mass spectrometry [GCMS]. Unlike their parent acids which adsorb to the stationary phase, the methyl esters **6** and **7** are readily analysed by GCMS. As shown in Figure 2.6 preliminary GCMS studies of methyl 8-camphanylphosphinate (**6**) [50°C to 250°C at 5°C per mins] gave one major component eluting at 5.92 mins [R_f=0.15, M^+ at 216]. When a less concentrated sample along with a temperature programme of 50°C to 250°C at 1°C per mins is used, the major component is found to consist of two overlapping signals eluting at 33.10 [R_f=0.165] and 33.15 mins [R_f=0.166]. These two signals, which have identical parent ion masses, and equal area, confirm the existence of a pair of diastereoisomers. Also given in Figure 2.6 is the mass spectrum of a minor component (**6a**) [R_f=0.162] which is similar to that of **6**. As separation of the diastereoisomers using column chromatography was only partially successful, preparative separation of the diastereoisomers was not undertaken. An additional minor component, methyl di(8-camphanyl)phosphinate (**8**) [R_f=0.70, M^+ at *m/z* 352], formed by the methylation of di(8-camphanyl)phosphinic acid (**2**), was also detected by GCMS. In the GCMS studies of methyl 8-camphanyl(phenyl)phosphinate (**7**), which are included in the experimental section, both the minor addition product **7a** and the diastereoisomers of **7** are detected. The mass spectrum of **7** is included in Figure 2.6.

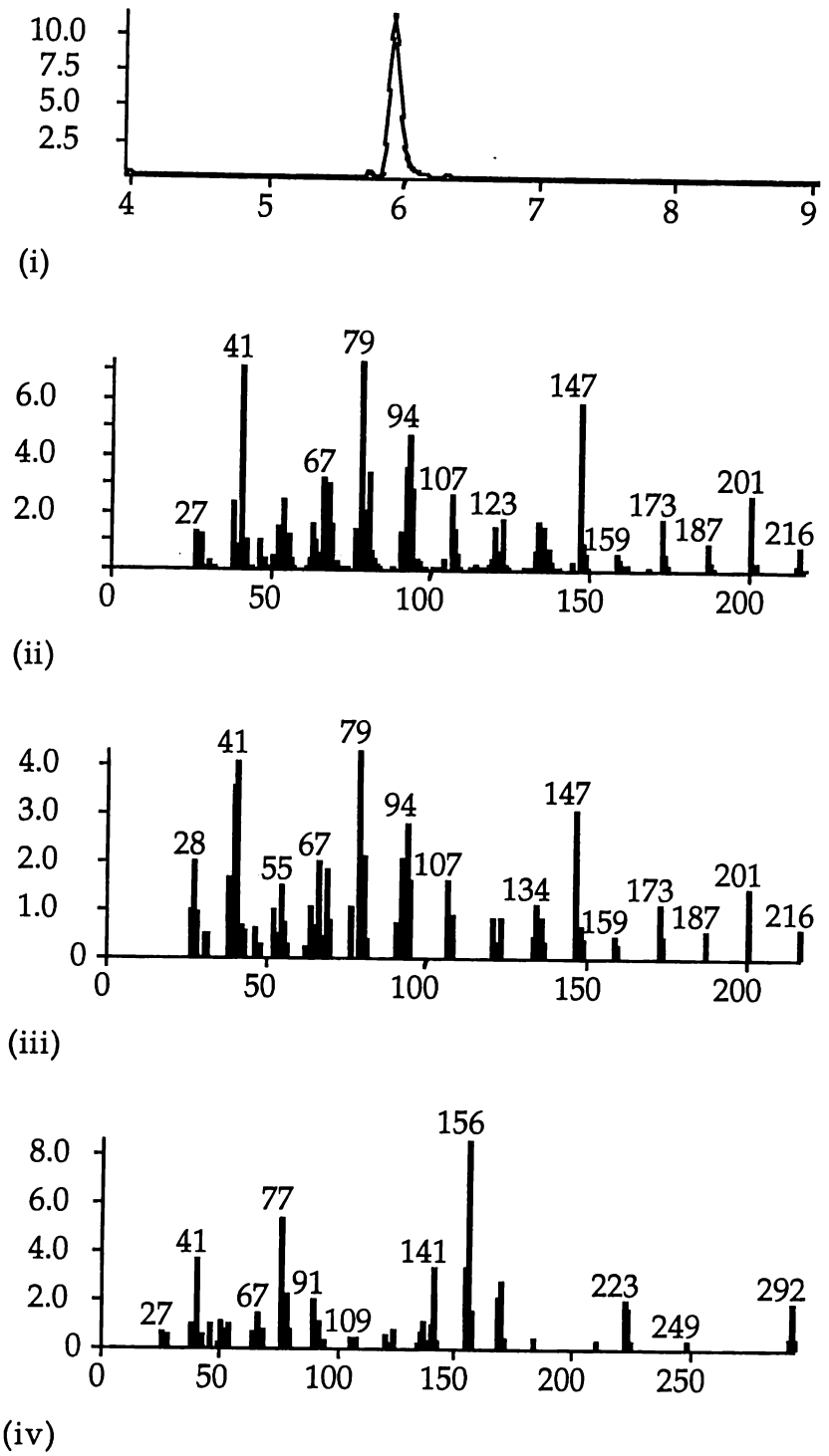

Figure 2.6: (i) total ion chromatogram of **6** from 4 to 9 mins. (ii) mass spectrum of major product methyl 8-camphanylphosphinate (**6**) eluting at 5.92 mins. (iii) mass spectrum of minor addition product **6a** eluting at 5.74 mins. (iv) mass spectrum of methyl 8-camphanyl(phenyl)phosphinate (**7**).

2.2.4 NMR analysis of methyl 8-camphanyl(phenyl)phosphinate (7)

One- and two-dimensional NMR studies were carried out to fully assign the ^{1}H and ^{13}C NMR spectra of methyl 8-camphanyl(phenyl)-phosphinate (7) which, as previously stated in section 2.2.3, exists as a pair of diastereoisomers. A summary of the ^{1}H and ^{13}C NMR data of both isomers is included in Tables 2.7 and 2.8 respectively. The assignment of the absolute configuration of each isomer of 7 by NOE-difference spectroscopy is not possible as ^{1}H NMR resonances in the 1D-^{1}H NMR spectrum are indistinguishable.

	$C_{10}H_{17}P(OH)(O)(Ph)$ 3	$C_{10}H_{17}P(OMe)(O)(Ph)$ isomer of 7	$C_{10}H_{17}P(OMe)(O)(Ph)$ isomer of 7
H_4	2.14, br, s	2.28, br, s	1.98, br , s
H_3	1.75, m	1.74, m	1.81, m
H_1	1.67, br ,s	1.66, br ,s	1.66, br ,s
$H_{8'/8''}$	1.79, m	1.96-1.67, m	1.85, m
$H_{8'/8''}$	1.76, m	1.96-1.67, m	1.85, m
$H_{7''}$	1.49, d	1.53, d	1.53, d
$H_{6''}$	1.43, m	1.47, m	1.42, m
$H_{5''}$	1.18, m	1.28, m	0.95, m
$H_{5'}$	1.16, m	1.28, m	0.95, m
$H_{6'}$	1.19-1.14, m	1.18, m,	1.10, m
$H_{7'}$	1.05, d	1.05	1.01
Me'	0.83, s	0.79, s	0.88, s
Me"	0.71, s	0.68, s	0.75, s

Table 2.7: A comparison of ^{1}H NMR data [δ in $CDCl_3$] of the isomers of 7 with their parent acid 3.

The ^{13}C NMR spectra of the isomers of **7** [refer to the ^{13}C NMR spectrum given in Figure 2.7 and Table 2.8] consists of three resonances which are equivalent [δ 37.0, 31.6 and 24.6] for each isomer and seven resonances which are inequivalent for each isomer [δ (48.5, 48.4), (43.8, 43.7), (42.4, 42.2), (37.6, 37.4), (26.9, 26.8), (22.2, 22.1), (20.2, 19.9)]. The equivalent resonances which belong to C(6), C(7) and C(10) are assigned by comparison with the ^{13}C NMR spectrum of their parent acid **3** [see Table 2.8].

	$C_{10}H_{17}P(OH)(O)(Ph)$ **3**	$C_{10}H_{17}P(OMe)(O)(Ph)$ isomer of **7**	$C_{10}H_{17}P(OMe)(O)(Ph)$ isomer of **7**
C(5)	20.1	19.9	20.2
C(9) Me"	22.0	22.2	22.1
C(6)	24.6	24.6	24.6
C(8)	27.9	26.8	26.9
$^1J_{P\text{-}C(8)}$	101.1 Hz	101.1 Hz	101.1 Hz
C(10) Me'	31.6	31.6	31.6
C(7)	37.0	37.0	37.0
C(2)	37.5	37.4	37.6
$^3J_{P\text{-}C\text{-}C\text{-}C(2)}$	11.9 Hz	6.4 Hz	6.4 Hz
C(4)	42.8	42.2	42.4
$^3J_{P\text{-}C\text{-}C\text{-}C(4)}$	4.4 Hz	3.9 Hz	3.9 Hz
C(3)	43.8	43.7	43.8
$^2J_{P\text{-}C\text{-}C(3)}$	3.2 Hz	3.1 Hz	3.1 Hz
C(1)	48.5	48.4	48.5
OMe	-	50.90, d*; 50.85, d*	50.90, d*; 50.85, d*

Table 2.8: A comparison of the ^{13}C NMR data [δ in $CDCl_3$] of the isomers of **7** with their parent acid **3**.

* denotes tentative assignment of signals

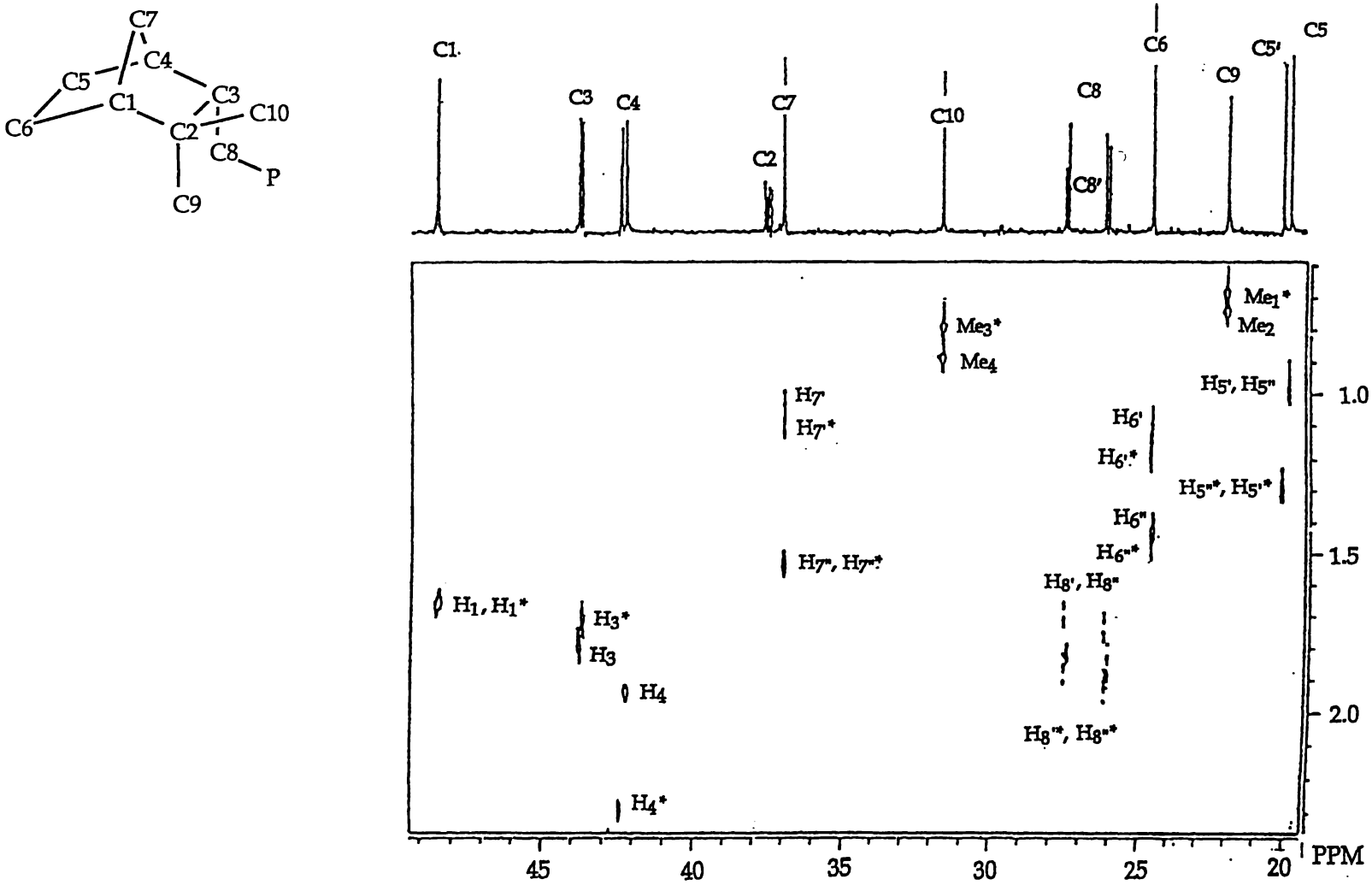

Figure 2.7: The ^{13}C-^{1}H correlated NMR spectrum of the camphanyl moiety of methyl 8-camphanyl(phenyl)phosphinate isomers (7), recorded in $CDCl_3$ at 300 MHz.

The ^{13}C-^{1}H correlated NMR spectrum, Figure 2.7, of the camphanyl moiety of **7** gave two sets of correlation peaks. Each set of correlation peaks defines the ^{1}H NMR resonances belonging to a given isomer [sets are differentiated by the presence or absence of an asterisk]. In the ^{13}C-^{1}H correlated NMR spectrum the cross peaks belonging to C(4) and C(4)', hereafter labelled H_4 and H_4^*, are of particular interest as they are sufficiently separated from each other, and from other ^{1}H NMR resonances to allow partial interpretation of their correlations in the COSY45 spectrum.

In the COSY45 spectrum of **7** shown in Figure 2.8, the H_4^* correlation peaks of **7** are identical to its parent acid **3** and include the easily distinguished correlation peaks which arise from the coupling of H_4^* to H_3^* (1), H_1^* (2), $H_{7''}^*$ (3), $H_{5''}^*$ and/or $H_{5'}^*$ (4) and $H_{7'}^*$ (5). For the H_4 proton resonance only three of the five expected correlation peaks are easily identified; $H_{7''}$ (6), $H_{5''}$ and/or $H_{5'}$ (8) and $H_{7'}$ (7). A strong five-bond *exo*-Me to $H_{7'}$ coupling observed in the COSY45 spectrum of the parent acid **3** [refer to section 2.1.5.3], is also observed in the COSY45 spectrum of **7** [(12) and (13)]. This correlation links the methyl groups to their respective $H_{7'}$ protons and therefore their associated H_4 protons. The methyls are linked to each other by a strong four-bond coupling. The assignment of the correlation peaks that arise from the coupling of $H_{6'}$ to $H_{6''}$ and H_3 to $H_{8'/8''}$ for each isomer is not possible as these correlation peaks fall amongst crowded areas of the COSY45 spectrum. However NOE's, which are included in Table 2.9, are able to resolve ambiguous ^{1}H NMR assignments and reaffirm postulated assignments. Particularly diagnostic are the observed NOE's of both H_4 and H_4^* to their associated protons H_3, H_1, $H_{7''}$, $H_{5'',5'}$ and $H_{7'}$ and the observed NOE's of the *endo* -methyl groups to their associated $H_{6''}$ [and not $H_{6'}$] and $H_{8'/8''}$ protons. Recognition of the H_1, H_1^*, H_3, H_3^*, $H_{5'}$, $H_{5'}^*$, $H_{5''}$, $H_{5''}^*$, $H_{8'}$, $H_{8'}^*$, $H_{8''}$, $H_{8''}^*$ and Me_1^*, Me_2 resonances, as revealed by crosspeaks in the COSY45 and enhancements observed in the NOE-difference spectra, identified the C(1), C(1)', C(3), C(3)', C(5), C(5)', C(8), C(8)' and C(9), C(9)' ^{13}C NMR resonances, *via* correlation peaks observed in the ^{13}C-^{1}H correlated NMR spectrum of **7**.

Irradiated hydrogen	*Enhanced signal (%)*
H_4*	$H_{7''}$* (4.9), $H_{5''/5'}$* (7.3), $H_{7'}$* (5.8), H_1* (x), H_3*(y), x+y=6.9
H_4	$H_{7''}$ (1.2), $H_{5''/5'}$(1.4), $H_{7'}$ (1.4), H_1 (x), H_3 (y), x+y=7.4
Me''*	Me'* (1.7), $H_{6''}$* (5.1), H_1* (x), $H_{8'/8''}$*(y), x+y=8.0
Me''	Me' (2.4), $H_{6''}$ (5.9), H_1 (2.0), $H_{8'/8''}$ (5.2)
Me'*	Me''* (1.7), $H_{7''}$* (4.3), H_1*+ H_3 x+y=8.8)
Me'	Me'' (1.9), $H_{7''}$ (3.9), H_1 (3.1), H_3 (4.5)

Table 2.9: NOE's observed for the protons of 7 [% enhancements are given in brackets].

A comparison of the ^{1}H- and ^{13}C- NMR spectra of 3 and its methyl ester 7, Tables 2.7 and 2.8, shows that there is no significant difference between commonly assigned resonances. There is, however, a significant variation between the ^{1}H NMR resonances assigned to H_4 and $H_{5''/5'}$ of the diastereomers of 7. The difference between these resonances can be explained by the spatial orientation of the phenyl group with respect to the H_4 and $H_{5''/5'}$ protons.

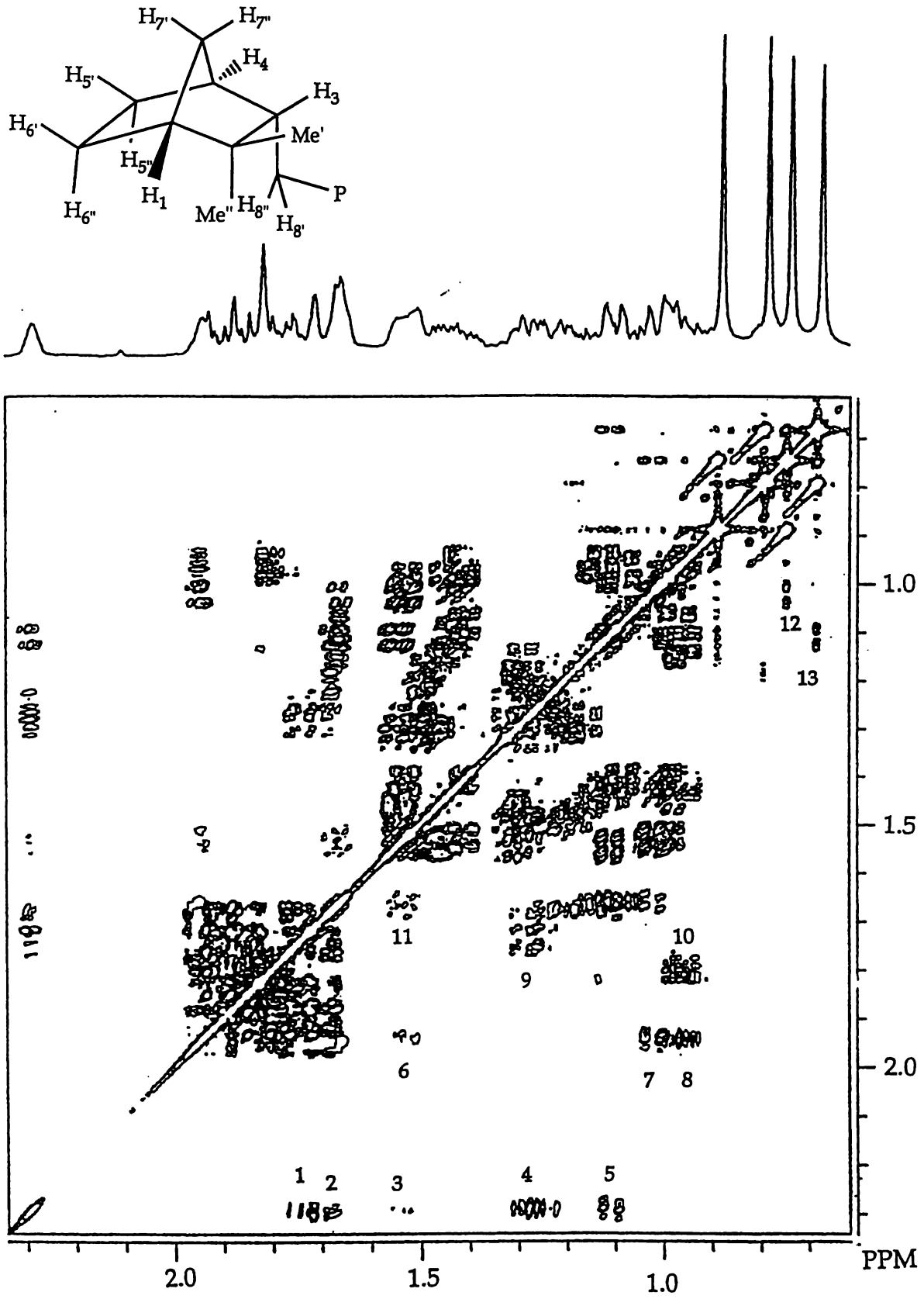

Figure 2.8: The COSY45 spectrum of the camphanyl moiety of methyl 8-camphanyl(phenyl)phosphinate (7) recorded in $CDCl_3$ at 300 MHz.

Crosspeaks : 1: H_4*/H_3* 2: H_4*/H_1* 3: H_4*/$H_{7"}$* 4: H_4*/$H_{5'}$* and/or H_1*/$H_{5"}$* 5: H_4*/$H_{7'}$* 6: H_4/$H_{7"}$ 7 H_4/$H_{7'}$ 8: H_4/$H_{5'}$ and/or H_1/$H_{5"}$ 9: H_3*/$H_{5'}$* and/or $H_{5"}$* 10: H_3/$H_{5'}$ and/or H_3/$H_{5"}$ 11: H_1/$H_{7"}$* 12: $H_{7'}$/Me_2 13: $H_{7'}$*/Me_1.

2.3 Synthesis and characterisation of some 8-camphanylphosphinic acid derivatives

2.3.1 Introduction

The reaction of phosphinic acids with aldehydes and ketones to give hydroxyalkylphosphinic acids is well established and is essentially the same reaction developed around the turn of the century for hypophosphorous acid[25, 27]. The acid-catalysed addition of formaldehyde to phosphinic acids to give hydroxymethylphosphinic acids, illustrated in Scheme 2.18, has been subsequently developed to shorten the reaction time.

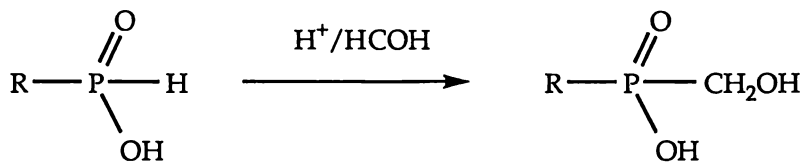

Scheme 2.18: The acid-catalysed addition of formaldehyde to phosphinic acids to give hydroxymethylphosphinic acids.

As illustrated in Scheme 2.19 addition products are also formed by the reaction of phosphorous acids with Schiff bases[28, 29] [formed *in situ* from HCOH and R_2NH] and aryl isocyanates[30].

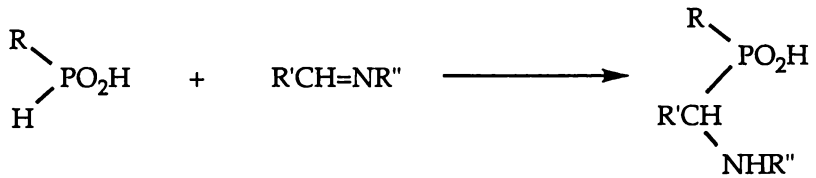

R and R'= H, alkyl, aryl

Scheme 2.19: Addition products formed by the reaction of phosphorous acids with Schiff's bases [formed *in situ* from HCOH and R_2NH].

Several methods are also available in the literature for the preparation of phosphonic dichlorides[31, 32]. One of the most widely used procedures consists of the conversion of phosphonates to phosphonic

dichlorides by reaction with PCl_5[30, 31], $SOCl_2$[31, 33, 34] or $COCl_2$[31]. The chlorination of phosphonates by $SOCl_2$, Scheme 2.20, can also be catalysed by pyridine, hexamethylphosphoric triamide and *N,N*-disubstituted formamides[30].

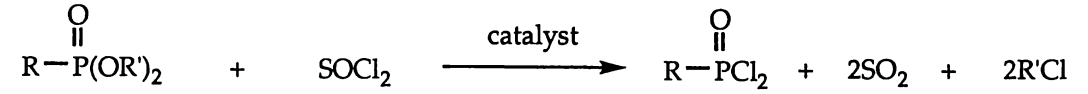

Scheme 2.20: Chlorination of phosphonates with thionyl chloride [$SOCl_2$].

The phosphinic acids **1** and **3** are ideal precursors in the synthesis of new camphene-derived hydroxymethyl and chlorinated phosphorus compounds. Thus an investigation into their reactivity particularly relating to the addition of formaldehyde and chlorine was undertaken.

2.3.2 Results and discussion

(i) Acid-catalysed addition of formaldehyde and formaldehyde /dimethylamine to phosphinic acid 1

At an elevated temperature [150°C] **1** reacts with an excess of paraformaldehyde to form two major products, one of which is hydroxymethyl camphanylphosphinic acid (**9**); Scheme 2.21. Formed in moderate yield, **9** is readily purified by recrystallisation from a methanol/ether solution. Attempts to isolate and identify the other major product met with no success. **1** also reacts with an excess of concentrated formaldehyde heated at reflux and hydrochloric acid to form **9**. However due to longer reaction times, lower yields and the formation of a greater number of products, this route is least preferred [*c.f.* the use of paraformaldehyde]. The formulated structure of **9** is consistent with elemental data. As shown in Scheme 2.21, 8-camphanylphosphinic acid (**1**) also reacts with a mixture of formaldehyde and dimethylamine to give 8-camphanyl-N,N-dimethyl-aminomethylphosphinic acid hydrochloride (**10**), a white crystalline solid, in high yield. Elemental microanalytical data of **10**

confirms the formation of the hydrochloride salt and not, as initially suspected, the free amine. Both **9** and **10** are insoluble in organic solvents such as chloroform and are readily recrystallised from methanol/ether.

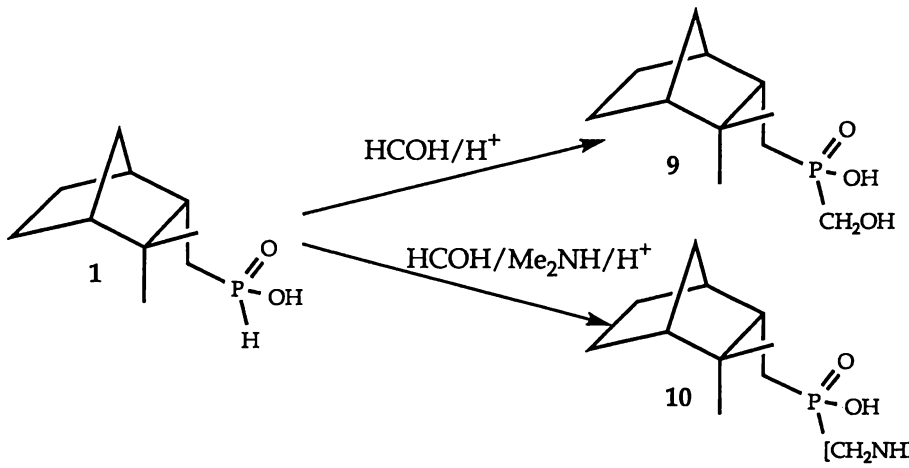

Scheme 2.21: The acid-catalysed addition of HCOH and $HCOH/Me_2NH$ to **1**.

Detailed characterisation of **9** and **10** by ESMS and NMR spectroscopy is presented in sections 2.3.3 and 2.3.4 respectively.

(ii) Chlorination of the phosphinic acids 1 and 3

The oxidative chlorination of **1** involves **1** heated at reflux and the catalyst pyridine [1 drop per 0.16 g of **1**] in a solution of thionyl chloride [$SOCl_2$] for 1.5 h. Upon completion of the reaction, which is determined by ^{31}P NMR, the excess thionyl chloride, pyridine and byproducts [HCl, SO_2] are simply removed under vacuum yielding a pale yellow liquid, 8-camphanylphosphonic dichloride (**11**), in quantitative yield; Scheme 2.22. A catalyst [*i.e.* pyridine] must be used, otherwise the oxidative chlorination of **1** occurs slowly yielding a large number of products which are not easily separated.

8-Camphanyl(phenyl)phosphinic acid (**3**) readily reacts with an excess of thionyl chloride [with a pyridine catalyst] affording 8-camphanyl(phenyl)-phosphinic chloride (**12**), in quantitative yield (see Scheme 2.22). As a result of the chlorine substitution a chiral phosphorus centre is generated which combines with the chiral camphanyl moiety [refer to section 2.2.2] to give

four isomers. Two of the four isomers are chemically similar and physically different, *i.e.* diastereoisomers, and thus are detectable by ^{31}P NMR [δ 57.8 and 57.2].

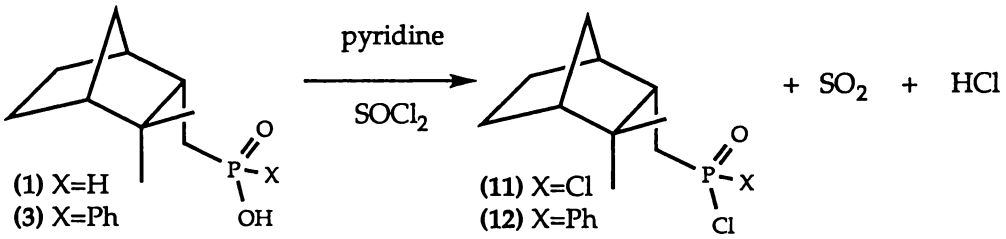

Scheme 2.22: The pyridine-catalysed chlorination of **1** and **3** with $SOCl_2$.

Detailed characterisation of **11** and **12** by NMR spectroscopy is presented in section 2.3.4.

*2.3.3 Electrospray mass spectrometric analysis of camphene-derived phosphinic acids **9** and **10***

The ESMS data of **9** and **10** in both positive and negative ion modes are given in Table 2.10. Results clearly indicate that to obtain simple mass spectra the phosphinic acid **9** should be analysed using similar conditions to those specified for the phosphinic acids **1** and **3** [refer to section 2.1.4]. However mass spectral data of the phosphinic acid **10** suggests that positive ion mode is recommended for spectral simplicity.

Compound	Mode (cone voltage)	Principal ion *(m/z)*	Other Ions *(m/z)*
9	positive (45 V)	$[RP(O)(OH)CH_2OH+H]^+$ (233, 100%)	$[2M+H]^+$ (465, 70%); $[3M+H]^+$ (697, 55%); $[4M+H]^+$ (929, 45%)
9	negative (45V)	$[RP(O)(OH)CH_2OH-H]^-$ (231, 100%)	$[2M-H]^+$ (463, 13%)
10	positive (15V)	$A=[RP(O)(OH)CH_2NHMe_2]^+$ (260, 100%)	$[2A-H]^+$ (519, 55%)
10	negative (15V)	$B=[RP(O)(O)CH_2NMe_2]^-$ (258, 100%)	$[B+2H_2O]^-$ (294, 85%); $[2B+H]^-$ (517, 35%); $[2B+H+2H_2O]^-$ (553, 25%); $[3B+2H]^-$ (776, 10%); $[3B+2H+2H_2O]^-$ (812, 7%)

Table 2.10: A comparison of electrospray mass spectral data of **9** and **10** collected in positive and negative ion modes.
M is defined as the molecular ion and *A* and *B* are defined as charged species, the formula of which are described above.

2.3.4 NMR analysis of 8-camphanylphosphinic acid derivatives

2.3.4.1 NMR analysis of 8-camphanylphosphonic dichloride (11)

One- and two-dimensional NMR studies were carried out to fully assign the ^{1}H and ^{13}C NMR spectra of 8-camphanylphosphonic dichloride (**11**). A summary of the ^{1}H- and ^{13}C-NMR data of **11**, along with the analogous resonances of **1**, are presented in Tables 2.11 and 2.12 respectively.

	$C_{10}H_{17}P(OH)(O)(H)$ **1**	$C_{10}H_{17}P(O)Cl_2$ **11**
H_4	2.26, br, s	2.34, br, s
H_3	1.79, m	1.93, m
H_1	1.75, m	1.71, br ,s
$H_{8'/8''}$	1.75,m	2.54, m
$H_{8'/8''}$	1.71, m	2.49, m
$H_{7''}$	1.64, d,^{2}J 9.9	1.59, d, ^{2}J 10.1
$H_{6''}$	1.53, m	1.46, m
$H_{5''}$	1.29, m	1.36, m
$H_{5'}$	1.29, m	1.31, m
$H_{6'}$	1.24, m	1.21, d, J 4.8
$H_{7'}$	1.18, dt, ^{2}J 9.9, ^{3}J 1.7	1.15, d, ^{2}J 10.1
Me'	0.95, s	0.91, s
Me''	0.78, s	0.74, s

Table 2.11: A comparison of the ^{1}H NMR data [δ in $CDCl_3$] of the camphanyl moieties of **11** and **1**.

The ^{31}P NMR chemical shift of 8-camphanylphosphonic dichloride (**11**) occurs at δ 51.6 and is consistent with n-hexylphosphonic dichloride [$C_6H_{13}P(O)Cl_2$] which has a chemical shift of δ 62.0[22].

The ^{13}C NMR spectrum of **11** is assigned by comparison with its precursor **1** [see Table 2.12]. Recognition of the carbon resonances of the

camphanyl moiety identified all camphanyl related proton resonances, *via* correlation peaks observed in the ^{13}C-^{1}H correlated NMR spectrum of **11**.

	$C_{10}H_{17}P(O)(OH)(H)$ **1**	$C_{10}H_{17}P(O)Cl_2$ **11**
C(5)	20.2	20.3
C(9) Me"	21.1	21.9
C(6)	24.6	24.5
C(8)	26.6	41.9
$^{1}J_{P\text{-}C(8)}$	93.5 Hz	95.7 Hz
C(10)Me'	31.8	31.6
C(7)	37.6	37.0
C(2)	37.5	38.2
$^{3}J_{P\text{-}C\text{-}C\text{-}C(2)}$	12.2 Hz	17.5 Hz
C(4)	42.1	41.9
$^{3}J_{P\text{-}C\text{-}C\text{-}C(4)}$	6.2 Hz	5.2 Hz
C(3)	43.4	45.1
$^{2}J_{P\text{-}C\text{-}C(3)}$	1.5 Hz	6.5 Hz
C(1)	48.4	48.3

Table 2.12: A comparison of the ^{13}C NMR data (δ in $CDCl_3$) of **11** with **1**.

The correlations observed in the COSY45 NMR spectrum are consistent with the assignment of ^{1}H NMR resonances obtained *via* correlations in the ^{13}C-^{1}H correlated NMR spectrum of **11**. Proton resonances belonging to $H_{5"}$ [δ 1.36] and $H_{5'}$ [δ 1.31] are assigned assuming that the chemical shift of the *exo*-proton is greater than the *endo*- proton [refer to section 2.1.5 for more detail]. No discrepancies exist between the ^{1}H-^{1}H and ^{13}C-^{1}H correlated NMR spectra.

A comparison of the ^{1}H- and ^{13}C-NMR spectra of **11** with **1**, Table 2.12, shows that there is a pronounced difference between the resonances assigned to C(8) and $H_{8'/8"}$. For **11** the signals assigned to C(8) and $H_{8'/8"}$ are δ 41.9 and δ 2.54 respectively while the equivalent resonances in the

phosphinic acid **1** are δ 26.6 and δ 1.75-1.71 respectively. This is expected to be the result of the substitution of less electronegative chlorine atoms for the oxygen atoms at the phosphorus centre. This phenomenon is also observed for the chlorination of carboxylic acids, *e.g.* 2-methylpropanoic acid, where the β carbon atom shifts upfield δ 12.4[35].

2.3.4.2 *NMR analysis of **9** and **10***

The ^{13}C NMR spectra of **9** and **10** are assigned by comparison with **1** [see Table 2.13]. The methylene signals [δ 63.3 for **9** and δ 58.2 for **10**] which exhibit large $^{1}J_{P\text{-}C}$ coupling constants [108.4 Hz for **9** and 84.4 Hz for **10**] are assigned to the $-CH_2OH$ group of **9** and $-CH_2N$ group of **10**. A DEPT90 experiment performed on **10** clearly distinguished the methine signals belonging to C(1), C(3), C(4) [δ 51.9, 47.1 and 45.9 respectively] from the methyl signals belonging to the $-N(CH_3)_2$ group [δ 48.6]. The hydroxymethyl assignment for **9** is similar to that in the carbon analogue hydroxyethanoic acid (glycolic acid), where the equivalent atom has a chemical shift of δ 60.4[35].

Compound	RP(O)(OH)(H)	RP(O)(OH)(CH_2OH)	RP(O)(OH)(CH_2NHMe_2)Cl
	1	**9**	**10**
solvent	$CDCl_3$	CD_3CN	CD_3CN
C(5)	20.2	23.8	23.8
C(9) Me''	21.1	25.7	25.7
C(6)	24.6	28.2	28.2
C(8)	26.6	26.7	31.2
$^1J_{\text{P-C(8)}}$	93.5 Hz	89.2 Hz	96.4 Hz
C(10)Me'	31.8	35.5	35.5
C(7)	37.6	40.5	40.5
C(2)	37.5	37.8	41.2
$^3J_{\text{P-C-C-C(2)}}$	12.2 Hz	10.7 Hz	11.8 Hz
C(4)	42.1	45.9	45.9
$^3J_{\text{P-C-C-C(4)}}$	6.2 Hz	3.1 Hz	3.1 Hz
C(3)	43.4	47.2	47.1
$^2J_{\text{P-C-C(3)}}$	1.5 Hz	4.6 Hz	4.6 Hz
C(1)	48.4	52.0	51.9
CH_2X	-	63.3 (X=OH)	58.2 (X=N)
$^1J_{\text{P-CH}_2\text{X}}$	-	108.4 Hz (X=OH)	84.4 Hz (X=N)
$NH(CH_3)_2$	-	-	48.6#

Table 2.13: A comparison of the ^{13}C NMR chemical shifts [75 MHz] of 8-camphanylphosphinic acid (**1**) and derivatives **9** and **10** .

R = $C_{10}H_{17}$ = 8-camphanyl.

# denotes multiplicity not resolved

The influence of electronegativity upon $^1J_{\text{P-C}}$ coupling constants is demonstrated by the difference between the $^1J_{\text{P-C(8)}}$ [89.2 Hz] and $^1J_{\text{P-CH}_2\text{OH}}$ [108.4 Hz] coupling constants within **9**. A comparison of carbon atoms of the camphanyl moiety [C(8)] and the hydroxymethyl group [CH_2OH] shows that these atoms only differ in that the hydroxymethyl group has the more electronegative hydroxyl group directly attached, which in turn results in a larger $^1J_{\text{P-C}}$ coupling constant. The $^1J_{\text{P-C(8)}}$ and $^1J_{\text{P-CH}_2\text{N}}$ coupling constants

within **10** [84.4 and 96.4 Hz respectively] are unlike those of **9** [108.4 and 89.2 Hz respectively] in that the magnitude of the $^{1}J_{\text{P-C(8)}}$ and $^{1}J_{\text{P-}\ \text{CH}_2\text{N}}$ coupling constants have been reversed.

Compound	RP(O)(OH)(H)	RP(O)(OH)(CH_2OH)	[RP(O)(OH)(CH_2NHMe_2)]Cl
	1	**9**	**10**
solvent	$CDCl_3$	CD_3CN	CD_3CN
$^{1}J_{\text{P-C(8)}}$	93.5 Hz	89.2 Hz	96.4 Hz
$^{1}J_{\text{P-CH}_2\text{X}}$	-	108.4 Hz (X=OH)	84.4 Hz (X= $CH_2NHMe_2^+$)

Table 2.14: One-bond phosphorus-to-carbon coupling constants of **1**, **9** and **10**.

2.4 Synthesis and characterisation of polymeric calcium 8-camphanylphosphinate (13)

2.4.1 Introduction

The cooperative assembly of molecular precursors into complex structures, termed "self-assembly", is an area of significant interest as these materials tend to have both novel structures and novel applications. One such example is the self-assembly of nanostructures using metal phosphates, phosphonates, and phosphinates which have applications in catalysis, ion exchange, and sorptive processes[36]. Specific examples include molecular sieve alumino- and gallo-phosphates, layered phosphonates having the ability to undergo shape-[37] and enantioselective[38] intercalation reactions, and a vanadium phosphate which adopts a novel chiral double-helix structure[39]. However studies to date have been largely restricted to salts of relatively simple, sterically non-demanding organophosphorus acids.

The newly synthesised camphene-derived phosphinic acid **1** thus represented an ideal precursor to the synthesis of metal derivatives which contain a sterically demanding organophosphorus acid. The objective of this part of the thesis was therefore to synthesise and characterise new metal salts of 8-camphanylphosphinic acid (**1**).

The synthesis of metal phosphinates usually involves the precipitation of the metal phosphinate from a solution of a metal salt and phosphinic acid, Scheme 2.23.

$$n\text{R-PO}_2\text{H}_2 + \text{M}^{n+} \longrightarrow (\text{R-PO}_2\text{H})_n\text{M} + n\text{H}^+$$

Scheme 2.23: The precipitation of metal phosphinates from the phosphinic acid and metal salt.

Although preparation of the metal phosphinate is straightforward the difficulty of this type of research often lies in the production of single crystals of suitable quality for structural characterisation by X-ray diffraction. Single

crystals can be obtained *via* a number of methods, most of which involve the slow evaporation of a solution of the metal salt and phosphinic acid. The pH of the solution may also be controlled to facilitate slow crystallisation of the metal phosphinate. One such example, which is illustrated in Scheme 2.24, is the use of urea which hydrolyses slowly to ammonia and reacts with the phosphinic acid to form the ammonium phosphinate [$(R\text{-}PO_2H^-)(NH_4^+)$]. The intermediate subsequently reacts with a metal ion [M^{2+}] to form the desired metal phosphinate [$(R\text{-}PO_2H)_2M$]. It is worth noting that restricting the amount of water present controls the rate of formation of the metal phosphinate by controlling the rate at which ammonium phosphinate is formed. This ensures the slow crystallisation of the metal phosphinate and hence an improved chance of obtaining crystals of X-ray diffraction quality.

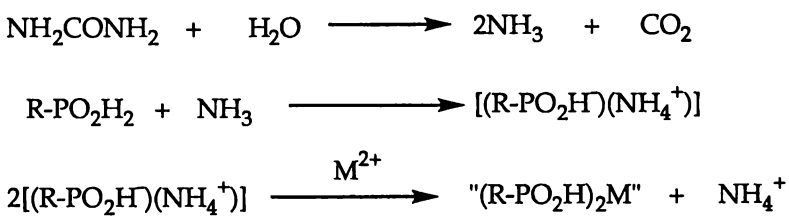

Scheme 2.24: The schematic formation of divalent metal phosphinates by the slow hydrolysis of urea.

2.4.2 Results and discussion

The reaction of 8-camphanylphosphinic acid (**1**) with 0.5 mol equivalent of $Ca(NO_3)_2.4H_2O$ and excess urea [for pH control] for 5 days yields a colourless solution which, upon slow evaporation, afforded colourless prismatic crystals (see Scheme 2.25). These were characterised as the polymeric calcium salt $[Ca(RPO_2H)_2(RPO_2H_2)(H_2O)]_n$ {R=8-camphanyl} (**13**) on the basis of a single-crystal X-ray study [refer to section 2.4.3 for more detail].

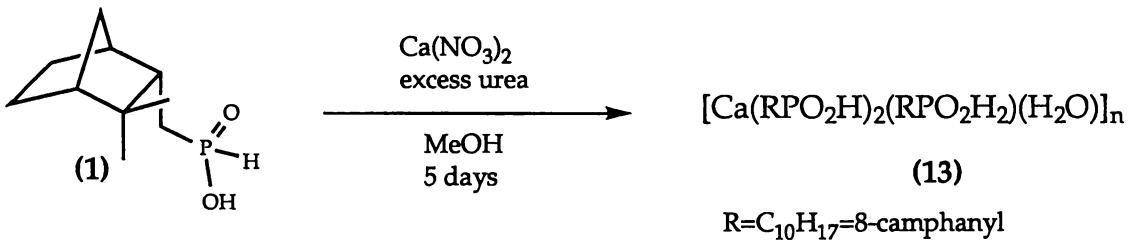

Scheme 2.25: The synthesis of polymeric calcium phosphinate.

Crystals of **13** are soluble in methanol, and the ^{31}P-$\{^1H\}$ NMR spectrum of the resulting solution shows a single peak at δ 29.1, close to the predicted weighted average position for two camphanylphosphinates [δ *ca.* 26.5] and one 8-camphanylphosphinic acid [δ 35.4], indicating that the polymeric structure of **13** is not retained in solution.

2.4.3 X-ray structure of polymeric calcium phosphinate (13)

In order to unambiguously characterise the nature of **13**, a single-crystal X-ray diffraction study was carried out. Crystal data, intensity measurements and structure solution and refinement details for **13** are presented in the experimental section. Full tables of bond lengths and angles are presented in Appendix III.

Because of the relatively poor quality of the crystals, and the disorder of the camphanyl groups, arising from librational effects and possibly also from superposition of (+) and (-) enantiomers, the structure determination is less precise than usual [R = 0.148]. A detailed discussion of bond parameters is therefore unfortunately precluded. Nevertheless, the overall structural features are clear and of interest.

The asymmetric unit formally consists of two Ca^{2+} ions, four $C_{10}H_{17}PO_2H^-$ anions, two $C_{10}H_{17}PO_2H_2$ molecules, and two water molecules, linked to form a buckled ladder-like chain polymer. The coordination geometries about the Ca^{2+} ions are given in Figure 2.9 along with Table 2.15, which contains selected bond lengths and angles. Each of the crystallographically distinct, but chemically equivalent, Ca^{2+} ions is six-coordinate, being bonded to one H_2O ligand, to two oxygen atoms from terminally-bonded phosphinates, to two oxygen atoms which bridge symmetry-related Ca^{2+} ions, and to one oxygen atom from a phosphinate which bridges between the two independent Ca^{2+} ions.

There are two types of phosphinate groups. Two of them in the backbone of the ladder [labelled P(5) and P(6) in Figure 2.9] are present as the anion $C_{10}H_{17}PO_2H^-$, and have one oxygen bonded terminally to one Ca^{2+} ion, and the other oxygen doubly bridging the other Ca^{2+} ions. The other four ligands are terminally bonded, two to each of the two distinct Ca^{2+} ions. Formally, these are present as two $C_{10}H_{17}PO_2H^-$ and two $C_{10}H_{17}PO_2H_2$, but the OH group of one ligand is H-bonded to the free oxygen of an adjacent ligand, rendering them equivalent. The net result of these interactions is to generate a buckled ladder consisting of alternating four-membered Ca_2O_2 and eight-membered Ca-O-P-O-Ca-O-P-O rings, supported by the P-O-

H···O=P H-bonding interactions between ligands on adjacent Ca^{2+} ions, which further serve to bind the chain together.

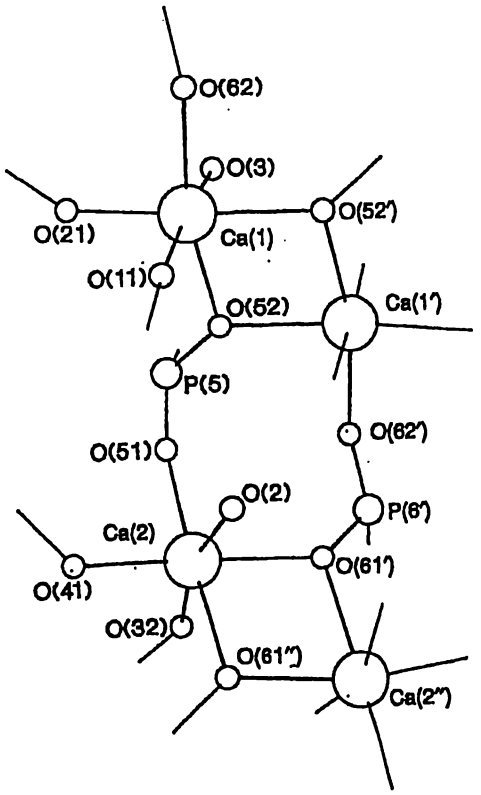

Figure 2.9: Coordination geometry about the calcium atoms in the polymeric chain of **13**, showing the alternating four- and eight-membered rings and the atom numbering scheme.

Ca(1)-O(3)	2.413(13)	Ca(2)-O(2)	2.414(13)
Ca(1)-O(52)	2.361(13)	Ca(1)-O(52)'	2.366(12)
P(5)-O(51)	1.45(2)	P(5)-O(52)	1.496(13)
Ca(2)-O(51)	2.26(2)	Ca(1)-O(11)	2.29(2)
Ca(1)-O(21)	2.34(2)	Ca(2)-O(32)	2.32(2)
Ca(2)-O(41)	2.29(2)	O(52)-Ca(1)-O(52)'	78.1(5)
Ca(1)-O(52)-Ca(1)'	101.9(5)	O(51)-P(5)-O(52)	119.5(9)
P(5)-O(51)-Ca(2)	158.9(11)	P(5)-O(52)-Ca(1)	124.3(7)
O(3)-Ca(1)-O(52)'	81.4(4)	O(11)-Ca(1)-O(52)'	98.3(5)

Table 2.15: Selected bond lengths (Å) and angles (°) of **13**. Estimated standard deviations are in parentheses.

The dominance of the bulky camphanyl groups are clearly illustrated in the space-filling diagram of **13**, Figure 2.10. These groups form a coherent, essentially 'close-packed' hydrocarbon sheath around the central hydrophilic inorganic Ca/O/P core. Individual chains resemble an 'insulated wire'. It is worth noting that equal numbers of *1R, 4S-* and *1S, 4R*-enantiomers of **1** were located in the structure of **13**.

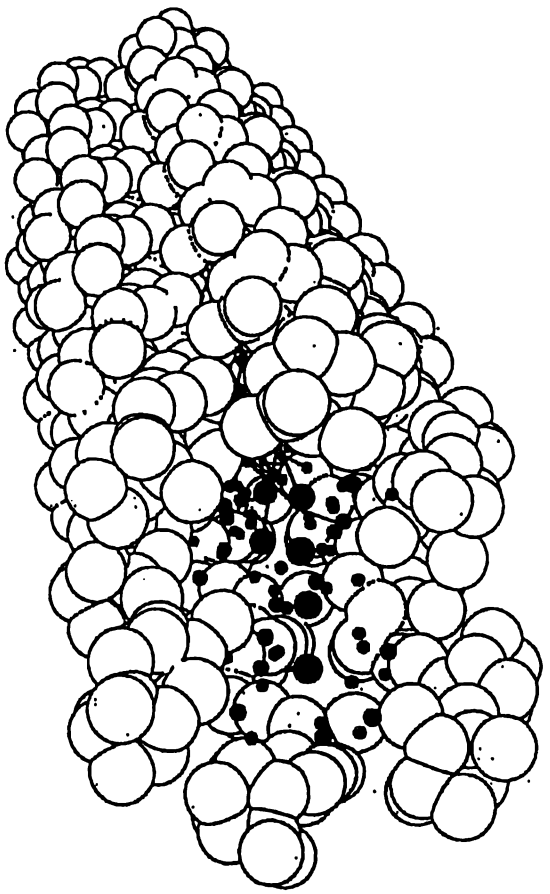

Figure 2.10: Space-filling representation of the polymeric chain, with calcium, phosphorus and oxygen atoms of the central hydrophilic core shown by the smaller black circles, and the carbon atoms of the camphanyl group by the larger open circles.

In contrast to the metal phosphonates, relatively few metal derivatives of phosphinic [or dialkyl phosphoric] acids have been structurally characterised. The chain-like structure adopted by **13** is not unique to this system and has been observed in other metal phosphinates[40].

However the incorporation of neutral coordinated phosphinic acids is unique and appears to be a new feature in the structural chemistry of this system. It seems reasonable to propose that the self-assembly of **13** is largely directed by the steric requirements of the bulky camphanyl moieties.

To conclude it also seems reasonable to propose that these bulky camphanyl moieties and their steric requirements, will feature predominantly in the structural chemistry of camphanyl-metal salts which contain metals of different coordination requirements. This may in turn lead to the development of other novel structural materials.

2.5 *Experimental*

General instrumental techniques are as described in Appendix II. The following reagents were used as supplied from commercial sources: benzoyl peroxide (BDH), (+)-1R, 4S-camphene (BDH 94%), hypophosphorous acid (Albright & Wilson Ltd., 50% w/w aqueous solution) and phenylphosphinic acid (Aldrich). Analytical grades of aqueous formaldehyde, hydrochloric acid, paraformaldehyde, potassium hydroxide, urea and triethylamine were all used as supplied. Other reagents used were laboratory grade and were used as supplied. All solvents used were of reagent grade. Petroleum spirit refers to the fraction of b.p. 40-60°C. Diazomethane was synthesised by a standard literature procedure[41].

2.5.1 Synthesis of 8-camphanylphosphinic acid (1)

A mixture of 50% hypophosphorous acid solution (660 mL, 399.3 g, 6.06 mol), isopropanol (600 mL) and technical grade camphene (215.5 g, 1.58 mol) was heated to reflux. Approximately 22.4 g of benzoyl peroxide, in approximately 5 g portions, was added over 14 h. Progress of the reaction was monitored by ^{31}P NMR. When complete, water (400 mL) was added and the volatile organics removed on a rotary evaporator. The oily product was taken up into CH_2Cl_2 (400 mL) and the crude 8-camphanylphosphinic acid extracted into an excess of 15% aqueous sodium hydroxide and washed with CH_2Cl_2 (200 mL). The aqueous layer was acidified to pH 0 with concentrated HCl and the organics extracted with CH_2Cl_2 (600 mL). The organic phase was dried over dry magnesium sulfate and evaporated to dryness to give a white crystalline solid. The crude 8-camphanylphosphinic acid (**1**) was recrystallised from CH_2Cl_2/petroleum spirit to give white needle-like crystals (265 g, 83% based on camphene content), m.p. 93-95°C. (Found: C, 59.30; H, 9.43%. $C_{10}H_{19}O_2P$ requires C, 59.37; H, 9.47 %.) Fast-atom

bombardment MS (*m*-nitrobenzyl alcohol matrix, positive ion mode) $[M+H]^+$ at *m/z* 203. ESMS (cone 45 V, negative ion); $[M-H^+]^-$ at *m/z* 201.

NMR: $^{31}P-\{^1H\}$: δ 38.8 [s]; ^{31}P: δ 38.8 [m, ^1J(PH) 556.6].

^1H: δ 12.49 [1H, s, br, OH], 7.06 [1H, dt, P-H, $^1J_{P-H}$ 538.2, ^3J 2.0], 2.26 [1H, s, br, H_4], 1.79 [1H, m, H_3]$_a$, 1.75 [2H, m, H_1, $H_{8'/8''}$]$_b$, 1.71 [1H, m, $H_{8'/8''}$]$_b$, 1.64 [1H, d, ^2J 9.9, $H_{7''}$]$_a$, 1.53 [1H, m, $H_{6''}$], 1.29 [2H, m, $H_{5''/5'}$]$_b$, 1.24 [1H, m, $H_{6'}$]$_b$, 1.18 [1H, dt, ^2J 9.9, ^3J 1.7, $H_{7'}$]$_a$, 0.95 [3H, s, Me'], 0.78 [3H, s, Me''].

a: partially overlapping signals

b: overlapping signals

^{13}C: δ 48.4 [s, C(1)], 43.4 [d, $^2J_{P-C-C}$ 1.5 Hz, C(3)], 42.1 [d, $^3J_{P-C-C-C}$ 6.2 Hz, C(4)], 37.5 [d, $^3J_{P-C-C-C}$ 12.2 Hz, C(2)], 37.6 [s, C(7)], 31.8 [s, C(10)], 26.6 [d, $^1J_{P-C}$ 93.5 Hz, C(8)], 24.6 [s, C(6)], 22.1 [s, C(9)], and 20.2 [s, C(5)].

I.R. : υ(P=O) region (1300-1140 cm^{-1}) 1200.9, 1193.4 strong

υ(P-OH) region (1040-910 cm^{-1}) 996.3, 980.0, 963.4 broad, strong

Due to the large number of overlapping I.R. signals the above stretching frequencies were only tentatively assigned.

The attempted preparation of chiral **1** starting from (R)-(+)-camphene (Aldrich; 94% (R)-(+)-camphene, 6% tricyclene) yielded only racemic material. The ORD and CD spectra of **1** in methanol, which were obtained by Dr M. Prinsep at the University of Canterbury, gave no polarisation of light.

2.5.2 *Synthesis of 8-camphanyl(phenyl)phosphinic acid (3)*

Phenylphosphinic acid (5.06 g, 0.018 mol) and technical camphene (17.9 g, 0.13 mol) were refluxed in isopropanol (100 mL), and benzoyl

peroxide (*ca.* 1 g) in 0.2 g portions was added over 6 h. The reaction workup was as above for **1**. The crude product was recrystallised from CH_2Cl_2/petroleum spirit to give white needle-like crystals of **3** (8.02g, 81%), m.p. 158-159 °C. (Found C, 69.01; H, 8.06%. $C_{16}H_{23}O_2P$ requires C, 69.03; H, 8.33 %.) ESMS (cone 45, negative ion); $[M\text{-}H^+]^-$ at *m/z* 277.

NMR: $^{31}P\text{-}\{^1H\}$: δ 47.1 [s]

^1H: δ 11.14, [1H, s, br, OH], 7.74-7.70, 7.46-7.43, 7.40-7.36 [5H, m, br, Ph]$_b$, 2.14 [1H, s, br, H_4], 1.79 [1H, d, ^2J 11.0, $H_{8'/8''}]_a$, 1.76 [1H, m, br, $H_{8'/8''}]_b$, 1.75 [1H, m, br, $H_3]_b$, 1.67 [1H, s, br, $H_1]_b$, 1.49 [1H, d, ^2J 10.6, $H_{7''}]_a$, 1.43 [1H, m, br, $H_{6''}]_a$, 1.18 [1H, m, $H_{5''}]_b$, 1.16 [1H, m, $H_{5'}]_b$, 1.19-1.14 [1H, m, $H_{6'}]_b$, 1.05 [1H, d, ^2J 10.6, $H_{7'}]_a$, 0.83 [3H, s, Me'], and 0.72 [3H, s, Me'']

a: partially overlapping signals

b: overlapping signals

$^{13}C\text{-}\{^1H\}$: δ 131.7 [d, $^4J_{P\text{-}C\text{-}C\text{-}C\text{-}C}$ 9.8 Hz, C(14)], 131.0 [d, $^2J_{P\text{-}C\text{-}C}$ 12.2 Hz, C(12)/C(16)], 128.4 [d, $^3J_{P\text{-}C\text{-}C\text{-}C}$ 12.2 Hz, C(13)/C(15)], 48.6 [s, C(1)], 44.3 [s, C(3)], 42.3 [s, C(4)], 37.5 [s, C(2)], 37.0 [s, C(7)], 31.8 [s, C(10)], 27.9 [d, $^1J_{P\text{-}C}$ 101.1 Hz, C(8)], 24.6 [s, C(6)], 22.0 [s, C(9)], 20.1 [s, C(5)].

Note: C(12)/C(16)=*ortho* carbon atoms, C(13)/C(15)=*meta* carbon atoms, C(14)=*para* carbon atom.

I.R.: υ(P=O) region (1300-1140 cm^{-1}): 1185.2, 1142.1, 1130.2 broad, strong

υ(P-OH) region (1040-910 cm^{-1}), υ(P-Ph) region (1130-1090, 1010-990): 1083.1, 1068.0, 983.6, 971.9, 958.7 broad, strong.

Due to the large number of overlapping I.R. signals the above stretching frequencies were only tentatively assigned.

2.5.3 Synthesis of methyl 8-camphanylphosphinate (6)

An excess of diazomethane was added to 8-camphanylphosphinic acid (**1**) (0.30 g, 1.4 mmol) and the resulting solution stoppered. After 24 h the excess diazomethane was removed by evaporation at atmospheric pressure yielding a colourless oil **6** (0.31 g, 98%) that was further dried under vacuum. GCMS *m/z* at 216 (M^+, 16%).

NMR: $^{31}P-\{^1H\}$: δ 43.1 [s, P], 42.6 [s, P'].

^{13}C: δ 52.7 [d, $^2J_{P\text{-}C\text{-}C}$ 3.3 Hz, OMe]*, 48.4 [s, C(1)], 43.3, 43.2 [s, C(3)], 42.2, 42.0 [d, $^3J_{P\text{-}C\text{-}C\text{-}C}$ 5.6 Hz, C(4)], 37.5 [d, $^2J_{P\text{-}C\text{-}C}$ 12.5 Hz, C(2)], 37.1 [s, C(7)], 31.75, 31.70 9 [s, C(10)], 26.35, 26.25 [d, $^1J_{P\text{-}C}$ 92.8 Hz, C(8)], 24.5 [s, C(6)], 22.0 [s, C(9)], 20.1 [s, C(5)].

* denotes a tentative assignment

I.R. : υ(P=O) region (1300-1140 cm^{-1}): 1247.9, 1226.2 broad, strong

υ(P-OH) region (1040-910 cm^{-1}): 1042.9, 1002, 973.0 broad, strong

Due to the large number of overlapping I.R. signals the above stretching frequencies were only tentatively assigned.

Methyl 8-camphanylphosphinate hydrolyses over 24 h in the presence of air to form 8-camphanylphosphinic acid (**1**). Despite several attempts to purify the methyl ester by vacuum distillation [126°C at 0.5 mm Hg] a sample suitable for elemental analysis was not obtained.

Preliminary GCMS studies [50°C to 250°C at 5°C per mins] gave one major component eluting at 5.92 mins [R_f=0.15, M^+ at *m/z* 216] which was resolved into two overlapping signals [(R_f=0.165, M^+ at *m/z* 216) and (R_f=0.166, M^+ at *m/z* 216)] using a temperature programme of 50°C to 250°C at 1°C per mins. Preparative separation of the diastereoisomers was not undertaken. The minor addition product **6a** [R_f=0.162, M^+ at *m/z* 216] and minor component, methyl di(8-camphanyl)phosphinate (**8**) [R_f=0.70, M^+ at *m/z* 352] were also detected by GCMS.

2.5.4 Synthesis of methyl 8-camphanyl(phenyl)phosphinate (7)

An excess of diazomethane was added to 8-camphanyl(phenyl)-phosphinic acid (**3**) (0.30 g, 1.0 mmol) and the resulting solution stoppered. After 24 h the excess diazomethane was removed by evaporation at atmospheric pressure yielding a colourless oil which was dried further under vacuum. Recrystallisation of the colourless oil from $CHCl_3$/petroleum spirit gave a white solid **7** (0.30 g, 96%), m.p. 69-89°C. (Analysis: Found: C, 69.94%; H, 8.62%. $C_{17}H_{25}O_2P$ requires C, 69.82; H, 8.62 %.) GCMS *m/z* at 292 (M^+, 21%);
NMR: $^{31}P\text{-}\{^1H\}$: δ 47.1 [s, P], 46.8 [s, P']

Isomer 1: ^1H: δ 8.02-7.05 [5H, m, Ph]$^{\#}$, 3.55, 3.51 [3H, s, OMe]$^{\#}$, 2.28 [1H, br, s, H_4*], 1.96-1.67 [2H, m, $H_{8'/8''}$*], 1.74 [1H, br, m, H_3*], 1.66 [1H, br, s, H_1*], 1.53 [1H, d, ^2J 10.6, $H_{7''}$*], 1.47 [1H, m, $H_{6''}$*], 1.28 [2H, m, $H_{5''/5'}$*], 1.18 [1H, m, $H_{6'}$*], 1.05 [1H, $H_{7'}$*], 0.79 [3H, s, Me'''*], 0.68 [3H, s, Me'*].

$^{13}C\text{-}\{^1H\}$: δ 132.5-128.0 [6C, m, Ar]$^{\#}$, 50.85, 50.95 [d, $^2J_{P\text{-}C\text{-}C}$ 4.4 Hz, OMe]$^{\#}$, 48.4 [s, C(1)*], 43.7 [d, $^2J_{P\text{-}C\text{-}C}$ 3.1 Hz, C(3)*], 42.2 [d, $^3J_{P\text{-}C\text{-}C\text{-}C}$ 3.9 Hz, C(4)*], 37.6, 37.4 [d, $^1J_{P\text{-}C\text{-}C}$ 6.4 Hz, C(2)*]$^{\#}$, 37.0 [s, C(7)*], 31.6 [s, C(10)*], 26.9, 26.8 [d, $^1J_{P\text{-}C}$ 101.1 Hz, C(8)*]$^{\#}$, 24.6 [s, C(6)*], 22.1 [s, C(9)*], 20.2 [s, C(5)*].

Isomer 2 :^1H : δ 8.02-7.05 [5H, m, Ph]$^{\#}$, 3.55, 3.51 [3H, OMe]$^{\#}$, 1.98 [1H, br, s, H_4], 1.85 [2H, m, $H_{8'/8''}$], 1.81 [1H, br, m, H_3], 1.66 [1H, br, s, H_1], 1.53 [1H, d, ^2J 10.6, $H_{7''}$], 1.42 [1H, m, $H_{6''}$], 0.95 [2H, m, $H_{5''/5'}$], 1.10 [1H, m, $H_{6'}$], 1.01 [1H, $H_{7'}$], 0.88 [3H, s, Me''], 0.75 [3H, s, Me'].

$^{13}C\text{-}\{^1H\}$: δ 132.5-128.0 [6C, m, Ar]$^{\#}$, 50.85, 50.95 [d, ^2J (PC) 4.4, OMe]$^{\#}$, 48.4 [s, C(1)], 43.8 [d, $^2J_{P\text{-}C\text{-}C}$ 3.1 Hz, C(3)], 42.4 [d, $^3J_{P\text{-}C\text{-}C\text{-}C}$ 3.9 Hz, C(4)], 37.6,

37.4 [d, $^{3}J_{\text{P-C-C-C}}$ 6.4 Hz, C(2)]#, 37.0 [s, C(7)], 31.6 [s, C(10)], 26.9, 26.8 [d, $^{1}J_{\text{P-C}}$ 101.1 Hz, C(8)]#, 24.6 [s, C(6)], 22.2 [s, C(9)], 19.9 [s, C(5)].

# denotes signals not assigned to an isomer, * denotes tentative assignment of resonances.

All proton signals except for H_4 and the Me signals of each isomer overlapped.

Due to the complexity of I.R. spectrum of **7** no signals were assigned.

The GCMS analysis of the reaction product [50°C to 250°C at 1°C per mins] gave two major products with similar retention times [R_f=0.180 and 0.81], identical parent ion masses [M^+ at m/z 277] and equal areas. Preparative separation of the diastereoisomers was not pursued. Also present was the ester of the minor addition product **7a** [R_f=0.78 M^+ at m/z 277].

2.5.5 Synthesis of hydroxymethyl 8-camphanylphosphinic acid (9)

An excess of paraformaldehyde (2.1 g) was added to a vigorously stirred melt of 8-camphanylphosphinic acid (**1**) (5.0 g, 0.02 mol) at 150°C. Upon addition of paraformaldehyde the reaction mixture effervesced and after 20 mins went pale yellow in colour. After 10 h of vigorous stirring at 150°C the reaction mixture was cooled, water (2 mL), HCl (2 mL), methanol (20 mL) added and the resulting solution refluxed for a further 1 h. The solvent was removed under vacuum and the white solid dissolved in a minimum amount of ether/methanol (90-10). Petroleum spirit was added slowly to this solution until a faint precipitate appeared. The solvent was then removed under vacuum until approximately one third of the solid had precipitated out of solution at which time the crystalline solid was filtered. The supernatant was reconcentrated and the process repeated to give a white solid **9** (2.1 g, 45%), m.p. 146-148°C. (Analysis: Found: C, 56.67; H, 9.39%. $C_{11}H_{21}O_3P$ requires C, 58.87; H, 9.12%.) ESMS (cone 45 V, positive ion);

$[M+H]^+$ at *m/z* 233, $[2M+H]^+$ at *m/z* 465, $[3M+H]^+$ at *m/z* 697, $[4M+H]^+$ at *m/z* 929. ESMS (cone 45 V, negative ion); $[2M-H]^-$ at *m/z* 463.

NMR: $^{31}P-\{^1H\}$: (CD_3OD): δ 51.0 [s].

$^{13}C-\{^1H\}$: δ 63.3 [d, $^1J_{P-C}$ 108.4 Hz, CH_2OH], 52.0 [s, C(1)], 47.2 [d, $^2J_{P-C-C}$ 4.0 Hz, C(3)], 45.9 [d, $^3J_{P-C-C-C}$ 3.1 Hz, C(4)], 37.8 [d, $^3J_{P-C-C-C}$ 10.7 Hz, C(2)], 40.5 [s, C(7)], 35.5 [s, C(10)], 28.2 [s, C(6)], 26.7 [d, $^1J_{P-C}$ 89.2 Hz, C(8)], 25.7 [s, C(9)], 23.8 [s, C(5)].

*2.5.6 Synthesis of 8-camphanyl-N,N-dimethylaminomethylphosphinic acid hydrochloride (**10**)*

To **1** (3.82 g, 0.019 mol) was added isopropanol (50 mL), concentrated hydrochloric acid (4.5 mL) and dimethylamine (3.5 mL, 26%w/v). The resulting solution was heated to reflux and while being vigorously stirred, formaldehyde [5.5 mL (40%w/v) in 10 mL H_2O] was added dropwise. After 10 h a further 6 mL of formaldehyde was added dropwise and the solution refluxed for another 5 h. Upon removal of the solvent a yellow oil formed which solidified upon addition of $CHCl_3$ (150 mL). The white solid **10** (1.88 g, 90%) was filtered and washed with $CHCl_3$. A sample suitable for elemental analysis was obtained by recrystallisation from methanol/ether. (Found: C, 49.39; H, 9.16%. $C_{13}H_{27}NO_2PCl.H_2O$ requires C, 49.82; H, 9.33 %.) The presence of H_2O was confirmed by ^1H NMR studies.

ESMS (cone 15 V, positive ion); *A*=[$C_{10}H_{17}P(O)(OH)CH_2NHMe_2]^+$ at *m/z* 260, (100%), $[2A-H]^+$ at *m/z* 519 (55%).

ESMS (cone 15 V, negative ion); *B*=$[C_{10}H_{17}P(O)(O)CH_2NMe_2]^-$ at *m/z* 258 (100%); $[B+2H_2O]^-$ at *m/z* 294 (85%); $[2B+H]^-$ at *m/z* 517 (35%); $[2B+H+2H_2O]^-$ at *m/z* 553 (25%); $[3B+2H]^-$ at *m/z* 776 (10%); $[3B+2H+2H_2O]^-$ at *m/z* 812 (7%).

B is defined as the principal ion (*i.e.* 100% intensity)

NMR: ^{31}P-{^{1}H}: δ 40.5 [s].

^{13}C-{^{1}H}: δ 58.2 [d, $^{1}J_{P\text{-}C}$ 84.4 Hz, $\underline{C}H_2N$], 51.9 [s, C(1)], 48.6 [m, -$N(CH_3)_2$]#, 47.1 [d, $^{2}J_{P\text{-}C\text{-}C}$ 4.6 Hz, C(3)], 45.9 [d, $^{3}J_{P\text{-}C\text{-}C\text{-}C}$ 3.1 Hz, C(4)], 41.2 [d, $^{3}J_{P\text{-}C\text{-}C\text{-}C}$ 11.8 Hz, C(2)], 40.5 [s, C(7)], 35.5 [s, C(10)], 31.2 [d, $^{1}J_{P\text{-}C}$ 96.4 Hz, C(8)], 28.2 [s, C(6)], 25.7 [s, C(9)], 23.8 [s, C(5)].
# denotes multiplity not resolved.

*2.5.7 Synthesis of 8-camphanylphosphonic dichloride (**11**)*

An excess of thionyl chloride (40 mL) was added to 8-camphanyl-phosphinic acid (**1**) (1.67g, 8.2 mmol). While being stirred, pyridine (10 drops) was added and the resulting yellow solution refluxed for 7.5 h. Removal of the thionyl chloride under reduced pressure gave **11** as a light yellow oil (1.88 g, 90%). (Found: C, 47.92; H, 6.97%. $C_{10}H_{17}OPCl_2$ requires C, 47.24; H, 6.74 %.) GCMS *m/z* at 255 (M^+, 16%).

NMR: ^{31}P-{^{1}H}: δ 51.6 [s]

^{1}H: δ 2.54 [1H, m, br, $H_{8'/8''}$], 2.49 [1H, m, br, $H_{8'/8''}$], 2.34 [1H, br, s, H_4], 1.93 [1H, m, br, H_3], 1.71 [1H, br, s, H_1], 1.59 [1H, d, ^{2}J 10.1, $H_{7''}$], 1.46 [1H, m, br, $H_{6''}$], 1.36 [1H, m, br, $H_{5''}$]$_a$, 1.31 [1H, m, br, $H_{5'}$]$_b$, 1.21 [1H, d, *J* 4.8, $H_{6'}$]$_b$, 1.15 [1H, d, ^{2}J 10.1, $H_{7'}$]$_a$, 0.91 (3H, s, Me'], and 0.74 [3H, s, Me''].

^{13}C-{^{1}H}: δ 48.3 [s, C(1)], 45.1 [d, $^{2}J_{P\text{-}C\text{-}C}$ 6.5 Hz, C(3)], 41.9 [d, $^{3}J_{P\text{-}C\text{-}C\text{-}C}$ 5.2 Hz, C(4)], 41.85 [d, $^{1}J_{P\text{-}C}$ 95.7 Hz, C(8)], 38.2 [d, $^{3}J_{P\text{-}C\text{-}C\text{-}C}$ 17.5 Hz, C(2)], 37.0 [s, C(7)], 31.6 [s, C(10)], 24.5 [s, C(6)], 21.9 [s, C(9)], 20.3 [s, C(5)].

a: partially overlapping signals

b: overlapping signals

2.5.8 *Synthesis of 8-camphanyl(phenyl)phosphinic chloride (12)*

To 8-camphanyl(phenyl)phosphinic acid (**3**) (0.61g, 2.1 mmol) and pyridine (8 drops) was added an excess of thionyl chloride (20 mL) and the resulting solution refluxed for 1.5 h. The thionyl chloride was removed under vacuum to give **12** as a yellow liquid (0.55 g, 86%). The ^{31}P NMR spectrum gave 2 signals at δ 57.8 and 57.2.

2.5.9 *Synthesis of polymeric calcium camphanylphosphinate (13)*

A solution of $Ca(NO_3)_2.4H_2O$ (0.585 g, 2.48 mmol) with **1** (1.00 g, 4.95 mmol) and urea (1.5 g, excess) in reagent grade methanol (30 mL) was warmed to 65°C for 5 days. The resulting solution was filtered to remove a small quantity of white solid, and the filtrate allowed to spontaneously evaporate, producing colourless needles which were filtered, washed with cold methanol (2 x 10 mL) and air dried, to give **13** (0.568 g, 35% based on Ca) m.p. fracture and turn opaque>100 °C, soften >210°C. (Found: C, 54.1; H, 9.7. $C_{30}H_{57}CaO_7P_3$ requires C, 54.4; H, 8.7%.)

NMR ^{31}P-{^1H} (CH_3OH, D_2O external lock) : δ 29.1 [s].

X-ray structure of polymeric calcium phosphinate (13)

Data were measured at -173 °C on a Nicolet R3 diffractometer with graphite monochromated Cu-Kα radiation using ω-scans. A total of 5302 reflections were collected with 4935 unique (R_{int} 0.048). After absorption correction (Φ scan method, $T_{max, min}$ 0.96, 0.66) 2834 reflections had $I > 2\sigma(I)$.

Crystal data: $C_{60}H_{100}Ca_2O_{14}P_6$, M_r =1311.46, triclinic, space group $P\bar{1}$, a =12.501(3), b=18.154(4), c = 18.474(4) Å, α=117.80(3), β=96.40(3),γ =102.20(3)°, U =3516.3(14) Å^3, Z = 2, D_c =1.239 g cm^{-3}.

Solution and refinement

The structure was solved by direct methods to give the Ca^{2+} ion and the P atom positions, and a subsequent difference map revealed the O atoms and the P-C-C carbons of the camphanyl groups, which refined cleanly in subsequent cycles. The remaining parts of the camphanyl groups showed significant disorder, so were refined with restrained C-C bond lengths of 1.54(5) Å. In the final cycles of least-squares refinement only the Ca and P atoms were refined anisotropically, while all C-C distances were restrained to 1.54(5) Å. H atoms were not included. Convergence gave $R_1 = 0.148$ [for 2834 data with $I > 2\sigma(I)$], 0.221 (all data), and $wR_2 = 0.431$ (all data), where $w = [s2(F_o^2) + (0.2072P)^2 + 70.21P]^{-1}$ and $P = 1/3\ [F_o^2 + 2F_c^2]$. Goodness of fit was 1.027. Programs used were SHELXS86[42] and SHELXL93[43].

References

1 D.F. Peppard, G.W. Mason, C.M. Andrejasich, *J. Inorg. Nucl. Chem.*, (1965), **27**, 2065; R.H. Williams, L.A. Hamilton, *J . Am. Chem. Soc.*, (1955), **77**, 3411.

2 U.S.A. Patent No. 2957931, (1960).

3 G. Quesnel, M. De Botton, A. Chambolle, R. Dulou, *Compt. Rend.*, (1960), **251**, 1074.

4 U.K. Patent, Albright and Wilson Ltd, GB 2268178 A, (1994).

5 W. Henderson, Personal communication, Waikato University

6 W.R. Vaughan, R. Perry, *J. Am. Chem. Soc.*, (1953), **75**, 3618.

7 W.R. Vaughan, C. T. Goetschel, M.H. Goodrow, C.L. Warren, *J. Am. Chem. Soc.*, (1963), **85**, 2282.

8 W.R. Vaughan, C.W. David, B.W. Everling, R.J. Kilian, J. Stochers, *J. Am. Chem. Soc.*, (1973), **95**, 1265, and references therein.

9 W.R. Vaughan, D.M. Teegarden, *J. Am. Chem. Soc.*, (1974), **96**, 4902.

10 M.E. Druyan, A.H. Reis, E. Gebert, S.W. Peterson, G.W. Mason, D.F. Peppard, *J. Am. Chem. Soc.*, (1976), 16, 4801.

11 J.R. Ferraro, G.W. Mason, D.F. Peppard, *J. Inorg. Nucl. Chem.*, (1961), **22**, 285.

12 P.C. Moews, J.R. Knox, W.R. Vaughan, *J. Am. Chem. Soc.*, (1978), **100**, 260.

13 F.H Allen, O. Kennard, D.G. Watson, L. Brammer, A.G. Orpen, R. Taylor, *J. Chem. Soc. Perkin Trans. II*, (1987), S1-S19.

14 W. Sawka-Dobrowolska, *Acta Cryst.*, (1988), **C44**, 2193.

15 J.B. Fenn, M. Mann, C.K. Meng, S.F. Wong, C.M. Whitehouse, *Mass Spectrometry Reviews*, (1990), **9**, 37; P. Kebarle, L. Tang, *Analytical Chemistry*, (1993), **65**, 972.

16 R. Colton, J.C. Traeger , J. Harvey, *Org. Mass Spectrom.*, (1992), **27**, 1030.

17 C.E.C.A. Hop, D.A. Saulys, D.F. Gaines, *Inorg. Chem.*, (1995), 34, 1977.

18 R. Colton, J.C. Traeger, *Inorg. Chim. Acta*, (1992), **201**, 153.

19 V.T. Borrett, R. Colton, J.C. Traeger, *Eur. Mass Spectrom.*, (1995), **1**, 131.

20 K. Laihia, E. Kolehmainen, P. Malkavaara, J. Kovola, P. Manttari, R. Kauppinen, *Magnetic Resonance in Chemistry*, (1992), 30, 754; A. Badjah-Hadj-Ahmed, B. Meklati, H. Watson, Q. Pham, *Magnetic Resonance in Chemistry*, (1992), 30, 807.

21 W.B. Smith, *Magnetic Resonance in Chemistry*, (1994), **32**, 316.

22 J.C. Tebby in *Phosphorus-31 NMR Spectroscopy in Stereochemical Analysis*, VCH Publishers Inc. (1987), 1-59 and references therein.

23 D.G. Gorenstein in *Handbook of Organophosphorus Chemistry*, Ed R. Engel, Published by Marcel Dekker Inc, New York (1992), 435-482.

24 G. Klose, *Ann.Phys.*, (1962), **9**, 262; G. Buchanan, J. Bowen, *Can. J. Chem.*, (1977), **55**, 604; G. Buchanan, C. Benezra, *Can. J. Chem.*, (1975), **54**, 231.

25 P.C. Crofts in *Organic Phosphorus Compounds*, Ed by G.M. Kosolapoff, L. Maier, Wiley and Sons (1973), **6**, 1-209 and references therein.

26 A.W. Frank in *Organic Phosphorus Compounds*, Ed by G.M. Kosolapoff, L. Maier, Wiley and Sons (1973), **4**, 255-462 and references therein.

27 C. Marie, *Ann. Chim. Phys.*, (1904), **3**, 335; A. Pudovik, I. Gur'yanova, L. Banderova, G. Romanov, *Zh. Obshch. Khim.*, (1969), **39**, 2418; (1970), **72**, 79164.

28 A. Pudovik, L. Spirina, M. Pudovik, Y. Kargin, L. Andreeva, *Zh. Obshch. Khim.*, (1969), **39**, 1715; (1969), **71**, 124597.

29 L. Maier, *Helv. Chim. Acta*, (1967), **50**, 1742.

30 R. Fox, W. Bailey, *J. Org. Chem.* , (1960), 25, 1447.

31 L. Maier, *Phosphorus, Sulphur and Silicon*, (1990), **47**, 465-470.

32 M. Fild, R. Schmutzler, S.C. Peake in *Organic Phosphorus Compounds*, Ed by G.M. Kosolapoff, L. Maier, Wiley and Sons (1973), 4, 155-253 and references therein.

33 T. Dawson, J. Armstrong, U.S.A. Patent No. 2847469, (1958).

34 K. Moedritzer, R. Millar, *Syn. React. Inorg. Metal-Org. Chem.*, (1974) **4**, 417.

35 E. Breitmaier in *Carbon-13 NMR Spectroscopy*, 3rd Ed, VCH Publishers, (1987).

36 M.E. Thompson, *Chem. Mater.*, (1994), **6**, 1168; S.L. Suib, *Chem. Rev.*, (1993), **93**, 803; G. Cao, H.G. Hong, T.E. Mallouk, *Acc. Chem. Res.*, (1992), **25**, 420; A. Clearfield, *Comments Inorg. Chem.*, (1990), **10**, 89.

37 G. Cao, V.M. Lynch, L.N. Yacullo, *Chem. Mater.*, (1993), **5**, 1000; G. Cao, T. Mallouk, *Inorg. Chem.*, (1991), **30**, 1434.

38 G. Cao, M.E. Garcia, M. Alcalá, L.F. Burgess, T.E. Mallouk, *J. Am. Chem. Soc.*, (1992), 114, 7574.

39 V. Soghomonian, Q. Chen, R.C. Haushalter, J. Zubieta, C.J. O'Connor, *Science*, (1993), **259**, 1596.

40 See, for example, W.T.A. Harrison, T.M. Nenoff, T.E. Gier, G.D. Stucky, *Inorg. Chem.*, (1992), **31**, 5395; S.J. Liu, R.J. Staples, J.P. Fackler (Jr), *Polyhedron*, (1992), **11**, 2427; M. Shieh, K.J. Martin, P.J. Squattrito, A. Clearfield, *Inorg. Chem.*, (1990), **29**, 958; P. Colamarino, P.L. Orioli, W.D. Benzinger, H.D. Gillman, *Inorg. Chem.*, (1976), **15**, 800.

41 *Org. Synth. Coll.*, (1943), Volume II, 165.

42 G.M. Sheldrick, SHELXS86 Program for the solution of crystal structures, University of Göttingen, (1986).

43 G.M. Sheldrick, SHELXL93 Program for the refinement of crystal structures, University of Göttingen, (1993).

Chapter Three

Synthesis and chemistry of 8-camphanyl-phosphonic acid and derivatives

*3.1 Synthesis and characterisation of 8-camphanyl-phosphonic acid (**14**)*

3.1.1 Introduction

The general reaction scheme for the oxidation of phosphinic acids to phosphonic acids is given in Scheme 3.1.

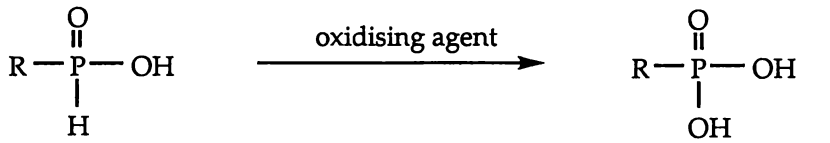

phosphinic acid — phosphonic acid

Scheme 3.1: The oxidation of phosphinic [RPO_2H_2] to phosphonic acid [RPO_3H_2] {R=alkyl group}.

Strong oxidising agents[1] such as concentrated hydrogen peroxide[2, 3], nitric acid[4, 5], alkaline permanganate[6, 7], mercuric chloride[6, 8], aqueous bromine[9], iodine[3, 7] and sulfur dioxide[10] are usually required. Aromatic phosphinic acids may suffer ring nitration if nitric acid is employed[11]. Phosphinic acids reduce ammoniacal silver nitrate and other metallic salts to the free metals[12].

More recent work involves the oxidation of phenylphosphinic acid [$PhPO_2H_2$] to phenylphosphonic acid [$PhPO_3H_2$] at room temperature using a solution of $Cu_2(\mu\text{-}O_2CCH_3)_4\,(H_2O)_2$[13] in pyridine. The phosphonic acid is

recovered as the monomeric copper(II) complex $Cu(PhPO_3H_2)(C_5H_5N)_4$-$.2CH_3OH$.

The synthesis of phosphonic acids can also be achieved by the hydrolysis of phosphonic dichlorides [$RP(O)Cl_2$]. This procedure, given in Scheme 3.2, is well documented in the literature and usually requires no more than stirring in ice or water[14]. More difficulty is encountered if the organic group is bulky but in such cases heating with dilute nitric acid[15, 16] or aqueous alkali[17, 18] is usually adequate.

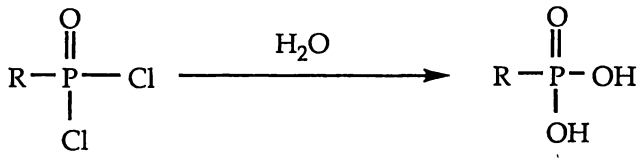

Scheme 3.2: The hydrolysis of phosphonic dichloride to phosphonic acid.

The camphene-derived phosphinic acid **1** and phosphonic dichloride **11** are both ideal precursors to the camphene-derived phosphonic acid 8-camphanylphosphonic acid. Hence an investigation of the feasibility of oxidising agents upon **1** and the hydrolysis of **11**, was undertaken.

3.1.2 Results and discussion

The camphene-derived phosphinic acid 8-camphanylphosphinic acid (**1**) is oxidised to 8-camphanylphosphonic acid (**14**) by the use of sulfur dioxide [SO_2] in isopropanol heated at reflux, Scheme 3.3. In this case the byproduct, elemental sulfur, is readily removed by simple filtration. Copper(II) nitrate in methanol heated at reflux also oxidises **1** to **14**, producing metallic copper, a byproduct that is also readily removed by filtration. Although posing practical problems, the use of gaseous SO_2 [*c.f.* Cu salt] is the preferred oxidising agent as higher yields are consistently obtained.

Alkaline hypochlorite may also be used for the oxidation of **1**, however this leads to an impure product. Alkaline hydrogen peroxide and

concentrated nitric acid were found to be completely ineffective oxidising agents for **1**[19].

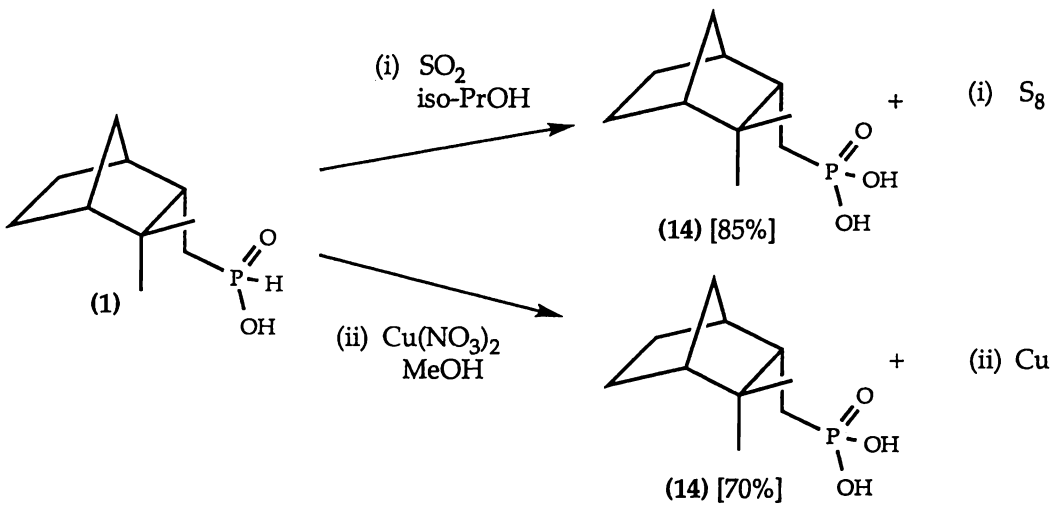

Scheme 3.3 : The oxidation of **1** to 8-camphanylphosphonic acid (**14**) using either (i) SO_2 or (ii) $Cu(NO_3)_2$. Percentage yields are presented in brackets.

An alternative synthetic route to **14**, Scheme 3.4, involves the oxidative chlorination of **1** to afford 8-camphanylphosphonic dichloride (**11**) [refer to section 2.3.2 for details on the preparation of **11**], which in turn is hydrolysed in mild conditions [water heated at reflux] precipitating **14** in high yield. This synthetic route involves an additional step [*c.f.* direct oxidation of **1**] and as a result is the least preferred.

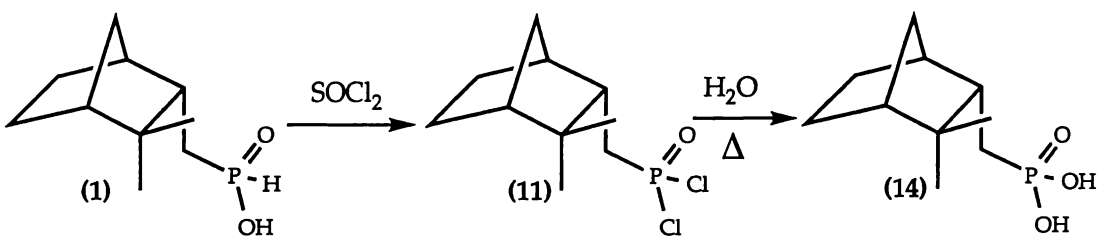

Scheme 3.4 : The synthesis of phosphonic acid **14** by the hydrolysis of 8-camphanylphosphonic dichloride (**11**).

The phosphonic acid **14** is a white solid which is only slightly soluble in organic solvents and water but readily soluble in low molecular weight alcohols. Detailed characterisation of **14** by X-ray crystallography and NMR spectroscopy is presented in sections 3.1.3 and 3.1.4 respectively. Elemental

microanalytical data collected for **14** are consistent with its formulated structure.

It is worth noting that the trace amount of **1a** [refer to section 2.1.2 for details of synthesis] present in **1**, is also expected to be oxidised by SO_2 to its corresponding phosphonic acid **14a**.

*3.1.3 X-ray crystal structure of 8-camphanylphosphonic acid (**14**)*

An investigation of the synthesis of new metal-phosphonate salts of 8-camphanylphosphonic acid (**14**) was undertaken. As with the synthesis of the metal-phosphinate salts of 8-camphanylphosphinic acid (**1**) [see section 2.4] this synthesis involved the heating of a methanol/water solution of **14** with urea and a metal salt. From one trial using strontium nitrate colourless hexagonal crystals were grown which were initially thought to be a strontium phosphonate salt. However refinement of the X-ray crystal data at Waikato University when strontium was included, met with little success. The examination of the data by Dr Mark Turnbull of Clark University revealed that strontium was not present, *i.e.* we were dealing not with a metal-phosphonate but with the phosphonic acid **14**. The growth of crystals of **14** are thought to arise from the slow evaporation of methanol from the methanol/water mixture and not from the action of urea [see section 2.4 for details].

The molecular structure of 8-camphanylphosphonic acid (**14**) together with the atom numbering scheme is shown in Figure 3.1. Bond lengths and selected bond angles of **14** are presented in Table 3.1. Crystal data, intensity measurements and structure solution and refinement details for **14** are presented in the experimental section. Full tables of bond lengths and angles are presented in Appendix III.

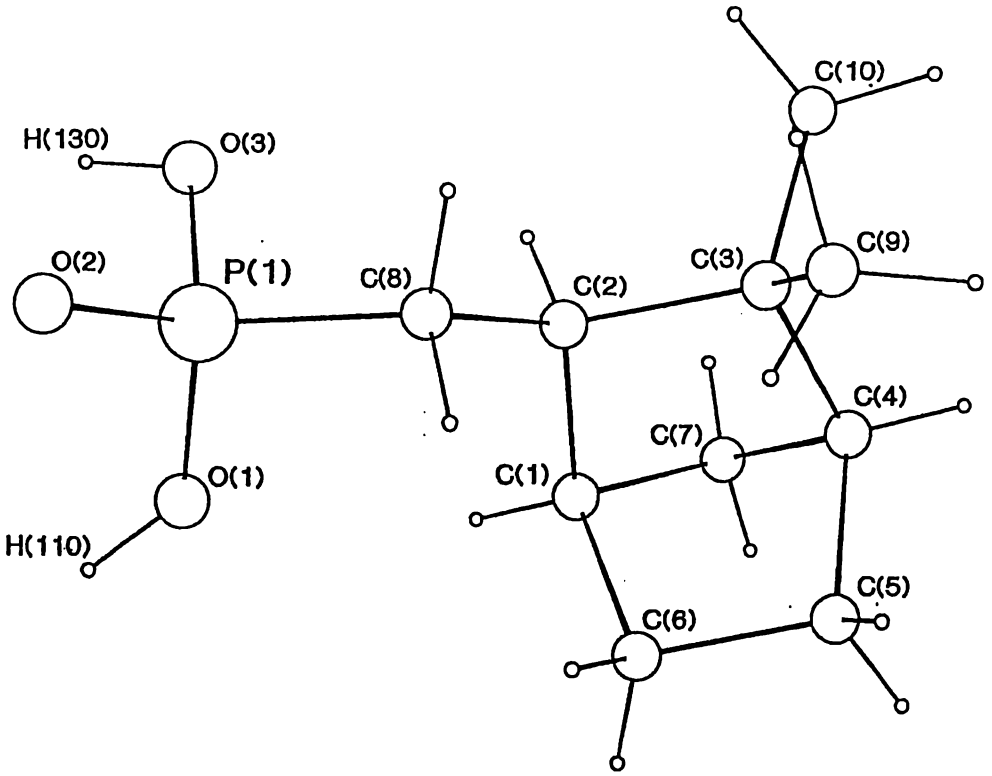

Figure 3.1: Molecular structure of 8-camphanylphosphonic acid (**14**) together with the atom numbering scheme.

P(1)-O(2)	1.511(5)	P(1)-O(1)	1.534(6)
P(1)-O(3)	1.548(6)	P(1)-C(8)	1.762(8)
C(4)-C(5)	1.521(11)	C(4)-C(7)	1.521(12)
C(4)-C(3)	1.555(11)	C(3)-C(8)	1.532(10)
C(3)-C(2)	1.576(11)	C(2)-C(1)	1.520(12)
C(2)-C(10)	1.522(12)	C(2)-C(9)	1.541(11)
C(1)-C(6)	1.529(12)	C(1)-C(7)	1.547(12)
C(6)-C(5)	1.538(12)		
O(1)-P(1)-C(8)	106.4(3)	O(1)-P(1)-O(3)	110.8(3)
O(3)-P(1)-C(8)	104.0(4)		

Table 3.1: Bond lengths (Å) and selected bond angles (°) of 8-camphanylphosphonic acid (**14**). Estimated standard deviations are in parentheses.

The structure confirms the formulation of the compound as 8-camphanylphosphonic acid, containing an *endo*-$CH_2PO_3H_2$ group. The marked asymmetry of the bridgehead observed in **1** [refer to section 2.1.3] is not observed in **14** where the bond distances to the bridgehead carbon C(7), Table 3.2, are crystallographically equivalent. A comparison of the C(8)-C(2)-C(3)-C(9) and C(8)-C(2)-C(3)-C(10) torsion angles of **1** and **14** shows that these torsion angles are also crystallographically equivalent.

Compound	C(1)-C(7)	C(4)-C(7)	C(8)-C(2)-C(3)-C(9)	C(8)-C(2)-C(3)-C(10)
1	1.59(1)	1.49(1)	-11.3(7)	109.3(7)
14	1.54(1)	1.52(1)	-10.35(11)	108.88(8)

Table 3.2: A comparison of selected bond lengths (Å) and torsion angles (°) of the phosphinic acid **1** and phosphonic acid **14**.

This suggests that if the asymmetry of the bridgehead of **1** was due to the steric interaction between the *exo*-methyl group [C(10)] and the bridgehead [C(7)] it follows that the bridgehead of **14** should experience a similar distortion. However this is not the case indicating that the bridgehead distortion observed in crystallographic studies of **1** is as postulated previously in section 2.1.3, the result of intermolecular contacts and not intramolecular contacts.

All other C-C bond lengths for **14**, which lie between 1.576(11)-1.520(12) Å, are comparable with that of 8-camphanylphosphinic acid (**1**) [1.54(18)-1.497(9) Å, section 2.1.3]. The average P-O bond length of **14** [1.531(5) Å] is similar to the average P-O bond lengths of the amino phosphonic acids $PhCH_2CH(NH_2)PO_3H_2$[20] and $HC(NH_2)(CH_2COOH)PO_3H_2$[21] [1.524(5) and 1.528(3) Å respectively] [Table 3.3]. Although the P-C(8) bond length of **14** [1.762(8) Å] is not comparable with the P-C bond length of the amino phosphonic acids mentioned above, the P-C bond length of **14** is similar to the equivalent bond lengths within the phosphinic acid **1** [1.785(6) Å], R-$(CH_2)_2P(Me)(O)OH$ {R=$C(NH_3)(COOH)Cl$}[22] [1.786(3) Å] and the phosphonic acid 4-methyl-2,6-bis(phosphonomethyl)phenol dihydrate[23] [an average of

1.787(1) Å]. This suggests that the P-C bond length of amino phosphonic acids are themselves anomalous and thus are not comparable with the P-C bond length of **14**. Owing to the bulk of the camphanyl moiety the O-P-O bond angles of **14** are not comparable with the equivalent bond angles of $PhCH_2CH(NH_2)PO_3H_2$ and $HC(NH_2)(CH_2COOH)PO_3H_2$.

	14	$PhCH_2CH(NH_2)PO_3H_2$	$HC(NH_2)(CH_2COOH)PO_3H_2$
P-C(8)	1.762(8)	1.826(4)	1.846(4)
P-O(2)	1.511(5)	1.495(3)	1.500(3)
P-O(1)	1.534(6)	1.505(3)	1.509(3)
P-O(3)	1.548(6)	1.573(3)	1.576(3)
O(2)-P(1)-O(3)	111.9(3)	117.6(2)	117.7(2)
O(2)-P(1)-O(1)	111.2(3)	112.5(2)	107.7(2)
O(2)-P(1)-C(8)	112.2(3)	105.8(2)	106.1(8)

Table 3.3: A comparison of bond lengths (Å) and bond angles (°) of **14** with 1-amino-2-phenylethyl)phosphonic acid monohydrate [$PhCH_2CH(NH_2)PO_3H_2$] and 3-amino-3-phosphonopropionic acid [$HC(NH_2)(CH_2COOH)PO_3H_2$].

The crystal is made up from H-bonded hexamers of $RP(O)(OH)_2$ packed about the three-fold axis. As shown in Figure 3.2, a stereo view of the $P(O)(OH)_2$ core, three molecules are linked in a ring by O(3) [red]-H(130)...O(2) [black] interactions between adjacent molecules, then these trimers are linked together by six O(1) [blue]-H(110)...O(2) [black] bonds. This core of $RP(O)(OH)_2$ hexamers stack upon each other [see Figure 3.3 which depicts two $RP(O)(OH)_2$ hexamers] to give a discontinuous hydrophilic central core. As depicted in Figure 3.4, a stereo view of the unit cell, the bulky camphanyl groups surround this central core.

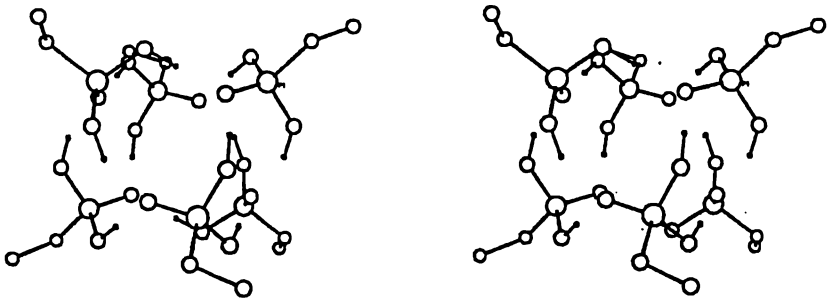

Figure 3.2: Stereo view of the $CH_2P(O)(OH)_2$ core in which three molecules are linked in a ring by O(3) [red]-H(130)...O(2) [black] hydrogen bonding. These trimers are linked together by six O(1) [blue]-H(110)...O(2) [black] bonds. With the exception of the C(3) atom, all other atoms relating to the camphanyl moiety are omitted for clarity.

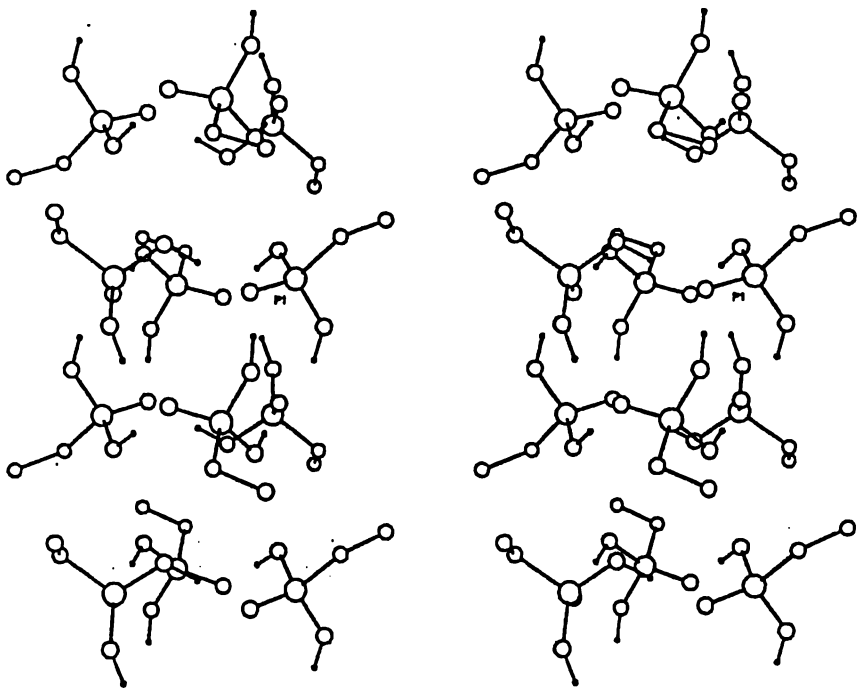

Figure 3.3: Stereo view of the core of two $CH_2P(O)(OH)_2$ hexamers which stack upon each other giving a discontinuous hydrophilic central core. With the exception of the C(3) atom, all other atoms relating to the camphanyl moiety are omitted for clarity. The phosphorus atoms are shaded.

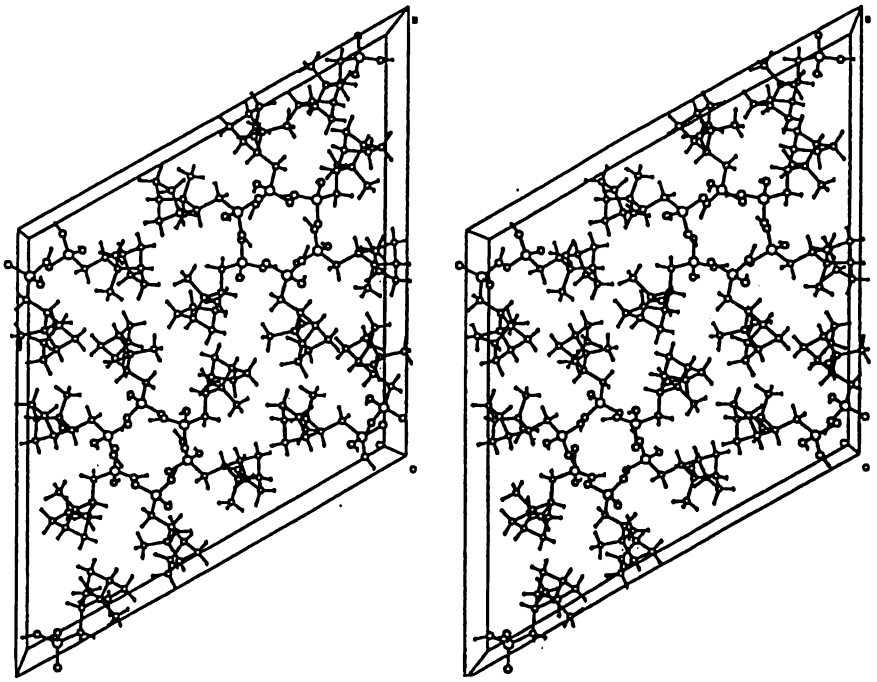

Figure 3.4: Stereo view of the unit cell depicting the bulky camphanyl groups that surround the central core.

A comparison of the packing tendencies of **14** with the Ca-phosphinate **13** [see section 2.4.3] clearly indicate that these camphene-derived compounds pack such that there is maximum separation of the hydrophilic inorganic moiety from the hydrophobic organic moiety. Thus as a consequence both **13** and **14** form central hydrophilic inorganic cores which are surrounded by the bulky hydrophobic camphanyl groups.

These crystallographic tendencies suggest that metal salts of the phosphonic acid **14** may also retain, in part, or in whole, this novel columnar structure and not the more traditional layer structures of metal phosphonates[24]. Although initial attempts to crystallise the Cu salt of **14** using the urea method described in section 2.4 were successful, the crystals instantly became opaque upon removal from the methanolic solution. As this was expected to result from solvent molecules encapsulated in the crystal lattice escaping, further trials using the higher boiling point solvents ethylene glycol and propanol were undertaken. However, these subsequent trials did not produce crystals of suitable quality for crystallographic studies. Despite varying the amount of urea and water present, all attempts to crystallise the Sr salt of **14** were also unsuccessful, and repeating the synthesis of the Cu salt in methanol was also unsuccessful.

3.1.4 NMR analysis of 8-camphanylphosphonic acid (14)

One- and two-dimensional NMR studies were carried out on 8-camphanylphosphonic acid (**14**) to fully assign the ^{1}H and ^{13}C NMR data. A summary of these results is presented in Tables 3.4 and 3.5. The structure of the camphanyl moiety deduced by NMR spectroscopy is consistent with that determined by X-ray crystallography.

Atom	^{13}C NMR data	^{1}H NMR data	Assignment
C(4)	43.5, d, $^{3}J_{P\text{-}C\text{-}C\text{-}C}$ = 3.6 Hz	2.38, br, s	H_4
	[42.1, d, $^{3}J_{P\text{-}C\text{-}C\text{-}C}$ = 6.2 Hz]		
C(3)	46.0, d, $^{2}J_{P\text{-}C\text{-}C}$ = 3.9 Hz	1.82, m	H_3
	[43.4, d, $^{2}J_{P\text{-}C\text{-}C}$ = 1.5 Hz]		
C(2)	38.3, d, $^{3}J_{P\text{-}C\text{-}C\text{-}C}$ = 14.1 Hz	-	-
	[37.5, d, $^{3}J_{P\text{-}C\text{-}C\text{-}C}$ = 12.2 Hz]		
C(1)	50.1 [48.4]	1.77, br, s *	H_1
C(8)	25.2, d, $^{1}J_{P\text{-}C}$ = 138.3 Hz	1.72, m	$H_{8'/8''}$
	[26.6, d, $^{1}J_{P\text{-}C}$ = 93.5 Hz]	1.65, m	
C(7)	37.8 [37.6]	1.66, m	$H_{7''}$
		1.20, dt	$H_{7'}$
C(6)	25.6 [24.6]	1.60, m	$H_{6''}$
		1.32, m	$H_{6'}$
C(5)	21.0 [20.2]	1.44, m	$H_{5''}$
		1.34, m	$H_{5'}$
C(10)	32.3 [31.8]	0.98, s	Me'
C(9)	22.3 [21.1]	0.83, s	Me''

Table 3.4: Summary of the ^{1}H and ^{13}C NMR data [δ in CD_3OD] for 8-camphanylphosphonic acid (**14**).

* denotes an unresolved resonance

[ ] represents the equivalent ^{13}C NMR data obtained for 8-camphanyl-phosphinic acid (**1**).

The ^{31}P NMR chemical shift of 8-camphanylphosphonic acid (**14**) occurs at δ 23.8 and is consistent with the phosphonic acids $MeP(O)(OH)_2$ and $HOCH_2P(O)(OH)_2$ which have ^{31}P NMR chemical shifts of δ 24.8 and 22.8 respectively[25].

The ^{13}C NMR spectrum of **14** was assigned by comparison with the ^{13}C NMR spectrum of its precursor **1** [see Table 3.4]. In the ^{13}C-^{1}H correlated NMR spectrum of **14** the cross peaks relating to the ^{13}C NMR signals of the camphanyl moiety identified their corresponding camphanyl moiety ^{1}H NMR resonance(s).

As the ^{1}H and COSY45 spectra of **14**, Figure 3.5, showed many similarities to its precursor **1** [Figure 2.5], complete assignment of the ^{1}H and COSY45 NMR spectra of **14** was possible. As in the phosphinic acid **1**, examination of the H_4 cross peaks of **14** readily identifies the proton resonances belonging to H_4 [δ 2.38], H_3 (1) [δ 1.82], H_1 (2) [δ 1.77], $H_{7''}$ (3) [δ 1.66], $H_{5'}$ (4) [δ 1.34], $H_{8'/8''}$ (6) [δ 1.72, 1.65] and $H_{7'}$ (5) [δ 1.20].

Unlike **1** [see section 2.1.5], the $H_{5''}$ and $H_{5'}$ proton resonances of **14** [δ 1.44 and δ 1.34 respectively] are sufficiently separated to be distinguished. This assignment results from the observation of correlation peaks arising from the coupling of H_4 to $H_{5'}$ [but not to $H_{5''}$] (4), H_3 to $H_{5'}$ [but not to $H_{5''}$] (7) and $H_{7''}$ to $H_{5''}$ [but not to $H_{5'}$] (12). Further confirmation is obtained by the presence of an NOE from Me'' to $H_{5''}$. A summary of the NOE's observed for **14** is presented in Table 3.5. Again, as in the phosphinic acid, NOE's are observed from Me' to H_3 and $H_{7''}$, and from Me'' to $H_{8'/8''}$, $H_{6''}$ and $H_{5''}$, proving the *endo* disposition of the $-CH_2PO_3H_2$ group.

Irradiated Hydrogen	*Enhanced Signal (%)*
H_4 (δ 2.38)	H_3 (2.0), $H_{7''}$ (1.8), $H_{5'}$ (0.6), $H_{5''}$ (1.6), $H_{7'}$ (2.3)
$H_{6''}$ (δ 1.60)	H_4 (1.2), Me'' (0.7)
$H_{7'}$ (δ 1.20)	H_4 (3.0), H_1 (1.7), $H_{7''}$(11.3)
Me' (δ 0.98)	H_3 (3.5), H_1 (4.3), $H_{7''}$ (4.1), Me'' (1.2)
Me'' (δ 0.83)	H_1 (3.3), $H_{8'}$ (x) and $H_{8''}$ (y), x + y = 8.0, $H_{6''}$ (7.0), $H_{5''}$ (0.9), Me' (1.5)

Table 3.5: NOE's observed for the protons of **14** [% enhancements are given in brackets].

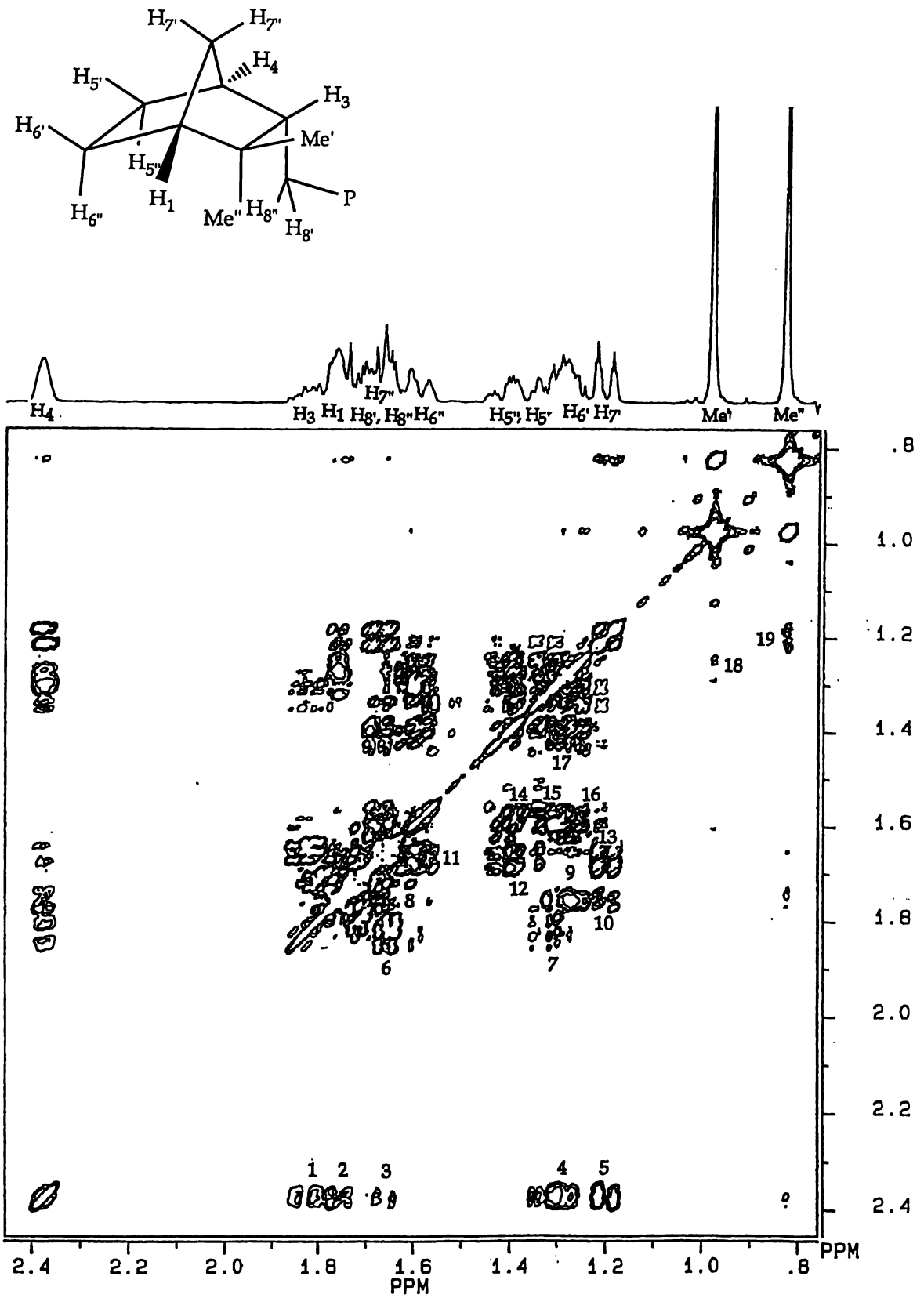

Figure 3.5: COSY45 spectrum of 8-camphanylphosphonic acid (**14**) recorded in $CDCl_3$ at 300MHz.

Crosspeaks 1:H_4/H_3 2:H_4/H_1 3:$H_4/H_{7"}$ 4:$H_4/H_{5'}$ 5:$H_4/H_{7'}$ 6:$H_3/H_{8'}$,$H_{8"}$ 7:$H_3/H_{5'}$ 8:$H_1/H_{7"}$ 9:$H_1/H_{6'}$ 10: $H_1/H_{7'}$ 11: $H_{7"}/H_{6"}$ 12:$H_{7"}/H_{5"}$ 13: $H_{7"}/H_{7'}$ 14: ,$H_{6"}/H_{5"}$ 15: $H_{6"}/H_{5'}$ 16: $H_{6"}/H_{6'}$ 17: $H_{5"}/H_{5'}$, $H_{5"}/H_{6'}$, $H_{5'}/H_{6'}$ 18: $H_{6'}$/Me' 19: $H_{7'}$/Me"

3.2 Synthesis and characterisation of the dimethyl 8-camphanylphosphonate (15)

3.2.1 Results and discussion

The esterification of phosphorus acids using diazomethane is well documented in the literature[26]. Hence the treatment of 8-camphanylphosphonic acid (**14**) with an excess of diazomethane, Scheme 3.5, affords dimethyl 8-camphanylphosphonate (**15**), a colourless oil, in quantitative yield. Detailed characterisation of **15** by NMR spectroscopy is presented in section 3.2.2.

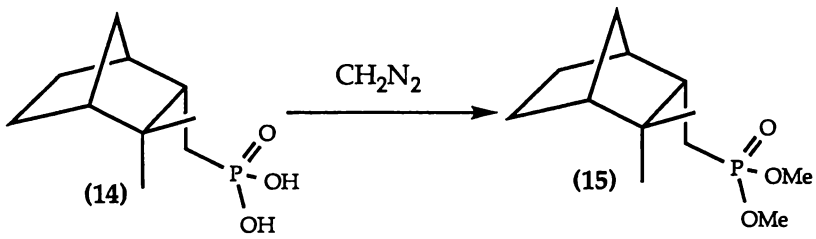

Scheme 3.5 : The methylation of **14** with an excess of diazomethane.

The methyl ester **15** contained a small amount of **14** which, despite several attempts using vacuum distillation, could not be removed. It is suggested that, like the related methyl ester **6** which is hydrolysed in air to its corresponding phosphinic acid [consult section 2.2.2 for more detail], **15** also undergoes hydrolysis in air to form the corresponding phosphonic acid **14**, Scheme 3.6. It is worth noting that it is unlikely that the impurity **14** is due to the presence of unreacted starting material as a large excess of diazomethane was used to ensure complete reaction.

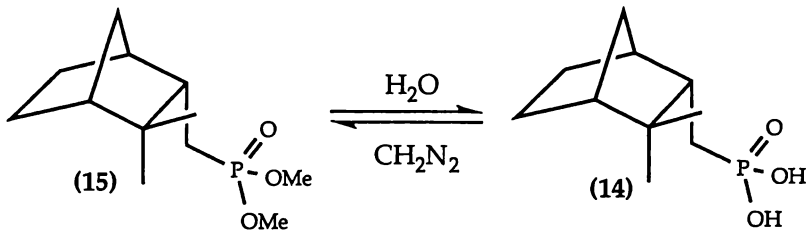

Scheme 3.6: The hydrolysis of dimethyl 8-camphanylphosphonate (**15**) in air.

As illustrated in Scheme 3.7, the minor addition product **15a**, formed by the methylation of the minor addition product **14a** [refer to section 3.1.2 for more detail] was also detected by GCMS in trace amounts. The GCMS data of **15a** were consistent with that of a minor addition product, *i.e* an identical parent ion [M^+ at *m/z* 246] and similar retention time [R_f=0.150] to the major product **15** [R_f=0.148] was obtained. The minor addition product **15a** is expected to have the -PO(OMe)$_2$ group in an *endo* rather than *exo*-position to minimise steric interactions between the -PO(OMe)$_2$ group and the bridgehead C(7) [see section 2.1.3 for more detail].

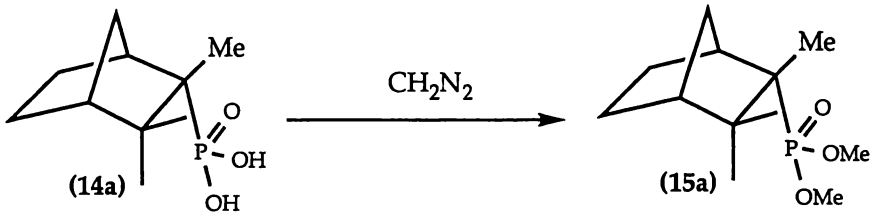

Scheme 3.7: The methylation of the minor addition product **14a** with diazomethane.

3.2.2 NMR analysis of dimethyl 8-camphanylphosphonate (15)

One- and two-dimensional NMR studies were undertaken to fully assign the ^{1}H and ^{13}C NMR spectra of dimethyl 8-camphanylphosphonate (**15**). A summary of these results is presented in Tables 3.6 and 3.7.

The ^{31}P NMR chemical shift of **15** occurs at δ 35.8 and is comparable with the dialkylphosphonates MeP(O)(OEt)$_2$ and PhP(O)(OEt)$_2$ which have ^{31}P NMR chemical shifts of δ 29.6 and 20.5 respectively[25].

Atom/Group	^{13}C NMR	^{1}H NMR	Assignment
OMe	52.2, d*	3.69, br, s	
	52.1, d*	3.65, br, s	
C(4)	42.3, d, $^{3}J_{P\text{-}C\text{-}C\text{-}C}$ = 3.9 Hz	2.26, br, s	H_4
	[43.5, d, $^{3}J_{P\text{-}C\text{-}C\text{-}C}$ = 3.6 Hz]		
C(3)	44.3, d, $^{2}J_{P\text{-}C\text{-}C}$ = 3.7 Hz	1.73, m	H_3
	[46.0, d, $^{2}J_{P\text{-}C\text{-}C}$ = 3.9 Hz]		
C(2)	37.5, d, $^{3}J_{P\text{-}C\text{-}C\text{-}C}$ = 14.3 Hz	-	-
	[38.3, d, $^{3}J_{P\text{-}C\text{-}C\text{-}C}$ = 14.1 Hz]		
C(1)	48.6 [50.1]	1.72, m	H_1
C(8)	22.0, d, $^{1}J_{P\text{-}C}$ = 140.1 Hz	1.72-1.66, m	$H_{8'/8''}$
	[25.2, d, $^{1}J_{P\text{-}C}$ = 138.3 Hz]		
C(7)	36.9 [37.8]	1.62, m	$H_{7''}$
		1.15, d*	$H_{7'}$
C(6)	24.6 [25.6]	1.49, m	$H_{6''}$
		1.23, m	$H_{6'}$
C(5)	20.0 [21.0]	1.31-1.20, m	$H_{5''}$
			$H_{5'}$
C(10)	31.8 [32.3]	0.92, s	Me'
C(9)	21.9 [22.3]	0.74, s	Me''

Table 3.6: Summary of the ^{1}H and ^{13}C NMR data [δ in $CDCl_3$] for dimethyl 8-camphanylphosphonate (**15**).

* denotes tentative assignment of signal

[ ] represents the equivalent ^{13}C NMR data obtained for 8-camphanylphosphonic acid (**14**)

The ^{13}C NMR spectrum of **15** is assigned by comparison with 8-camphanylphosphonic acid (**14**) [see Table 3.6]. Recognition of the ^{13}C NMR resonances of the camphanyl moiety identified all camphanyl-related ^{1}H NMR resonances, *via* correlation peaks observed in the ^{13}C-^{1}H correlated NMR spectrum of **15**.

The ^1H and COSY45 NMR spectra of dimethyl 8-camphanyl phosphonate (**15**) are similar to its precursor 8-camphanylphosphonic acid (**14**). Consequently resonances belonging to H_4 (δ 2.26), H_3 (δ 1.73), $H_{8'/8''}$ (δ 1.72-1.66), $H_{7''}$ (δ 1.62), $H_{5'}$ (δ 1.31-1.20), $H_{7'}$ (δ 1.15) are readily identifiable.

Remaining structural ambiguities were resolved by NOE difference spectroscopy. Again, as in the phosphonic acid, the irradiation of the *endo*-methyl (Me') gives enhancement of *endo* protons $H_{8'/8''}$ thus confirming the *endo* position of the $CH_2PO(OMe)_2$ group. The remainder of the NOE data are summarised in Table 3.7. No discrepancies exist between the ^1H-^1H and ^{13}C-^1H correlated NMR spectra of **15**.

Irradiated Hydrogen	*Enhanced Signal (%)*
H_4 (δ 2.26)	H_3(4.2); $H_{7''}$(3.5); $H_{5'}$ and/or $H_{5''}$(5.7), $H_{7'}$(3.5)
$H_{6''}$ (δ 1.49)	$H_{6'}$(8.2), Me'' (5.6)
$H_{7'}$ (δ 1.15)	$H_{7''}$(15.6), H_4(3.8)
Me'' (δ 0.92)	Me'(1.0), H_4(x), $H_{8''}$(y), $H_{8'}$(z); x + y + z = 11.0
Me' (δ 0.74)	Me''(1), H_3(3.7), $H_{7''}$(2.5)

Table 3.7: NOE's observed for protons of **15** [% enhancements are given in brackets].

*3.3 A comparison of NMR data of the organophosphorus acids **1** and **14** with dimethyl 8-camphanylphosphonate (**15**)*

A comparison of the ^{1}H and ^{13}C NMR data of **1**, **14** and **15**, given in Table 3.8 and Table 3.9, shows that the multiplicities between analogous resonances are identical. Chemical shifts are also seen to vary only slightly between analogous resonances.

Compound	$C_{10}H_{17}P(O)(OH)(H)$	$C_{10}H_{17}P(O)(OH)_2$	$C_{10}H_{17}P(O)(OMe)_2$
	1	**14**	**15**
Solvent	$CDCl_3$	CD_3OD	$CDCl_3$
OMe	-	-	3.69, br, s
			3.65, br, s
H_4	2.26, br, s	2.38, br, s	2.26, br, s
H_3	1.79, m	1.82, m	1.73, m
H_1	1.75, m	1.77, br, s*	1.72, m
$H_{8'/8''}$	1.75, m	1.72, m	1.72-1.66, m
$H_{8'/8''}$	1.71, m	1.65, m	1.72-1.66, m
$H_{7''}$	1.64, m	1.66, m	1.62, m
$H_{6''}$	1.53, m	1.60, m	1.49, m
$H_{5''}$	1.29, m	1.44, m	1.31-1.20, m
$H_{5'}$	1.29, m	1.34, m	1.31-1.20, m
$H_{6'}$	1.24, m	1.32, m	1.23, m
$H_{7'}$	1.18, dt	1.20, d*	1.15, d*
Me'	0.95, s	0.98, s	0.92, s
Me''	0.78, s	0.83, s	0.74, s

Table 3.8: A comparison of the ^{1}H NMR data [300 MHz] of organophosphorus acids **1** and **14** with dimethyl 8-camphanylphosphonate (**15**).
$C_{10}H_{17}$=8-camphanyl
* denotes an unresolved resonance

Compound	$C_{10}H_{17}P(O)(OH)(H)$	$C_{10}H_{17}P(O)(OH)_2$	$C_{10}H_{17}P(O)(OMe)_2$
	1	**14**	**15**
Solvent	$CDCl_3$	CD_3OD	$CDCl_3$
C(5)	20.2	21.0	20.0
C(9) [Me'']	21.1	22.3	21.9
C(6)	24.6	25.6	24.6
C(8)	26.6	25.2	22.0
$^1J_{P\text{-}C(8)}$	93.5 Hz	138.3 Hz	140.1 Hz
C(10) [Me']	31.8	32.3	31.8
C(7)	37.6	37.8	36.9
C(2)	37.5	38.3	37.5
$^3J_{P\text{-}C\text{-}C\text{-}C(2)}$	12.2 Hz	14.1 Hz	14.3 Hz
C4	42.1	43.5	42.3
$^3J_{P\text{-}C\text{-}C\text{-}C(4)}$	6.2 Hz	3.6 Hz	3.9 Hz
C(3)	43.4	46.0	44.3
$^2J_{P\text{-}C\text{-}C(3)}$	1.5 Hz	3.9 Hz	3.7 Hz
C(1)	48.4	50.1	48.6
OMe	-	-	52.2, d*; 52.1, d*

Table 3.9: A comparison of the ^{13}C NMR data [75 MHz] of organophosphorus acids **1** and **14** with dimethyl 8-camphanylphosphonate (**15**).

* denotes the tentative assignment of signals

$C_{10}H_{17}$=8-camphanyl

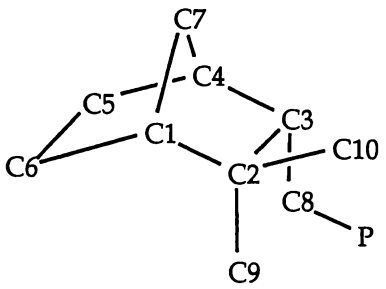

3.4 Synthesis and characterisation of platinum complexes derived from 8-camphanylphosphonic acid

3.4.1 Introduction

A wide variety of four-membered platinacyclic compounds have been reported and a comprehensive review outlining the main routes to their synthesis has been produced[27]. In recent years the utility of silver(I) oxide as a mediator in syntheses of a number of four-membered platinacycles has been shown[28, 29]. The structural diversity of platinacyclic compounds synthesised using silver(I) oxide is shown diagrammatically in Scheme 3.8 and illustrates the ease with which substitutents can be varied within and attached to the ring by the use of different ligands. Of the ligand examples given, which include phosphine oxides (i), phosphonic diamides (ii), sulfonamides (iii) and phosphonic acids (iv), the use of phosphonic acids as ligands in the synthesis of metallacyclic compounds is most relevant to this thesis and thus will be discussed in detail.

Platinum complexes containing phosphonic acid ligands are of considerable interest as recent studies have shown this type of compound to have antitumor activity[30].

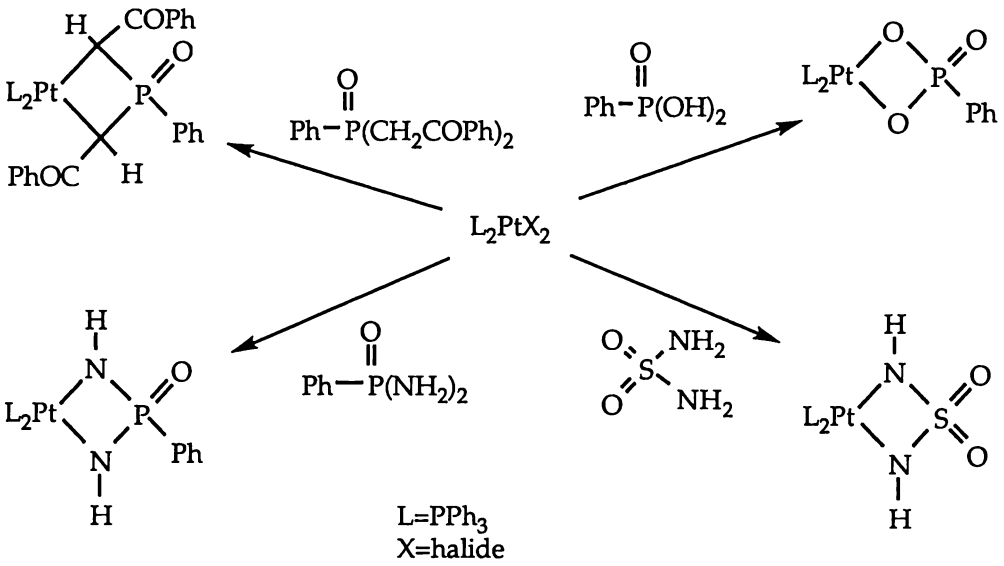

Scheme 3.8: The synthesis of four-membered platinacycles using silver(I) oxide as a base and halide-abstracting agent.

The general reaction scheme for the synthesis of four-membered platinacycles derived from a phosphonic acid is given in Scheme 3.9.

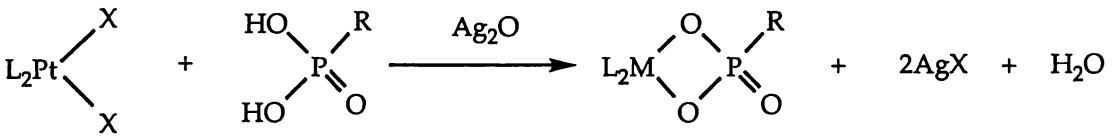

X=halide
R=alkyl, aryl group
L=PPh_3

Scheme 3.9: General reaction scheme for the synthesis of four-membered phosphonic acid-derived platinacycles using silver(I) oxide as a base and halide-abstracting agent.

The simple alkyl and aryl phosphonic acid-derived platinacycles, shown in Figure 3.6, have been synthesised and fully characterised[28]. However an investigation of bulky terpene-phosphonic acid-derived metallacycles has not as yet been carried out.

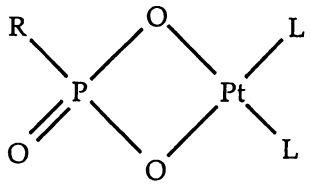

(1) R = Me, L = PPh_3
(2) R = Ph, L = PPh_3
(3) R = Me, L_2 = dppe
(4) R = Me, L_2 = dppe
(5) R =Ph, L =$PMePh_2$

Figure 3.6: The phenyl and methyl phosphonic acid-derived platinacycles.

The camphene-derived phosphonic acid **14** therefore represents an important derivative from which new terpene-derived metallacyclic complexes can be synthesised. Thus its reactivity, particularly that relating to metallacyclic chemistry, was investigated.

3.4.2 Results and discussion

*3.4.2.1 Synthesis of the 8-camphanylphosphonic acid-derived platinacycles **16, 17** and **18***

The general synthetic route to the 8-camphanylphosphonic acid-derived Pt(II) complexes **16, 17** and **18**, Scheme 3.10, is achieved by the reaction of an excess of silver oxide with equimolar quantities of the platinum dichloride complexes *cis*-$[PtCl_2L_2]$ {L=PPh_3, $PPhMe_2$; L_2=DPPE [1,2-bis(diphenylphosphane)ethane]} and phosphonic acid **14**. The reaction proceeds in dichloromethane heated at reflux with complete reaction, as determined by ^{31}P NMR, typically occurring within a 36 h period. Upon completion, the unreacted silver oxide and silver chloride, a byproduct of the reaction, are simply removed by filtration.

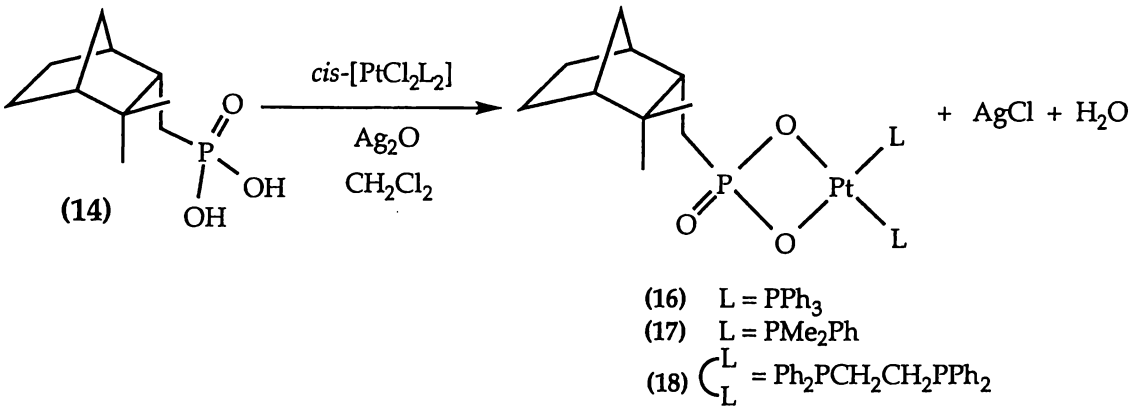

(16) L = PPh_3
(17) L = PMe_2Ph
(18) $\overset{L}{\underset{L}{\frown}}$ = $Ph_2PCH_2CH_2PPh_2$

Scheme 3.10: The synthesis of 8-camphanylphosphonic acid-derived platinacycles **16, 17** and **18** using silver(I) oxide as a base and a halide-abstracting agent.

Platinacycles **16** and **18** are readily purified by recrystallisation from chloroform/petroleum spirit while the purification of platinacycle **17** is achieved by repeatedly washing the crude product with small volumes of acetone. Synthesised in moderate yield, the crystalline platinacycles **16, 17** and **18** are stable both in air and in organic solvents such as dichloromethane and methanol. Detailed characterisation of **16, 17** and **18** by ^{31}P, ^{1}H and ^{13}C NMR spectroscopy is presented in section 3.4.3. Characterisation of **16, 17** and **18** by ESMS is presented in section 3.4.5.

Attempts to obtain crystallographic data for **16** were hindered somewhat by the incorporation of solvent within the crystal lattice upon crystallisation. The loss of this solvent, which is detected by the weakening of the diffracted X-rays as preliminary studies progressed, resulted in the crystal cracking which rendered the single crystal useless. These complications are easily remedied by the use of low temperature diffraction studies. However single crystals obtained from further recrystallisation of **16** from chloroform/petroleum spirit were not of suitable quality to resume crystallographic studies. Attempts to recrystallise diffraction quality single crystals from higher boiling point solvents also met with no success. ^{1}H NMR studies show that most solvents used, which include methanol, water, chloroform and dichloromethane, are incorporated. The incorporation of these solvents meant reliable analytical data were difficult to obtain. However after careful handling and prolonged drying [48 h at 0.5

mmHg] analytical data consistent with that of the ^1H NMR spectrum of **16** as a trihydrate was obtained.

The attempted synthesis of the analogous COD (1,5-cyclooctadiene) platinacycle [Pt{OP(O)($C_{10}H_{17}$)O(COD)}] met with little success. The reaction of equimolar amounts of **14** and $PtCl_2$(COD) with an excess of silver oxide in dichloromethane heated at reflux afforded a large number of products by ^{31}P NMR, which were not investigated further.

*3.4.2.2 Attempted synthesis of 8-camphanylphosphonic acid (**14**) derived palladacycles:*

Unlike the chemistry of its platinum counterpart the analogous palladium chemistry of **14** is non-selective, forming a large number of unidentifiable products. The reaction, which involves a dichloromethane solution of **14** and $PdCl_2(PPh_3)_2$ heated at reflux with an excess of silver oxide, did not afford the characteristic ^{31}P NMR chemical shifts of a cyclised product. Thus further investigation was not deemed productive.

3.4.2.3 Attempted synthesis of 8-camphanylphosphinic acid-derived platinacycles

Research was extended to an investigation of the action of platinum(II) complexes upon the camphene-derived phosphinic acid (**1**). Experimental results to date clearly indicate that camphene-derived phosphonic acid **14** undergoes reasonably clean and moderate-yielding cyclisation reactions with platinum(II) complexes. As the monodentate ligand phosphinic acid **1** is not able to undergo cyclisation with platinum(II) complexes an investigation of the platinum chemistry of the phosphinic acid **1** was undertaken. These results are included within this section as they are relevant to the platinum chemistry described within this section.

In an attempt to synthesise the di-substituted non-cyclised platinum(II) complex of **1**, Scheme 3.11, the reaction was performed as described for the phosphonic analogue **16** but with two equivalents of **1**. Although this reaction, as evidenced by the ^{31}P NMR data, gave a large number of unidentifiable products, the result clearly indicates that ring formation is a driving force and in its absence, as described here, reaction to form the desired product does not occur.

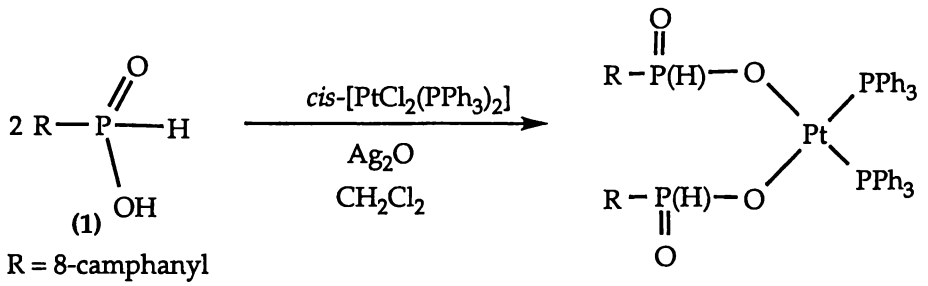

Scheme 3.11: The attempted synthesis of the di(8-camphanyl)phosphinic acid-derived platinum(II) complex.

An additional factor may be the steric congestion produced between adjacent camphanyl moieties and the bulky triphenyl phosphine ligands. To further complicate matters, the P-H bond of **1** can also act as a reducing agent reducing Pt(II) to Pt(0), or more likely, Ag(I) to Ag(0).

3.4.3 *Spectroscopic characterisation of* **16, 17** *and* **18**

3.4.3.1 *NMR analysis of* $[Pt\{OP(O)(C_{10}H_{17})O\}(PPh_3)_2]$ **(16)**

(i) ^{31}P*:* The resonances belonging to the triphenylphosphine ligands P_x and P_y are inequivalent, coupling to each other to produce two doublets at δ 5.4 and 7.5. Each of these doublets is further split by P_z to produce the two distinctive doublet of doublet patterns [$^2J_{P_x\text{-}Pt\text{-}P_y}$ 26 Hz, $^3J_{P_x\text{-}Pt\text{-}O\text{-}P_z}$ 7 Hz] shown in Figure 3.7. The chemical inequivalence of P_x and P_y is expected to result from the steric congestion produced by the close proximity the bulky camphanyl moiety to the triphenylphosphine ligands. An indepth discussion is presented in section 3.4.4. The assignment of the resonances belonging to P_z is straightforward as a distinctive triplet-like pattern is observed at δ 55.3 [$^3J_{P_z\text{-}O\text{-}Pt\text{-}P_{x(y)}}$ 7 Hz]. It is worth noting that the expected multiplicity for P_z, a doublet of doublet pattern, was not observed. The simplification of this doublet of doublet pattern to the observed triplet-like pattern occurs as the result of the P_z-to-P_x and -P_y coupling constants being approximately equal.

As ^{195}Pt is NMR active, spin $^1/_2$ and 33% abundant, Pt-to-P coupling is also observed. The one- and two-bond Pt-to-P coupling constants [$^1J_{P_x\text{-}Pt}$ 3732, $^1J_{P_y\text{-}Pt}$ 3843, $^2J_{P_z\text{-}O\text{-}Pt}$ 117 Hz] and three-bond P-to-P coupling constant of **16** are consistent with $[Pt\{OP(O)(R)O\}(PPh_3)_2]$ where R=Me [$^1J_{P\text{-}Pt}$ 3848 Hz, $^2J_{P\text{-}O\text{-}Pt}$ 122 Hz, $^3J_{P\text{-}Pt\text{-}O\text{-}P}$ 10 Hz], R=Ph [$^1J_{P\text{-}Pt}$ 3877 Hz][28]. It is important to note that the phenyl analogue is reported[28] to have a $^2J_{P\text{-}O\text{-}Pt}$ coupling constant of 27 Hz. This is not consistent with other $^2J_{P\text{-}O\text{-}Pt}$ coupling constants reported in this publication and therefore assumed to be in error. It is suggested that this is a typing error and should read 127 Hz.

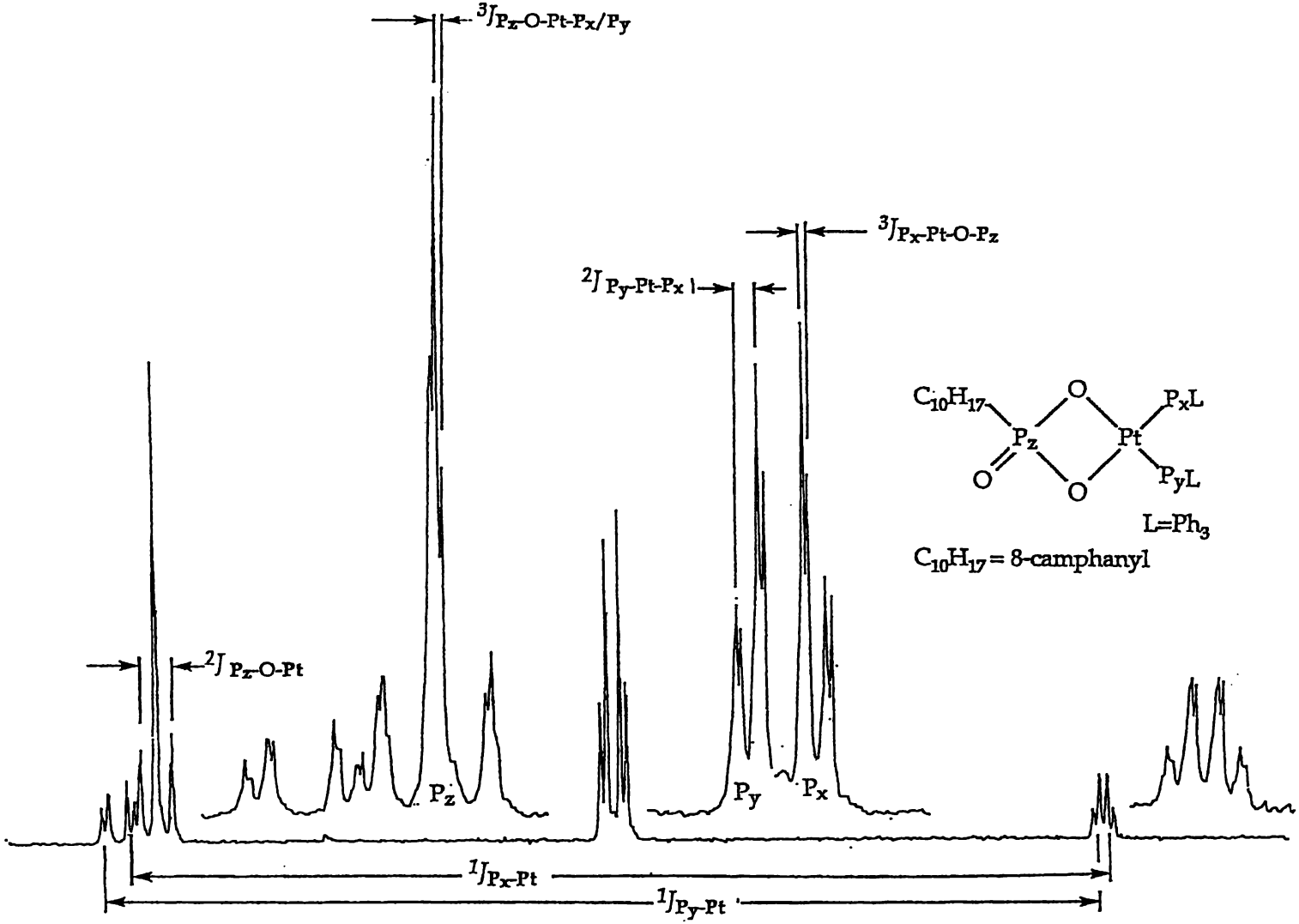

Figure 3.7: The ^{31}P NMR spectrum of **16**, recorded in $CDCl_3$ at 36 MHz.

(ii) ^{13}C*:* The ^{13}C NMR spectrum of the camphanyl region of **16** comprised ten resonances, consisting of two methyl, three methine, four methylene and a quaternary resonance. The methylene signal [δ 27.9] which exhibited a large one-bond carbon to phosphorus coupling [*J* 121.9 Hz] is assigned to C(8). The other three methylene signals [δ 20.1, 24.8 and 37.1] belonging to C(5), C(6) and C(7) respectively are assigned by comparison with those chemical shifts obtained for 8-camphanylphosphonic acid (**14**) [δ 21.0, 25.6 and 37.8 respectively]. The methine signal [δ 49.0] which is not seen to couple to phosphorus is assigned to C(1) as $^{4}J_{\text{P-C-C-C-C}}$ coupling is not expected to be seen. The other two methine signals (δ 46.1 and 42.5) belonging to C(3) and C(4) respectively exhibiting two and three phosphorus-to-carbon couplings [*J* 3.4 Hz and 13.1 Hz respectively] are assigned by comparison with those chemical shifts obtained for 8-camphanylphosphonic acid (**14**) [δ 46.0, d, *J* 3.9 Hz and δ 43.5, *J* 3.9 Hz respectively]. The comparatively small coupling exhibited by C(3) [3.4 Hz] is consistent with the tendency for $^{3}J_{\text{P-C-C-C}}$ coupling to be greater than $^{2}J_{\text{P-C-C}}$ coupling[31]. The assignment of quaternary carbon C(2) [δ 37.5] which is coupled to phosphorus [*J* 3.3 Hz] is confirmed by its absence in the DEPT experiment. Due to the complexity of the aryl region of **16** the signals [δ 131.5-128.4] belonging to the phenyl rings of triphenylphosphine are not assigned. Full ^{13}C NMR data for **16** are given in section 3.4.4, Table 3.15.

In the ^{13}C-^{1}H correlated NMR spectrum of **16** the cross peaks relating to these camphanyl carbon signals identified all proton resonances relating to the camphanyl moiety.

(iii) ^{1}H*:* Identification of many of the ^{1}H NMR resonances is possible by examination of H_4 cross peaks in the COSY45 spectrum. Consequently resonances belonging to H_4 (δ 2.58), H_3 (δ 1.96), $H_{8'/8''}$ (δ 1.60, 1.54), $H_{7''}$ (δ 1.68), $H_{5''}$ (δ 1.26), $H_{7'}$ (δ 1.05) are readily identified. Other trends in the COSY45 spectrum are as described for 8-camphanylphosphinic acid (**1**) in section 2.1.5. Full ^{1}H NMR data for **16** are given in section 3.4.4, Table 3.14. No discrepancies exist between the ^{1}H-^{1}H and ^{13}C-^{1}H correlated NMR spectra.

(iv) NOE data: Remaining structural ambiguities are resolved by NOE difference spectroscopy. Particularly diagnostic are the NOE's observed from Me' to $H_{7''}$ and to H_3 [but not significantly from Me' to $H_{8'/8}$] indicating that $H_{7''}$ and H_3 are on the same side of the molecule, confirming the *endo* disposition of the -$CH_2PO_2H_2$ group. Other NOE's of significance are those of H_4 to $H_{5'}$ (and not to $H_{5''}$), $H_{7'}$ to $H_{6'}$ (and not $H_{6''}$) and H_3 to $H_{7'}$ (and not $H_{7''}$). These NOE's along with a 1-D spectrum of **16** are presented in Figure 3.8. The remainder of the NOE data, Table 3.10, along with the COSY spectrum, gives the complete spectral assignment.

Irradiated hydrogen	*Enhanced signal (%)*
H_4 (δ 2.58)	H_3 (5.5), $H_{7''}$(1.9), $H_{7'}$(3.0), $H_{5'}$(3.0), [Ar; *ortho*-[11.5], *meta*- (2.5), *para*- (4.0)]
H_3 (δ 1.96)	H_4 (6.2), $H_{7''}$(6.0), Me_1(5.5), Me_2(1.0), Ar; *ortho*-(13.0), *meta*- (2.5), *para*- (6.0)]
$H_{1/7''}$ (δ 1.68)	H_4 (3.0), H_3 (10.0), $H_{7'}$(29.0), Me'(3.0), Me''(0.8), [Ar; *ortho* -(5.6), *meta*- (2.8), *para*- (6.5)]
Me''(δ 0.71)	Me'(1.3), $H_{8'/8''}$ (7.0)
$H_{5'}$ (δ 0.82)	$H_{5''}$ (17.0), H_4 (4.7),
Me' (δ 0.95)	Me'' (0.7), $H_{7''}$ (7.8), H_3 (8.4),
$H_{7'/6'}$ (δ 1.05)	H_4 (3.3), $H_{6''}$ (6.5), $H_{7''}$(22.0), $H_{5'}$(0.4)
$H_{5''}$ (δ 1.26)	H_4 (1.6), H_3(1.0), $H_{5'}$(12.5), $H_{6'/6''}$(5.7)
ortho- Ar (δ 7.42)	*meta*- Ar (11.9), H_4 (0.5), H_3 (0.4)
meta- Ar (δ 7.20)	[Ar; *ortho*- (7.7), *para*- (10.3)]
para- Ar (δ 7.30)	*meta*- Ar (9.5)

Table 3.10: NOE's observed for protons of **16** [% enhancements are given in brackets].

Interestingly, an NOE between H_4 [attached to the camphanyl moiety] and the *ortho*-phenyl protons [δ 7.49-7.37] of the triphenylphosphine ligand was observed. Although at first glance this NOE seems unlikely, construction of a molecular model of **16** reveals the close proximity of the triphenylphosphine ligand protons to the camphanyl proton H_4 and therefore the possibility of an enhancement. Further NOE studies of the three phenyl regions [δ 7.49-7.37, 7.36-7.28 and 7.25-7.13 signals present in ratios of 2:1:2] indicate that the phenyl protons at δ 7.49 to 7.37 are the *ortho* protons. That is, the irradiation of the *meta* protons [δ 7.25 to 7.13] results in an enhancement of both the *ortho* [δ 7.49-7.37] and *para* [δ 7.36-7.28] proton resonances whereas irradiation of the *ortho* proton [δ 7.49-7.37] gives an enhanced *meta* [δ 7.36-7.28] proton signal along with an enhancement of the H_4 signal.

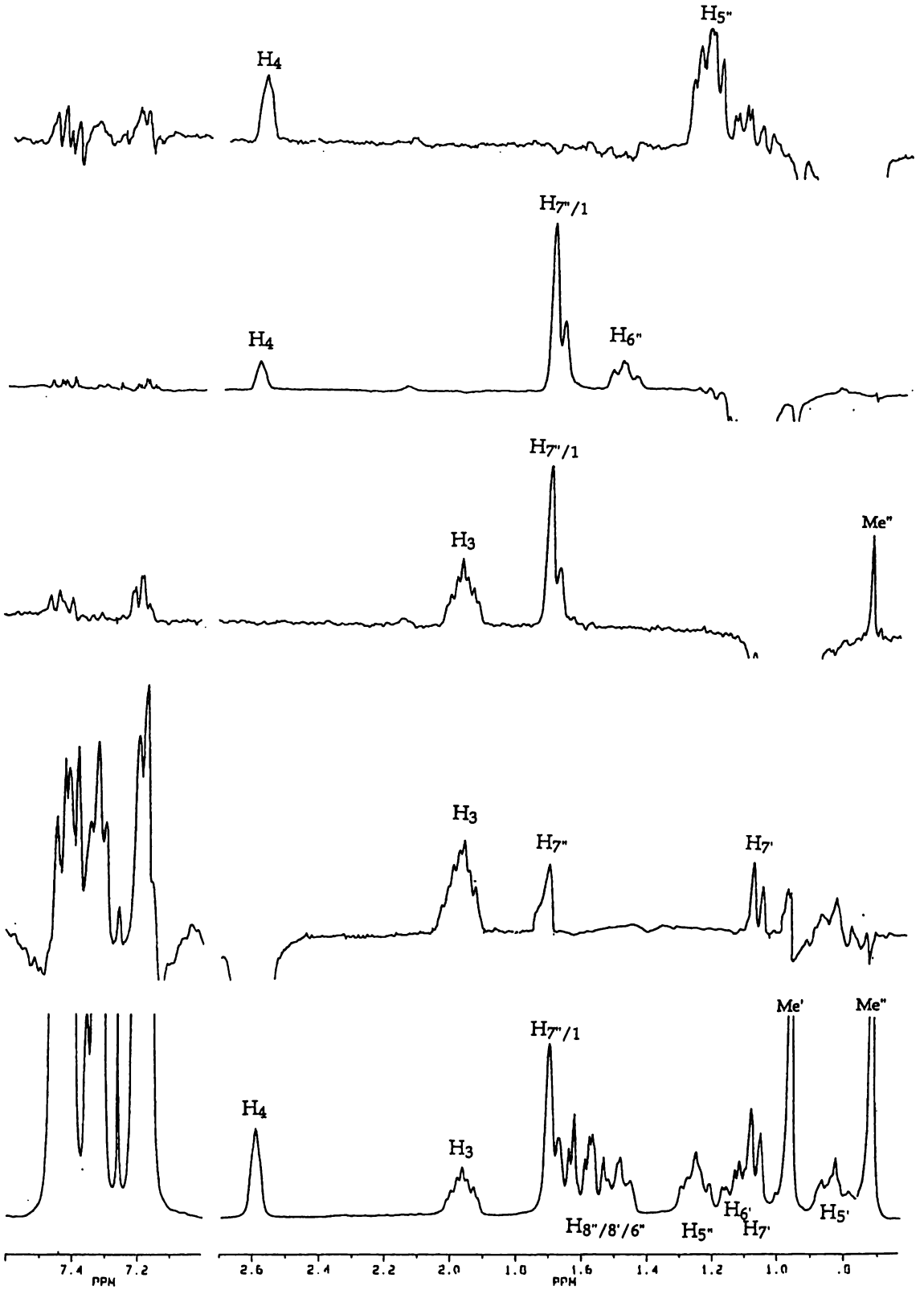

Figure 3.8: NOE difference spectra of **16** recorded in $CDCl_3$ at 300 MHz. (a) ^1H NMR spectrum of **16** (b) Irradiation of H_4 (δ 2.29) (c) Irradiation of Me' (δ 0.95) (d) Irradiation of $H_{7'/1}$ (δ 1.05) (e) Irradiation of $H_{5'}$ (δ 0.83).

3.4.3.2 *NMR analysis of* $[\overline{Pt\{OP(O)(C_{10}H_{17})O\}}(PPhMe_2)_2]$ (17)

(i) ^{31}P*:* As shown in Figure 3.9, the assignment of the resonances belonging to P_Z is straightforward as a triplet-like pattern [d of d where $J_1 \approx J_2$ (consult 3.4.3.1 for more details)] at δ 53.2 [$^3J_{P_Z\text{-O-Pt-}P_X/P_Y}$ 4 Hz] is observed. In contrast to the PPh_3 analogue **16**, the dimethylphenyl phosphine ligands [P_X and P_Y] of **17** are equivalent, both coupling to P_Z to produce a doublet at δ -20.9 [$^3J_{P_Z\text{-Pt-O-}P_X/P_Y}$ 4 Hz]. This difference, which is discussed in detail in section 3.4.4, is expected to result from the difference in steric requirements of the donor phosphorus ligands. The one- and two-bond P-to-Pt coupling constants of **17** [$^1J_{P_X/P_Y\text{-Pt}}$ 3654, $^2J_{P_Z\text{-O-Pt}}$ 100 Hz] are consistent with the related complexes $[\overline{Pt\{OP(O)(R)O\}}(PPh_2Me)_2]$ where R=Me [$^1J_{\text{P-Pt}}$ 3755 Hz, $^2J_{\text{P-O-Pt}}$ 112-Hz], R=Ph [$^1J_{\text{P-Pt}}$ 3755 Hz, $^2J_{\text{P-O-Pt}}$ 107 Hz][28].

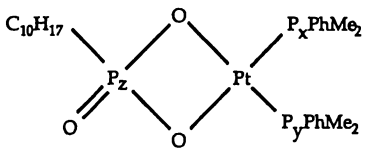

(ii) ^1H *and* ^{13}C*:* One- and two-dimensional NMR studies were carried out to fully assign the ^1H and ^{13}C NMR data of **17**. A summary of these results is presented in Table 3.11. The ^{13}C NMR spectrum of the camphanyl region of **17** is assigned by comparison with **16** [see Table 3.11]. Due to the complexity of the aryl region the ^{13}C NMR signals [δ 131.5-128.5] belonging to the phenyl rings of dimethylphenylphosphine are not assigned. The COSY45 spectrum of **17** is similar to **16** allowing assignment of the resonances belonging to H_4 (δ 1.75) , H_3 (δ 2.01), $H_{7''/7'}$ (δ 1.67, 1.15), $H_{8''/8'}$ (δ 1.61, 1.59), H_1 (δ 1.74) and $H_{5''/5'}$ (δ 1.49, 1.22). Resonances belonging to $H_{6''}$ and $H_{6'}$ [δ 1.56, 1.21] are assigned by comparison with **16** [δ 1.47, 1.10]. No discrepancies exist between the ^1H-^1H and ^{13}C-^1H correlated NMR spectra of **17**.

Atom	^{13}C NMR	^{1}H NMR	Assignment
C(4)	42.8, d, $^{3}J_{P\text{-}C\text{-}C\text{-}C}$ = 3.2 Hz	2.75, br, s	H_4
	[42.5, d, $^{3}J_{P\text{-}C\text{-}C\text{-}C}$ = 13.1 Hz]		
C(3)	46.4, d, $^{2}J_{P\text{-}C\text{-}C}$ = 3.1 Hz	2.01, m	H_3
	[46.1, d, $^{2}J_{P\text{-}C\text{-}C}$ = 3.4 Hz]		
C(2)	37.6, d, $^{3}J_{P\text{-}C\text{-}C\text{-}C}$ = 13.0 Hz	-	-
	[37.5, d, $^{3}J_{P\text{-}C\text{-}C\text{-}C}$ = 13.1 Hz]		
C(1)	49.0 [49.0]	1.74, m	H_1
C(8)	28.6, d, $^{1}J_{P\text{-}C}$ = 122.0 Hz	1.61, d, 11.7 Hz	$H_{8'/8''}$
	[27.0, d, $^{1}J_{P\text{-}C}$ = 121.9 Hz]	1.59, br, m	
C(7)	37.0 [37.1]	1.67, d, 13.0	$H_{7''}$
		1.15, d*	$H_{7'}$
C(6)	24.8 [24.8]	1.56, s	$H_{6''}$
		1.21, s	$H_{6'}$
C(5)	20.5 [20.1]	1.49, br, m	$H_{5''}$
		1.22, br, m	$H_{5'}$
C(10)	32.3 [32.4]	1.01, s	Me'
C(9)	22.2 [22.0]	0.81, s	Me''

Table 3.11: ^{1}H and ^{13}C NMR data [δ in $CDCl_3$] of **17**.

* denotes tentative assignment of signal

[ ] represents the equivalent ^{13}C NMR signal obtained for **16**

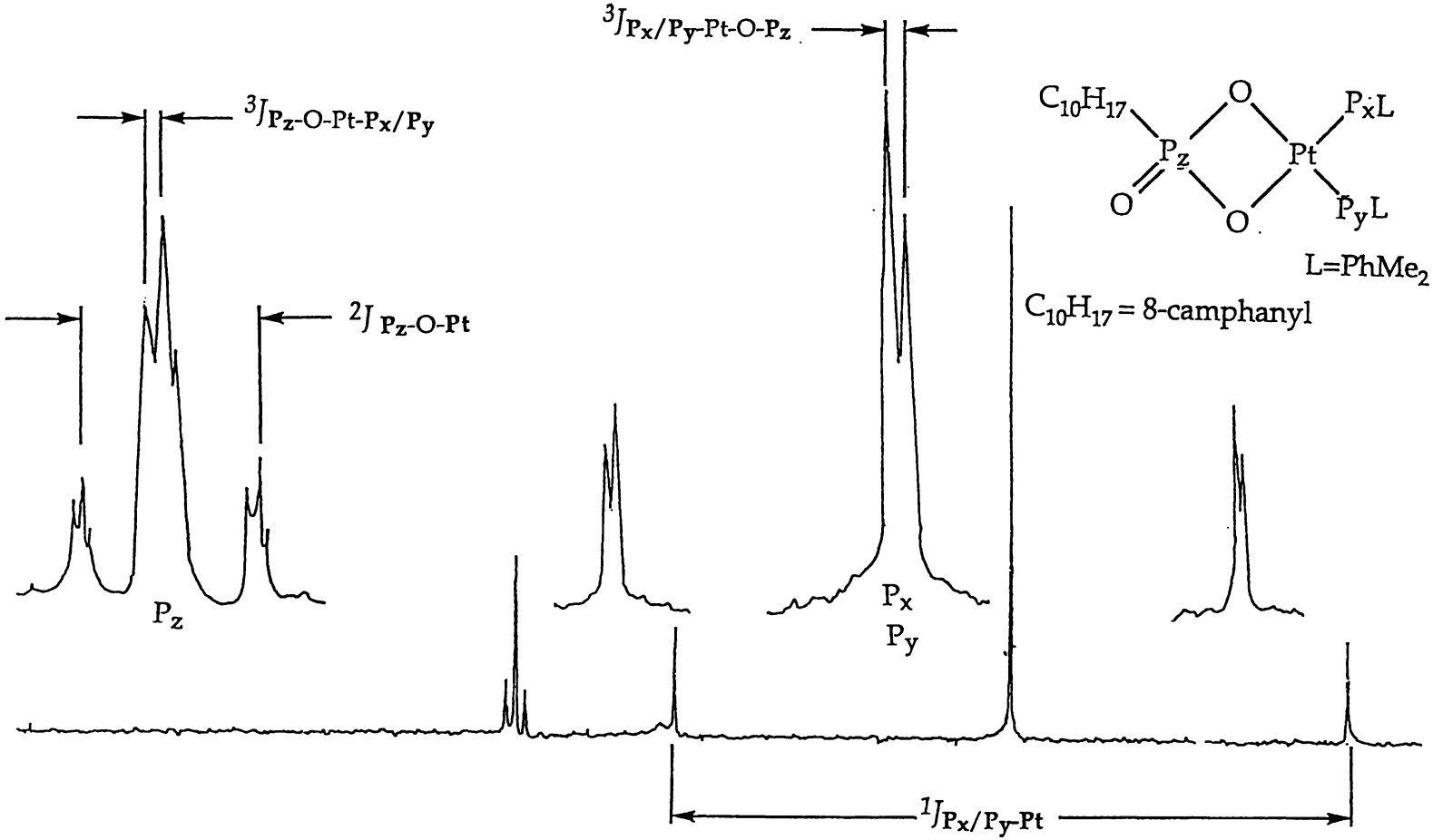

Figure 3.9: The ^{31}P NMR spectrum of **17**, recorded in $CDCl_3$ at 36MHz.

3.4.3.3 *NMR analysis of [Pt{OP(O)($C_{10}H_{17}$)O}(DPPE)] (18)*

(i) ^{31}P*:* The assignment of the resonance belonging to P_z is straightforward as a triplet pattern pattern [d of d where $J_1 \approx J_2$ (consult 3.4.3.1 for more details)] at δ 53.2 [$^3J_{P_x/P_y\text{-Pt-O-}P_z}$ 7 Hz] is observed. The donor phosphorus ligands [P_x and P_y] are inequivalent, coupling to each other to produce two doublets at δ 30.5 and 31.0. Each of the doublets are further split by P_z producing a distinctive doublet of doublets pattern [$^2J_{P_x\text{-Pt-}P_y}$ 20 Hz, $^3J_{P_x/P_y\text{-Pt-O-}P_z}$ 7 Hz]. The chemical inequivalence of P_x and P_y is expected to result from the steric congestion produced by the close proximity the bulky camphanyl moiety to the triphenylphosphine ligands. An indepth discussion is presented in section 3.4.4. The one- and two- Pt-to-P bond coupling constants [$^1J_{P_x\text{-Pt}}$ 3730, $^1J_{P_y\text{-Pt}}$ 3701, $^2J_{P_z\text{-O-Pt}}$ 102 Hz] and three bond P-to-P coupling constant [$^3J_{P_x/P_y\text{-Pt-O-}P_z}$ 7 Hz] of **18** are consistent with [Pt{OP(O)(R)O}(DPPE)] where R=Me [$^1J_{P\text{-Pt}}$ 3848 Hz, $^2J_{Pt\text{-O-}P}$ 122 Hz, $^3J_{P\text{-Pt-O-}P}$ 10 Hz], R=Ph [$^1J_{P\text{-Pt}}$ 3877 Hz][28].

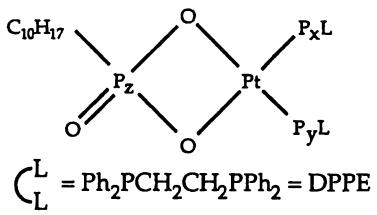

(ii) ^{13}C *and* ^1H*:* One- and two-dimensional NMR studies were undertaken to fully assign the ^1H and ^{13}C NMR data of **18**. A summary of these results is presented in Table 3.12. The ^{13}C NMR spectrum of the camphanyl region of **18** is assigned by comparison with **16** [see Table 3.12]. Due to the complexity of the aryl region within the ^{13}C and ^1H NMR spectrum the signals [δ 131.5-128.5 and δ 7.95-7.20 respectively] belonging to the phenyl rings of dimethylphenylphosphine are not assigned. The ^1H and COSY spectra of **18** are assigned in a similar manner to that described for **16** and **17**. No discrepancies are found to exist between the ^1H-^1H and ^{13}C-^1H correlated NMR spectra of **18**.

Atom	^{13}C NMR data	^{1}H NMR data	Assignment
C(4)	42.0, d, $^{3}J_{P\text{-}C\text{-}C\text{-}C}$ = 3.1 Hz	2.49, br, s	H_4
	[42.5, d, $^{3}J_{P\text{-}C\text{-}C\text{-}C}$ = 13.1 Hz]		
C(3)	46.2, d, $^{2}J_{P\text{-}C\text{-}C}$ = 3.1 Hz	1.84, m	H_3
	[46.1, d, $^{2}J_{P\text{-}C\text{-}C}$ = 3.4 Hz]		
C(2)	37.5, d, $^{3}J_{P\text{-}C\text{-}C\text{-}C}$ = 13.9 Hz	-	-
	[37.5, d, $^{3}J_{P\text{-}C\text{-}C\text{-}C}$ = 13.1 Hz]		
C(1)	48.8 [49.0]	1.56, m	H_1
C(8)	28.0, d, $^{1}J_{P\text{-}C}$ = 121.3 Hz	1.66, br, s*	$H_{8'/8''}$
	[27.0, d, $^{1}J_{P\text{-}C}$ = 121.9 Hz]	1.61, br, m	
C(7)	37.1 [37.1]	1.35, d, 10.6 Hz	$H_{7''}$
		0.84, d, 10.6 Hz	$H_{7'}$
C(6)	24.7 [24.8]	1.39, s	$H_{6''}$
		1.04, s	$H_{6'}$
C(5)	20.2 [20.1]	1.28, br, m	$H_{5''}$
		0.87, br, m	$H_{5'}$
C(10)	32.2 [32.4]	0.80, s	Me'
C(9)	22.1 [22.0]	0.66, s	Me''

Table 3.12: ^{1}H and ^{13}C NMR data [δ in $CDCl_3$] of **18**.

* denotes an unresolved signal

[ ] represents the equivalent ^{13}C NMR signal obtained for **16**

*3.4.4 A comparison of the NMR data of the platinacyclic complexes **16, 17 and 18***

*3.4.4.1 A comparison of the ^{31}P NMR of **16, 17 and 18***

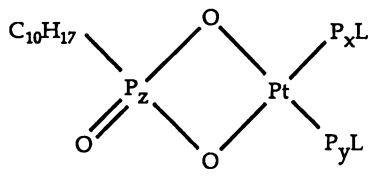

16 L = Ph_3
17 L = $PhMe_2$
18 L_2 = DPPE

	P_x δ	P_y δ	P_z δ	$^1J_{P_x\text{-}Pt}$ Hz	$^1J_{P_y\text{-}Pt}$ Hz	$^2J_{P_z\text{-}O\text{-}Pt}$ Hz	$^2J_{P_x\text{-}Pt\text{-}P_y}$ Hz	$^3J_{P_x\text{-}Pt\text{-}O\text{-}P_z}$ Hz
16	5.4 (dd)	7.5 (dd)	55.3 (t)	3732	3843	117	26	7
17	-20.9 (d)	-20.9 (d)	53.2 (t)	3654	3654	100	0	4
18	30.5 (dd)	31.0 (dd)	58.4 (t)	3730	3701	102	20	7

Table 3.13: ^{31}P NMR data of platinacycles **16, 17** and **18**, together with an atom labelling scheme.
coupling constants ± 3 Hz.

The ^{31}P NMR data of the camphene-derived platinacycles **16** and **18**, Table 3.13, are more complicated than the analogous methyl and phenyl platinacycles {[Pt{OP(O)(R)O}L_2] (R=Me, L= PPh_3 or L_2=DPPE; R=Ph, L= PPh_3 or L_2=DPPE)}[28] previously reported. The ^{31}P NMR spectra show that the donor phosphorus ligands of the methyl and phenyl platinacycles are equivalent; a singlet split by $^3J_{P\text{-}Pt\text{-}O\text{-}P}$ coupling to produce a doublet.

In contrast to these methyl and phenyl platinacycles, the donor phosphorus ligand environments [P_x and P_y] of the camphanyl equivalents, **16** and **18**, are inequivalent, coupling to each other to produce two doublets in the ^{31}P NMR spectra. As with the methyl and phenyl platinacycles mentioned above these doublets are further split by $^3J_{P\text{-}Pt\text{-}O\text{-}P}$ coupling to produce a pair of doublet of doublets. The inequivalence of the donor phosphorus ligand environments of **16** and **18** is also reflected in the difference between the Pt-P_x and Pt-P_y coupling constants.

As **16** and **18** differ only by the attached organic moiety [*c.f.* {[Pt{OP(O)(R)O}L_2] (R=Me or Ph, L= PPh_3 or L_2=DPPE)}] one must conclude that the inequivalence of the donor phosphorus ligand environments of **16** and **18** arises from the steric restriction produced by the substitution of a less bulky organic moiety, such as an organic group in the methyl and phenyl platinacycles, for the more sterically demanding camphanyl moiety in **16** and **18**. It is postulated that this steric restriction prevents the free rotation of the donor phosphorus ligands which in turn renders them chemically inequivalent. Although this postulate seems unreasonable, the construction of a molecular model shows that this interaction is indeed possible. NOE studies of **16** also reveal that the camphanyl and triphenyl phosphine ligands are of close proximity. This suggests that steric interaction between these two groups is possible which results in the inequivalence observed in the ^{31}P NMR studies.

In contrast to **16**, the ^{31}P NMR spectrum of the donor phosphorus ligands of **17** shows a singlet split by $^3J_{P_{x,y}\text{-}Pt\text{-}O\text{-}P_z}$ coupling, indicating that, even though the bulky camphanyl moiety is present, the donor phosphorus ligand environments are equivalent. It is therefore postulated that unlike **16** and **18**, where the bulky donor phosphorus ligands are restricted by the camphanyl moieties [an NOE observed from the camphanyl group to the triphenylphosphine moieties of **16** (refer to section 3.4.3 for details)], the decreased steric bulk of the dimethylphenylphosphine ligand in **17** is such that free rotation of this ligand is possible. This free rotation enables the two phenyl groups of the dimethylphenylphosphine ligands to orient themselves in such a way as to minimise the steric interaction with the

bulky camphanyl moiety which in turn renders the donor phosphorus ligands equivalent.

These results suggest that both a bulky organic group and a bulky donor phosphorus ligand are required to produce the steric interaction that results in an inequivalence of the donor phosphorus ligand environments.

As mentioned previously both ^{31}P and ^{195}Pt are NMR active and of spin 1/2 which results in the coupling of P to Pt. A comprehensive review[32] describes how a ligand *trans* to the P-Pt bond affects the P-Pt coupling constant. A *trans*-influence series is well established with ligands in order of increasing $^{1}J_{\mathbf{P\text{-}Pt}}$ coupling constants. The $^{1}J_{\mathbf{P\text{-}Pt}}$ coupling constants of **16, 17** and **18**, which lie between 3843 and 3654, are comparable with this series as having a Pt-P bond *trans* to oxygen. These $^{1}J_{\mathbf{P\text{-}Pt}}$ coupling constants are also comparable with the complexes [Pt{OP(O)(Ph)O}L_2] where L=$(PPh_3)_2$, $PPhMe_2$, L_2=DPPE which also have Pt-P bond *trans* to oxygen [see section 3.4.3 for more detail].

3.4.4.2 A comparison of the ^{1}H and ^{13}C NMR of 16, 17 and 18

A comparison of the ^{1}H NMR signals of the platinacycles **16, 17** and **18**, given in Table 3.14, indicates that the $H_{7''/7'}$ proton signals of **18** vary significantly. Also observed is a shift to higher field of the protons H_1 and $H_{6''/6'}$ of **18**. These anomalies are expected to be the result of substitution effects. Other anomalies that exist are the $H_{5''/5'}$ and H_4 protons of **17**. The ^{13}C NMR data of the platinacyclic complexes **16, 17,** and **18** [Table 3.15] are consistent with each other and consistent with 8-camphanylphosphonic acid (**14**).

Compound	$RP(O)(OH)_2$	$[Pt\{OP(O)(R)O\}(PPh_3)_2]$	$[Pt\{OP(O)(R)O\}(PPhMe_2)_2]$	$[Pt\{OP(O)(R)O\}(DPPE)]$
	14	**16**	**17**	**18**
Solvent	CD_3OD	$CDCl_3$	$CDCl_3$	$CDCl_3$
H_4	2.38, br, s	2.58, br, s	2.75, br, s	2.49, br, s
H_3	1.82, m	1.96, br, m	2.01, br, m	1.84, br, m
H_1	1.77, br, s	1.69, br, s	1.74, br, s	1.56, br, s
$H_{8'/8''}$	1.72, m*	1.60, d, ^2J 12.2 Hz	1.61, d, ^2J 11.7 Hz	1.66, br, s*
	1.65, m	1.54, br, m	1.59, br, m	1.61, br, m
$H_{7''}$	1.66, m	1.68, br, s*	1.67, d, ^2J 13.0 Hz	1.35, d, ^2J 10.6 Hz
$H_{6''}$	1.60, m	1.47, s	1.56, s	1.39, s
$H_{6'}$	1.32, m	1.10, s	1.21, s	1.04, s
$H_{7'}$	1.20, d	1.05, d, ^2J 9.8 Hz	1.15, d, ^2J 13.0 Hz	0.84, d,^2J 10.6 Hz
$H_{5''}$	1.44, m	1.26, m	1.49, br, m	1.28, br, m
$H_{5'}$	1.34, m	0.83, br, m	1.22, br, m	0.87, br, m
Me'	0.98, s	0.95, s	1.01, s	0.80, s
Me"	0.83, s	0.71, s	0.81, s	0.66, s
Ar	-	7.50-7.18	7.37-7.28	7.95-7.20

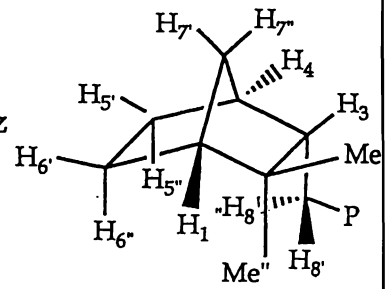

Table 3.14: ^1H NMR data of platinacyclic complexes **16, 17** and **18,** along with the atom numbering scheme.

* denotes multiplicity not detectable, R=$C_{10}H_{17}$=8-camphanyl, coupling constants ±1.2 Hz

Compound	$RP(O)(OH)_2$	$[Pt\{OP(O)(R)O\}(PPh_3)_2]$	$[Pt\{OP(O)(R)O\}(PPhMe_2)_2]$	$[Pt\{OP(O)(R)O\}(DPPE)]$
	14	**16**	**17**	**18**
Solvent	CD_3OD	$CDCl_3$	$CDCl_3$	$CDCl_3$
C(5)	21.0	20.1	20.5	20.2
C(9) Me"	22.3	22.0	22.2	22.1
C(6)	25.6	24.8	24.8	24.7
C(8)	25.2	27.9	28.6	28.0
$^1J_{\text{P-C(8)}}$	138.3 Hz	121.9 Hz	122.0 Hz	121.3 Hz
C(10) Me'	32.3	32.4	32.3	32.2
C(7)	37.8	37.1	37.0	37.1
C(2)	38.3	37.5	37.6	37.5
$^3J_{\text{P-C-C-C(2)}}$	14.1 Hz	13.1 Hz	13.0 Hz	13.9 Hz
C(4)	43.5	42.5	42.8	42.0
$^3J_{\text{P-C-C-C(4)}}$	3.6 Hz	3.3 Hz	3.2 Hz	3.1 Hz
C(3)	46.0	46.1	46.4	46.2
$^2J_{\text{P-C-C(3)}}$	3.9 Hz	3.4 Hz	3.1 Hz	3.1 Hz
C(1)	50.1	49.0	49.0	48.8

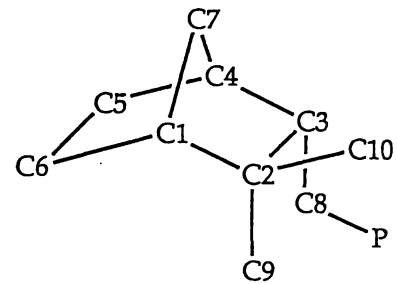

Table 3.15: ^{13}C NMR data of the camphanyl moiety of platinacyclic complexes **16, 17** and **18,** along with the atom numbering scheme. R=$C_{10}H_{17}$=8-camphanyl

3.4.5 Electrospray mass spectrometric analysis of **16, 17** *and* **18**

Surprisingly, the ESMS spectra for these metallacyclic compounds are complex, giving a large number of fragments which are not easily interpreted. The complex **16** gave a weak parent ion $[M+H]^+$ in positive-ion mode at a cone voltage of 20 V which is consistent with the isotope pattern [see Figure 3.10]. Varying the cone voltage made little difference to the complexity of the mass spectrum of **16**. The ESMS spectra of **17** and **18** are not assignable.

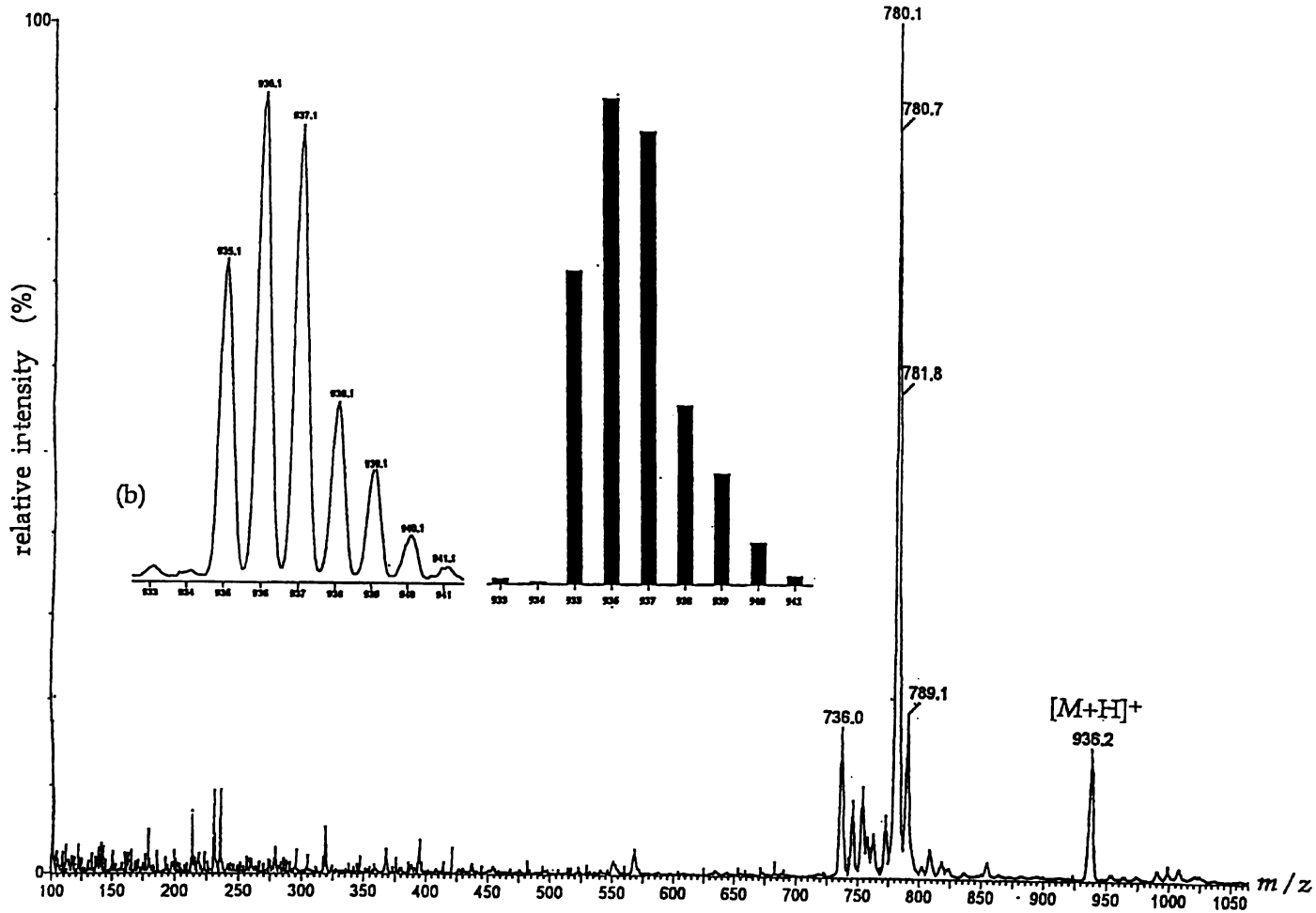

Figure 3.10: Positive-ion electrospray mass spectrum of **16** in 1:1 MeCN/H_2O at a cone voltage of 20 V. The insert shows observed (LHS) and calculated (RHS) isotope distribution pattern of $[M+H]^+$ at m/z 936.

3.5 *Experimental*

General instrumental techniques are as described in Appendix II. Analytical grades of silver(I) oxide (BDH) and sulfur dioxide (BDH) were used as supplied. Other reagents used were laboratory grade and were used as supplied. All solvents used were of reagent grade. Petroleum spirit refers to the fraction of b.p. 40-60°C. Diazomethane[33], $[PtCl_2(COD)]$[34], *cis*-$[PtCl_2(PPh_3)_2]$[35], $[PtCl_2(DPPE)]$[36], *cis*-$[PtCl_2(PPhMe_2)_2]$[36], $[PdCl_2(COD)]$[37] and $[PdCl_2(PPh_3)_2]$[36] were all prepared by standard literature procedures.

*3.5.1 Synthesis of 8-camphanylphosphonic acid (**14**) by direct oxidation using SO_2*

8-Camphanylphosphinic acid (**1**) (77.4 g, 0.38 mol) was dissolved in a mixture of isopropanol (500 mL) and water (100 mL), the solution heated to reflux and sulfur dioxide bubbled through for 4 h. The reaction mixture was cooled and nitrogen bubbled through it for 30 mins. Sulfur was removed by filtration through a celite bed. Removal of solvent by rotary evaporation gave 8-camphanylphosphonic acid (**14**) as a white crystalline solid (71.0 g, 85%), m.p. 171-173°C. (Found: C, 55.04; H, 8.85; P, 14.16. $C_{10}H_{19}O_3P$ requires C, 55.02; H, 8.78; P, 14.19%.). ESMS (cone 45 V, negative ion); $[M\text{-}H]^-$ at m/z 217.

NMR : $^{31}P\text{-}\{^1H\}$ (D_2O/NaOH): δ 23.8, [s].

^1H (CD_3OD): δ 9.97 [2H, s, br, OH], 2.38 [1H, s, br, H_4], 1.82 [1H, m, $H_3]_a$, 1.77 [1H, s, br, $H_1]_b$, 1.72 [1H, m, $H_{8'/8''}]_b$, 1.66 [1H, m, $H_{7''}]_b$, 1.65 [1H, m, $H_{8'/8''}]_b$, 1.60 [1H, m, $H_{6''}]_a$, 1.44 [1H, m, $H_{5''}]_a$, 1.34 [1H, m, $H_{5'}]_a$, 1.32 [1H, m, $H_{6'}]_b$, 1.20 [1H, dt, ^2J 9.7, ^3J 1.7, $H_{7'}]_a$, 0.98 [3H, s, Me'], 0.83 [3H, s, Me''].

a: partially overlapping signals

b: overlapping signals

^{13}C-{^{1}H} (CD_3OD) : δ 50.1 [d, $^{4}J_{P\text{-}C\text{-}C\text{-}C}$ 3.9 Hz, C(1)], 46.0 [d, ^{2}J(PC) 3.9 Hz, C(3)], 43.5 [d, $^{3}J_{P\text{-}C\text{-}C\text{-}C}$ 3.6 Hz, C(4)], 38.3 [d, $^{3}J_{P\text{-}C\text{-}C\text{-}C}$ 14.1 Hz, C2], 37.8 [s, C(7)], 32.3 [s, C(10)], 25.6 [s, C(6)], 25.2 [d, $^{1}J_{P\text{-}C}$ 138.3 Hz, C(8)], 22.3 [s, C(9)], 21.0 [s, C(5)].

I.R. : υ(P=O) region (1300-1140 cm^{-1}) 1122 broad, strong

υ(P-OH) region (1040-910 cm^{-1}) 1053 broad, strong

Note that due to the complexity of the I.R. spectrum, the above signals were only tentatively assigned.

*X-ray crystal structure of 8-camphanylphosphonic acid (**14**)*

Cell parameters and intensity data were obtained at 163 K using a Nicolet R3 four-circle diffractometer with monochromated Mo-K_α radiation (λ = 0.7107Å). A total of 1522 reflections (1193 unique) in the range $5^\circ<2\theta<50^\circ$ were collected, and corrected for Lorentz and polarisation effects. No absorption correction was deemed necessary because of the low value of the linear absorption coefficient.

Crystal data: $C_{10}H_{19}O_3P$, *M* 218.22, trigonal, space group $\overline{R3}$, *a*=*b*=27.012(5), *c*=8.041(4)Å, *U*=5081(3) $Å^3$. D_c 1.284 g cm^{-3} for *Z*=18. *F*(000) 2124, μ(Mo-Kα) 0.22 mm^{-1}.

*Solution and refinement of 8-camphanylphosphonic acid (**14**)*

This structure was solved by Dr Mark Turnbull at Clark University and fully developed at Waikato University using direct methods. Refinement included all non-hydrogen atoms with anisotropic temperature factors. The hydrogen atoms attached to carbon were included in calculated positions. The hydrogen atom on O(1) was located in a hydrogen-bonding position between O(1) and O(2) in a penultimate difference map and was

included with fixed coordinates. The hydrogen atom on O(3) was not found so was included in a calculated position on the O(3)..O(2) vector. Refinement converged at R_1 [for 1193 reflections with $I>2\sigma(I)$]=0.0842, wR_2 [all data]=0.1985, GoF 0.916. In the last cycle of refinement no parameter shifted by more than a maximum (Δ/σ) of 0.003. The largest features in a final difference map were +0.619/-0.408 e $Å^{-3}$. The high R factor reflects the poor data set collected, the result of a small, weakly diffracting crystal.

*3.5.2 Synthesis of 8-camphanylphosphonic acid (**14**) by direct oxidation using $Cu(NO_3)_2$*

8-Camphanylphosphinic acid (**1**) (2.0 g, 9.9 mmol) and $Cu(NO_3)_2.3H_2O$ (2.39 g, 9.8 mmol) were dissolved in a methanol (70 mL)/water (10 mL) mixture and heated to reflux for 4.5 h. After cooling, the brown precipitate of copper metal[Ψ] , was removed by filtration. Removal of solvent by rotary evaporation gave a white solid which was found to be 8-camphanylphosphonic acid (**14**) (2.1 g, 70%) by ^{31}P NMR and by melting point.

*3.5.3 Synthesis of 8-camphanylphosphonic acid (**14**) by hydrolysis of **11***

An aqueous solution (30 mL) of 8-camphanylphosphonic dichloride (**11**) (0.36 g, 1.41 mmol), prepared as described in section 2.5.4, was heated to reflux for 6 h. The white precipitate was filtered off and found to be 8-camphanylphosphonic acid (**14**) (0.24 g, 80%) by ^{31}P NMR, ^{1}H NMR and melting point.

[Ψ] The brown precipitate was found to be copper metal as it was insoluble in dilute HNO_3 [*c.f.* similarly coloured Cu_2O which is soluble in dilute HNO_3].

3.5.4 Synthesis of dimethyl 8-camphanylphosphonate (15)

An excess of diazomethane was added to 8-camphanylphosphonic acid (**14**) (0.29 g, 1.3 mmol) and the resulting solution stoppered for 24 h. The excess diazomethane was removed by evaporation at atmospheric pressure and the solution concentrated to yield dimethyl 8-camphanylphosphonate (**15**) as a colourless oil (0.30 g, 98%). GCMS *m/z* at 246 (M^+, 21%).

NMR : ^{31}P-{^{1}H}: δ 35.8 [s].

^{1}H: δ 3.69, 3.65 [6H, br, s, OMe], 2.26 [1H, br, s , H_4], 1.73 [1H, br, m, H_3]$_a$, 1.72 [1H, br, s, H_1]$_a$, 1.72-1.66 [2H, m, $H_{8'/8''}$]$_b$, 1.62 [1H, d, ^2J 9.7, $H_{7''}$]$_a$, 1.49 (1H, br, m, $H_{6''}$], 1.31-1.20 [2H, m, $H_{5''/5'}$]$_b$, 1.23 [1H, br, m, $H_{6'}$]$_b$, 1.15 [1H, d, ^2J 9.7, $H_{7'}$]$_a$, 0.92 [3H, s, Me'], 0.74 [3H, s, Me''].

a: partially overlapping signals

b: overlapping signals

^{13}C-{^{1}H} : δ 52.20 [d, $^2J_{\text{P-C-C}}$ 6.8 Hz, OMe]*, 52.10 [d, $^2J_{\text{P-C-C}}$ 6.8 Hz, OMe]*, 48.6 [s, C(1)], 44.3 [d, $^2J_{\text{P-C-C}}$ 3.7 Hz, C(3)], 42.3 [d, $^3J_{\text{P-C-C-C}}$ 3.9 Hz, C(4)], 37.5 [d, $^3J_{\text{P-C-C-C}}$ 14.3 Hz, C(2)], 36.9 [s, C(7)], 31.8 [s, C(10)], 24.6 [s, C(6)], 22.0 [d, $^1J_{\text{P-C}}$ 140.1 Hz, C(8)], 21.9 [s, C(9)], 20.0 [s, C(5)].

* denotes a tentative assignment.

I.R. :	υ(P=O) region (1300-1140 cm^{-1})	1253, 1237, 1184 broad, strong
	υ(P-O-C) region (1050-970 cm^{-1})	1057, 1032, broad, strong

Due to the complexity of the I.R. spectrum, the above signals were only tentatively assigned.

Raman : υ(P=O) 924 cm^{-1} sharp, strong

A trace amount of **14**, produced by the air hydrolysis of **15**, was detected in the ^{31}P NMR spectrum of dimethyl 8-camphanylphosphonate (**15**). Unfortunately reliable analytical data were not obtainable, even with the vacuum sealing of a vacuum distilled (140°C at 0.5 mmHg) sample.

GCMS studies [50°C to 250°C at 1°C per mins] gave a major product **15** [M^+ at m/z 246, R_f=0.148] and the minor product **15a** [M^+ at m/z 246, R_f=0.150].

Synthesis of platinum-phosphonate complexes

The typical preparation and purification procedure utilised for the formation of four-membered ring metallacyclic complexes is illustrated in the preparation of **16** in section 3.5.5.

3.5.5 Synthesis of $[\overline{Pt\{OP(O)(C_{10}H_{17})O\}}(PPh_3)_2]$ *(16)*

8-Camphanylphosphonic acid (**14**) (0.06 g, 0.27 mmol), *cis*-$[PtCl_2(PPh_3)_2]$ (0.21 g, 0.27 mmol) and an excess of silver(I) oxide (0.17 g, 0.73 mmol) were added in succession to dichloromethane (30 mL). After 36 h heated at reflux and vigorous stirring the excess silver(I) oxide was removed by filtration and the yellow solution evaporated to dryness under vacuum. Recrystallisation of the yellow oil from chloroform/petroleum spirit gave **16** as a colourless needle-like crystalline solid (0.15 g, 60%), m.p. 224-225°C. (Found C, 55.75%; H, 5.28%. $C_{46}H_{47}PtP_3O_3.3H_2O$ requires C, 55.80; H, 5.40%.) The existence of **16** as a trihydrate was confirmed by the integration of the water signal in the ^1H NMR. ESMS (cone 40 V, positive ion); $[M+H]^+$ at m/z 937.

NMR: ^{31}P-{^1H}:

δ 5.37 [dd, $^1J_{\mathbf{P_x\text{-}Pt}}$ 3732 Hz, $^2J_{\mathbf{P_x\text{-}Pt\text{-}P_y}}$ 26 Hz, $^3J_{\mathbf{P_x\text{-}Pt\text{-}O\text{-}P_z}}$ 7 Hz, P_x]

δ 7.49 [dd, $^1J_{\mathbf{P_y\text{-}Pt}}$ 3843 Hz, $^2J_{\mathbf{P_y\text{-}Pt\text{-}P_x}}$ 26 Hz, $^3J_{\mathbf{P_y\text{-}Pt\text{-}O\text{-}P_z}}$ 7 Hz, P_y]

δ 55.26 [t, $^2J_{P_z\text{-O-Pt}}$ 117 Hz, $^3J_{P_z\text{-O-Pt-}P_x\,/(P_y)}$ 7 Hz, P_z]

^{1}H : δ 7.80-7.30 [30H, m, aryl]$_b$, 2.58 [1H, br, s, H_4], 1.96 [1H, br, m, H_3], 1.69 [1H, br, s, H_1]$_a$, 1.68 [1H, br, s, $H_{7''}$]$_b$, 1.60 [1H, d, ^2J 12.2, $H_{8'/8''}$]$_b$, 1.54 [1H, m, $H_{8'/8''}$]$_b$, 1.47 [1H, s, $H_{6''}$]$_a$, 1.26 [1H, m, $H_{5''}$], 1.10 [1H, s, $H_{6'}$]$_b$, 1.05 [1H, d, ^2J 9.75, $H_{7'}$]$_a$, 0.95 [3H, s, Me'), 0.83 [1H, br, m, $H_{5'}$], 0.71 [3H, s, Me''].

a: partially overlapping signals

b: overlapping signals

^{13}C-{^{1}H} : δ 131.5-128.4 [m, aryl], 49.0 [s, C(1)], 46.1 [d, $^2J_{\text{P-C-C}}$ 3.4 Hz, C(3)], 42.5 [s, $^3J_{\text{P-C-C-C}}$ 3.3 Hz, C(4)], 37.5 [d, $^3J_{\text{P-C-C-C}}$ 13.1 Hz, C(2)], 37.1 [s, C(7)], 32.4 [s, C(10)], 27.9 [d, $^1J_{\text{P-C}}$ 121.9 Hz, C(8)], 24.8 [s, C(6)], 22.0 [s, C(9)], 20.1 [s, C(5)].

3.5.6 *Synthesis of* $[Pt\{OP(O)(C_{10}H_{17})O\}(PPhMe_2)_2]$ *(17)*

The platinacyclic complex $[Pt\{OP(O)(C_{10}H_{17})O\}(PPhMe_2)_2]$ (17) was prepared by the method described in section 3.5.5. Purification of the crude reaction mixture was achieved by removing the solvent under vacuum and washing the resulting yellow solid with acetone (0.5 ml) to remove impurities. The white crystalline solid obtained, 17 (0.08 g, 67%), gave the following physical and spectral properties. M.p. 233-234°C. (Found C, 45.35%; H, 5.97%. $C_{26}H_{39}PtP_3O_3$ requires C, 45.40; H, 5.72 %.)

NMR: ^{31}P-{^{1}H}:

δ 20.9 [d, $^1J_{P_x\text{-Pt}}$ 3654 Hz, $^3J_{P_x\text{-Pt-O-}P_z}$ 4 Hz, P_x]

δ 20.9 [d, $^1J_{P_y\text{-Pt}}$ 3654 Hz, $^3J_{P_y\text{-Pt-O-}P_z}$ 4 Hz, P_y]

δ 53.2 [t, $^2J_{P_z\text{-O-Pt}}$ 100 Hz, $^3J_{P_z\text{-Pt-O-}P_x/(P_y)}$ 4 Hz, P_z]

^1H : δ 7.37-7.28 [10, m, Ar]$_b$, 2.75 [1H, br, s, H_4], 2.01 [1H, br, m, H_3], 1.74 [1H, br, s, H_1]$_b$, 1.67 [1H, br, s, $H_{7''}$]$_b$, 1.65-1.49 [1H, br, m, CH_3]$_b$, 1.61, [1H, d, ^2J 11.7, $H_{8'/8''}$]$_b$, 1.59 [1H, m, $H_{8'/8''}$]$_b$, 1.56 [1H, s, $H_{6''}$]$_b$, 1.49 [1H, br, m, $H_{5''}$]$_b$, 1.22 [1H, br, m, $H_{5'}$]$_b$, 1.21 [1H, s, $H_{6'}$]$_b$, 1.15 [1H, d, ^2J 11.1, $H_{7'}$]$_a$, 1.01 [3H, s, Me'], 0.81 [3H, s, Me''].

a: partially overlapping signals

b: overlapping signals

^{13}C-{^1H} : δ 131.5-128.5 [12C, m, aryl], 49.0 [s, C(1)], 46.4 [d, $^2J_{P\text{-}C\text{-}C}$ 3.1 Hz, C(3)], 42.8 [s, $^3J_{P\text{-}C\text{-}C\text{-}C}$ 3.2 Hz, C(4)], 37.6 [d, $^3J_{P\text{-}C\text{-}C\text{-}C}$ 13.0 Hz, C(2)], 37.0 [s, C(7)], 32.3 [s, C(10)], 28.6 [d, $^1J_{P\text{-}C}$ 122.0 Hz, C(8)], 24.8 [s, C(6)], 22.2 [s, C(9)], 20.5 [s, C(5)], 12.5, 12.9 [t, $^1J_{P\text{-}C}$ 30.9 Hz, 2 x CH_3].

3.5.7 Synthesis of [Pt{OP(O)($C_{10}H_{17}$)O} (DPPE)] (18)

The platinacyclic complex [Pt{OP(O)($C_{10}H_{17}$)O}(DPPE)] (**18**) was prepared by the standard method described in section 3.5.5. Purification of **18** was achieved by the recrystallisation of the crude reaction mixture, a yellow oil, from chloroform/petroleum spirit at room temperature. The colourless needle-like crystals of **18** (0.09 g, 70%) gave the following physical and spectral properties. M.p. >140°C decomposes upon heating.

NMR: ^{31}P-{^1H} :

δ 30.50 [dd, $^1J_{P_x\text{-}Pt}$ 3730 Hz, $^2J_{P_x\text{-}Pt\text{-}P_y}$ 20 Hz, $^3J_{P_x\text{-}Pt\text{-}O\text{-}P_z}$ 7 Hz, P_x]

δ 31.0 [dd, $^1J_{P_y\text{-}Pt}$ 3701 Hz, $^2J_{P_y\text{-}Pt\text{-}P_x}$ 20 Hz, $^3J_{P_y\text{-}Pt\text{-}O\text{-}P_z}$ 7 Hz, P_y]

δ 58.4 [t, $^2J_{P_z\text{-}O\text{-}Pt}$ 102 Hz, $^3J_{P_z\text{-}O\text{-}Pt\text{-}P_x\,/(P_y)}$ 7 Hz, P_z]

^1H : δ 7.95-7.20 [20H, m, aryl]$_b$, 2.54-2.37 [4H, m, CH_2]$_a$, 2.49 [1H, br, s, H_4]$_a$, 1.84 [1H, br, m, H_3], 1.66 [1H, br, s, $H_{8'/8''}$]$_b$, 1.61 [1H, m, $H_{8'/8''}$]$_b$, 1.56 [1H, br, s, H_1]$_a$, 1.39 [1H, s, $H_{6''}$]$_b$, 1.35 [1H, d, ^2J 10.6, $H_{7''}$]$_b$, 1.28 [1H, m, $H_{5''}$]$_b$,

1 .04 [1H, s, $H_{6'}$], 0.82 [1H, d, ^2J 10.6, $H_{7'}]_b$, 0.87 [1H, m, $H_{5'}]_b$, 0.84 [3H, s, Me'], 0.70 [3H, s, Me''].

a: partially overlapping signals

b: overlapping signals

^{13}C-{^1H} : δ 133.2-129.1 (24C, m, aryl], 48.8 [s, C(1)], 46.2 [d, $^2J_{P\text{-}C\text{-}C}$ 3.2 Hz, C(3)], 42.0 [s, $^3J_{P\text{-}C\text{-}C\text{-}C}$ 3.0 Hz, C(4)], 37.5 [d, $^3J_{P\text{-}C\text{-}C\text{-}C}$ 13.9 Hz, C(2)], 37.1 [s, C(7)], 32.2 [s, C(10)], 28.0 [d, $^1J_{P\text{-}C}$ 121.3 Hz, C(8)], 27.2, 26.6 [t, $^1J_{P\text{-}C}$ 3.8 Hz, CH_2], 24.7 [s, C(6)], 22.1 [s, C(9)], 20.2 [s, C(5)].

3.5.8 *Attempted synthesis of* $[Pt\{HP(O)(C_{10}H_{17})O\}_2(PPh_3)_2]$

8-Camphanylphosphinic acid (0.05 g, 0.24 mmol), *cis*-$[PtCl_2(PPh_3)_2]$ (0.09 g, 0.11 mmol) and an excess of silver(I) oxide (0.1 g, 0.43 mmol) were added in succession to dichloromethane (30 mL). After 36 h of vigorous stirring and heating at reflux the excess silver(I) oxide was removed by filtration and the yellow/orange solution evaporated to dryness under vacuum to give a yellow oil.

A ^{31}P NMR spectrum of the crude reaction mixture gave a large number of signals. Over a period of 9 days the crude reaction mixture went from yellow to orange to brown. The examination of the ^{31}P NMR spectrum after 5 days showed a large number of broad multiplets present. As decomposition was occurring no further investigation was undertaken.

3.5.9 *Attempted synthesis of* $[Pt\{OP(O)(C_{10}H_{17})O\}(COD)]$

8-Camphanylphosphonic acid (**14**) (0.05 g, 0.23 mmol), $[PtCl_2COD]$ (0.08 g, 0.22 mmol) and an excess of silver(I) oxide (0.10 g, 0.43 mmol) were added in succession to dichloromethane (30 mL). The mixture was refluxed and stirred vigorously for 48 h. The excess silver(I) oxide was removed by filtration and the brown solution evaporated to dryness to give a brown oil.

No further investigation was undertaken due to the complexity of the ^{31}P NMR spectrum.

3.5.10 Attempted synthesis of $[Pd\{OP(O)(C_{10}H_{17})O\}(PPh_3)_2]$

8-Camphanylphosphonic acid (**14**) (0.07 g, 0.3 mmol), $[PdCl_2(PPh_3)_2]$ (0.19 g, 0.28 mmol) and an excess of silver(I) oxide (0.17 g, 7.5 mmol) were added in succession to dichloromethane (30 mL). After 36 h of heating at reflux and vigorous stirring the excess silver(I) oxide was removed by filtration and the solution evaporated to dryness. The ^{31}P NMR spectrum of the crude reaction mixture gave a large number of unexpected signals that were not consistent with the Pt analogue. As it was clear that reactions other than cyclisation had occurred, that were not obvious, no further investigation was undertaken.

References

1 A.W. Frank in *Organic Phosphorus Compounds*, Ed by G.M. Kosolapoff, L. Maier, Wiley and Sons (1973), 4, 295.

2 G.M. Burch, H. Goldwhite, R.N. Haszeldine, *J. Chem. Soc.*, (1964), 572.

3 H.J. Emeleus, J.D. Smith, *J. Chem. Soc.*, (1959), 375.

4 H.C. Brown, U.S Patent 2, (1952), 584, 112.

5 F. Guichard, *Ber.*, (1899), **32**, 1572.

6 H.J. Emeleus, R.N. Haszeldine, R.C. Paul, *J. Chem. Soc.*, (1955), 563.

7 H.H. Hatt, *J. Chem. Soc.*, (1933), 776.

8 D.Davies, *J. Chem. Ind.* (London), (1964), 1755.

9 D. Fiat, M. Halmann, L. Kugel, J. Reuben, *J. Chem. Soc.*, (1962), 3837.

10 P.A.T. Hoye in *Mellor's Comprehensive Treatise on Inorganic Chemistry*, Scetion XXXIII, p. 1082

11 G.B. Arnold, C.S. Hamilton, *J. Amer. Chem. Soc.*, (1941), **63**, 2637.

12 A.W. Frank, *Chem. Rev.*, (1961), **61**, 389.

13 M. McCann, E. Murphy, C. Cardin, M. Convery, *Polyhedron*, (1992), **11**, 3101.

14 P.C. Crofts in *Organic Phosphorus Compounds*, Ed by G.M. Kosolapoff, L. Maier, Wiley and Sons (1973), **6**, 38.

15 P.J. Biddle, J. Kennedy, J.L. Williams, *J. Chem. Ind.* (London), (1957), 1481.

16 L.M. Yagupol'skii, P.A Yufa, *Zh. Obshch. Khim.*, (1960), **30**, 1294.

17 B.I. Stepanov, A.I. Bokanov, E.N. Karpova, N.V. Danilova, *Zh. Obshch. Khim.*, (1970), **40**, 2217.

18 Yu.M. Zinov'ev, L.Z. Soborovskii, *Zh. Obshch. Khim.*, (1956), **26**, 3030.

19 Personal communication, W. Henderson, Waikato University

20 J. Kowalik, W. Sawka-Dobrowolska, T. Glowiak, *J. Chem. Soc. Chem. Comm.*, (1984), 446.

21 J. Kowalik, W. Sawka-Dobrowolska, T. Glowiak, *Acta Cryst.*, (1992), **C48**, 288.

22 W. Sawka-Dobrowolska, *Acta Cryst.*, (1988), **C44**, 2193.

23 G. Ferguson, J.F. Gallagher, *Acta Cryst.*, (1993), **C49**, 1024-1026.

24 G. Cao, V.M. Lynch, L.N. Yacullo, *Chem. Mater.*, (1993), **5**, 1000; G. Cao, T. Mallouk, *Inorg. Chem.*, (1991), **30**, 1434.

25 J.C. Tebby in *Phosphorus-31 NMR Spectroscopy in Stereochemical Analysis*, VCH Publishers Inc. (1987), 1-59, and references therein.

26 P.C. Crofts in *Organic Phosphorus Compounds*, Wiley and Sons, Ed by G.M. Kosolapoff, L. Maier, (1973), 6, 45 and references therein.

27 S.D. Chappell, D.J. Cole-Hamilton, *Polyhedron*, (1982), 11-12, 739.

28 R.D.W. Kemmitt, S. Mason, J. Fawcett, D.R. Russell, *J. Chem. Soc. Dalton Trans.*, (1992), 851.

29 R.D.W Kemmitt, S. Mason, M.R. Moore, J. Fawcett, D.R. Russell, *J. Chem. Soc. Chem. Comm.*, (1990), 1535.

30 M.J. Bloemink, J.P. Dorenbos, R.J. Heeterbrij, B.K. Keppler, J. Reedijk, H. Zahn, *Inorg. Chem.*, (1994), **33**, 1127-1132 and references therein.

31 G. Klose, *Ann.Phys.*, (1962), **9**, 262; G. Buchanan, J. Bowen, *Can. J. Chem.*, (1977), **55**, 604; G. Buchanan, C. Benezra, *Can. J. Chem.*, (1975), **54**, 231.

32 T.G. Appleton, H.C. Clark, L.E. Manzer, *Coordination Chemistry Reviews*, (1973), **10**, 335-422.

33 *Org. Synth. Coll.*, (1943), Vol II, 165

34 J.X. Mc Dermott, J.F. White, G.M. Whitesides, *J. Am. Chem. Soc.*, (1976), **98**, 6521.

35 D.L. Oliver, G.K. Anderson, *Polyhedron*, (1992), 11, 2415; G.K. Anderson, H.C. Clark, J.A. Davies, *Inorg. Chem.*, (1981), **20**, 3607

36 Pt(II) and Pd(II) complexes were synthesised by the general preparation described in reference 35.

37 D. Drew, J.R. Doyle, *Inorg. Synth.*, (1972), **13**, 52.

Chapter Four

Syntheses and characterisation of camphene-derived phosphines and their derivatives

4.1 Introduction

The development of much of modern coordination chemistry has been facilitated by the continuing rapid development in the chemistry of tertiary phosphines. Metal complexes of such ligands find application in areas as diverse as homogeneous catalysis[1] and medicine[2]. For simplicity, the chemistry of phosphines has been categorised into the four general areas outlined below, which are of relevance to this current study. The extensive volume of chemistry that exists within each of these classes is such that a summary of the chemistry within this context is not practical. Thus, the aim of this overview is to direct the reader to the key/novel reviews available. It is worth noting that the examples quoted in this review are only relevant in that they briefly illustrate the chemistry of the general field in question.

(i) Achiral phosphines

The numerous methods for the synthesis of achiral phosphines have been exhaustively reviewed by Maier within Volume 5 of *Progress in Inorganic Chemistry* (1963)[3] and later revised by Maier within Volume 1 of *Organic Phosphorus Compounds* (1972)[4]. More recent comprehensive reports include publications by *Cotton et al* (1994)[5], which describe the synthesis and selected applications of polydentate phosphines, and Gilheany *et al* (1990)[6].

(ii) Chiral phosphines

An area of some significance is the synthesis of chiral phosphines and the applications of the metal phosphine derivatives in asymmetric catalysis. Kagan and Sasaki (1990)[7] review the diverse range, preparation and applications of chiral phosphines and their derivatives. More recent reports which review specific areas of chiral phosphine chemistry include reports by Pietrusiewicz and Zablocka (1994)[8], which describe the synthesis of scalemic P-chiral phosphines and their derivatives, and Mayer and Kaska (1994)[9].

(iii) Water-soluble phosphines

There is significant and continued interest in the chemistry of water-soluble phosphine derivatives, which have significant potential for the development of new and improved catalytic systems. The potential of a water soluble catalyst is clearly demonstrated by the hydroformylation process operated by Rhone-Poulenc, which utilises the sulphonated rhodium phosphine catalyst $HRh(CO)L_3$ [$L=Ph_2P(C_6H_4SO_3Na)$][10]. The preparation and applications of water soluble phosphines in homogeneous catalysis has been recently reviewed[1]. A recent comprehensive report by Herrmann and Kohlpaintner (1993)[11] outlines the synthesis of water-soluble phosphines and their metal derivatives. The application of these phosphines as two-phase catalysts is also discussed within this report. A recent novel example describes the catalytic hydrogenation of aldehydes in an aqueous two-phase solvent system using a 1,3,5-triaza-7-phosphaadamantane (PTA) complex of ruthenium[12]. Another example is the Ru(II) complex of sulphonated BINAP as an asymmetric catalyst where a 90% enantiomeric excess is obtained for the hydrogenation of 2-acylamino acid precursors and methylenesuccinic acid[13].

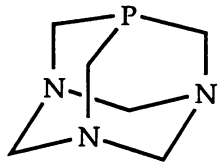

PTA

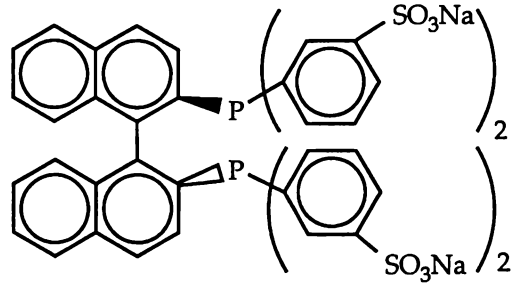

BINAP-4-SO_3Na

(iv) Hydroxymethylphosphines

Hydroxymethylphosphines have been known for some years, however an increased interest in the catalytic and biomedical applications of water-soluble phosphines has led to a renewed interest in hydroxymethyl-phosphorus chemistry. This resurgence of interest is clearly demonstrated with tris(hydroxymethyl)phosphine [THP] where a renewed interest in its chemistry[14] has been generated by an interest in the application of THP metal derivatives as homogeneous catalysts[15]. The reactivity of THP with amines, amino acids and model peptides has also been recently studied[16].

A general review on the synthesis of hydroxymethylphosphorus compounds[17] (which includes phosphines) describes the importance of this class of compound. The applications of water-soluble phosphines (1979 to 1991) has been reviewed[18]. Cristau and Plenat (1990)[19] review the preparation, properties and reactions of phosphonium salts (using phosphines).

Katti *et al* have published comprehensive reviews (1996 and 1999)[20] on the advances, synthesis and applications of bis-, tri- and tetra-hydroxymethylphosphines and their metal derivatives. Hydroxymethyl-phosphines have also been utilised in the development of dendrimers[21].

The diverse range of chemistry that is accessible through phosphines suggests that an investigation of the chemistry of camphene-derived phosphines may be a highly attractive starting point for the development of novel phosphines.

4.2 Synthesis and characterisation of 8-camphanylphosphine

4.2.1 Introduction

Two well established methods for the synthesis of primary phosphines are the disproportionation of phosphinic acids of the type RP(O)(OH)(H)[22, 23], Scheme 4.1, and the use of reducing agents such as silanes[24], H_2S[25], LiH[26], Li[27], $LiBH_4$[28] and $LiAlH_4$. Although the former method, which affords the corresponding phosphonic acid as a byproduct, is straightforward, an inherent problem is that a maximum 33% yield based on the starting phosphinic acid suggests that this synthetic route is best suited to inexpensive starting materials which are themselves easily synthesised.

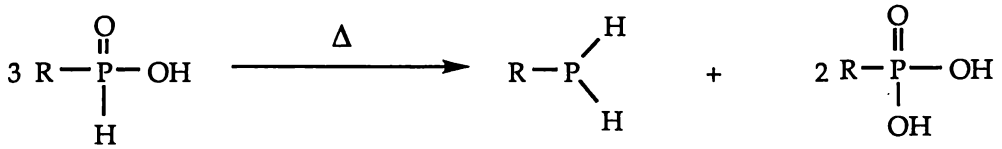

Scheme 4.1: The disproportionation of phosphinic acids.

The latter method, which involves the use of a reducing agent, is the most common method employed for the preparation of primary phosphines. The diverse range of starting materials is clearly illustrated in Scheme 4.2 and includes dihalophosphines [equation (i)], phosphonic dichlorides [equation (ii)], phosphonic acids [equation (iii)], phosphonates [equation (iv)], phosphonites [equation (v)] and phosphonothionates [equation (vi)]. Of the various starting materials and reducing agents available, the treatment of phosphorus compounds with the reducing agent $LiAlH_4$ [equations (i) and (ii) in Scheme 4.2], which was first introduced by Hovat and Furst[29], is the most widely used method. Studies suggest that the reduction probably proceeds through the formation of complexes of the type $Li[H_{4-x}Al(PRH)_x]$ (value of x is unknown)[30].

(i) $2RPCl_2 + LiAlH_4 \longrightarrow 2RPH_2 + LiAlCl_4$

(ii) $4RP(O)Cl_2 + 3LiAlH_4 \longrightarrow 4RPH_2 + 2LiAlCl_4 + LiAl(OH)_4$

(iii) $2RP(O)(OH)_2 + LiAlH_4 \longrightarrow 2RPH_2 + LiAl(OH)_4$

(iv) $4RP(O)(OR')_2 + 3LiAlH_4 \longrightarrow 4RPH_2 + LiAl(OH)_4 + 2LiAl(OR')_4$

(v) $2RP(OR')_2 + LiAlH_4 \longrightarrow 2RPH_2 + LiAl(OR')_4$

(vi) $4RP(S)Cl_2 + 3LiAlH_4 \longrightarrow 4RPH_2 + 2\,LiAlCl_4 + LiAl(SH)_4$

Scheme 4.2: The reduction of phosphorus compounds with $LiAlH_4$.

The camphene-derived phosphinic acid **1** [refer to section 2.1.2 for more detail] and phosphonic dichloride **11** [refer to section 2.3.2 for more detail] are therefore ideal precursors in the synthesis of camphene-derived phosphines. Thus an investigation of their reactivity, particularly that relating to phosphine chemistry, was undertaken.

4.2.2 Results and discussion

The treatment of 8-camphanylphosphonic dichloride (**11**) with an excess of lithium aluminium hydride [$LiAlH_4$], Scheme 4.3, yields a white solid with spectral properties consistent with 8-camphanylphosphine (**19**). The purification of phosphine **19** is accomplished by the addition of dichloromethane to the reaction mixture, which allows the insoluble lithium aluminium salts to be filtered from the dichloromethane-soluble **19**.

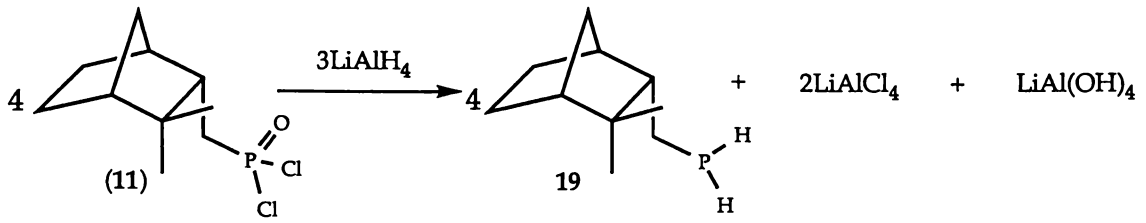

Scheme 4.3: The reduction of 8-camphanylphosphonic dichloride (**11**) with lithium aluminium hydride [$LiAlH_4$].

Despite affirmation of the presence of **19** by both the proton-coupled ^{31}P NMR spectrum, which gave a characteristic 1:2:1 triplet signal [^{1}J(PH) 194 Hz] at δ -140.4, and the ^{1}H NMR spectrum, which gave no discrepancies with the formulated structure, the microanalytical data suggests that this material was either impure or did not possess simple stoichiometry [Analysis: Found C, 28.47; H, 5.83%. $C_{10}H_{17}PH_2$ requires C, 70.54; H, 11.26%]. However repeatedly performing the purification process noted above made no significant difference to subsequent microanalytical results. Furthermore, attempts to vacuum distil **19**, a technique routinely employed for the purification of phosphines, also met with no success despite the use of high temperatures [>200°C at 0.5 mmHg]. It is therefore concluded, after taking into account the experimental results and observations, that phosphine **19** is not the free phosphine $C_{10}H_{17}PH_2$ but a metal-phosphine adduct which is observed in this type of reaction[31].

The availability of the inexpensive, easily manufactured starting material **1** means that despite the inherently low yield, which is discussed in the previous section, the disproportionation of **1** on a large laboratory scale appears to be a viable means to the synthesis of primary phosphines.

Thus, when **1** is heated to 140°C under vacuum [0.5 mmHg], it disproportionates to yield 8-camphanylphosphine (**20**) as an air-sensitive odorous liquid (see Scheme 4.4). Full characterisation of **20** by ^{1}H, ^{13}C and ^{31}P NMR spectroscopy is presented in section 4.2.3.

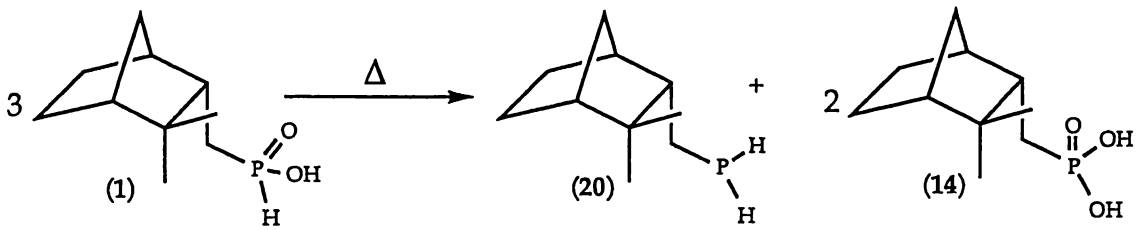

Scheme 4.4: The thermal reduction of 8-camphanylphosphinic acid (**1**).

The apparatus shown in Figure 4.1 enables the disproportionation and distillation to occur simultaneously *in situ*. The heating [140°C at 0.5 mmHg] of the reaction vessel initiates the disproportionation of the phosphinic acid **1** to the phosphine **20** and phosphonic acid **14**. The gaseous phosphine **20** is drawn under vacuum into a trap cooled with liquid nitrogen where it then condenses. To prevent contamination of phosphine **20** with the phosphonic acid **14**, which distils above 200°C [0.5 mmHg], the phosphinic acid **1** is not heated above 150°C [0.5 mmHg]. It is worth noting that both the reaction vessel and delivery tube are insulated to prevent condensation of the phosphine.

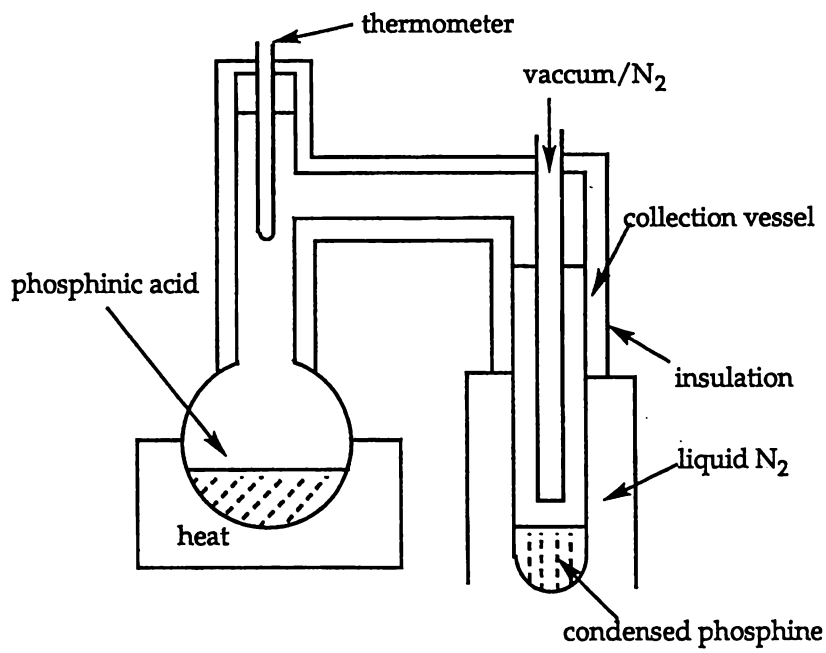

Figure 4.1: Apparatus designed to facilitate both the disproportionation of phosphinic acid **1** and the distillation of the primary phosphine **20**.

Primary phosphines, particularly the lower aliphatic phosphines, which spontaneously ignite in air, are easily oxidised. As illustrated in

Scheme 4.5 8-camphanylphosphine (**20**) is also oxidised in the presence of air to 8-camphanylphosphine oxide (**21**). The proton-coupled ^{31}P NMR spectrum of the phosphine oxide **21** [δ 9.2, t, $^{1}J_{P\text{-}H}$ 416.4 Hz] is consistent with that of the primary phosphine oxide $C_{10}H_{25}P(O)H_2$ [δ 3.9, t, $^{1}J_{P\text{-}H}$ 457][32].

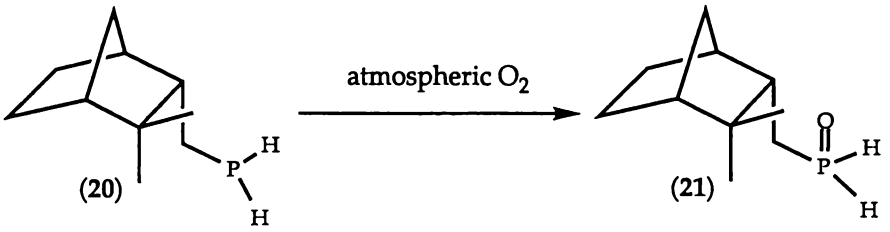

Scheme 4.5: The oxidation of phosphine **20** to the phosphine oxide **21**.

It is worth noting that primary phosphine oxides $RP(O)H_2$ are known to be generally unstable towards disproportionation to the primary phosphine RPH_2 and the phosphinic acid RPO_2H_2[33].

4.2.3 NMR analysis of 8-camphanylphosphine (20)

The proton-coupled ^{31}P NMR spectrum of **20** shows a 1:2:1 triplet [$^{1}J_{P\text{-}H}$ 194 Hz at δ -140.4] as a result of the two directly attached protons coupling to phosphorus. These values are very similar to those obtained for other primary phosphines, which typically appear in the range δ -110 to -160[34] and 180-225 Hz, for example $H_2PCH_2CH_2PH_2$ [δ -130.8, $^{1}J_{P\text{-}H}$ 193 Hz][35], PH_3 [$^{1}J_{P\text{-}H}$ 193 Hz][36] and $MePH_2$ [δ -163.0].

The ^{1}H and ^{13}C NMR spectra of **20**, which are included in Table 4.1, are assigned in an analogous manner to that described for **1** [refer to section 2.1.5]. No discrepancies exist between the one- and two-dimensional NMR spectra of **20**.

^{1}H NMR	R-PO_2H_2 **1**	R-PH_2 **20**	^{13}C NMR	R-PO_2H_2 **1**	R-PH_2 **20**
PH	7.06, dt	2.95, 2.30, br, m	C(2)	37.5, d, $^3J_{P\text{-}C\text{-}C\text{-}C}$ 12.2	37.8, d, $^3J_{P\text{-}C\text{-}C\text{-}C}$ 3.9
H_4	2.26, br, s	2.25, br, s	C(4)	42.1, d, $^3J_{P\text{-}C\text{-}C\text{-}C}$ 6.2	41.1, d, $^3J_{P\text{-}C\text{-}C\text{-}C}$ 4.4
H_3	1.79, m	1.74, br, s	C(3)	43.4, d, $^2J_{P\text{-}C\text{-}C}$ 1.5	49.3, d, $^2J_{P\text{-}C\text{-}C}$ nd
H_1	1.75, s	1.46, br, s	C(1)	48.4	52.8
$H_{8'/8''}$	1.75, m 1.71, m	1.49, br, s	C(8)	26.6, d, $^1J_{P\text{-}C}$ 93.5	10.8, d, $^1J_{P\text{-}C}$ 7.1
$H_{7''}$	1.64, m	1.60, d	C(7)	37.6	36.8
$H_{7'}$	1.18, dt	1.14, d			
$H_{6''}$	1.53, m	1.54, m	C(6)	24.6	24.6
$H_{6'}$	1.24, m	1.25, m			
$H_{5''/5'}$	1.29, m	1.25, m	C(5)	20.2	19.6
Me'	0.95, s	0.91, s	C(9)	21.1	21.4
Me''	0.78, s	0.80, s	C(10)	31.8	32.4

Table 4.1: A comparison of the ^{1}H NMR [δ in $CDCl_3$] and ^{13}C NMR [δ in $CDCl_3$] data of phosphinic acid **1** and primary phosphine **20**.
R denotes 8-camphanyl
nd denotes coupling not resolved
All coupling constants are given in Hz.

With the exception of the ^{1}H NMR resonances belonging to $H_{8'/8''}$, H_1 and the ^{13}C NMR signals belonging to C(8) and C(3), the ^{1}H and ^{13}C NMR chemical shifts of phosphinic acid **1** and phosphine **20** are comparable. These discrepancies which are included in Table 4.1, are expected to be the result of substituting the PO_2H_2 moiety for the PH_2 moiety.

A comparison of the one-bond P-to-C(8) coupling constants of **1** [93.5 Hz] and **20** [7.1 Hz] suggests that they too are also affected by substitution of a PO_2H_2 moiety, as in **1** with a PH_2 moiety, as in **20**. The observed P(III)-to-

C(8) coupling constant of **20** is consistent with those quoted in the literature [0-45 Hz][37].

In the P-H region of the ^{1}H NMR spectrum of the primary phosphine **20**, Figure 4.2(a), the PH_2 protons are highly coupled giving two very broad multiplets at δ 2.95 and 2.30. Although it was initially thought that each multiplet belonged to a given P-H proton, examination of the COSY45 spectrum of **20** gave no correlation linking these resonances together. The only correlation peaks observed for these multiplets was to the resonances assigned to $H_{8'/8''}$. It is therefore suggested that these resonances are in fact a single multiplet split by phosphorus. [In this case a correlation linking the resonances is not seen]. Irradiation of the signals assigned to $H_{8'/8''}$ [δ 1.49], Figure 4.2(b), simplifies the P-H multiplets to a pair of doublets indicating that the PH_2 protons are inequivalent, coupling to each other to produce a pair of doublets which are split by phosphorus [H_a δ 2.69, $^1J_{\mathbf{P\text{-}H_a}}$ 192 Hz, $^2J_{\mathbf{H_a\text{-}P\text{-}H_b}}$ 15 Hz], [H_b δ 2.58, $^1J_{\mathbf{P\text{-}H_b}}$ 192 Hz, $^2J_{\mathbf{H_b\text{-}P\text{-}H_a}}$ 15 Hz]. The $^1J_{\mathbf{P\text{-}H}}$ coupling observed in the ^{1}H NMR spectrum [192 Hz] is similar to the $^1J_{\mathbf{P\text{-}H}}$ coupling observed in the ^{31}P NMR spectrum [194 Hz].

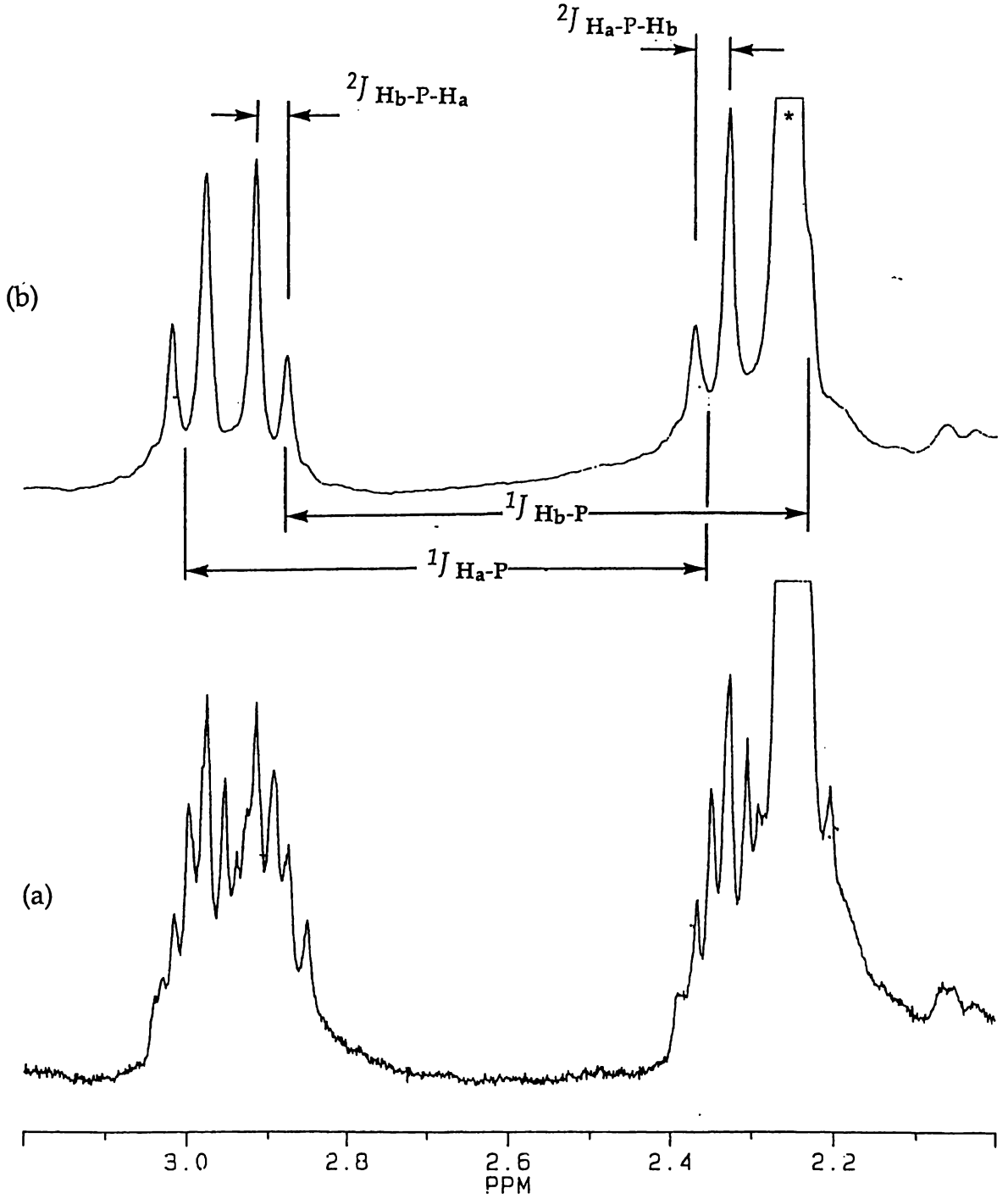

Figure 4.2: The P-H region of the ^1H NMR spectrum of **20** displaying (a) the highly coupled PH_2 signals (b) the result of irradiating the signals assigned to $H_{8'/8''}$ [δ 1.49].

* denotes the resonance belonging to H_4

4.3 The gas phase decomposition of 8-camphanyl-phosphine

Berrigan and Russell (Auckland University) have investigated the gas phase decomposition of 8-camphanylphosphine (**20**) using I.R. Laser Powered Homogeneous Pyrolysis. Their results indicate that phosphine is firstly eliminated followed by the rearrangement and decomposition of camphene through two distinct pathways. These pathways, which are presented diagrammatically in Scheme 4.6, involve either (a) the conversion to tricyclene and then decomposition through bridge opening or (b) the conversion of camphene to methylethylnorbornene and subsequent retro Diels-Alder decomposition. The methods of identification, which are summarised in Appendix V, allow all products to be unambiguously identified.

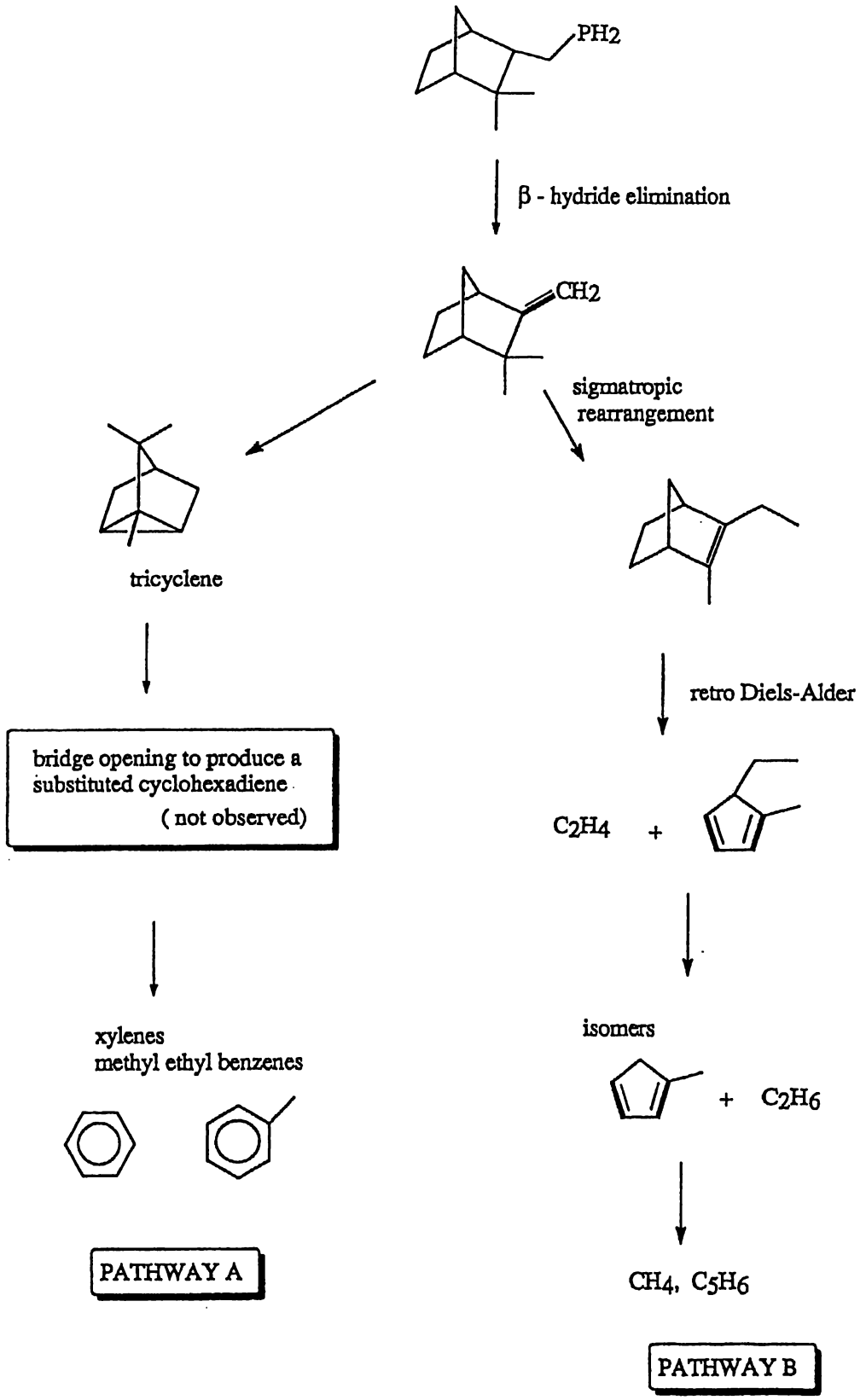

Scheme 4.6: Proposed pathways to the gas phase decomposition of 8-camphanylphosphine (**20**).

4.4 Synthesis and characterisation of 8-camphanyl tris(hydroxymethyl)phosphonium chloride (22)

4.4.1 Introduction

Primary phosphines are known to have high reactivity and examples include the controlled oxidation with H_2O_2[38, 39] to form phosphine oxides and phosphorus acids, the reaction with group VI elements sulfur and selenium to form the phosphine sulfides[39, 32] and selenides[32] and the reaction with aqueous hydrochloric acid/formaldehyde to form hydroxymethylphosphonium salts[40]. The latter reaction, which was first developed by Hoffman[41] and later modified for industry and laboratory work, is currently of great interest as the introduction of hydroxymethyl groups within phosphines, Scheme 4.7, results in the formation of a product with increased water-soluble characteristics.

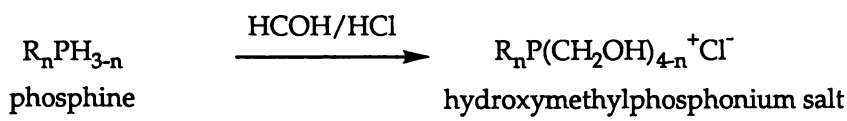

Scheme 4.7: The synthesis of bis(hydroxymethyl)phosphonium salt by treatment of primary phosphine with HCl/HCOH.

The primary phosphine **20** therefore represents an important new derivative as a precursor for the synthesis of a camphene-derived hydroxymethylphosphonium salt and thus its reactivity, with aqueous hydrochloric acid/formaldehyde, was investigated.

4.4.2 Results and discussion

Under a nitrogen atmosphere, the addition of an excess of aqueous hydrochloric acid/formaldehyde to freshly prepared **20** affords an air-stable white crystalline solid, 8-camphanyl tris(hydroxymethyl)phosphonium

chloride (**22**) [^{31}P NMR δ 29] in moderate yield (Scheme 4.8). Detailed characterisation of **22** by X-ray crystallography, NMR spectroscopy and ESMS is presented in sections 4.4.3 and 4.4.4 respectively. Elemental microanalytical data obtained for **22** are consistent with the formulated structure.

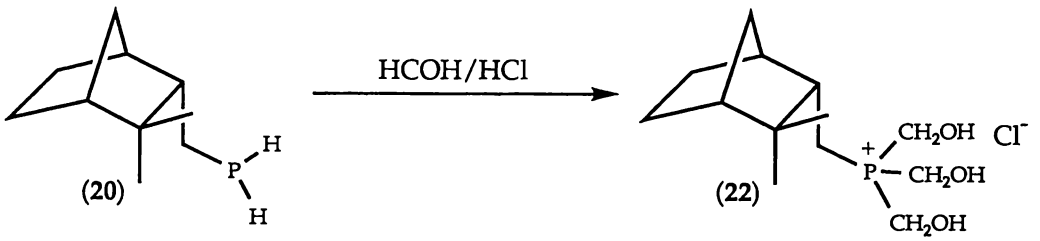

Scheme 4.8: The synthesis of the phosphonium salt **22** by addition of excess HCl/HCOH to the primary phosphine 8-camphanylphosphine (**20**).

4.4.3 X-ray crystal structure of 8-camphanyl tris(hydroxymethyl)-phosphonium chloride (22)

The crystallographic study of **22** was deemed necessary as a Cambridge Structure Database search revealed that no single crystal X-ray structures of a tris(hydroxymethyl)phosphonium salt presently exist and only a relatively small number of structures have been reported on bis(hydroxymethyl)-phosphonium salts, for example, $[Ph_2P(CH_2OH)_2]Cl$[40], $[PhMe_2P\{CMe(OH)-C(O)Me\}]Cl$[42] and $[FcCH_2PMe(CH_2OH)]I$[43] (Fc=ferrocenyl).

The molecular structure of **22**, together with the atom numbering scheme and a stereoview of the cell packing diagram, are shown in Figure 4.3. Selected bond lengths and angles of **22** associated with interionic interactions are presented in Table 4.2. Crystal data, intensity measurements and structure solution and refinement details for **22** are presented in the experimental section.

The compound exists as a quaternary phosphonium cation with a chloride counter ion. The cell packing diagram shown in Figure 4.3(b) reveals that each chloride anion experiences interionic contacts to the hydroxyl groups of three different phosphonium cations. These interionic

contacts, which have also been observed in the bis(hydroxymethyl) phosphonium salt $[Ph_2P(CH_2OH)_2]Cl$ and more elaborately in $[Fe(\eta\text{-}C_5H_5)\{\eta\text{-}C_5H_4CH_2P(CH_2OH)_2\}]$[43], are indicated by the short Cl····H distances given in Table 4.2. The Cl····O distances [3.03-3.10 Å] are also typical for Cl····HO hydrogen bonds[44].

Cl(1)····H(110)	2.336 Å	Cl(1)····O(1)	3.104 Å
Cl(1)····H(210)	2.218 Å	Cl(1)····O(2)	3.029 Å
Cl(1)····H(310)	2.280 Å	Cl(1)····O(3)	3.067 Å
O(1)-H(110)····Cl(1)	156°	O(2)-H(210)····Cl(1)	170°
O(3)-H(310)····Cl(1)	160°		

Table 4.2: Bond lengths (Å) and angles (°) of 8-camphanyl tris(hydroxymethyl)phosphonium chloride (**22**) associated with interionic H-bonding interactions.

The geometry around phosphorus is essentially tetrahedral with the C-P-C angles in the range 107-113°. A comparison of selected bond lengths, Table 4.3, indicates that the average P-CH_2OH and average CH_2-OH bond lengths of **22** [1.815(3) and 1.413(4) Å respectively] are comparable with those of $[Ph_2P(CH_2OH)_2]Cl$ [1.830(3) and 1.405(7) Å respectively]. The C(8)-P bond length of **22** [1.794(3) Å] is similar to the average P-CH_3 bond length in the phosphonium salt $[PhMe_2P\{C(OH)MeC(O)Me\}]Cl$ [1.782(3) Å], and to the average C(sp^3)-P^+ bond distances in phosphonium salts [1.800(15) Å][45].

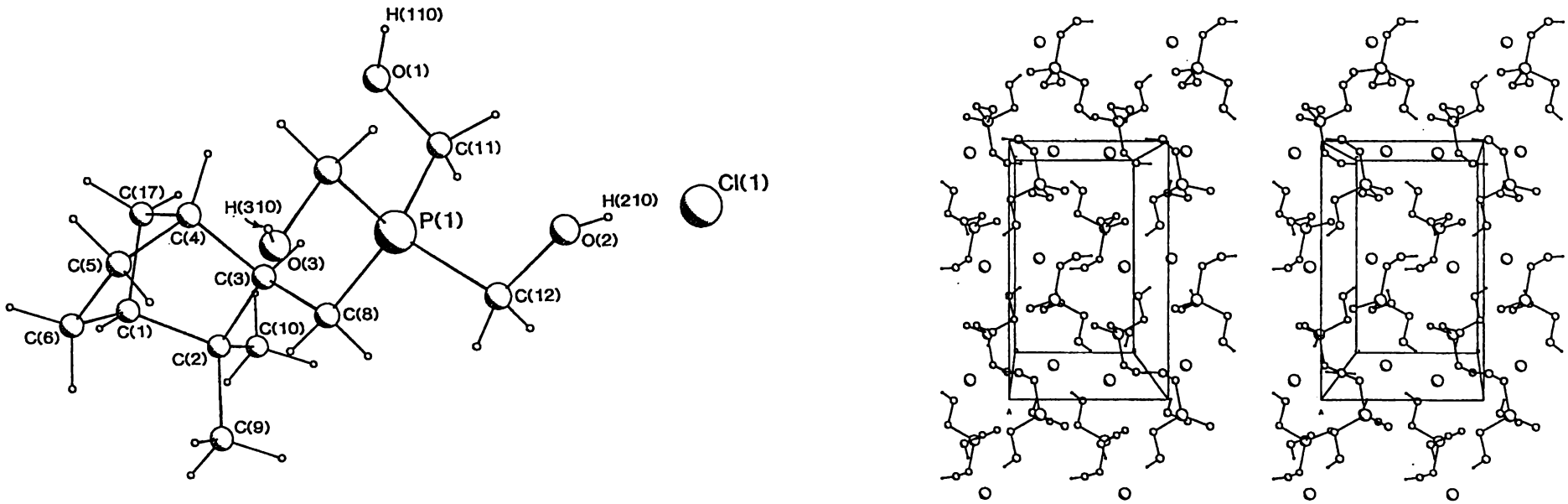

Figure 4.3: (a) Molecular structure of 8-camphanyl tris(hydroxymethyl)phosphonium chloride (**21**), together with the atom numbering scheme (b) stereoview of the cell packing diagram of **22** [the camphanyl ring has been omitted for clarity].

Bond length	$[RP(CH_2OH)_3]Cl$	$[Ph_2P(CH_2OH)_2]Cl$
$P-CR_1R_2$	1.794(3) [$R_1=R_2=H$]	1.786(3) [$R_1=R_2=C$]
		1.781(3) [$R_1=R_2=C$]
$P-CH_2OH$	1.819(3)	1.822(5)
	1.820(3)	1.838(6)
	1.808(3)	
C-OH	1.412(4)	1.400(7)
	1.410(4)	1.409(7)
	1.419(3)	

Table 4.3: A comparison of selected bond lengths of **22** with the analogous bond lengths of $[Ph_2P(CH_2OH)_2]Cl$.
R = 8-camphanyl.

The bond lengths and angles of the camphanyl moiety of **22**, **1** (8-camphanylphosphinic acid) and **14** (8-camphanylphosphonic acid), which are all included in Appendix III, are comparable. The methylene-phosphorus moiety of **22**, as in the starting phosphinic acid **1** adopts the expected *endo* position.

4.4.4 Spectroscopic analyses of 8-camphanyl tris(hydroxymethyl)-phosphonium chloride (22)

4.4.4.1 NMR analysis

One- and two-dimensional NMR studies were carried out on 8-camphanyl tris(hydroxymethyl)phosphonium chloride (**22**). A summary of the ^1H NMR and ^{13}C NMR data of **22** is presented in Table 4.4.

The ^{31}P NMR chemical shift of **22** [δ 29] is similar to tris(hydroxy-methyl)phosphonium chloride $[P(CH_2OH)_4]Cl$ which has a ^{31}P NMR resonance of δ 25.8[46].

The ^{13}C NMR spectrum of the camphanyl region of **22** comprised ten resonances, consisting of two methyl signals, three methine signals, four methylene signals and one quaternary signal. The quaternary carbon C(2)

which shows coupling to phosphorus [$^3J_{P\text{-}C\text{-}C\text{-}C}$ 12.4 Hz] is readily assigned by the absence of the signal [δ 37.6] in the DEPT experiment. The methylene signal exhibiting a large one-bond carbon-to-phosphorus coupling [$^1J_{P\text{-}C}$ 38.3 Hz] is assigned to C(8). The only methine signal that exhibits a carbon to phosphorus coupling [$^2J_{P\text{-}C\text{-}C}$ 4.9 Hz] is assigned to C(3). The magnitude of the observed coupling constant is consistent with two-bond carbon-to-phosphorus coupling constants reported in the literature[37]. The remaining methine resonances [δ 48.8 and 42.3] are assigned to be C(1) and C(4) respectively by comparison with other camphanyl derivatives.

The CH_2OH signal [δ 50.7] exhibiting a large one-bond carbon-to-phosphorus coupling [$^1J_{P\text{-}C}$ 54.7 Hz] is assigned as C(11). A standard gated decoupling experiment was performed on **22** which enabled the direct comparison of the CH_2OH and C(1) peak areas [nuclear Overhauser enhancement of the peak intensities of methylene and methine signals prevents the direct comparison of carbon signals. A gated decoupling experiment eliminates nuclear overhauser enhancements by permitting the decoupler to be operational only during acquisition]. The peak intensity ratio of the CH_2OH and C(1) signals is 3:1 confirming the existence of three equivalent CH_2OH groups.

The ^1H NMR data of **22**, which is included in Table 4.4, is assigned in an analogous manner to that described for **1** [see section 2.1.5]. No discrepancies exist between the one- and two-dimensional NMR spectra of **22**.

Atom/Group	^{13}C NMR	^{1}H NMR	Assignment
CH_2OH	50.7, d, $^{1}J_{P\text{-}C}$ 54.7 Hz	4.70, br, s	CH_2OH
C(1)	48.1	1.98, s	H_1
C(3)	43.6, d, $^{2}J_{P\text{-}C\text{-}C}$ 4.9 Hz	2.02, br, m	H_3
C(4)	42.3	2.33, br, m	H_4
C(2)	38.5, d, $^{3}J_{P\text{-}C\text{-}C\text{-}C}$ 12.4 Hz	-	-
C(7)	36.9	1.85, m	$H_{7''}$
		1.43, d	$H_{7'}$
C(10)	31.1	0.99, s	Me''
C(6)	24.4	1.73, m	$H_{6''}$
		1.46, m	$H_{6'}$
C(9)	21.3	1.12, s	Me'
C(5)	19.7	1.48, br, m	$H_{5'/5''}$
C(8)	11.8, d, $^{1}J_{P\text{-}C}$ 38.3 Hz	2.55, m	$H_{8'/8''}$

Table 4.4: ^{1}H NMR [δ in $CDCl_3$] and ^{13}C NMR[δ in $CDCl_3$] data of **22**.

4.4.4.2 Electrospray mass spectrometric analysis

Positive ion electrospray mass spectral studies of phosphonium salts[47] show that aggregates are especially common since the P-CH_2OH groups promote aggregation *via* H-bonding. In the ESMS of **22** (cone 16 V), Table 4.5, the principal ion {$[C_{10}H_{17}P(CH_2OH)_3]^+$} and $[2M+Cl^-]^+$ aggregate are observed. Increasing the cone voltage does not produce additional ions.

Compound	*Mode*	*Principal ion (m/z)*	*Ions (m/z)*
22	positive	$[RP(CH_2OH)_3]^+$ 261	$[2M+Cl^-]^+$ 557

Table 4.5: Electrospray mass spectral data of 8-camphanyl tris(hydroxymethyl)phosphonium chloride (**22**) in 1:1 H_2O/CH_3CN.

* denotes peaks not assigned.

4.5 Synthesis and characterisation of 8-camphanyl bis(hydroxymethyl)phosphine (23) and derivatives

4.5.1 Introduction

(i) Synthesis of hydroxymethylphosphines

The general synthetic route to hydroxymethylphosphines is achieved by careful neutralisation of the phosphonium salt with a base, usually potassium hydroxide or triethylamine (see Equation 4.1)[48]. It is worth noting however, that the addition of an excess of hydroxide, as shown in Equation 4.2, results in the formation of the undesired phosphine oxide[49].

$$[R_nP(CH_2OH)_{4-n}]Cl \xrightarrow{KOH} R_nP(CH_2OH)_{3-n} + CHOH + NaCl + H_2O$$

Equation 4.1: Synthesis of hydroxymethylphosphines by the treatment of a phosphonium salt with potassium hydroxide.

$$[R_nP(CH_2OH)_{4-n}]Cl \xrightarrow{\text{excess KOH}} R_n-\overset{\overset{O}{\|}}{P}(CH_2OH)_{3-n}$$

Equation 4.2: Synthesis of hydroxymethylphosphine oxides by treatment of a phosphonium salt with an excess of potassium hydroxide.

Phosphines which contain large organic groups such as the camphanyl group can be separated from the byproducts by performing the reaction within the immiscible layers of an organic and aqueous solvent. The byproducts and unreacted phosphonium salt remain in the aqueous layer while the product, a hydroxymethylphosphine, extracts into the organic phase. The product is therefore isolated by the separation and evaporation of the organic phase.

(ii) Synthesis of hydroxymethylphosphine derivatives

The potential of hydroxymethylphosphines is illustrated in Scheme 4.9 where the synthesis of some of the numerous hydroxymethylphosphine derivatives are presented for $P(CH_2OH)_3$[17, 48]. These syntheses include the reaction of hydroxymethylphosphines with the group 16 elements oxygen, sulfur, selenium and tellurium [equation (1)] to form the corresponding phosphine sulfide, selenide and telluride; with metal (group 8) dichloride complexes to form metal complexes of phosphines [equation (2)]; with monosubstituted and unsymmetrically disubstituted ureas to produce tris(4-substituted ureidomethyl)phosphine oxides [equation (3)]; with acrylonitrile to form tris(2-cyanoethyl)phosphine [equation (4)]; with alkyl halides to form quaternary phosphonium salts [equation (5)]; with silyl chlorides to form silyl ethers [equation (6)]; and with isocyanates and isothiocyanates to form carbamate esters [equation (7)].

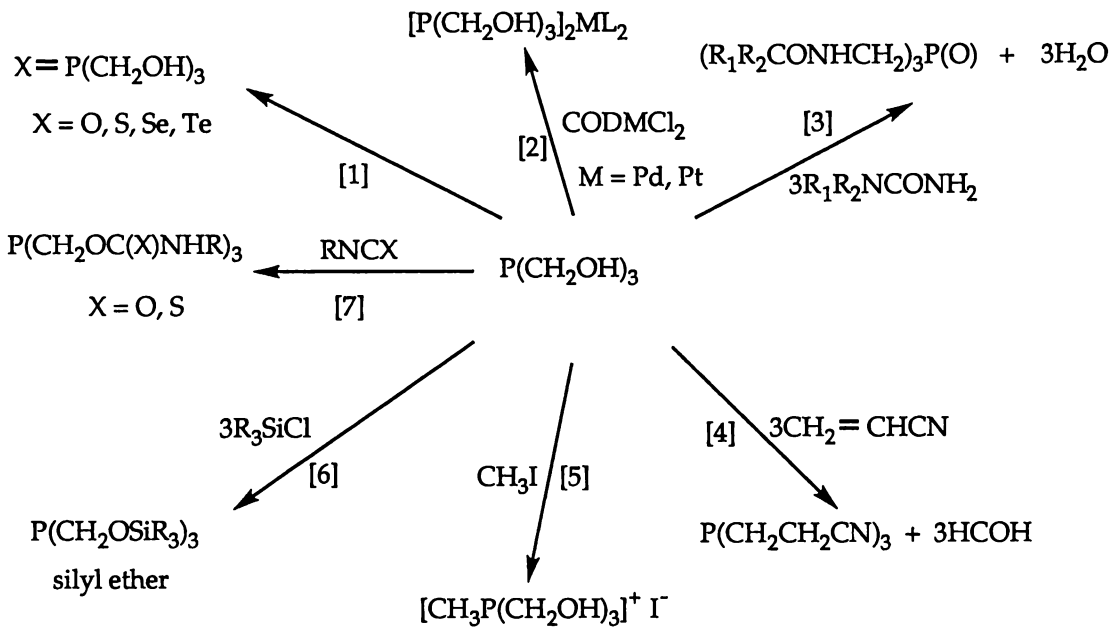

Scheme 4.9: A summary of some reactions of tris(hydroxymethyl)phosphine.

The experimental procedure commonly employed involves the preparation and isolation of the hydroxymethylphosphine [refer to section above] which, in turn, is reacted with a substrate. This two-step reaction can be simplified somewhat by the addition of the substrate to the aqueous solution

containing the phosphonium salt. The subsequent addition of hydroxide to the aqueous solution facilitates hydroxymethylphosphine formation which, in turn, reacts with the substrate [usually contained in an aqueous layer] to form the desired organic-soluble hydroxymethylphosphine derivative. This single step procedure eliminates the direct handling of the air-sensitive hydroxymethylphosphine thereby reducing the amount of hydroxymethylphosphine oxide, a contaminant caused by air oxidation of hydroxymethylphosphine.

The tris(hydroxymethyl)phosphonium salt **22** therefore represents an important new derivative and thus its reactivity, particularly that pertaining to bis(hydroxymethyl)phosphine chemistry, was investigated

4.5.2 Results and discussion

Under a nitrogen atmosphere the treatment of a deoxygenated water/dichloromethane mixture containing 8-camphanyl tris(hydroxymethyl)-phosphonium chloride (**22**) with equimolar amounts of either potassium hydroxide or triethylamine affords 8-camphanyl bis(hydroxymethyl)phosphine (**23**) [^{31}P NMR δ -25.4] (Scheme 4.10). Phosphine **23** is easily isolated from the unwanted byproducts by separating and drying [with anhydrous magnesium sulfate] the organic phase. Subsequent removal of solvent under vacuum yields the colourless, air-sensitive oil **23**. Detailed characterisation of **23** by NMR spectroscopy is presented in section 4.5.3.

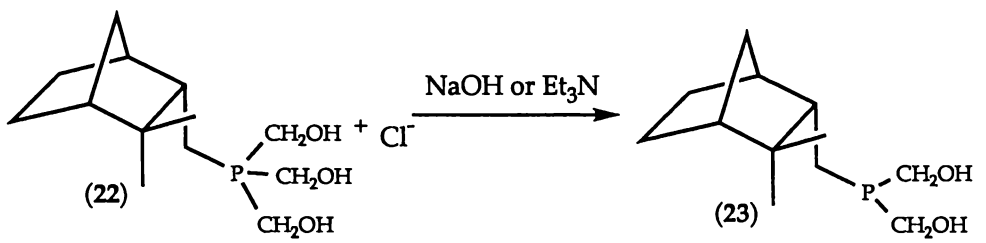

Scheme 4.10: Synthesis of hydroxymethylphosphine **23** by treatment of **22** with potassium hydroxide or Et_3N.

Although high yields are obtained with the use of either base, the use of triethylamine results in the formation of phosphine-formaldehyde adducts. These adducts, shown in Scheme 4.11, are formed by the addition of formaldehyde produced in the reaction with the phosphine[50]. Reversal of these addition products is achieved by heating the mixture [85°C under vacuum] while nitrogen is bubbled through the liquid, thus driving off the formaldehyde to form the free phosphine.

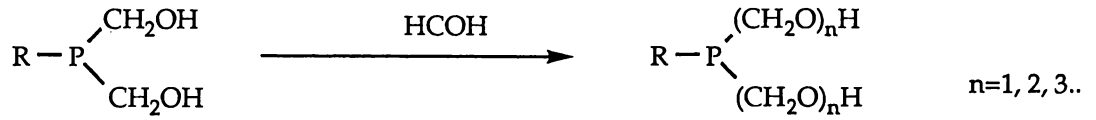

R = $C_{10}H_{17}$ = 8-camphanyl

Scheme 4.11: Synthesis of formaldehyde adducts of 8-camphanyl bis(hydroxymethyl)phosphine (**23**).

The treatment of a deoxygenated water/dichloromethane mixture containing 8-camphanyl tris(hydroxymethyl)phosphonium chloride (**22**) and sulfur [in excess] with potassium hydroxide, Scheme 4.12, affords 8-camphanyl bis(hydroxymethyl)phosphine sulfide (**24**) in high yield.

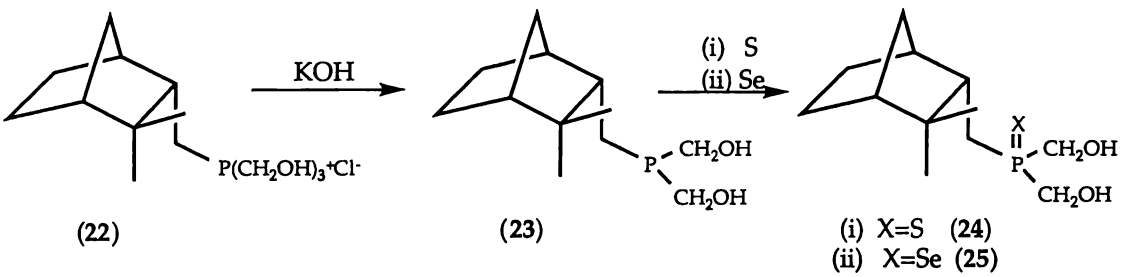

(**22**) (**23**) (i) X=S (**24**) (ii) X=Se (**25**)

Scheme 4.12: The synthesis of the phosphine sulfide **24** and selenide **25**.

The phosphine selenide **25**, shown in Scheme 4.12, is synthesised in a similar manner to that of the phosphine sulfide **24**. However, in the case of the phosphine selenide, an aqueous solution is heated [85°C] for four hours to facilitate reaction. Subsequent isolation of the phosphine selenide **25** is easily achieved by the extraction of the aqueous reaction mixture with dichloromethane. The organic phases containing **24** and **25**, when dried over anhydrous magnesium sulfate and evaporated to dryness, both afford

crystalline solids with spectral properties consistent with the formulated structures.

Detailed characterisation of the phosphine sulfide **24** [^{31}P NMR δ 55.6] and phosphine selenide **25** [^{31}P NMR δ 43.4 *J*(PSe) 683 Hz] by NMR spectroscopy and ESMS is presented in section 4.5.3. Analytical data obtained for **24** and **25** are consistent with the formulated structures.

The controlled oxidation of 8-camphanyl bis(hydroxymethyl)phosphine (**23**) with hydrogen peroxide, Scheme 4.13, precipitates the white crystalline solid, 8-camphanyl bis(hydroxymethyl)phosphine oxide (**26**) [^{31}P δ 46.9] in high yield. Analytical data collected on **26** recrystallised from methanol is consistent with the ^{1}H NMR spectrum of **26** as a di-methanol solvate.

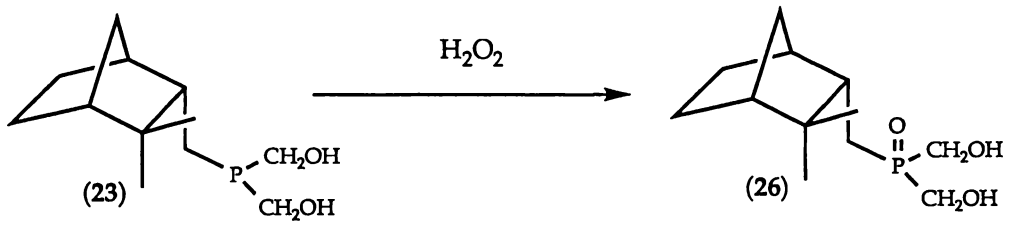

Scheme 4.13: The oxidation of **23** to the hydroxymethylphosphine oxide **26**.

4.5.3 Spectroscopic analyses of camphene-derived hydroxymethyl-phosphines and their derivatives

One- and two-dimensional NMR studies were performed to fully assign the ^{1}H and ^{13}C NMR data of **23** and its derivatives [**24-26**]. Summaries of the ^{1}H and ^{13}C assignments are presented in section 4.7; Tables 4.9 and 4.10. As the general NMR patterns seen for the organophosphorus acids [refer to chapters 2 and 3 for more detail] apply for these derivatives no in-depth discussion on ^{13}C and ^{1}H NMR assignments of the camphanyl moiety is included. The points of ^{13}C and ^{1}H NMR discussion are restricted to areas where discrepancies or uncertainties exist.

4.5.3.1 NMR analysis of 8-camphanyl bis(hydroxymethyl)phosphine (23)

The ^{31}P NMR chemical shift of $C_{10}H_{17}P(CH_2OH)_2$ (**23**) [δ -25.4] is similar to the ^{31}P NMR shift of bis(hydroxymethyl)phosphine [$P(CH_2OH)_3$] [δ -24.5[48]].

The two hydroxymethyl groups, which have ^{13}C NMR signals of δ 61.3 and 61.1 are split by phosphorus [$^1J_{P\text{-}C}$ 14.9 Hz] to produce a pair of doublets. The "triplet-like" appearance of these adjacent doublets allowed absolute assignment of the ^{13}C NMR signals and therefore the $^1J_{P\text{-}C}$ coupling constants associated with the hydroxymethyl groups. However insufficient resolution in the ^1H NMR window [δ 4.3 to 0.0] of the ^{13}C-^1H correlated NMR spectrum meant that only the tentative assignment of the hydroxymethyl protons was possible. The presence of two hydroxymethyl groups was confirmed in a standard inverse gated experiment, where the peak intensity ratios of the hydroxymethyl signals were compared to an averaged C(1), C(2), C(3) peak intensity.

4.5.3.2 NMR analysis of 8-camphanyl bis(hydroxymethyl)phosphine sulfide (24), selenide (25) and oxide (26)

(i) *8-camphanyl bis(hydroxymethyl)phosphine sulfide (24)*

The ^{31}P NMR shift of $C_{10}H_{17}P(S)(CH_2OH)_2$ (**24**) [δ 55.6] is comparable with the ^{31}P NMR chemical shift of $PhP(S)(CH(Me)(OH))_2$ [δ 53.2[32]].

In the ^{13}C NMR spectrum of **24** two hydroxymethyl signals [δ 60.5, 59.7] split by phosphorus [$^1J_{P\text{-}C}$ 30.5 Hz] are observed indicating that these groups are inequivalent. In the ^{13}C-^1H correlated NMR spectrum the cross peaks relating to the ^{13}C NMR signals at δ 60.5 and 59.7 identify the corresponding hydroxymethyl ^1H NMR signals [δ 4.00 and δ 3.98 respectively]. Full

assignment of the ^{13}C and ^{1}H NMR data of **24** is achieved by careful examination of the one- and two-dimensional NMR spectra. No discrepancies are found to exist between the ^{1}H-^{1}H and ^{13}C-^{1}H correlated NMR spectra.

(ii) *8-camphanyl bis(hydroxymethyl)phosphine selenide (25) and oxide (26)*

The ^{31}P NMR chemical shift of $C_{10}H_{17}P(Se)(CH_2OH)_2$ (**25**) [δ 43.4] is consistent with that of a phosphine selenide, for example $PhPH(Se)(CMe_2OH)_2$ gives a ^{31}P NMR resonance at δ 35.6[32]. As ^{77}Se is NMR active and of the same spin as ^{31}P, *i.e* spin 1/2, selenium satellites also appear in ^{31}P NMR spectra. The selenium satellites of **25** [$^{1}J_{P\text{-}Se}$ 683 Hz] are consistent with those obtained for the phosphine selenide $Ph_3P{=}Se$ [$^{1}J_{P\text{-}Se}$ 730 Hz][37]. The ^{31}P NMR chemical shift of $C_{10}H_{17}P(O)(CH_2OH)_2$ (**26**) [δ 46.9] is similar to that of bis(hydroxymethyl)phosphine oxide [$O{=}P(CH_2OH)_3$] which has a ^{31}P NMR signal of δ 45.4[48].

The ^{13}C NMR spectrum of **25** shows two hydroxymethyl signals split by phosphorus to produce a pair of doublets. The close proximity of these signals means there are two viable combinations of these four signals that result in a pair of doublets. That is, firstly as overlapping doublets with a $^{1}J_{P\text{-}CH_2OH}$ coupling constant of 47.4 Hz or secondly as two adjacent doublets which do not overlap giving a $^{1}J_{P\text{-}CH_2OH}$ coupling constant of 27.8 Hz. In the ^{13}C NMR spectrum of **26** the hydroxymethyl signals, which are as described for **25**, combine firstly as overlapping doublets with a $^{1}J_{P\text{-}CH_2OH}$ coupling constant of 72.5 Hz or secondly as two adjacent doublets which do not overlap giving a $^{1}J_{P\text{-}CH_2OH}$ coupling constant of 3.1 Hz. Included in Table 4.6 are the one bond phosphorus-to-carbon coupling constants of all the camphene-derived hydroxymethylphosphorus compounds along with the preferred coupling constants for derivatives **25** and **26**.

	22	23	24	25	26
$^1J_{P\text{-}C(8)}$	38.3	9.2	17.6	39.2	39.5
$^1J_{P\text{-}CH_2OH}$	54.7	14.9	30.0	*47.4	*72.5
				[§27.8]	[§3.1]

Table 4.6: A comparison of the $^1J_{P\text{-}C(8)}$ and $^1J_{P\text{-}CH_2OH}$ coupling constants of the phosphine **23**, phosphine sulfide **24**, selenide **25** and oxide **26** with phosphonium salt **22**.

* denotes the coupling constant which results from overlapping hydroxymethyl signals and § denotes the coupling constant which results from adjacent hydroxymethyl signals that do not overlap. [ ] represents the least preferred coupling constant.

The ^{13}C NMR hydroxymethyl signals of **25** and **26** are assigned such that their one bond phosphorus-to-carbon coupling constants are consistent with the other camphene-derived hydroxymethylphosphorus derivatives, *i.e*, the magnitude of the $^1J_{P\text{-}C(8)}$ coupling constant is less than its $^1J_{P\text{-}CH_2OH}$ coupling constant.

It was initially thought that the $^1J_{P\text{-}CH_2OH}$ coupling constant would be of a similar magnitude to the $^1J_{P\text{-}C(8)}$ coupling constant, which is unambiguously known. However it is not applicable in this case as previous studies in chapter 2, section 2.3.4, indicate that the relationship between the $^1J_{P\text{-}CH_2OH}$ and $^1J_{P\text{-}C(8)}$ coupling constants is highly dependant on the type of directly attached groups.

The one-dimensional ^1H and ^{13}C NMR spectra of the phosphine selenide **25** was assigned by comparison with the ^1H and ^{13}C NMR spectra of the phosphine sulfide **24** [see section 4.7, Tables 4.9 and 4.10].

A comparison of the ^1H and ^{13}C NMR data of the hydroxymethylphosphine **23** and its derivatives **[24-26]** is included in section 4.7.

4.5.3.3 Electrospray mass spectrometric analysis of camphene-derived phosphine derivatives

The use of Ag(I) complexes as an aid in the characterisation of phosphines, hydroxymethylphosphines and their sulfide derivatives by electrospray mass spectrometry, has been investigated[47]. This involves the preparation of silver adducts *in situ* by the addition of a small quantity of aqueous $AgNO_3$ to a 1:1 H_2O/MeCN solution of the phosphine or phosphine sulfide. Silver also has two isotopes [^{107}Ag, ^{109}Ag] of similar abundance, so that complexes containing one, two, or three silver atoms can be readily distinguished by inspecting the isotope patterns in the mass spectra.

The positive-ion ESMS spectrum of the phosphine sulfide **24** in MeCN/H_2O [containing aqueous $AgNO_3$], Figure 4.4, gives two Ag-phosphine adducts $[M+CH_3CN+Ag]^+$ and $[2M+Ag]^+$. The observed isotope patterns for these Ag-adducts are consistent with their calculated isotope patterns [Figures 4.4(b) and 4.4(c)]. Aqueous $AgNO_3$ is an ionising reagent and without its use the positive-ion ESMS of the phosphine sulfide **24** is complex giving a large number of peaks which are not assignable. The positive-ion ESMS spectrum of the phosphine selenide **25** in MeCN/H_2O is not obtained irrespective of whether aqueous $AgNO_3$ is present or not.

Compound	*Mode*	*Principal ion (m/z)*	*Ions (m/z)*
24 [$AgNO_{3\,(aq)}$ added]	positive		214*, 234*, $[M+CH_3CN+Ag]^+$; 412, $[2M+Ag]^+$ 633
26	positive	$[M+H]^+$ 247	$[2M+H]^+$ 493; $[3M+H]^+$ 739.

Table 4.7: Electrospray mass spectral data of camphene-derived hydroxymethylphosphine derivatives in 1:1 MeCN/H_2O.
* denotes peaks not assigned, *M* denotes parent molecule.

The positive-ion electrospray mass spectrum of the phosphine oxide **26**, Table 4.7, gives the protonated parent ion $[M+H]^+$ and the protonated adducts

$[2M+H]^+$ and $[3M+H]^+$. Alkali metals [KCl, NaCl] may also be used to facilitate the ionisation of the P=O moiety[47]. However, in the case of the oxide **26**, this was not deemed necessary, presumably because of the ease with which the P=O group is protonated.

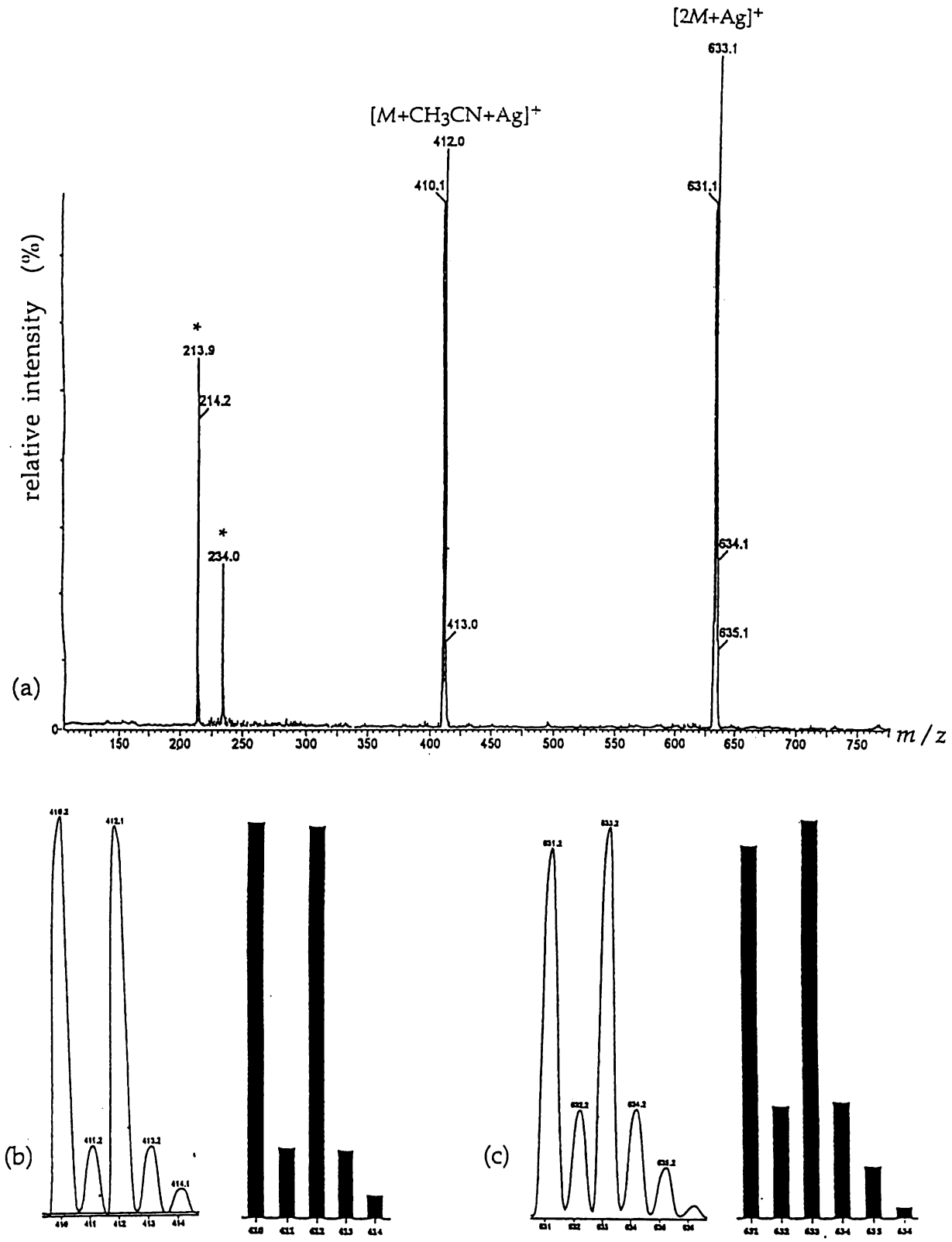

Figure 4.4: (a) Electrospray mass spectrum of $C_{10}H_{17}P(S)(CH_2OH)_2$ **(24)** in 1:1 H_2O/CH_3CN [containing $AgNO_3$] at a cone voltage of 20 V. (b) observed [LHS] and calculated [RHS] isotope patterns of peak at *m/z* 412. (c) observed [LHS] and calculated [RHS] isotope patterns of peak at *m/z* 633.

* denotes an unidentified ion

4.6 Synthesis and characterisation of metal complexes of 8-camphanyl bis(hydroxymethyl) phosphine (23)

4.6.1 Introduction

The coordination and organometallic chemistry of hydroxymethylphosphines is extensive and recent research has been driven by their possible medical and catalytic applications. The metal complexes of THP illustrate well the applications of hydroxymethylphosphine-metal derivatives. The Ni, Pd and Pt complexes of THP are, as mentioned in section 4.1, useful homogeneous catalysts, while the analogous Au complex has potential therapeutic applications[51]. The coordination of hydroxymethylphosphines to other metal centres has been extensively studied and includes coordination to Mo[52], Tc[53], Pd[54], Pt[55, 56], Au[57, 58], Ru and Re[59].

The hydroxymethylphosphine **22** therefore represents an important new derivative in which to synthesise camphene-derived metal complexes. An investigation of the coordination of **22** to the metal centres Pt, Pd and Au, was therefore undertaken.

4.6.2 Results and discussion

Under a nitrogen atmosphere, the treatment of a deoxygenated dichloromethane solution of 8-camphanyl bis(hydroxymethyl)phosphine (**23**) with $CODPtCl_2$ {COD = 1, 5-cyclooctadiene}, Scheme 4.14, directly precipitates the platinum dichloride complex **27** [^{31}P NMR δ 10.70, 10.65, $^{1}J_{Pt\text{-}P}$ 3420.3] in high yield. Characterisation of **27** by NMR spectroscopy and ESMS is presented in section 4.6.3. Elemental analysis of **27** is consistent with the formulated structure.

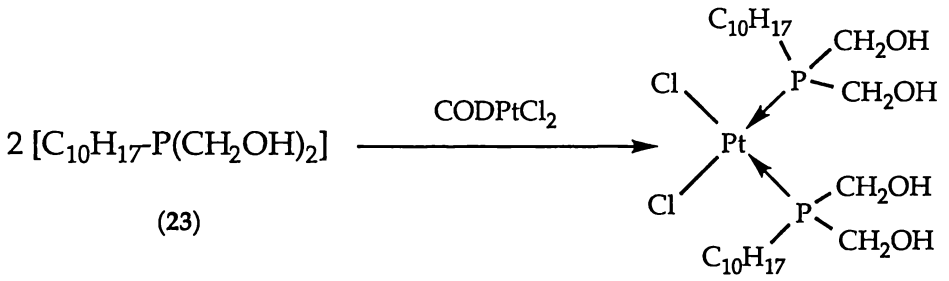

(23)

(27)

$C_{10}H_{17}$ = 8-camphanyl
COD = 1, 5 cyclooctadiene

Scheme 4.14: The synthesis of the platinum dichloride complex **27**.

The presence of two chiral camphanyl moieties [consult section 2.3.2 for more detail] within **27** suggests that diastereoisomers of **27** should exist. Although initial ^{31}P NMR studies [JEOL FX90Q spectrometer; 36 MHz field] indicated that this was not the case as only one signal was observed, further ^{31}P NMR studies on a Bruker AC300NMR spectrometer, which has higher resolution [121.51 MHz field], confirmed the existence of diastereoisomers by obtaining two distinguishable signals, Figure 4.5.

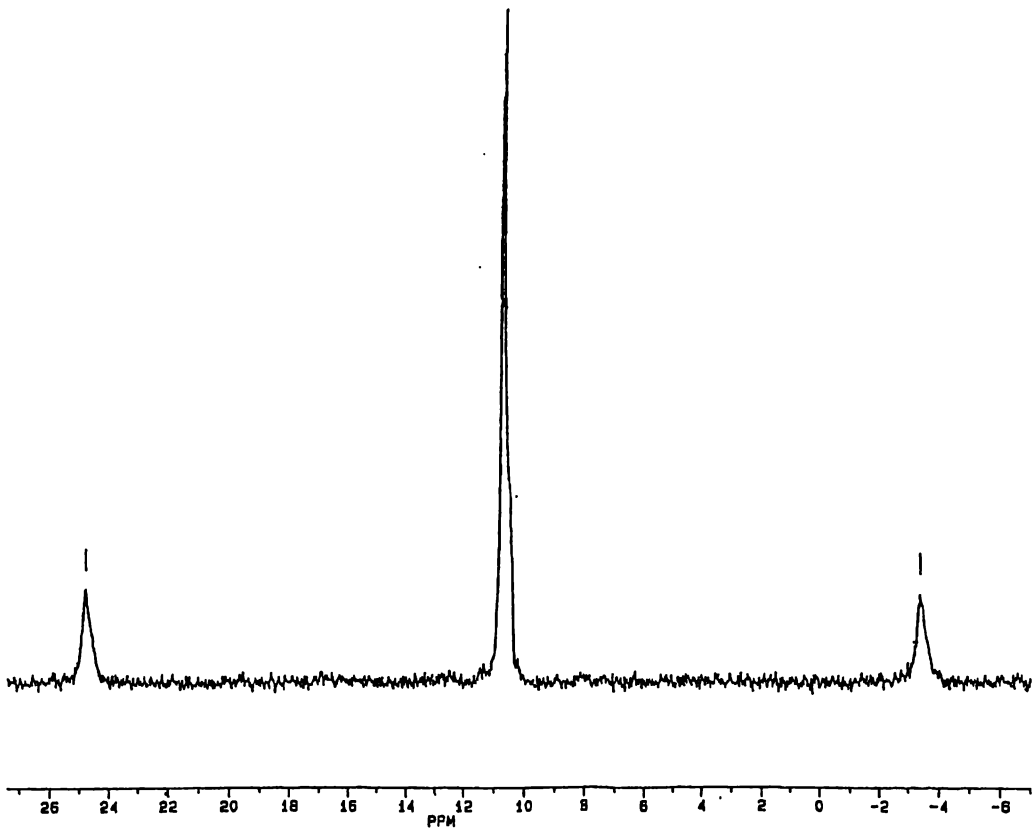

Figure 4.5: The ^{31}P NMR spectrum of the platinum dichloride complex **27** at 121.51 MHz.

In contrast to the platinum chemistry of **23**, the palladium chemistry of **23** was not easily resolved. The reaction of **23** with $CODPdCl_2$ does not afford the analogous palladium dichloride complex of **27**. Instead the reaction is non-selective forming, as evidenced by ^{31}P NMR, a large number of products. Owing to the large number of products, the palladium chemistry relating to **23** was not further investigated.

A large number of gold(I) complexes are reported in the literature, most involving ligands with the donor atoms phosphorus, arsenic and sulfur. The general synthetic route, Equation 4.3, makes use of tetrahydrothiophene gold(I) chloride [thtAuCl], a gold(I) complex formed by the action of tetrahydrothiophene upon sodium chloroaurate(III) or the corresponding acid in acid conditions[60].

$$R_3P + thtAuCl \longrightarrow (R_3P)AuCl + tht$$

tht= tetrahydrothiophene

Equation 4.3: General reaction scheme for the synthesis of gold(I) complexes containing donor phosphorus ligands.

The treatment of a deoxygenated dichloromethane solution of 8-camphanyl bis(hydroxymethyl)phosphine (**23**) with tetrahydrothiophene gold(I) chloride [thtAuCl], Scheme 4.15, precipitates the gold(I) chloride complex $C_{10}H_{17}P(CH_2OH)_2AuCl$ (**28**) [^{31}P NMR δ 21.7] in high yield. Characterisation of **28** by NMR spectroscopy and ESMS is presented in section 4.6.3.

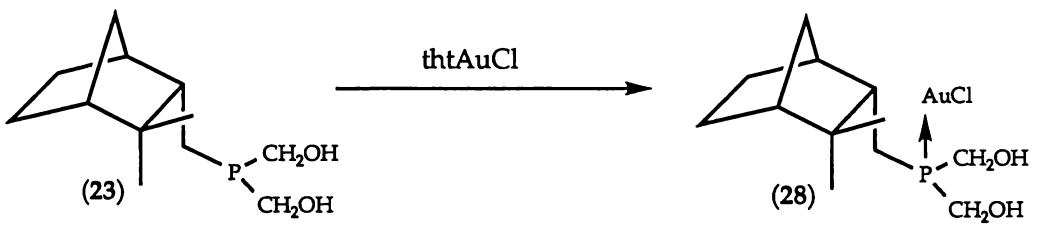

tht=tetrahydrothiophene

Scheme 4.15: The synthesis of the gold(I) chloride complex **28**.

4.6.3 Spectroscopic analyses of the metal complexes of 8-camphanyl bis(hydroxymethyl)phosphine (23)

4.6.3.1 NMR analysis

The ^{31}P NMR chemical shift of the platinum dichloride complex **27** [δ 10.70, 10.65, $^{1}J_{P\text{-}Pt}$ 3420.3 Hz] is similar to the ^{31}P NMR shift of the platinum dichloride complex $PtCl_2(Ph_2PCH_2OH)_2$ [δ 7.3, $^{1}J_{P\text{-}Pt}$ 3687 Hz][61].

The ^{13}C NMR spectrum of **27** is assigned by examination of the DEPT spectrum and by comparison with other phosphine derivatives [see section 4.7.2, Table 4.10]. As **27** exists as diastereoisomers [see previous section] additional signals were expected to be observed. These include the C(8), C(5) and CH_2OH signals which are not assigned to a given diastereoisomer.

The ^{31}P NMR chemical shift of $C_{10}H_{17}P(CH_2OH)_2AuCl$ (**28**) [^{31}P NMR δ 21.7] is consistent with that of gold(I) chloride complex, for example $[Au(Ph_2PCH_2OH)_3]Cl$ gives a ^{31}P NMR signal of δ 31.4[51]. The pronounced downfield shift of **28** compared to its parent phosphine [Δδ=47.1] is also consistent with that of $[Au(Ph_2PCH_2OH)_3]Cl$ compared to its parent phosphine [Δδ=51.8].

The ^{1}H and ^{13}C NMR spectra of the gold(I) chloride complex **28** [included in Section 4.7.2, Tables 4.9 and 4.10] are assigned by examination of the ^{1}H, ^{1}H-^{1}H and ^{13}C-^{1}H correlated NMR spectra. No discrepancies exist between the ^{1}H-^{1}H and ^{13}C-^{1}H correlated NMR spectra.

4.6.3.2 Electrospray mass spectrometric analysis

The electrospray mass spectral data for $C_{10}H_{17}P(CH_2OH)_2AuCl$ (**28**) is presented diagrammatically in Figure 4.6 and summarised in Table 4.8. Results show that the gold complex **28** readily dissociates in solution to give the

positive ion $[M+Au]^+$. This molecular ion along with the $[M+Au+CH_3CN]^+$, $[2M+Au]^+$ and $[2M+2Au+Cl]^+$ aggregates are all observed in the ESMS spectrum [cone 50 V, H_2O/MeCN] of **28**. These aggregates are consistent with the calculated isotope patterns of gold, which has only the one isotope [^{197}Au], Figure 4.7. Attempts to obtain an electrospray mass spectrum of the platinum dichloride complex **27** were unsuccessful.

Compound	*Mode*	*Observed Ions (m/z)*
28	positive	42*, $[M+Au]^+$ 427; $[M+Au+CH_3CN]^+$ 468; $[2M+Au]^+$ 657; $[2M+2Au+Cl]^+$ 889.

Table 4.8: Electrospray mass spectral data of the gold(I) chloride complex **28** recorded in 1:1 H_2O/MeCN at a cone voltage of 50V.

* denotes peak not assigned.

R=8-camphanyl

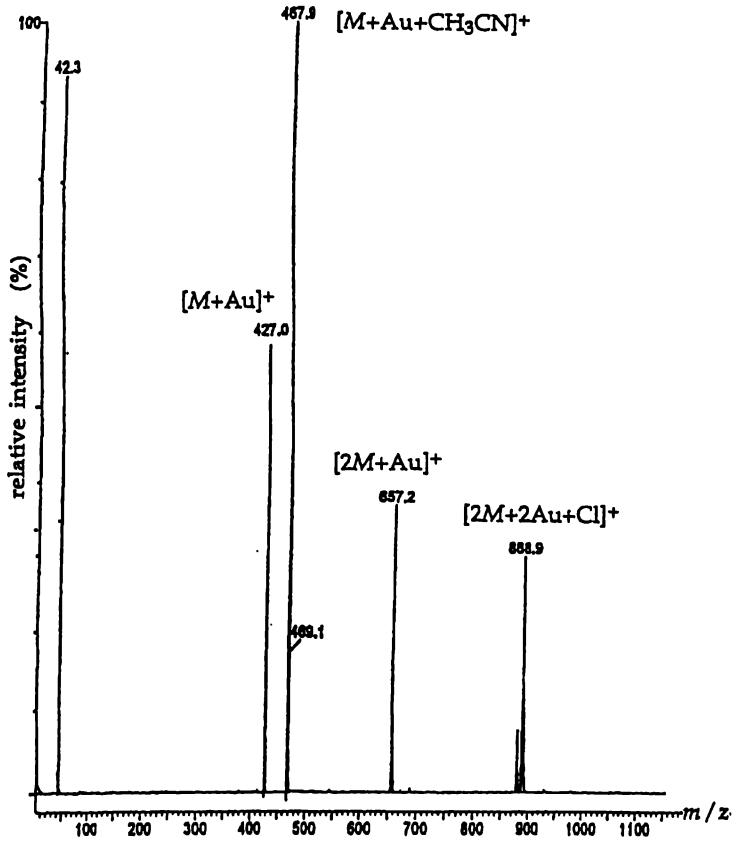

Figure 4.6: Positive-ion electrospray mass spectrum of the gold(I) chloride complex **28** recorded in 1:1 H_2O/MeCN at a cone voltage of 50V.

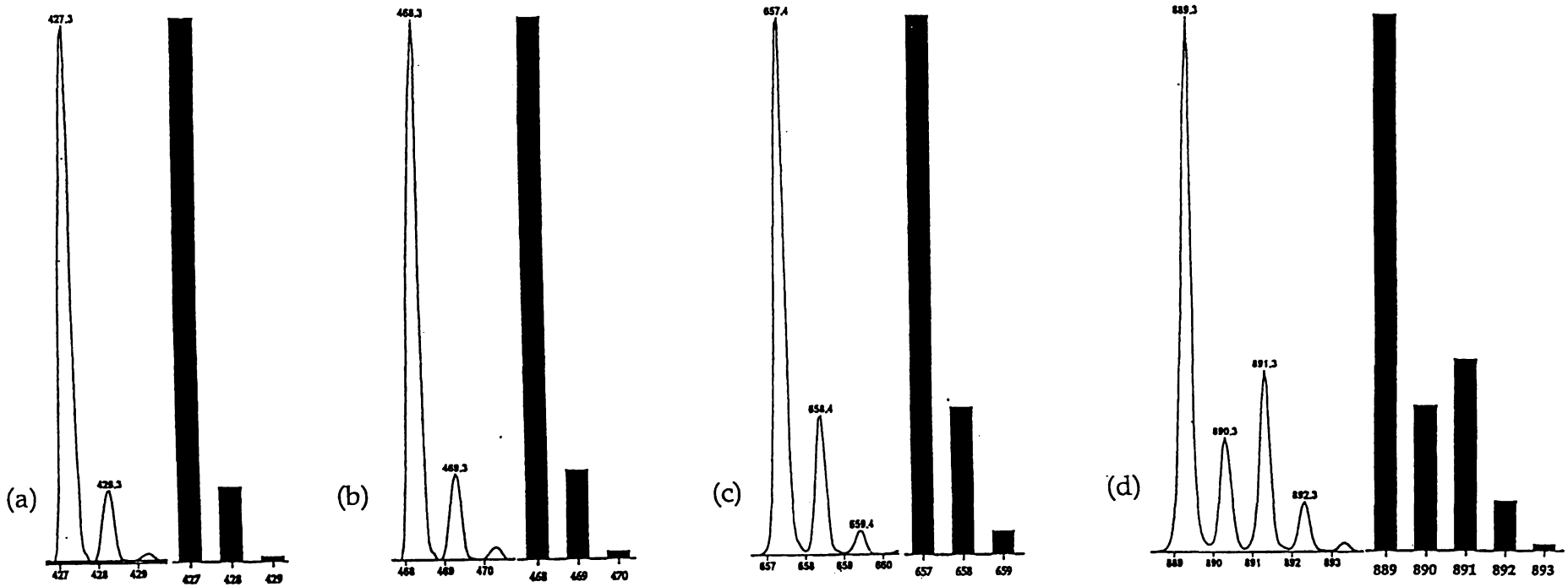

Figure 4.7: Observed (LHS) and calculated (RHS) isotope patterns for the gold(I)-phosphine adducts (a) $[M+Au]^+$ at m/z 427. (b) $[M+Au+CH_3CN]^+$ at m/z 468. (c) $[2M+Au]^+$ at m/z 657. (d) $[2M+2Au+Cl]^+$ at m/z 889.

R denotes 8-camphanyl. M denotes the parent phosphine.

4.7 A comparison of NMR data of camphene-derived phosphines and their derivatives

4.7.1 Comparison of ^{31}P NMR data of camphene-derived phosphines and their derivatives

The characteristic ^{31}P NMR chemical shifts of the phosphines **20** [δ -140] and **23** [δ -25.4] clearly distinguish them from the phosphonium salt **22** [δ 29.0], hydroxymethylphosphine oxide, sulfide, selenide **24-26** [δ 55.6-43.4] and Pt, Au complexes **27-28** [δ 21.7, 10.65]. The proton-coupled phosphorus NMR of the hydroxymethylphosphine derivatives **[22, 24-28]** gives broad signals or undefined multiplets which are expected to result from the large number of protons attached to the hydroxymethyl groups coupling to phosphorus.

4.7.2 Comparison of ^{1}H and ^{13}C NMR data of camphene-derived phosphines and their derivatives

A summary of the ^{1}H NMR chemical shifts of camphene-derived phosphines and their derivatives is presented in Table 4.9, along with an atom numbering scheme. A comparison of the ^{1}H NMR resonances of the primary phosphine **20** with the phosphonium salt **22** reveals a general shift to higher field, the most significant shift being the ^{1}H NMR resonances belonging to $H_{8'/8''}$ [δ 1.49 to δ 2.55]. This shift is expected to be due to the net 1+ charge on the phosphonium salt [*c.f.* the phosphine which is neutral]. The resonances belonging to $H_{8'/8''}$ are most affected as they are adjacent to the substitution site.

The ^1H NMR resonances of the primary phosphine **20** and hydroxymethylphosphine **23** are comparable. A general shift back to higher field is observed when the ^1H NMR resonances of the phosphonium salt **22** are compared with those of hydroxymethylphosphine **23**. This too is expected to be the result of the difference in charges.

A comparison of the ^1H NMR data of **24** and **25** with **23** shows that the resonances most affected by the derivatisation of **23** to **24** or **25** are those in close proximity to the addition centre, *i.e*, resonances assigned to $H_{8'/8''}$ and H_3. The remaining ^1H NMR resonances for **23, 24** and **25** are consistent with respect to each other, only varying slightly in magnitude.

A summary of the ^{13}C NMR chemical shifts of the camphene-derived phosphines **[20, 22-28]** is presented in Table 4.10, along with an atom numbering scheme. The chemical shifts assigned to C(1)-C(7), C(9) and C(10) are remarkably consistent irrespective of the substituent or solvent used. The order in which these assigned ^{13}C NMR signals appear for all but one, the phosphine selenide **25**, are identical between derivatives. That is, the signal assigned to C(1) precedes the other assigned signals in the following order: C(3), C(4), C(2), C(7), C(10), C(6), C(9), C(5). The signal assigned to C(5) in all but two cases, precedes that signal assigned to C(8). These signals are easily distinguished as the relative intensity of the signal assigned to C(8), which was split by the directly attached phosphorus to produce a doublet, is considerably less than that signal assigned to C(5). The extent to which the signal relating to C(8) varies has been noted in previous chapters [section 2.3.4] and is a result of its close proximity to the phosphorus centre.

It is worth noting that the ^{13}C NMR spectra of the bis(hydroxymethyl) phosphine **23** and its bis(hydroxymethyl) derivatives **[24-26]** reveals that the hydroxymethyl groups are inequivalent. This is in direct contrast to their precursor, the tris(hydroxymethyl)phosphonium salt **22**, where the three hydroxymethyl groups are equivalent. This difference is expected be the result of diastereoisotopic effects, *i.e.* derivatives **23-26** forming conformers, and therefore distinct chemical environments, which minimise steric interaction between the $P(CH_2OH_2)_2X$ [X=O, S, Se] and asymmetric camphanyl moiety. This is compared to **22** where the free rotation of the

asymmetric camphanyl moiety interacts equally with all three -CH_2OH groups producing equivalent chemical environments and thus an equivalent ^{13}C NMR signals.

Although the ^{13}C NMR chemical shifts for the camphanyl moiety of the camphene-derived phosphorus compounds **[20, 22-28]** are consistent making identification possible at a glance, the same can not be said about the one-bond phosphorus to carbon coupling constants. These are not comparable and, in contrast to ^{13}C chemical shifts, vary significantly depending on substitution and nuclear charge at the phosphorus centre. However it is noted that the change in oxidation state of the phosphorus, as is the case with the transformation of both the phosphine **20** [$^1J_{P\text{-}C(8)}$ 7.1 Hz] to the phosphonium salt **22** [$^1J_{P\text{-}C(12)}$ 54.7 Hz; $^1J_{P\text{-}C(8)}$ 38.3Hz] and the phosphonium salt **22** to hydroxymethylphosphine **23** [$^1J_{P\text{-}C(12)}$ 14.9 Hz; $^1J_{P\text{-}C(8)}$ 9.2 Hz] is consistent with the general trends observed for one-bond phosphorus to carbon coupling constants[46].

	$C_{10}H_{17}PH_2$	$C_{10}H_{17}P^+(CH_2OH)_3$	$C_{10}H_{17}P(CH_2OH)_2$	$C_{10}H_{17}PS(CH_2OH)_2$	$C_{10}H_{17}PSe(CH_2OH)_2$	$C_{10}H_{17}P(CH_2OH)_2AuCl$
	20	**22**	**23**	**24**	**25**	**28**
	$CDCl_3$	$CDCl_3$	$CDCl_3$	$CDCl_3$	$CDCl_3$	CD_3OD
H_4	2.25, br, s	2.33, br, m	2.15, br, s	2.29, br, s	2.29, br, s	2.60, br, s
H_3	1.74, br, s	2.02, br, m	1.47, br, s	1.93, dt	1.90, m	1.80, m
$H_{7''}$	1.60, d, ^2J 12.1	1.85, m*	1.55, d, ^2J 10.2	1.67, d, ^2J 10.0	1.69, d, ^2J 10.0	1.73, d, ^2J 9.1
$H_{6''}$	1.54, m	1.73, m	1.49, m	1.55, m	1.55, br, m	1.64, br, m
$H_{8'/8''}$	1.49, br ,s	2.55, m	1.58, m	2.12-1.80, m	2.20, m	2.00, m
H_1	1.46, br, s	1.98, s	1.68, br, s	1.77, br, s	1.78, br, s	1.78, s
$H_{6'}$	1.25, m	1.46, m	1.18, m	1.28, m	1.29, m	1.32, m
$H_{5'/5''}$	1.25, m	1.48, br, m	1.32-1.10, m	1.30, br, m	1.30, m	1.35, m
$H_{7'}$	1.14, d, ^2J 12.1	1.43, d	1.10, d, ^2J 10.2	1.20, d, ^2J 10.0	1.20, d, ^2J 10.0	1.27, d, ^2J 9.1
Me'	0.91, s	1.12, s	0.89, s	0.97, s	0.98, s	1.08, s
Me''	0.80, s	0.99, s	0.79, s	0.80, s	0.82, s	0.90, s

Table 4.9: ^1H NMR data of camphene-derived phosphines and their derivatives, along with the atom numbering scheme.
$C_{10}H_{17}$=8-camphanyl * denotes unresolved signal

	RPH_2	$RP^+(CH_2OH)_3$	$RP(CH_2OH)_2$	$RP(S)(CH_2OH)_2$	$RP(Se)(CH_2OH)_2$	$RP(O)(CH_2OH)_2$	$[RP(CH_2OH)_2]_2PtCl_2$	$RP(CH_2OH)_2AuCl$
	20	**22**	**23**	**24**	**25**	**26**	**27**	**28**
	$CDCl_3$	$CDCl_3$	$CDCl_3$	$CDCl_3$	$CDCl_3$	DMSO	CD_3OD	CD_3OD
CH_2OH	-	50.7	61.3, 61.1	60.5, 59.7	59.8, 59.4	60.5, 60.4	59.1-58.0	57.9, 57.4
$^1J_{P-C}$	-	54.7 Hz	14.9 Hz	30.5 Hz	47.4 Hz	77.2 Hz	nm	42.9 Hz
C(1)	52.8	48.1	49.0	48.3	48.4	51.9	52.0	50.1
C(3)	49.3	43.6	47.6	44.1	44.8	47.1	50.0	48.7
$^2J_{P-C-C}$	nd	4.9 Hz	13.1 Hz	3.3 Hz	3.0 Hz	3.8 Hz	2.9 Hz	nd
C(4)	41.1	42.3	42.3	42.1	42.0	46.1	45.3	43.5
$^3J_{P-C-C-C}$	4.4 Hz	nd	7.5 Hz	1.5 Hz	nd	2.7 Hz	5.7 Hz	4.0 Hz
C(2)	37.8	38.5	37.6	38.0	37.0	40.9	41.6*	39.2
$^3J_{P-C-C-C}$	3.9 Hz	12.4 Hz	9.8 Hz	11.7 Hz	11.4 Hz	11.2 Hz	nm	10.9 Hz
C(7)	36.8	36.9	37.0	37.2	37.2	40.6	40.7	38.0
C(10)	32.4	31.1	32.3	31.7	31.7	35.4	35.5	32.5
C(6)	24.6	24.4	24.7	24.6	24.7	28.2	28.3	25.5
C(9)	21.4	21.3	21.7	22.1	22.4	25.8	25.9	22.4
C(5)	19.6	19.7	19.9	20.2	20.2	23.1	23.8*	21.0
C(8)	10.8	11.8	14.8	21.8	21.1	22.7	20.0*	17.2
$^1J_{P-C}$	7.1 Hz	38.3 Hz	9.2 Hz	17.6 Hz	39.5 Hz	61.7 Hz	nm	34.3 Hz

Table 4.10: ^{13}C NMR data of camphene-derived phosphines and their derivatives, along with the atom numbering scheme.

R=$C_{10}H_{17}$=8-camphanyl * denotes signal tentatively assigned nd denotes not detected nm denotes not measured

4.8 Experimental

General instrumental techniques are as described in Appendix II. Standard Schlenk and syringe techniques were used for all manipulations carried out under nitrogen. Lithium aluminium hydride (Aldrich) was used as supplied from commercial sources. Analytical grades of formaldehyde, hydrochloric acid, paraformaldehyde, potassium hydroxide, sulfur and selenium were all used as supplied. Other reagents used were laboratory grade and were used as supplied. All solvents were of reagent grade. Deoxygenated solvents were prepared by bubbling nitrogen gas through the solvent for 10 minutes. Tetrahydrofuran (THF) was distilled under a nitrogen atmosphere from sodium/benzophenone. Petroleum spirit refers to the fraction of b.pt. 40-60°C. Tetrahydrothiophene gold(I) chloride[62] and $CODPtCl_2$[63] were synthesised by standard literature procedures. 8-Camphanylphosphinic acid (**1**) and 8-camphanylphosphonic dichloride (**11**) were synthesised by the methods described in chapter 2, section 2.1.2 and section 2.3.2.

*4.8.1 Synthesis of 8-camphanylphosphine (**19**) via $LiAlH_4$ route*

Under a nitrogen atmosphere, 8-camphanylphosphonic dichloride (**11**) (7.0 g, 0.027 mol in 10 mL of dry THF) was added dropwise to $LiAlH_4$ (3.3 g, 0.08 mol in 30 mL of dry THF). The resulting mixture was refluxed for 4 h after which deoxygenated isopropanol was added to the ice-cooled mixture to destroy the excess $LiAlH_4$. The solvent was removed under vacuum and deoxygenated CH_2Cl_2 (50 mL) was added. Under nitrogen the supernatant was removed from a white solid by filtration. Concentration of the organic extract gave a cream-white solid which was found to be impure by elemental analysis. Despite repeated filtrations to remove "metal salts" purification was not possible. As the attempted vacuum distillation was also unsuccessful an alternative route was sought.

4.8.2 Synthesis of 8-camphanylphosphine (20) via disproportionation

Phosphinic acid **1** (62.8 g, 0.31 mol) was heated under vacuum (0.5 mmHg), and the fraction which distilled over at 140°C was collected in a trap cooled in liquid nitrogen, which upon warming to room temperature yielded the primary phosphine **20** (5.0 g, 28.5%) as a pale yellow liquid. Derivatisation of the freshly distilled phosphine was immediately carried out. Apparatus designed to facilitate both the disproportionation of **1** and the distillation of **20** is presented in section 4.2.2, Figure 4.1.

NMR : ^{31}P-{H}: δ -140.4 [t, $^{1}J_{P\text{-}H}$ 194.1 Hz]

^{1}H : δ 2.69 [br, m, PH_2], 2.58 [m, PH_2]$_a$, 2.25 [1H, br, s, H_4]$_a$, 1.74 [1H, br, s, H_3], 1.60 [1H, d, ^{2}J 12.1, $H_{7''}$]$_a$, 1.54 [1H, m, $H_{6''}$]$_b$, 1.49 [2H, br ,s , $H_{8'/8''}$]$_b$, 1.46 [1H, br, s, H_1]$_b$, 1.25 [3H, br, m, $H_{6'}$, $H_{5''/5'}$]$_b$, 1.14 [d, ^{2}J 12.1, $H_{7'}$]$_a$, 0.91 [3H, s, Me'], 0.80 [3H, s, Me''].

a: partially overlapping signals

b: overlapping signals

^{13}C-{H}: 52.8 [s, C(1)], 49.3 [s, C(3)], 41.1 [d, $^{3}J_{P\text{-}C\text{-}C\text{-}C}$ 4.4 Hz, C(4)], 37.8, [d, $^{3}J_{P\text{-}C\text{-}C\text{-}C}$ 3.9 Hz, C(2)], 36.8 [s, C(7)], 32.4 [s, C(10)], 24.6 [s, C(6)], 21.4 [s, C(9)], 19.6 [s, C(5)], 10.8 [d, $^{1}J_{P\text{-}C}$ 7.1 Hz, C(8)].

^{1}H NMR resonances belonging to $H_{5/5''}$ and $H_{8'/8''}$ were not distinguished. Irradiation of the signal assigned to $H_{8'/8''}$ simplified the PH_2 multiplet to a doublet of doublet pattern confirming the PH_2 assignment.

4.8.3 Synthesis of 8-camphanylphosphine oxide (21) via air oxidation

8-Camphanylphosphine (**20**) is readily oxidised in the presence of air to 8-camphanylphosphine oxide (**21**) [δ 9.2, t, $^{1}J_{P\text{-}H}$ 416.4 Hz]. Measurement

of the ^{31}P NMR peak areas indicated that half the phosphine **20** was present after 2 h. Further oxidation reduced the amount of **20** to one-third after 24 h. Other reaction products present were not identified.

4.8.4 Synthesis of 8-camphanyl tris(hydroxymethyl)phosphonium chloride (22)

To 8-camphanylphosphine (**20**) was added dropwise with stirring, 60 mL of a 1:1 mixture of deoxygenated 37% formaldehyde and concentrated hydrochloric acid. The two immiscible layers were stirred vigorously over two days, after which the resulting white solid was filtered, washed with a small amount of cold water, and recrystallised from methanol/petroleum spirit to give the phosphonium salt **22** as a white crystalline solid (9.2 g, 54 %) [1]. M.p. 137-139°C. (Analysis: Found: C, 52.43; H, 9.01% $C_{13}H_{26}O_3PCl$ requires C, 52.68; H, 8.85 %.) ESMS (cone 45, positive ion); $[M\text{-}Cl^-]^+$ at m/z 261, $[2M+Cl^-]^+$ at m/z 557.

NMR : ^{31}P-{H} (MeOH): δ 29.9 [s]

^1H : δ 4.70 [br, s, CH_2OH], 2.55 [2H, br, m, $H_{8'/8''}]_a$, 2.33 [1H, br, m, H_4], 2.02 [1H, br, m, $H_3]_b$, 1.98 [1H, s, $H_1]_b$, 1.85 [1H, m, $H_{7''}]_b$, 1.73 [1H, m, $H_{6''}]_b$, 1.48 [br, m, $H_{5''/5'}]_b$, 1.46, [1H, m, $H_{6'}]_b$, 1.43 [1H, d, ^2J 10.8, $H_{7'}]_b$, 1.12 [3H, s, Me'], 0.99 [3H, s, Me''].

a: partially overlapping signals

b: overlapping signals

^{13}C-{H}: δ 50.7 [d, $^1J_{P\text{-}C}$ 54.7 Hz, 3x CH_2OH], 48.1 [s, C(1)], 43.6 [d, $^2J_{P\text{-}C\text{-}C}$ 4.9 Hz, C(3)], 42.3 [s, C(4)], 38.5 [d, $^3J_{P\text{-}C\text{-}C\text{-}C}$ 12.4 Hz, C(2)], 36.9 [s, C(7)], 31.1 [s, C(10)], 24.4 [s, C(6)], 21.3 [s, C(9)], 19.7 [s, C(5)], 11.8 [d, $^1J_{P\text{-}C}$ 38.3 Hz, C(8)].

---

[1] yield calculated from the phosphinic acid **1**.

A C13NNE experiment was also performed and the peak intensity ratios of the CH_2OH signals to an averaged C(1), C(2), C(3) peak intensity was 3:1 which is consistent with the above assignment.

I.R. : 1055, 1044 broad, strong

X-ray crystal structure of 8-camphanyl tris(hydroxymethyl)phosphonium chloride (22)

Colourless plate-like crystals were obtained by slow evaporation of a methanol solution of **22**. Cell parameters (from 18 reflections with $10°<2\theta<30°$) and intensity data were obtained at -143°C using a Nicolet R3 four-circle diffractometer with monochromated Mo-Kα radiation (λ= 0.7107 Å). A total of 2798 reflections (2657 unique) in the range $2°<\theta<25°$ was collected. These were corrected for Lorentz and polarisation effects but not for absorption correction as the linear absorption coefficient was low.

Crystal data: $C_{13}H_{26}O_3PCl$, M 296.76, monoclinic, space group $P2_1/c$, a=12.1416(3), b=7.5611(5), c = 16.5044(7)Å, β = 92.541(2)°, U = 1513.6(8) $Å^3$. D_c 1.302 g cm^{-3} for Z = 4. F(000) 640, μ(Mo-Kα) 0.35 mm^{-1}, crystal size 0.57 x 0.10 x 0.16 mm.

Solution and refinement

The crystal structure was solved by direct methods using SHELX programs[64]. Subsequent difference maps revealed all non-hydrogen atoms. In the final cycle of full-matrix least-squares refinement (based on F^2, 163 parameters against 2657 data) the C, Cl, O and P atoms were assigned anisotropic temperature factors. Hydrogen atoms attached to carbon were included in their calculated positions with their isotropic temperature factors riding on the U_{iso} of the carbon to which they are attached. In the

penultimate difference map the hydrogen atoms attached to oxygen were located. These positions were included in the final refinement but with the O-H distances and C-O-H angles constrained to ideal values using the Affix 143 option of SHELXS93. Refinement converged at R_1 [for 2657 reflections with $I>2\sigma(I)$]= 0.0467, wR_2 [all data] = 0.0936, GoF 1.023. In the last cycle of refinement no parameter shifted by more than a maximum (Δ/σ) of 0.03. The largest features in a final difference map are +0.345/-0.215 e $Å^{-3}$.

4.8.5 Synthesis of 8-camphanyl bis(hydroxymethyl)phosphine (23) via the use of KOH

Under a nitrogen atmosphere 8-camphanyl tris(hydroxymethyl)-phosphonium chloride (**22**) (1.0 g, 3.4 mmol) was added to 60 mL of a 1:1 mixture of deoxygenated water and dichloromethane. While being vigorously stirred potassium hydroxide (0.21 g, 3.7 mmol in 10 mL of deoxygenated water) was added dropwise. After 2 h the dichloromethane layer was withdrawn by syringe from the aqueous layer and evaporated to dryness to give 8-camphanyl bis(hydroxymethyl)phosphine (**23**) (0.62 g, 80%) as a colourless oil.

NMR: ^{31}P-{H}: δ -25.4 [s]

^{1}H : δ 4.30 [2H, br, s, OH], 4.19-4.09, 3.99-3.91 [4H, br, m, $CH_2OH]_b$, 2.15 [1H, br, s, H_4)], 1.68 [1H, br, s, H_1], 1.60-1.57 [2H, m, $H_{8''/8'}$], 1.55 [1H, d, ^{2}J 10.2, $H_{7''}]_b$, 1.49 [1H, m, $H_{6''}]_b$, 1.47 [1H, br, s, $H_3]_b$, 1.32-1.10 [2H, br, m, $H_{5''/5'}]_b$, 1.18 [1H, m, $H_{6'}]_b$, 1.10 [1H, d, ^{2}J 10.2, $H_{7'}]_a$, 0.89 [3H, s, Me'], 0.79 [3H, s, Me''].

a: partially overlapping signals

b: overlapping signals

^{13}C-{H}: δ 61.3 [d, $^{1}J_{P\text{-}C}$ 14.9 Hz, CH_2OH)]*, 61.0 [d, $^{1}J_{P\text{-}C}$ 14.9 Hz, CH_2OH)]*, 49.0 [s, C1)], 47.6 [d, $^{2}J_{P\text{-}C\text{-}C}$ 13.1 Hz, C3)], 42.3 [d, $^{3}J_{P\text{-}C\text{-}C\text{-}C}$ 7.5 Hz,

C4)], 37.6 [d, $^3J_{P\text{-}C\text{-}C\text{-}C}$ 9.8 Hz, C2)], 37.0 [s, C7)], 32.3 [s , C10)], 24.7 [s, C6)], 21.7 [s, C9)], 19.9 [s, C5)], 14.8 [d, $^1J_{P\text{-}C}$ 9.2 Hz, C8)].

* denotes signals that were tentatively assigned

A C13NNE experiment was also performed and the peak intensity ratios of the CH_2OH signals to an averaged C(1), C(2) peak intensity was 2:1, which is consistent with the above assignment.

4.8.6 Synthesis of 8-camphanyl bis(hydroxymethyl)phosphine (23) via use of Et_3N

Under a nitrogen atmosphere 8-camphanyl tris(hydroxymethyl)-phosphonium chloride (**22**) (1.0 g, 3.4 mmol) was added to 60 mL of a 1:1 mixture of deoxygenated water and dichloromethane. While being vigorously stirred triethylamine (0.38 g, 3.7 mmol) was added dropwise. After 2 h the dichloromethane layer was syringed from the aqueous layer and evaporated to dryness to give a colourless oil. The ^{31}P NMR spectrum revealed that the colourless oil contained three components at δ -25.2, -28.1, -35.3. However after the oil was heated to 85°C under vacuum and had nitrogen bubbled through it for 4 h, only one ^{31}P NMR signal belonging to the hydroxymethylphosphine **23** (0.52 g, 66%) was present.

NMR: $^{31}P\text{-}\{H\}$: δ -25.4 [s]

4.8.7 Air oxidation of 8-camphanyl bis(hydroxymethyl)phosphine (23)

8-Camphanyl bis(hydroxymethyl)phosphine (**23**) readily reacts in the presence of air to form a large number of decomposition products. After 18 h all of the phosphine had decomposed. These decomposition products were not further analysed.

*4.8.8 Synthesis of 8-camphanyl bis(hydroxymethyl)phosphine sulfide (**24**)*

Under a nitrogen atmosphere 8-camphanyl tris(hydroxymethyl)-phosphonium chloride (**22**) (0.5 g, 1.7 mmol) and an excess of S_8 (1g) were added to a mixture of deoxygenated water (20 mL) and dichloromethane (30 mL). While being stirred potassium hydroxide (0.12 g, 2.1 mmol in 10 mL of deoxygenated water) was added dropwise. After 24 h the organic layer was separated, dried over anhydrous magnesium sulfate and evaporated to dryness to give a pale yellow solid which, when recrystallised from dichloromethane/petroleum spirit, gave 8-camphanyl bis(hydroxymethyl) phosphine sulfide (**24**) (0.35 g, 60%) as a yellow crystalline solid, m.p. 81-82°C. (Analysis: Found: C, 55.14; H, 8.84% $C_{12}H_{23}O_2PS$ requires C, 54.94; H, 8.84 %.) ESMS (cone 20 V, $AgNO_3$, positive ion); $[M+CH_3CN+Ag]^+$ at *m/z* 412, $[2M+Ag]^+$ at *m/z* 633. Observed isotope patterns for the Ag(I) aggregates of **24** are consistent with calculated isotope patterns.

NMR: ^{31}P-{H}: δ 55.6 [s]

^{1}H : δ 4.00 [2H, br, m, CH_2], 3.98 [2H, br, m, CH_2], 3.37 [2H, br, s, OH], 2.29 [1H, br, s, H_4], 2.05, 1.82 [2H, br, m, $H_{8''/8'}]_a$, 1.93 [1H, dt, ^2J 12.1, ^3J 3.1, H_3], 1.77 [1H, br, s, $H_1]_a$, 1.67 [1H, d, ^2J 10.0, $H_{7''}$], 1.55 [1H, m, $H_{6''}$], 1.30 [2H, br, m, $H_{5''/5'}]_b$, 1.28 [1H, m, $H_{6'}]_b$, 1.20 [1H, d, ^2J 10.0, $H_{7'}$], 0.97 [3H, s, Me'], 0.80 [3H, s, Me''].

a: partially overlapping signals

b: overlapping signals

^{13}C-{H}: δ 60.5 [d, $^1J_{P\text{-}C}$ 30.5 Hz, CH_2OH]*, 59.7 [d, $^1J_{P\text{-}C}$ 30.5 Hz, CH_2 OH]*, 48.3 [s, C(1)], 44.1 [d, $^2J_{P\text{-}C\text{-}C}$ 3.3 Hz, C(3)], 42.1 [d, $^3J_{P\text{-}C\text{-}C\text{-}C}$ 1.5 Hz, C(4)], 38.0 [d, $^3J_{P\text{-}C\text{-}C\text{-}C}$ 11.7 Hz, C(2)], 37.2 [s, C(7)], 31.7 [s, C(10)], 24.6 [s, C(6)], 22.1 [s, C(9)], 21.8 [d, $^1J_{P\text{-}C}$ 17.6 Hz, C(8)], 20.2 [s, C(5)].

* denotes tentative assignment of signals

I.R. : υ(P=O) region (1300-1140 cm^{-1}) 1040 broad, strong

υ(P=S) region (750-580 cm^{-1}) 686 sharp, strong

4.8.9 Synthesis of 8-camphanyl bis(hydroxymethyl)phosphine selenide (25)

Under a nitrogen atmosphere 8-camphanyl tris(hydroxymethyl)-phosphonium chloride (**22**) (0.47 g, 1.6 mmol) and an excess of selenium (0.7 g) were added to 30 mL of deoxygenated water. Potassium hydroxide (0.094 g, 1.7 mmol) was added and the resulting mixture was heated for 4 h at 85°C. Upon completion the aqueous phase was extracted with dichloromethane (30 mL), concentrated and recrystallised from dichloro-methane/petroleum spirit to give the phosphine selenide **25** (0.44 g, 70%) as a white needle-like crystalline solid, m.p. 90-92°C. (Analysis: Found C, 46.62; H, 7.60%. $C_{12}H_{23}O_2PSe$ requires C, 46.44; H, 7.48 %.)

NMR : ^{31}P-{^1H}: δ 43.4 [s, $^1J_{P\text{-}Se}$ 683 Hz]

^1H: δ 4.10 [4H, m, CH_2OH], 3.31 [2H, br, s, OH], 2.29 [1H, br, s, H_4], 2.20 [1H, m, $H_{8'/8''}$], 1.90 [1H, m, H_3], 1.88, [1H, br, m, $H_{8'/8''}$], 1.78 [1H, br, s, H_1], 1.69 [1H, d, ^2J 10.0, $H_{7''}$], 1.55 [1H, br, m, $H_{6''}$], 1.30 [2H, m, $H_{5''/5'}$]$_b$, 1.29 [1H, m, $H_{6'}$]$_b$, 1.20 [1H, d, ^2J 10.0, $H_{7'}$], 0.98 [3H, s, Me'], 0.82 [3H, s, Me''].

a: partially overlapping signals

b: overlapping signals

^{13}C-{H}: δ 59.8 [d, $^1J_{P\text{-}C}$ 47.4 Hz, CH_2OH)]*, 59.4 [d, $^1J_{P\text{-}C}$ 47.4 Hz, CH_2OH)]*, 48.4 [s, C(1)], 44.8 [d, $^2J_{P\text{-}C\text{-}C}$ 3.0 Hz, C(3)], 42.0 [s, C(4)], 37.0 [d, $^3J_{P\text{-}C\text{-}C\text{-}C}$ 11.4 Hz, C(2)], 37.2 [s, C(7)], 31.7 [s, C(10)], 24.7 [s, C(6)], 22.4 [s, C(9)], 21.1 [d, $^1J_{P\text{-}C}$ 39.2 Hz, C(8)], 20.2 [s, C(5)].

* denotes tentative assignment of signals

I.R. : υ(P-OH) 1031 broad, strong

4.8.10 Synthesis of 8-camphanyl bis(hydroxymethyl)phosphine oxide (26)

To 8-camphanyl bis(hydroxymethyl)phosphine (**23**) (0.20 g, 0.87 mmol) was added degassed acetone (10 mL) and hydrogen peroxide (1.5 mL , 60v/v in 5 mL of water). After 24 h a white precipitate was filtered and recrystallised by slow evaporation from methanol to give the phosphine oxide **26** (0.15 g, 68%) as a white plate-like crystalline solid, m.p. 80-95°C. (Analysis: Found C, 54.55; H, 10.09%. $C_{12}H_{23}O_3P.2CH_3OH$ requires C, 54.16; H, 10.07%). Analytical data collected on **26** recrystallised from methanol were consistent with the ^1H NMR spectrum of **26** as a di-methanol solvate. ESMS (cone 20, positive ion); $[M+H]^+$ at *m/z* 247, $[2M+H]^+$ at *m/z* 493, $[3M+H]^+$ at *m/z* 739.

NMR: ^{31}P-{H} (DMSO): δ 46.9 [s]

^{13}C-{H} (DMSO): δ 60.5 [d, $^1J_{P\text{-}C}$ 77.2 Hz, CH_2OH], 60.4 [d, $^1J_{P\text{-}C}$ 77.2 Hz, CH_2OH], 51.9 [s, C(1)], 47.1 [d, , $^2J_{P\text{-}C\text{-}C}$ 3.8 Hz, C(3)], 46.1 [d, , $^3J_{P\text{-}C\text{-}C\text{-}C}$ 2.7 Hz, C(4)], 40.9 [d, , $^3J_{P\text{-}C\text{-}C\text{-}C}$ 11.2 Hz, C(2)], 40.6 [s, C(7)], 35.4 [s, C(10)], 28.2 [s, C(6)], 25.8 (s, C(9)], 23.1 [s, C(5)], 22.7 [d, , $^1J_{P\text{-}C}$ 61.7 Hz, C(8)].

4.8.11 Synthesis of 8-camphanyl bis(hydroxymethyl)phosphine platinum dichloride (27)

Under a nitrogen atmosphere, the addition of $CODPtCl_2$ (0.18 g, 0.47 mmol in 10 mL of degassed CH_2Cl_2) to 8-camphanyl bis(hydroxymethyl) phosphine (**23**) (0.22g, 0.95 mmol in 5 mL of degassed CH_2Cl_2) precipitates the platinum dichloride complex **27** (0.24 g, 85%) as a white solid. Diethyl ether (30 mL) was added to further facilitate crystallisation. The white solid **27** was filtered, washed with ether and dried under vacuum. M.p. 219-223°C. (Analysis: Found C, 39.75; H, 6.50% $C_{24}H_{46}O_4PCl_2Pt$ requires C, 39.71; H, 6.39%.)

NMR: ^{31}P-{^{1}H} (121.51 MHz): δ 10.70 [P, s, $^{1}J_{P\text{-}Pt}$ 3420.3 Hz]; 10.65 [P', s, $^{1}J_{P\text{-}Pt}$ 3420.3 Hz]

^{13}C-{H} (CD_3OD): δ 59.1-58.0 [m, CH_2OH]*, 52.0 [s, C(1)], 50.0 [d, $^{2}J_{P\text{-}C\text{-}C}$ 2.9 Hz, C(3)], 45.3 [d, $^{3}J_{P\text{-}C\text{-}C\text{-}C}$ 5.6 Hz, C(4)], 41.7-41.5 [m, C(2)]*, 40.7 [s, C(7)], 35.5 [s, C(10)], 28.3 [s, C(6)], 25.9 [s, C(9)], 23.80, 23.75 [s, C(5)]*, 20.4-19.9 [m, C(8)]*.

* denotes signals not assigned

4.8.12 Synthesis of 8-camphanyl bis(hydroxymethyl)phosphine gold(I) chloride (28)

Under a nitrogen atmosphere tetrahydrothiophene gold(I) chloride (0.35 g, 1.1 mmol) was added to a deoxygenated dichloromethane solution of 8-camphanylbis(hydroxymethyl)phosphine (**23**) (0.30 g, 1.3 mmol). After 18 h of stirring, a white precipitate which had formed was filtered and washed with dichloromethane. The white solid was recrystallised from methanol to give the phosphine gold(I) chloride complex **28** (0.47g, 78%) as a white plate-like crystalline solid. M.p. 124.5-129.5°C. ESMS (cone 50, positive ion); $[M+Au]^+$ at m/z 427; $[M+Au+CH_3CN]^+$ at m/z 468; $[2M+Au]^+$ at m/z 657; $[2M+2Au+Cl]^+$ at m/z 889 (M = parent ion). Observed isotope patterns for the Au species are consistent with calculated isotope patterns. Elemental microanalytical data consistent with the formulated structure were not obtainable.

NMR: ^{31}P-{H}: (MeOH): δ 21.7 [s]

^{1}H (CD_3OD): δ 4.80 [2H, br, s, OH], 4.25 [4H, m, CH_2OH], 2.60 [1H, br, s, H_4], 2.00 (2H, br, m, $H_{8'/8''}$], 1.80 [1H, m, $H_3]_b$, 1.78 [1H, s, $H_1]_a$, 1.73 [1H, d, ^{2}J 9.1, $H_{7''}]_a$, 1.64 [1H, br, m, $H_{6''}$], 1.45, 1.35 [2H, br, m, $H_{5''/5'}]_b$, 1.32 [1H, m, $H_{6'}]_b$, 1.27 [1H, d, ^{2}J 9.1, $H_{7'}$], 1.08 [3H, s, Me'], 0.90 (3H, s, Me'').

a: partially overlapping signals

b: overlapping signals

^{13}C-{H} (CD_3OD): δ 57.9 [d, $^1J_{P\text{-}C}$ 42.9 Hz, CH_2OH]*, 57.4 [d, $^1J_{P\text{-}C}$ 42.4 Hz, CH_2OH]*, 50.1 [s, C(1)], 48.7 [s, C(3)], 43.5 [d, $^3J_{P\text{-}C\text{-}C\text{-}C}$ 4.0 Hz, C(4)], 39.2 [d, $^3J_{P\text{-}C\text{-}C\text{-}C}$ 10.9 Hz, C(2)], 38.0 [s, C(7)], 32.5 [s, C(10)], 25,5 [s, C(6)], 22.4 [s, C(9)], 21.0 [s, C(5)], 17.2 [d, $^1J_{P\text{-}C}$ 34.3 Hz, C(8)].

* denotes signals that were tentatively assigned

References

1 P. Kalck, F. Monteil, *Adv. in Organometallic Chem.*, (1992), **34**, 219.

2 K.V Katti, H. Gali, C.J. Smith, D.E. Berning, *Acc. Chem. Res.*, (1999), **32**, 9-17 and references therein.

3 L. Maier, *Progress in Inorganic Chemistry* (1963), **5**, 27.

4 L. Maier in *Organic Phosphorus Compounds*, Ed G.M. Kosolapoff, L. Maier, Wiley and Sons (1972), **1**, 1-287.

5 F.A. Cotton, B. Hong, *Progress in Inorganic Chemistry* , **40**.

6 D.G. Gilheany, C.M. Mitchell in *The Chemistry of Organophosphorus Compounds*, Ed F.R. Hartley, Wiley and Sons (1990), **1**, 151-190.

7 H.B. Kagan, M. Sasaki in *The Chemistry of Organophosphorus Compounds*, Ed F.R. Hartley, Wiley and Sons (1990), **1**, 52-102, 177-182.

8 K.M. Pietrusiewicz, M. Zablocka, *Chem. Rev.*, (1994), **94**, 1375-1411.

9 H.A. Mayer, W.C. Kaska, *Chem. Rev.*, (1994), **94**, 1239-1272.

10 P.G. Pringle, M.B. Smith, *Platinum Metals Rev.*, (1990), **34**, 74.

11 W.A. Herrmann, C.W. Kohlpaintner, *Angew. Chem. Int. Ed. Eng.*, (1993), **32**, 1524.

12 D.J. Darensbourg, F. Joo, M. Kannisto, A. Katho, J.H. Reibenspies, D.J. Daigle, *Inorg. Chem.*, (1994), **33**, 200.

13 K. Wan, M.E. Davis, *Tetrahedron: Asymmetry*, (1993), **12**, 2461.

14 For examples see D.W. Allen, D.E. Hibbs, M.B. Hursthouse, K.M. Abdul Malik, J. *Organometallic Chem.*, (1999), **572**, 259-264; K.N. Harrison, P.A.T. Hoye, A.G. Orpen, P.G. Pringle, M.B. Smith, *J. Chem. Soc., Chem. Comm.*, (1989), 1096-1097; B. Drieben-Holscher, J. Heinen, *J. Organometallic Chem.*, (1998), **570**, 141-146.

15 K.N Harrison, P.A.T. Hoye, A.G. Orpen, P.G. Pringle, M.B. Smith, *J. Chem. Soc. Chem. Comm.*, (1989), 1096; J.W. Ellis, K.N. Harrison, P.A.T. Hoye, P.G. Pringle, M.B. Smith, *Inorg. Chem.*, (1992), **31**, 3026.

16 D.E. Berning, K.V. Katti, C. L. Barnes, W.A. Volkert, *J. Am. Chem. Soc.*, (1999), **121**, 1658-1664.

17 A.W. Frank, D.J. Daigle, S.L. Vail, *Textile Research Journal*, (1982), 738.

18 J.W. Ellis, K.N. Harrison, P.A.T. Hoye, A.G. Orpen, P.G. Pringle, M.B. Smith, *Inorg. Chem.*, (1992), **31**, 3026.

19 H. Cristau, F. Plenat in *The Chemistry of Organophosphorus Compounds*, Ed F.R. Hartley, Wiley and Sons (1990), **3**, 45.

20 (1) Reviews: K.V. Katti, *Current Science*, (1996), **70**, 219-225; K.V Katti, H. Gali, C.J. Smith, D.E. Berning, *Acc. Chem. Res.*, (1999), **32**, 9-17 and references therein.

(2) For examples see G. Baxley, W.K. Millar, D.K. Lyon, B.E. Millar, G. Nieckarz, T.J.R. Weakley, D. Tyler, *Inorg. Chem.*, (1996), **35**, 6688-6693; V. Sreenivasa Reddy, K.V. Katti, C.L. Barnes, *J. Chem. Soc., Dalton Trans.*, (1996), 1301-1304; V. Sreenivasa Reddy, K.V. Katti, C.L. Barnes, *Inorg. Chim. Acta*, (1995), 367-370.

21 (1) Reviews: M.L. Lartigue, A.M. Caminade, J.P. Majoral, *Tetrahedron: Asymmetry*, (1997), **8**, 2697-2708 and references therein; C. Larre, D. Bressolles, C. Turrin, B. Donnadieu, A.M. Caminade, J.P. Majoral, *J. Am. Chem. Soc.*, (1998), **120**, 13070-13082 and references therein.

(2) For phosphine examples: M. Slany, M. Bardaji, M. Casanove, A.M. Caminade, J.P. Majoral, B. Chaudret, *J. Am. Chem. Soc.*, (1995), **117**, 9764-9765; C. Larre, A.M. Caminade, J.P. Majoral, *Angew. Chem. Int. Ed. Eng.*, (1997), **6**, 36; M. Slany, A.M. Caminade, J.P. Majoral, *Tetrahedron Letters*, (1996), **37**, 9053-9056 and references therein; M. Bardaji, A.M. Caminade, J.P. Majoral, B. Chaudret, *Organometallics*, (1997), **16**, 3489-3497.

22 Review: L. Maier in *Organic Phosphorus Compounds*, Ed G. Kosolapoff, L. Maier, Wiley and Sons (1972), **4**, 310.

23 For examples see B. Fontal, H. Goldwhite, D. Rowsell, *J. Org. Chem.*, (1966), **31**, 2424; V. Ginsburg, N. Privezentseva, *Zh. Obshch. Khim.*, (1958), **28**, 736; F. Mann, I. Millar, *J. Chem. Soc.*, (1952), 3039.

24 H. Fritzsche, U. Hasserodt, F. Korte, *Chem. Ber.*, (1965), **98**, 1681.

25 L.C.D. Groenweghe, U.S. Patent, (1965), 3223737.

26 L. Horner, H. Hoffmann, P. Beck, *Chem. Ber.*, (1958), **91**, 1583; T. Weil, B. Prijs, H. Erlenmeyer, *Helv. Chim. Acta*, (1952), **35**, 616.

27 P.R. Bloomfield, K. Parvin, *Chem. Ind.* (London), (1959), 541.

28 L.D. Freedmann, G.O. Doak, *J. Am. Chem. Soc.*, (1952), **74**, 3414.

29 R. Hovat, A. Furst, *J. Am. Chem. Soc.*, (1952), **74**, 562.

30 E. Fluck, H. Binder, *Z. Naturforsch., B*, (1967), **22**, 1001.

31 G.R. Knox, P.L. Pauson, D. Willison, *Organometallics*, (1992), **11**, 2930.

32 F. Uhlig, E. Herrmann, G. Ohms, G. Grobmann, S. Besser, R. Herbst-Irmer, *Z. Anorg. Allg. Chem.*, (1993) , **619**, 1962.

33 S.A. Buckler, M. Epstein, *Tetrahedron*, (1962), **18**, 1211; P.A.T. Hoye in Mellor's Comprehensive Treatise on Inorganic Chemistry, section XXXIII, 897.

34 K. Dixon in *Multinuclear NMR*, Ed J. Mason, Plenum Press, New York and London, (1987).

35 L. Maier, *Helv. Chim. Acta*, (1966), **49**, 842; K. Issleib and P.Thorausch, *Phosphorus Sulphur*, (1977), **3**, 203.

36 T. Birchall, W.L. Jolly, *Inorg. Chem.*, (1966), **5**, 2177.

37 D.G. Gorenstein in *Handbook of Organophosphorus Chemistry*, Ed R. Engel, Published by Marcel Dekker Inc, New York (1992), 435-482.

38 L. Maier in *Organic Phosphorus Compounds*, Ed G.M. Kosolapoff, L. Maier, Wiley and Sons (1972), **4**, 261.

39 H. Kohler, A. Michaelis, *Ber.*, (1877), **10**, 807; L. Maier, *Helv. Chim. Acta*, (1963), **46**, 1812.

40 J. Fawcett, P.A.T. Hoye, R.D.W. Kemmitt, D. Law, D.J. Russell, *J. Chem. Soc. Dalton Trans.*, (1993), 2563-2568.

41 A. Hoffman, *J. Am. Chem. Soc.*, (1921), **43**, 1684.

42 F.A. Jolon, P. Gomez-Sal, A. Otero, P. Royo, S. Garcia-Blanco, S. Martinez-Carrera, *J. Organomet. Chem.*, (1987), **332**, 289-298.

43 N.J. Goodwin, W. Henderson, B.K. Nicholson, J.K Sarfo, J. Fawcett, D.R. Russell, *J. Chem. Soc., Dalton Trans.*, (1997), 4377-4384

44 *International Tables for X-Ray Crystallography*, Kynoch Press, Birmingham, (1962), **3**.

45 F.H. Allen, O. Kennard, D.G. Watson, L. Brammer, A.G. Orpen, R. Taylor, *J. Chem., Perkin Trans. 2*, (1987), S1; *J. Chem. Soc, Dalton Trans.*, (1989), S1.

46 J.C. Tebby in *Phosphorus-31 NMR Spectroscopy in Stereochemical Analysis*,, Ed J.G. Verkade, L.D. Quin, VCH Publishers Inc., (1987), 1-59, and references therein.

47 W. Henderson, G.M. Olsen, *Polyhedron*, (1996), **15**, 2105.

48 A.W. Frank, D.J. Daigle, S.L. Vail, *Textile Research Journal*, (1982), 678.

49 A. Grayson, *J. Am. Chem. Soc.*, (1963), **85**, 79.

50 P.A.T. Hoye, P. G. Pringle, M.B. Smith, K. Worboys, *J. Chem. Soc. Dalton Trans.*, (1993), 269

51 D.E. Berning, K.V. Katti, C.L. Barnes, W.A. Volkert, *Chem. Ber./Recueil*, (1997), **130**, 907-911.

52 G. Nieckarz, T.J.R. Weakley, W.K. Millar, B.E. Millar, D.K. Lyon, D.R. Tyler, *Inorg. Chem.*, (1996), **35**, 1721-1724.

53 D.E. Berning, K.V. Katti, P.R. Singh, C. Higgenbotham, V.S. Reddy, W.A. Volkert, *Nuc. Med. Biol.*, (1996), **23**, 617-622.

54 K.N. Harrison, P.A.T. Hoye, A.G. Orpen, P.G. Pringle, M.B. Smith, *J. Am. Chem. Soc. Comm.*, (1989), 1096.

55 P.A.T. Hoye, P.G. Pringle, M.B. Smith, K. Worboys, *J. Chem. Soc. Dalton Trans.* (1993), 269.

56 M.N.I. Khan, C. King, J.P. Fackler, R.E.P. Winpenny, *Inorg. Chem.*, (1993), **32**, 2502.

57 S. Komiya, H. Awata, S. Ishimatsu, A. Fukuoka, *Inorg. Chim. Acta*, (1994), **217**, 201.

58 H. Schmidbaur, E. Zeller, J. Ohshita, *Inorg. Chem.*, (1993), **32**, 4524.

59 V. Sreenivasa Reddy, D.E. Douglas, K.V. Katti, C.L. Barnes, W.A. Volkert, A.R. Ketring, *Inorg. Chem.*, (1996), **35**, 1753-1757.

60 R. Uson, A. Laguna, M. Laguna, *Inorg. Synth.*, (1989), 26, 85.

61 D.L. Davies, J. Neild, L.J.S. Prouse, D.R. Russell, *Polyhedron*, (1994), **12**, 2121-2124.

62 R. Uson, A. Laguna, M. Laguna, *Inorg. Synth.*, (1989), 26, 85.

63 J.X. McDermott, J.F. White, G.M. Whitesides, *J. Am. Chem. Soc.*, (1976), **98**, 6521.

64 G.M. Sheldick, SHELXS86, University of Gottingen, (1986); SHELXL93, University of Gottingen, (1993).

Chapter Five

Uranyl nitrate complexes of camphene-derived phosphorylic compounds

5.1 Introduction

Compounds containing the phosphorylic unit (P=O) are known to possess excellent characteristics as donor ligands towards a wide range of metal centres, and the coordination chemistry of these ligands to metal centres is extensive[1, 2]. These types of ligands are often employed in industrial solvent extraction (hydrometallurgical) processes for the recovery and purification of a range of metal ions[3]. These metal extractants are typically highly lipophilic in nature, and this property is readily conferred by the use of large, branched hydrocarbon moieties, such as the inexpensive 2-ethylhexyl or 2,4,4-trimethylpentyl groups[4]. Branched hydrocarbon substituents are also known to impact selectivity in metal-ion separation processes by increasing steric crowding at the metal centre[5]. Other examples are presented within the report by Aparna, Krishnamurthy and Nethaji entitled "The coordination chemistry of lanthanides and actinides with ligands containing the phosphorylic unit and its relevance to practical liquid-liquid extraction"[6].

The bulky, lipophilic camphanyl group may show selectivity in metal-ion separation processes and therefore be utilised as an extractant. The synthesis of camphene-derived compounds which contain the phosphorylic group was therefore undertaken.

5.2 Synthesis and characterisation of 8-camphanyl-diphenylphosphine oxide (29)

5.2.1 Introduction

Grignard chemistry of the phosphorylic group, like that of the carbonyl group, is extensive and needs little introduction. One of the many synthetic applications of the Grignard reagent is the synthesis of phosphine oxides. The treatment of a phosphonic dichloride [$RP(O)Cl_2$] with a Grignard reagent [R'-MgCl], Scheme 5.1, yields a number of products [1-4] depending on the steric bulk of both the Grignard and phosphonic dichloride.

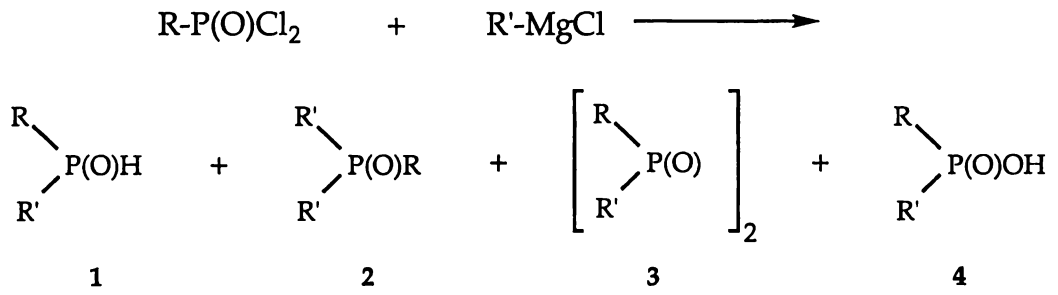

Scheme 5.1: The synthesis of phosphine oxides by the treatment of a phosphonic dichloride [$RP(O)Cl_2$] with a Grignard reagent [R'-MgCl].

Studies of the reaction of aliphatic phosphonic dichlorides with the bulky Grignard reagent t-BuMgCl indicate that the mono-substituted derivative **1** is preferentially formed along with low yields of both **2** and **4**. Studies of the reaction of aryl phosphonic dichlorides with t-BuMgCl indicate that the mono-substituted derivatives **1, 3** and **4** are preferentially formed, with the secondary phosphine oxide 1 once again being the primary product[7]. When less bulky Grignard reagents and phosphonic dichlorides are used the amount of the tertiary phosphine **2** increases but yields are still considered low.

The reactivity, particularly that relating to Grignard chemistry of the camphene-derived phosphonic dichloride $C_{10}H_{17}P(O)Cl_2$ (**11**) [section 2.3.2 gives details on synthesis and characterisation], was investigated.

5.2.2 Results and discussion

The general synthetic route to phosphine oxides involves the addition, under nitrogen, of a phosphonic dichloride to an ether solution containing a Grignard reagent. Thus, the addition of 8-camphanylphosphonic dichloride (**11**) to an ether solution of the Grignard reagent PhMgBr precipitates a brown oil which, when separated and purified, afforded a white crystalline solid. This mixture of products, as evidenced by ^{31}P NMR, was then further purified by recrystallisation from hot methanol to give the tertiary phosphine oxide 8-camphanyldiphenylphosphine oxide (**29**) [^{31}P-{H} NMR δ 31.4] as a colourless crystalline solid, Scheme 5.2. Detailed characterisation of **29** by NMR spectroscopy and ESMS is presented in section 5.2.3. Elemental data collected for **29** are consistent with the formulated structure.

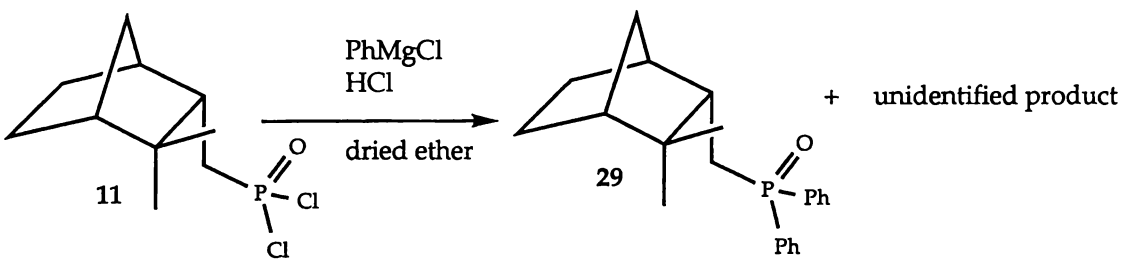

Scheme 5.2: The synthesis of 8-camphanyldiphenylphosphine oxide (**29**).

Attempts to separate the other minor product by fractional recrystallisation from chloroform/petroleum spirit were unsuccessful. The ^{31}P-{H} NMR spectrum of the minor product [δ 51.6, s] indicates that it is not the monosubstituted product suggested in Scheme 5.1. In fact the value obtained in the ^{31}P NMR suggests that this minor product is the disubstituted product 8-camphanylphenylphosphinic acid (**3**) [^{31}P-{H} 47.1

(section 2.1.2 gives details on synthesis and characterisation of **3**)] which is predicted in Scheme 5.1. However no further studies were undertaken to verify this conclusion.

5.2.3 Characterisation of 8-camphanyldiphenylphosphine oxide **29**

The ^{31}P NMR chemical shift of 8-camphanyldiphenylphosphine oxide (**29**) [δ 31.4] is is similar to Me_3PO which has a ^{31}P NMR chemical shift of δ 36.2. The ^{1}H and ^{13}C NMR spectra of the camphanyl moiety of **29** are assigned by examination of ^{1}H, ^{13}C and ^{1}H-^{1}H, ^{13}C-^{1}H correlated NMR spectra. Full assignment of ^{1}H and ^{13}C NMR data for **29** is included in the experimental section. Due to the complexity of the aryl region of **29** the signals [δ 131.5-128.4 and δ 7.77-7.38] belonging to the phenyl rings are not assigned. No discrepancies are found to exist between the ^{1}H-^{1}H and ^{13}C-^{1}H correlated NMR spectra.

ESMS studies of phosphine oxides are aided by the use of aqueous solutions of NaCl or KCl[8]. The ESMS [cone 80 V, positive ion] of the phosphine oxide **29** with added KCl, Figure 5.1, gave the $[M+H]^+$ parent ion as well as $[M+K]^+$ aggregates, which are consistent with the formulated structure.

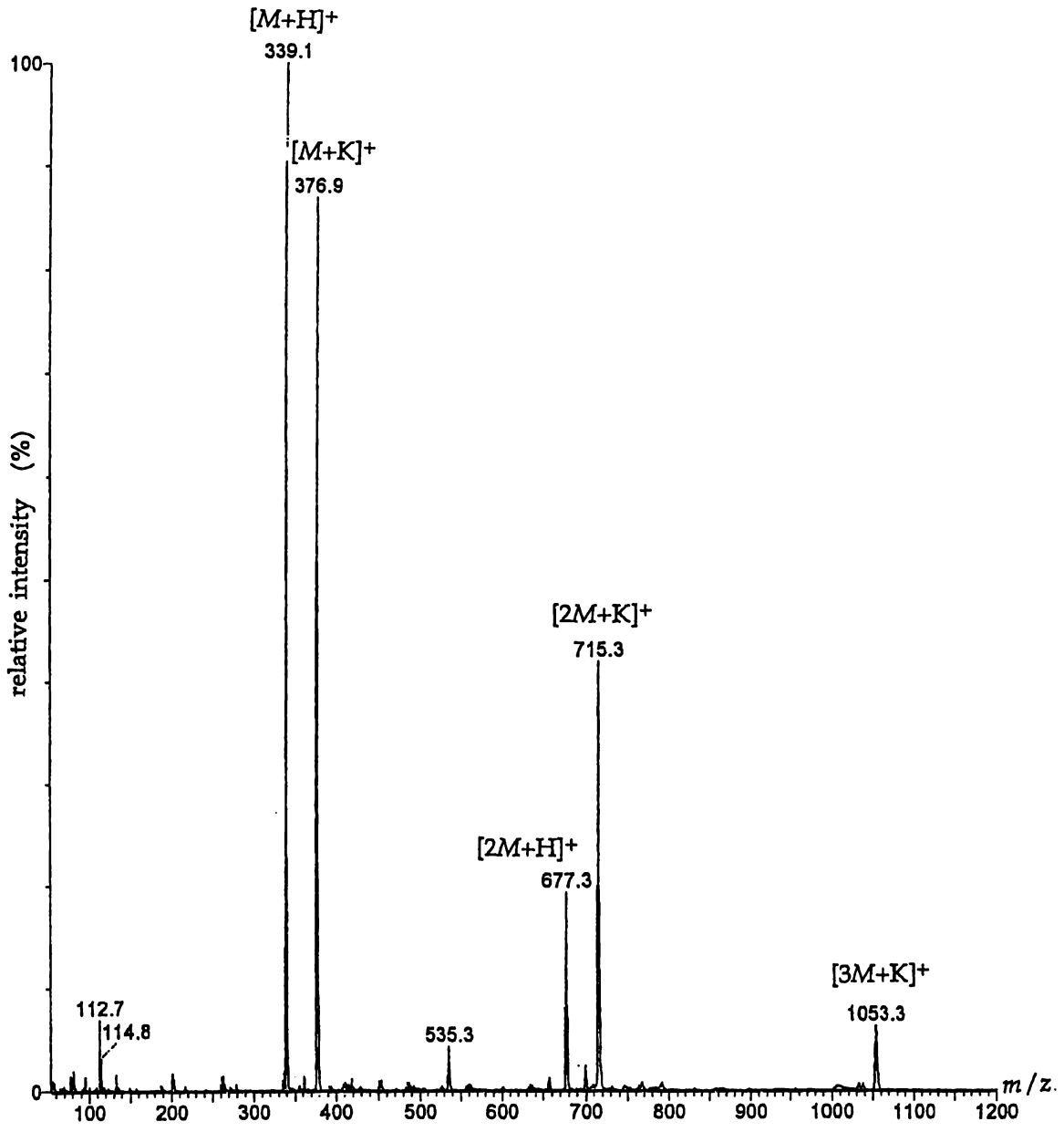

Figure 5.1: Positive-ion electrospray mass spectrum of **29** in 1:1 MeCN/H_2O [containing KCl] at 80 V.

*5.3 Syntheses and characterisation of camphanyl-derived uranyl(VI) nitrate complexes **30, 31** and **32***

5.3.1 Introduction

The coordination chemistry of ligands that contain the phosphorylic unit (P=O) to metal centres is, as previously mentioned, extensive[1, 2] and includes coordination to the uranyl group (UO_2^{2+})[9]. Their application as extractants is well illustrated by the use of tributylphosphate [$(BuO)_3P=O$] in the recovery of uranium and other fission products from spent nuclear fuel.

A wide range of uranyl(VI) nitrate complexes of the type $UO_2(NO_3)_2(L)_2$ [for example, L=phenacyldimethylphosphine oxide[10], methyldiphenylphosphate[11], triphenylphosphine oxide[12], and triethylphosphine oxide[13]] have been prepared by direct reaction of uranyl(VI) nitrate and the monodentate ligand in solvents such as ethanol (Scheme 5.3).

$$2\,R_3\text{-}P{=}O \;+\; UO_2(NO_3)_2.6H_2O \longrightarrow UO_2(NO_3)_2[R_3\text{-}P{=}O]_2$$

R = aryl/alkyl group.

Scheme 5.3: Synthesis of uranyl(VI) nitrate complexes of the type $UO_2(NO_3)_2(L)_2$.

The camphene-derived phosphorylic compounds [**7**, **15** and **29**], Figure 5.2, contain the bulky lipophilic camphanyl group and thus present excellent material from which to derive new solvent extraction reagents. Preliminary studies of the coordination chemistry of these ligands to the uranyl group were therefore carried out.

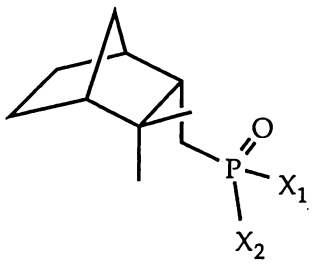

7: $X_1 = H, X_2 = OMe$
15: $X_1 = X_2 = OMe$
29: $X_1 = X_2 = Ph$

Figure 5.2: The molecular structure of the camphene-derived phosphorylic compounds **7, 15** and **29.**

5.3.2 Results and discussion

The spontaneous evaporation [over three days] of methanolic solutions containing uranyl(VI) nitrate and the monodentate ligands dimethyl 8-camphanylphosphonate (**15**), methyl phenyl 8-camphanylphosphinate (**7**) and 8-camphanyldiphenylphosphine oxide (**29**) yielded the uranyl(VI) nitrate complexes **30, 31** and **32** respectively as yellow crystalline solids, Scheme 5.4. Satisfactory microanalytical data were recorded for all these complexes.

$$UO_2(NO_3)_2.6H_2O \xrightarrow[MeOH]{\text{2 mol equi. L}} UO_2(NO_3)_2(L)_2$$

29: L= $C_{10}H_{17}PO(OMe)_2$
30: L= $C_{10}H_{17}PO(Ph)(OMe)$
31: L= $C_{10}H_{17}POPh_2$

Scheme 5.4: The synthesis of camphanyl-derived uranyl(VI) nitrate complexes **30, 31** and **32.**

Owing to the interest generated in the bonding of ligand **15** to the uranyl centre, a detailed characterisation of the uranyl(VI) nitrate complex **30** by X-ray crystallography and vibrational spectroscopy was carried out. The results of these studies are presented in sections 5.3.3 and 5.3.4 respectively.

5.3.3 X-ray crystal structure of uranyl(VI) nitrate complex **30**

The structural determination of $UO_2(NO_3)_2[C_{10}H_{17}PO(OMe)_2]_2$ (**30**), which was solved and refined by Professor Brian Nicholson at Waikato University, was not straightforward, and raises some interesting caveats concerning the need for evidence other than X-ray crystallography to provide absolute characterisation of compounds.

The first attempt at a crystal structure used a crystal of dimension 0.48 x 0.14 x 0.08 mm, which was mounted on a Nicolet R3 four-circle diffractometer at -143°C. The unit cell was then determined using the standard software and orientation procedures, which identified a monoclinic unit cell of dimensions a = 19.634(6), b = 8.082(1), c = 10.616(4) Å, β = 98.95(2)° from 20 reflections 10° < 2θ < 22°. Data (1643 of which 1588 were unique) were collected and corrected for absorption [$T_{max,\ min}$ 0.967, 0.761]. An examination showed no systematic absences other than those associated with the C-centering, indicating space groups C2, Cm or C2/m. Since a reasonable density required Z = 2, the first of these was assumed. The coordinates of the uranium atom were constrained to be at 0 0 0, and difference maps based on this allowed the development of a full structure. This model was refined [based on F^2, 94 parameters against all 1588 data] with only the U and P atoms treated anisotropically since the lighter atoms gave "non-positive definite" ellipsoids if they were assigned anisotropic parameters [not unexpectedly for light atoms in a uranium complex, especially since the camphanyl group is usually poorly defined because of partial disorder]. Convergence gave respectable agreement factors: R_1 0.0649, wR_2 0.1444, GoF 1.052. A Flack x parameter refined to 0.00(3) suggesting that the correct polarity had been selected, and a final difference map showed maximum features of +1.4/-1.3 e $Å^{-3}$. The structure of the final refined species is shown in Figure 5.3, with some bond parameters included in the caption. By all the usual criteria this was a satisfactorily determined structure -- reasonable R-factors, clean final difference map, acceptable temperature factors, sensible bond lengths and angles. However, the resulting structure incorporated a *cis*- UO_2 group which is unprecedented

among the many *trans* species previously reported. Furthermore the infrared and Raman spectra of **30** [consult 5.2.4 for more detail] each showed one, non-coincident U=O stretch which was strongly indicative of the usual *trans* arrangement. The problem was therefore investigated further.

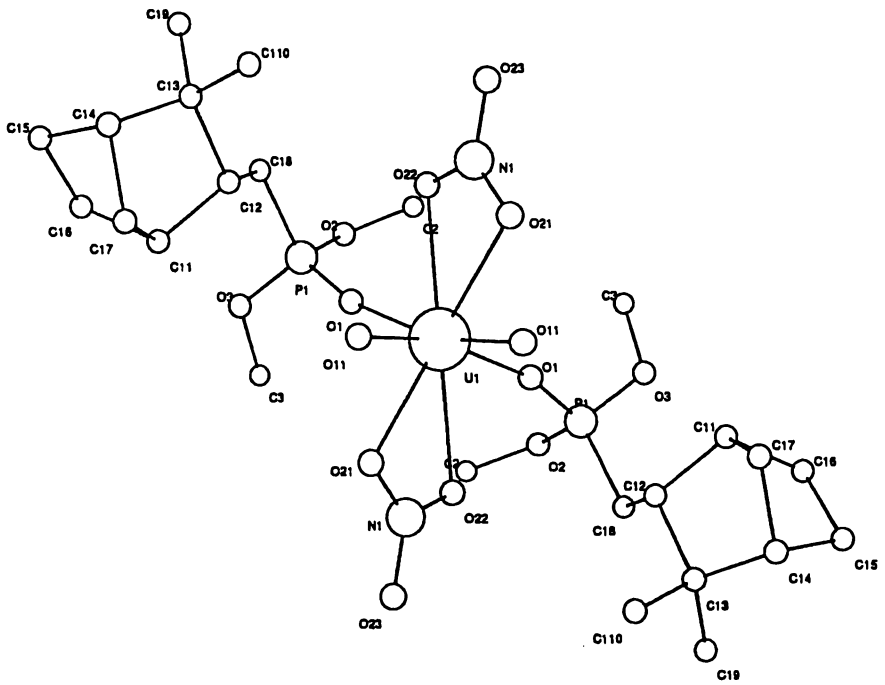

Figure 5.3: Molecular structure of the "*cis*-isomer" of **30**, together with the atom numbering scheme. Selected bond lengths (Å): U(1)-O(11) 1.795(18), U(1)-O(1) 2.289(18), U(1)-O(21) 2.582(14), U(1)-O(22) 2.544(17), P(1)-O(1) 1.526(19), P(1)-O(2) 1.619(41), P(1)-O(3) 1.560(14), P(1)-C(18) 1.741(20).

A new crystal from the original batch was subjected to a detailed photographic study. This showed that the diffractometer-located unit cell had halved one of the unit cell parameters by missing a weak class of reflection, and that the true cell was either Cc or C2/c with four molecules in the cell. A new data set, based on this correct cell was collected using a new crystal of dimensions 0.56 x 0.24 x 0.12 mm at -122 °C.

Crystal data: $C_{24}H_{46}N_2O_{14}P_2U$, M 886.60, monoclinic, space group C2/c or Cc (see below) a = 26.739(2), b = 8.137 (2), c = 19.782(2) Å, β = 127.90(2)°, U = 3396.4(9) $Å^3$. D_c 1.734 g cm^{-3} for Z = 4, F(000) 1752, μ(Mo-Kα) 4.94 cm^{-1}. Data:

2760 collected, 2218 unique after correction for absorption ($T_{max,\ min}$ 0.388, 0.292).

For the C2/c refinement the U coordinates were assigned to the inversion site at 0.25 0.25 0.00. Electron density maps phased on this allowed the slow development of the full structure although difficulty was encountered with accurately defining the camphanyl groups because of disorder. In the final refinement all non-hydrogen atoms were treated anisotropically, with H atoms included in calculated positions. Convergence gave R_1 0.0723 (for 1103 data with $F > 4\sigma(F)$), R_1 = 0.1486, wR_2 0.1621 GoF 0.908 for all 2218 data, with no residual features greater than +0.16/-1.21 e $Å^{-3}$. The low proportion of "observed" reflections, and the high R_1 figure for all data, can be attributed to the occupation of a special position by the U atom, leading to the k + l = odd class of reflection being nearly systematically absent.

Qualitative optical activity measurements of single crystals of **30** by Dr Olga Gladkikh [Victoria University, Wellington] using a polarised-light microscope suggests that these single crystals were optically active. Since the ligand used, *i.e* **15**, is racemic [refer to section 2.1 for details on synthesis of precursor **1**], the molecular structure of **30**, which contains two dimethyl 8-camphanylphosphonate ligands (**15**) for each uranyl nitrate molecule, must consist of either two R- or two S- isomers of the ligand [*c.f.* an R- and S-isomer of the ligand which does not give any optical activity]$^{\Psi}$. This strongly suggests that the true space group is in fact the non-centrosymmetric Cc. However a sensible refinement could not be carried out in this lower-symmetry space group because of the pseudo-centrosymmetry and the dominance of the U atom. The problems of refining near-centrosymmetric structures in lower symmetry space groups are well-known[14] and are exacerbated in this case by the presence of one dominant scatterer. Other examples involving uranium leading to incorrect structures[15] or giving difficulties in assigning space groups[16] are

available.

Although evidence from optical measurements [see above] and from the structure analysis [large U_{ij}'s for some of the atoms] suggest that Cc is the true space group, the structure of **30** is reported in C2/c. Individual bond parameters are therefore probably not very reliable so that little more than confirmation that it is indeed the *trans* UO_2^{2+} isomer can be deduced from the analysis. Figure 5.4 shows the geometry of the *trans*-isomer of **30**, with some bond parameters included in the caption.

Ψ It was also noted in these polarimetry experiments that individual crystals rotated plane-polarised light to different degrees. This suggests that there is a non-equal occupation of R-R and S-S camphanyl groups within each crystal.

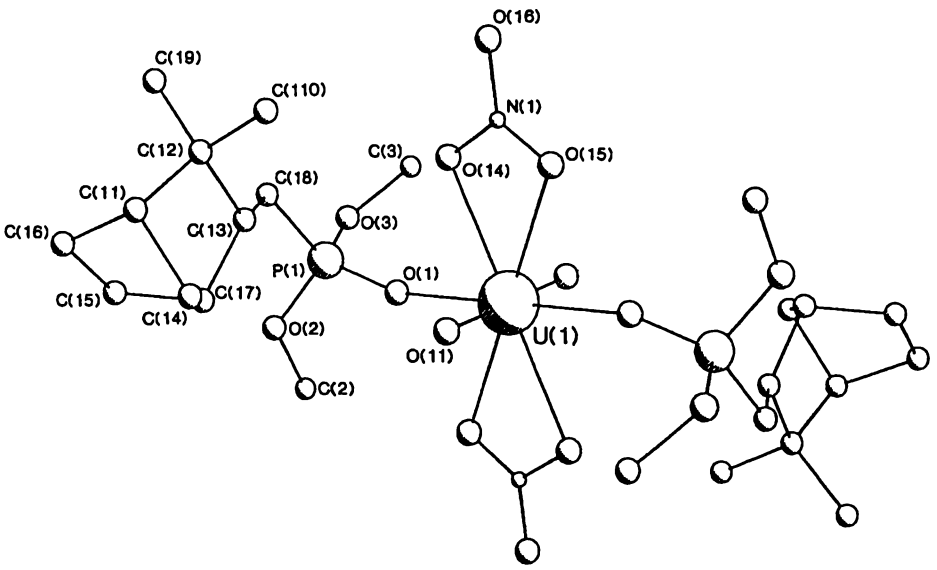

Figure 5.4: Molecular structure of the *trans*-isomer of **30**, together with the atom numbering scheme. Selected bond lengths (Å): U(1)-O(11) 1.668(14), U(1)-O(1) 2.345(14), U(1)-O(15) 2.51(2), U(1)-O(14) 2.52(2), P(1)-O(1) 1.52(2), P(1)-O(2) 1.557(13), P(1)-O(3) 1.57(2), P(1)-C(18) 1.74(2).

This structure provides an interesting insight into the reliability of X-ray crystallography. A data set collected in the wrong space group and unit cell allowed the successful refinement of a completely incorrect structural model, ending up with perfectly reasonable values for the criteria used to assess correctness of crystal structures. Indeed, the incorrect structure determination appears to be better, based on R-factors, than the correct one because of the pseudo-symmetry, space group ambiguity problems with the latter.

This is a different problem to that associated with false minima in refinement[17] which leads to an incorrect structure in the correct unit cell and space group. Rather it is associated with the presence of one extremely large scattering atom (U) which dominates any refinement, and is made worse by the probably disordered occupancy of the ligand sites by R and S camphanyl groups. These results reaffirm the need to not accept crystallographic determinations blindly, and to seek confirmatory evidence whenever possible. The uranyl nitrate complex $UO_2(NO_3)_2[C_{10}H_{17}PO(OMe)_2]_2$ (**30**) is one example where the simpler and cheaper technique of

vibrational spectroscopy proved to be more reliable than X-ray crystallography.

5.3.4 Vibrational spectroscopic analysis of the uranyl nitrate complex ***30***

The chemistry of U(VI) is largely confined to that of the linear uranyl group, UO_2^{2+}, the stability of the dioxo cation being unparalleled both in the solid state and in solution[18]. A *trans* geometry is always adopted, in contrast to the group VI *d*-block metals where the *cis*-dioxo group is the norm. The uranyl ion, of assumed $D_{\infty h}$ symmetry [*i.e.* a linear or *trans* model for UO_2^+], has four normal modes of vibration[19]. The two most useful modes of vibration are the non-degenerate symmetric stretching frequency, υ_1, and the non-degenerate asymmetric stretching frequency, υ_3. The non-degenerate symmetric stretching frequency, υ_1, is i.r-forbidden but has been reported as a weak absorption in the region 790-900 cm^{-1} in the i.r.. This vibration is Raman-allowed and occurs as a strong band at 810-880 cm^{-1}. The non-degenerate asymmetric stretching frequency, υ_3, is i.r-allowed and occurs in the range 911-960 cm^{-1}. This vibration is Raman-forbidden for the linear model and does not appear. The other modes of vibration include the doubly degenerate bending frequency, which absorbs in the region 260-212 cm^{-1} and hence is not detected easily[20].

The vibrational spectroscopy of the Group VI d-block metals clearly indicates that the *cis*- arrangement of the MO_2 is the norm. The complexes of the type MO_2L_2[21, 22] and related $MO_2L_4^{2-}$ species[23] have three vibrational modes associated with the MO_2 group. That is for the *cis*-(C_{2v})-form, this will have symmetry species [$2A_1$+ B_2] which are active in both the i.r. and Raman.

As only one stretching frequency [*c.f.* two expected for the *cis*-isomer] is obtained in the i.r. spectrum of **30**, Table 5.1, this complex is assumed to

have adopted the *trans*-isomer. As this broad i.r. signal may have contained a second underlying signal, the Raman spectrum of **30**, which is less ambiguous, was also recorded. The result, which is tabulated below, clearly shows that only one signal is present. This confirms the presence of the *trans*-isomer [*c.f.* two signals in the Raman spectrum expected for the *cis*-isomer].

	I.R	Raman
	υ_3 (cm^{-1})	υ_1 (cm^{-1})
phosphonate ligand **15**	-	924
Uranyl complex **30**	932	854

Table 5.1: Vibrational spectroscopic data for ligand **15** and the uranyl(VI) nitrate complex **30**.

The non-degenerate symmetric [υ_1] and asymmetric [υ_3] stretching frequencies of **30** are similar to the values of other *trans*-complexes. For example, the non-degenerate symmetric [υ_1] and asymmetric [υ_3] stretching frequencies of $[(EtO)_3PO]_2UO_2(NO_3)_2$ are 860 cm^{-1} [*c.f* 854 cm^{-1} for **30**] and 935 cm^{-1} [*c.f* 932 cm^{-1} for **30**] respectively [20].

5.4 Experimental

General experimental procedures and instrumental techniques are as described in Appendix II. Uranyl nitrate (BDH) was used as supplied. All solvents except for diethyl ether, which was dried over sodium and distilled under nitrogen, were of reagent grade. PhMgBr was synthesised by a standard literature method[24]. The ligands $C_{10}H_{17}P(O)(OMe)_2$ (**15**), $C_{10}H_{17}P(O)(Ph)(OMe)$ (**7**) and $C_{10}H_{17}P(O)Cl_2$ (**11**) were synthesised as described in sections 3.2.1, 2.2.2 and 2.3.2.

5.4.1 *Synthesis of 8-camphanyldiphenylphosphine oxide (29)*

To a solution of PhMgBr (0.022 mol) in dry ether (60 mL) was added 8-camphanylphosphonic dichloride (**11**) (2.94 g, 0.01 mole), and a brown oil immediately separated. After 24 h the supernatant was removed and the residue dissolved in chloroform (200 mL). The organic layer was washed with 10% hydrochloric acid (100 mL), dried over anhydrous magnesium sulfate and evaporated to dryness to give a cream solid. This was recrystallised from hot methanol to give **29** (2.92 g, 75%) as a colourless crystalline solid, m.p. 171.5-173.0°C. (Analysis: Found: C, 77.78; H, 7.97% $C_{12}H_{23}O_3P$ requires C, 78.06; H, 8.05%.) ESMS (cone 80 V, KCl, positive ion); $[M+H]^+$ at *m/z* 339, $[M+K]^+$ at *m/z* 376, $[2M+H]^+$ at *m/z* 677, $[2M+K]^+$ at *m/z* 715, $[3M+K]^+$ at *m/z* 1053.

NMR: ^{31}P-{H}: δ 31.4 [s].

^1H : δ 7.77-7.38 [10H, m, aryl]$_b$, 2.22 [2H, br, m, $H_{8'/8''}]_b$, 2.02 [1H, br, s , H_4], 1.87 [1H, br, m, H_3], 1.69 [1H, br, s, H_1], 1.50 [1H, d, ^2J 9.8, $H_{7''}]_b$, 1.49 [1H, br, m, $H_{6''}]_b$, 1.21 [1H, m, $H_{5''}]_b$, 1.15 [1H, m, $H_{6'}]_b$, 1.08 [1H, m, $H_{5'}]_b$, 1.04 [1H, d, ^2J 9.7, $H_{7'}]_a$, 0.85 [3H, s, Me'], 0.81 [3H, s, Me''].

^{13}C-{H}: δ 131.5-128.4 [m, Ar], 48.4 [s, C(1)], 44.0 [d, $^{2}J_{P\text{-}C\text{-}C}$ 4.0, C(3)], 42.3 [d, $^{3}J_{P\text{-}C\text{-}C\text{-}C}$ 3.1, C(4)], 37.8 [d, $^{3}J_{P\text{-}C\text{-}C\text{-}C}$ 10.7, C(2)], 37.0 [s, C(7)], 31.6 [s, C(10)], 27.3 [d, $^{1}J_{P\text{-}C}$ 62.6, C(8)], 24.7 [s, C(6)], 22.4 [s, C(9)], 20.3 [s, C(5)].

a: partially overlapping signals

b: overlapping signals

5.4.2 *Synthesis of* $UO_2(NO_3)_2(C_{10}H_{17}PO(OMe)_2)_2$ (**30**)

Dimethyl 8-camphanylphosphonate (**15**) (0.50 g, 2.03 mmol) and uranyl nitrate hexahydrate (0.512 g, 1.02 mmol) were dissolved in methanol (20 mL) and the resulting solution allowed to spontaneously evaporate at room temperature. Yellow microcrystalline **30** (0.79 g, 90%) precipitated out of solution and filtered off after 3 days, m.p. 107-111°C. (Found: C, 32.50 H, 5.25; N, 3.31% $C_{24}H_{42}N_2O_{14}P_2U$ requires C, 32.64; H, 4.81; N, 3.17 %.)

NMR: ^{31}P-{H}: δ 42.0 [s].

^{1}H : δ 4.14, 4.13, 4.10, 4.09 [12H, OMe]*, 2.35 [1H, s, br, $H_4]_b$, 2.04 [1H, m, H_3], 2.30 [2H, m, $H_{8'}/H_{8''}]_b$, 1.75 [1H, m, H_1], 1.55 [1H, d, ^{2}J 9.5, $H_{7''}]_a$, 1.55 [1H, m, $H_{6''}]_b$, 1.43-1.20 [3H, m, $H_{5''}$, $H_{5'}$, $H_{6'}]_b$, 1.14 [1H, d, ^{2}J 9.5, $H_{7'}$], 0.94 [3H, s, Me'], 0.85 [3H, s, Me''].

a: partially overlapping signals

b: overlapping signals

*: signals not assigned

^{13}C: δ 54.55, 54.45, 54.40, 54.30 [m, (OMe)]*, 44.3 [d, $^{2}J_{P\text{-}C\text{-}C}$ 4.4, C(3)], 42.3 [d, $^{3}J_{P\text{-}C\text{-}C\text{-}C}$ 3.5, C(4], 37.5 [d, $^{3}J_{P\text{-}C\text{-}C\text{-}C}$ 15.6, C(2)], 36.9 [s, C(7)], 31.8 [s, C(10)], 22.0 [d, $^{1}J_{P\text{-}C}$ 141.2, C(8)], 24.6 [s, C(6)], 21.9 [s, C(9)], 20.0 [s, C(5)].

5.4.3 Synthesis of $UO_2(NO_3)_2\{C_{10}H_{17}P(O)(OMe)(Ph)\}_2$ (31)

Methyl 8-camphanyl(phenyl)phosphinate (7) (0.11 g, 0.37 mmol) and uranyl nitrate hexahydrate (0.10 g, 0.19 mmol) were dissolved in methanol (30 mL) and the resulting solution allowed to spontaneously evaporate at room temperature. Yellow microcrystalline **31** (0.22 g, 60%) precipitated out of solution and filtered off after 3 days, m.p. 152-155°C. (Found: C, 41.55; H, 5.10; N, 2.80% $C_{34}H_{50}N_2O_{12}P_2U$ requires C, 41.70; H, 5.15; N, 2.86 %.)

5.4.4 Synthesis of $UO_2(NO_3)_2\{C_{10}H_{17}P(O)Ph_2\}_2$ (32)

8-Camphanyl(diphenyl)phosphine oxide (**28**) (0.10 g, 0.29 mmol) and uranyl nitrate hexahydrate (0.075 g, 0.15 mmol) were dissolved in hot methanol (50 mL) and the resulting solution allowed to spontaneously evaporate at room temperature. Yellow microcrystalline **32** (0.18 g, 60%) precipitated out of solution and was filtered off after 3 days, m.p. 226-245°C. (Found: C, 49.03; H, 5.06; N, 2.52% $C_{44}H_{54}N_2O_{10}P_2U$ requires C, 49.33; H, 5.08; N, 2.62 %.)

References

1 P. L. Goggin in *Comprehensive Coordination Chemistry*, Editor-in-Chief Sir G. Wilkinson, Pergamon Press, Oxford, (1987), **4**, Section 15.8; N. Burford, *Coord. Chem. Rev.*, (1992), **112**, 1.

2 *Comprehensive Inorganic Chemistry*, Executive Editor A. Trotman-Dickenson, Pergamon Press, (1973), **5**, 1-636.

3 D.F. Peppard, *Adv. Inorg. Chem. and Radiochem.*, (1996), 9,1; M. Laing, *Educ. in Chem.*, November (1996), 157; D. S. Flett, *Chem. Ind.*, (1977), 706; H. Eccles, A. Naylor, *Chem. Ind.*, (1987), 174.

4 M.J. Nicol, C.A. Fleming, J.S. Preston in *Comprehensive Coordination Chemistry*, Editor-in-Chief Sir G. Wilkinson, Pergamon Press, Oxford, (1987), **4**, 779.

5 G. W. Mason, A. F. Bollmeier, D. F. Peppard, *J. Inorg. Nucl. Chem.*, (1970), **32**, 1011; D.F. Peppard, G. W. Mason, A. F. Bollmeister, S. Lewey, *ibid*, (1971), **33**, 845.

6 K. Aparna, S. Krishnamurthy, M. Nethaji, *J. Chem. Soc., Trans*, (1995), 2991 and references therein.

7 L. Maier in *Organic Phosphorus Compounds*, Ed G. Kosolapoff, L. Maier, Wiley and Sons (1972), **4**, 468.

8 W. Henderson, G.M. Olsen, *Polyhedron*, (1996), **15**, 2105.

9 U. Casellato, P. Vigato, *Coord. Chem. Rev., (1981)*, **36**, 183-265.

10 C. Lestas, M. Truter, *J. Am. Chem. Soc.*, (1971), 738.

11 A. Apelblat, R. Levin, *J. Chem. Soc., Chem. Comm.*, (1970), 514.

12 C. Pannattoni, R. Graziani, U. Croatto, B. Zarli, G. Bombieri, *Inorg. Chim. Acta*, (1968), **2**, 43.

13 K. Bagnall, M. Wakkerley, *J. Chem. Soc., Dalton Trans*, (1974), 889.

14 R.E. Marsh, *Acta Cryst.*, B42, (1986), 193.

15 P.L. Ritger, J.H. Burns, G. Bombieri, *Inorg. Chim. Acta*, (1983), 77, L217.

16 N.W. Alcock, D.J. Flanders, *Acta Cryst.*, (1987), **C43**, 1480.

17 V.J. Murphy, D. Rabinovich, G. Parkin, *J. Amer. Chem. Soc.*, (1995), **117**, 9762.

18 D. Brown, R. Denning, R. Jones, *J. Chem. Soc., Chem. Comm.*, (1994), 2601.

19 G. Herzberg, *Infrared and Raman spectra of polyatomic molecules*, Van Nostrand, New York, (1945), 139.

20 J. I. Bullock, *Inorg. Phys. Chem.*, (1968), 781.

21 B. Soptrajanov, A. Nikolovski, I. Petrov, *Spectro. Acta*, 24a, 1617 and 1967 and references therein.

22 F.W. Moore, R.E. Rice, *Inorganic Chemistry*, (1968), 2150.

23 W.P. Griffith, T.D. Wickins, *J. Chem. Soc. A*, (1968), 400.

24 PhMgBr was synthesised by a standard method. That is, the addition of sodium dried ether solution of bromobenzene to magnesium.

Appendix I

Nomenclature of phosphorus compounds

Phosphorus compounds are named based upon their parent structures, making assignment and identification of these compounds relatively straightforward. Table I.1 contains a summary of parent structures of various phosphorus compounds, together with the appropriate nomenclature.

Name	Formula
Phosphinic acid	$RP(H)(O)(OH)$
Phosphinate	$RP(H)(O)(OMe)$
Phosphonic dichloride	$RP(O)(Cl)_2$
Phosphonic acid	$RP(O)(OH)_2$
Phosphonate	$RP(O)(OMe)_2$
Phosphite	$(RO)_3P$
Phosphine	R_3P
Phosphine oxide	$R_3P(O)$
Hydroxymethylphosphine oxide	$R_{3-n}P(O)(CH_2OH)_n$
Phosphine sulfide	$R_3P(S)$
Phosphine selenide	$R_3P(Se)$
Phosphonium ion	R_4P^+
Phosphorane	R_5P

Table I.1: The parent structures and appropriate nomenclature for various phosphorus compounds. R denotes an organic moiety.

The rules describing phosphorus compounds can be further simplified. They are as follows:

(i) phin e.g. phosphinate: contains 2 P-C bonds or 1 P-C and 1 P-H bond

(ii) phon e.g. phosphonate: contains only 1 P-C bond

(iii) ite e.g. phosphite: contains P(III) atom

(iv) ate e.g. phosphonate: contains P(V) atom

References

1 F. R. Hartley (Editor), *The chemistry of Organophosphorus Compounds*, John Wiley and Sons (1990), **1**, 1

Appendix II

Instrumental Techniques

AII.1 NMR spectroscopy

Unless otherwise stated all ^{31}P NMR spectra were recorded on a JEOL FX90Q spectrometer (36.23 MHz) in $CHCl_3$. Chemical shifts were externally referenced to 85% H_3PO_4 (δ 0.0) and a glass capillary containing D_2O used to provide a lock signal.

^1H (300.13 MHz) and ^{13}C (75.47 MHz) NMR spectra were recorded on a Bruker AC300P spectrometer in $CDCl_3$ (unless otherwise specified), with chemical shifts reported in p.p.m relative to $CDCl_3$ (δ ^1H 7.26 and ^{13}C 77.06), and coupling constants in Hz.

NOE difference spectra were measured on a solution that had not been degassed and were acquired with an irradiation time of 3s, typically achieving 50 to 60% saturation of the irradiated multiplet. Each multiplet was recorded in cycles of 16 scans for long term averaging. NOE difference spectra were obtained by subtracting the reference FID from the irradiated FID, and Fourier transforming the resulting difference-FID.

The COSY45 NMR spectra were acquired with 1K increments in the F2 dimension, 256 increments zero filled to 512 increments in the F1 dimension and 32 scans per increment. After transformation the data matrix was symmetrised.

The ^{13}C-^1H correlation spectra were acquired with 1K increments in F2 and 128 increments zero filled to 1K increments in F1 with 32 or 128 scans per increment.

AII.2 Mass spectrometry

(i) *Gas chromatography mass spectrometry (GCMS)*: GCMS data were recorded on a Hewlett Packard 5890 GC instrument interfaced with a HP5970B mass selective detector using a 25m x 0.22mm HP-1 methyl silicone column. Typical GCMS studies used a temperature programme of 50°C to 250°C at 1 to 5°C per min. The mass spectrometer scanned from 40 to 400 mass units and was calibrated with perfluorotributylamine which gave molecular ions at 69.95, 69.85, 218.95, 219.95, 502.00 and 503.00 mass units.

(ii) *Electrospray mass spectrometry (ESMS)* : Electrospray mass spectra were obtained using a VG Platform II mass spectrometer using a 1:1 v/v acetonitrile-water mobile phase. The compounds were dissolved in the mobile phase to give a solution typically of approximate concentration 0.1 mM and a small quantity of pyridine added to effect deprotonation of the parent acids. The diluted solution was injected into the spectrometer via a Rheodyne injector fitted with a 10mL sample loop. A Thermo Separation Products SpectraSystem P1000 LC pump delivered the solution to the mass spectrometer source at a flow rate of 0.01 mL min^{-1}, and nitrogen was employed both as a drying and nebulising gas. Spectra were recorded at varying cone voltages.

AII.3 Infrared spectroscopy

Spectra were recorded as solids with a resolution of 1 cm^{-1} on a BIO-RAD FTS-40 spectrometer. Solids were analysed as KBr discs. Full length spectra (4000-200 cm^{-1}) were routinely run.

AII.4 Raman spectroscopy

Spectra were recorded on a SPEX 1403 0.84m double beam spectrometer equipped with a water cooled Hamamatsu photomultiplier tube (R943-02). The laser is either a Spectra Physics HeNe laser (model 207B)

or a Spectra Physics Argon ion laser (model 165). Full length spectra (4000-200 cm^{-1}) with a resolution of 3 cm^{-1} were routinely run.

AII.5 Single crystal X-ray crystallography

Using preliminary procession photography (Cu-K_α radiation), the quality of the crystals was assessed. If no faults were found, zero and upper level photographs with Ni-filtered X-rays were taken, from which unit cell dimensions and space group were obtained. Full X-ray intensity data was collected at the University of Canterbury on a Nicolet model P3 diffractometer using Mo-K_α radiation.

AII.6 Elemental microanalysis

Elemental analyses were obtained by the University of Otago Microanalytical Laboratory.

AII.7 Melting points

Melting points were determined on a Reichert Thermoovar apparatus and are uncorrected.

Appendix III

AIII.1 Complete bond lengths, bond angles, and thermal and positional parameters for **1**

atom	x	y	z
P	0.3460(1)	0.1324(2)	0.5189(1)
O(1)	0.2273(3)	0.1709(5)	0.5215(3)
O(2)	0.3962(4)	-0.0555(6)	0.5639(4)
C(1)	0.6281(5)	0.3876(8)	0.8953(5)
C(2)	0.5395(6)	0.4744(9)	0.7879(6)
C(3)	0.4710(5)	0.3060(7)	0.7212(5)
C(4)	0.5385(7)	0.148(1)	0.7966(6)
C(5)	0.6630(6)	0.1303(8)	0.7947(6)
C(6)	0.7276(6)	0.286(1)	0.8715(6)
C(7)	0.5566(6)	0.217(1)	0.9118(5)
C(8)	0.4546(5)	0.2934(7)	0.5960(4)
C(9)	0.6016(5)	0.5848(8)	0.7235(5)
C(10)	0.4590(7)	0.601(1)	0.8174(6)
H(10)	0.363(8)	-0.13(1)	0.532(7)

Table AIII.1: Fractional atomic coordinates for **1**, with estimated standard deviations in parentheses.

	Angle		Angle
O(1)-P-O(2)	115.0(2)	C(9)-C(2)-C(10)	107.3(6)
O(1)-P-C(8)	113.2(2)	C(4)-C(3)-C(2)	101.7(5)
O(2)-P-C(8)	106.2(2)	C(4)-C(3)-C(8)	116.0(5)
C(6)-C(1)-C(2)	112.0(5)	C(2)-C(3)-C(8)	117.0(5)
C(6)-C(1)-C(7)	98.5(5)	C(3)-C(4)-C(5)	111.1(5)
C(2)-C(1)-C(7)	101.9(5)	C(3)-C(4)-C(7)	102.1(5)
C(3)-C(2)-C(1)	102.5(5)	C(5)-C(4)-C(7)	104.5(6)
C(3)-C(2)-C(9)	113.6(5)	C(4)-C(5)-C(6)	102.1(5)
C(3)-C(2)-C(10)	111.2(5)	C(5)-C(6)-C(1)	103.4(5)
C(1)-C(2)-C(9)	111.9(5)	C(4)-C(7)-C(1)	91.9(5)
O(1)-P-O(2)	115.0(2)	C(9)-C(2)-C(10)	107.3(6)
O(1)-P-C(8)	113.2(2)	C(4)-C(3)-C(2)	101.7(5)
O(2)-P-C(8)	106.2(2)	C(4)-C(3)-C(8)	116.0(5)
C(6)-C(1)-C(2)	112.0(5)	C(2)-C(3)-C(8)	117.0(5)
C(6)-C(1)-C(7)	98.5(5)	C(3)-C(4)-C(5)	111.1(5)
C(2)-C(1)-C(7)	101.9(5)	C(3)-C(4)-C(7)	102.1(5)
C(3)-C(2)-C(1)	102.5(5)	C(5)-C(4)-C(7)	104.5(6)
C(3)-C(2)-C(9)	113.6(5)	C(4)-C(5)-C(6)	102.1(5)
C(3)-C(2)-C(10)	111.2(5)	C(5)-C(6)-C(1)	103.4(5)
C(1)-C(2)-C(9)	111.9(5)	C(4)-C(7)-C(1)	91.9(5)
C(1)-C(2)-C(10)	110.4(5)	P-C(8)-C(3)	113.8(4)

Table AIII.2: Bond angles (°) for **1**, with estimated standard deviations in parentheses.

Atom	U11	U22	U33	U12	U13	U23
P	0.034(1)	0.027(1)	0.035(1)	0.0002(7)	0.0070(7)	0.0018(7)
O(1)	0.037(3)	0.027(2)	0.049(3)	-0.000(2)	0.009(2)	0.002(2)
O(2)	0.042(3)	0.026(3)	0.055(3)	-0.002(2)	0.006(2)	0.004(2)
C(1)	0.050(4)	0.044(4)	0.033(3)	0.004(3)	0.004(3)	0.002(3)
C(2)	0.055(4)	0.049(4)	0.058(4)	-0.016(4)	0.024(3)	-0.016(4)
C(3)	0.030(3)	0.038(4)	0.036(3)	-0.003(3)	0.010(3)	-0.007(3)
C(4)	0.083(6)	0.062(5)	0.038(4)	0.007(4)	0.016(4)	0.002(4)
C(5)	0.058(5)	0.043(4)	0.063(5)	0.016(3)	0.017(4)	-0.006(3)
C(6)	0.055(4)	0.067(5)	0.059(4)	-0.008(4)	0.008(4)	-0.003(4)
C(7)	0.071(5)	0.072(5)	0.054(5)	0.002(4)	0.021(4)	0.015(4)
C(8)	0.037(3)	0.027(3)	0.033(3)	0.001(3)	0.009(3)	0.001(3)
C(9)	0.048(4)	0.037(3)	0.041(3)	-0.016(3)	0.013(3)	-0.001(3)
C(10)	0.086(6)	0.056(5)	0.068(5)	-0.006(4)	0.045(4)	-0.012(4)
H(10)	0.07(3)					

Table AIII.3: Thermal Displacement Parameters for **1**, with estimated standard deviations in parentheses.

Atom	Distance	Atom	Distance
P-O(1)	3.511(4)	O(1)-C(8)	3.535(7)
P-O(2)	3.587(5)	O(2)-O(2)	3.564(9)
O(1)-O(2)	2.517(6)		

Table AIII.4: Intermolecular Distances (Å) for **1**, with estimated standard deviations in parentheses.

	Angle		Angle
P-C(8)-C(3)-C(4)	74.7(6)	C(5)-C(4)-C(3)-C(8)	59.6(7)
P-C(8)-C(3)-C(2)	-165.0(4)	C(5)-C(4)-C(7)-C(1)	56.3(6)
O(1)-P-C(8)-C(3)	59.1(4)	C(5)-C(6)-C(1)-C(2)	-65.4(7)
O(2)-P-C(8)-C(3)	-68.0(4)	C(5)-C(6)-C(1)-C(7)	41.1(6)
C(3)-C(4)-C(5)-C(6)	76.6(6)	C(6)-C(5)-C(4)-C(7)	-32.7(7)
C(3)-C(4)-C(7)-C(1)	-59.6(6)	C(6)-C(1)-C(2)-C(9)	-49.4(7)
C(3)-C(2)-C(1)-C(6)	72.6(6)	C(6)-C(1)-C(2)-C(10)	-168.9(5)
C(3)-C(2)-C(1)-C(7)	-31.7(6)	C(1)-C(6)-C(3)-C(8)	-132.1(5)
C(4)-C(3)-C(2)-C(1)	-4.6(6)	C(2)-C(3)-C(4)-C(7)	42.4(6)
C(4)-C(3)-C(2)-C(9)	116.3(6)	C(7)-C(4)-C(3)-C(8)	170.6(5)
C(4)-C(3)-C(2)-C(10)	-122.5(6)	C(7)-C(1)-C(2)-C(9)	-153.8(5)
C(4)-C(5)-C(6)-C(1)	-7.0(7)	C(7)-C(1)-C(2)-C(10)	86.8(6)
C(4)-C(7)-C(1)-C(6)	-58.5(5)	C(8)-C(3)-C(2)-C(9)	-11.3(7)
C(4)-C(7)-C(1)-C(2)	56.2(6)	C(8)-C(3)-C(2)-C(10)	109.9(6)
C(5)-C(4)-C(3)-C(2)	-68.5(6)		

Table AIII.5: Torsion or Conformation Angles (°) for **1**, with estimated standard deviations in parentheses.

AIII.2 Complete bond lengths, bond angles, and thermal and positional parameters for **13**

atom	x	y	z	U(eq)
Ca(1)	0.1180(3)	0.1005(3)	0.0647(2)	0.046(2)
Ca(2)	-0.3916(3)	0.0886(3)	0.0064(3)	0.047(2)
O(2)	-0.3005(11)	0.0690(8)	0.1157(7)	0.048(4)
O(3)	0.1667(11)	0.0456(8)	-0.0698(8)	0.050(4)
P(1)	-0.0059(5)	0.1756(5)	0.2488(3)	0.068(2)
O(11)	0.0521(13)	0.1497(10)	0.1845(9)	0.073(5)
O(12)	-0.1149(13)	0.1939(9)	0.2365(8)	0.062(4)
C(18)	0.0710(24)	0.2336(17)	0.3495(17)	0.092(9)
C(11)	-0.0294(37)	0.2050(27)	0.4461(26)	0.186(15)
C(12)	0.0086(22)	0.2714(16)	0.4219(15)	0.078(8)
C(13)	0.0827(37)	0.3562(28)	0.5104(26)	0.216(18)
C(14)	0.0476(29)	0.3240(22)	0.5679(22)	0.134(11)
C(15)	0.1105(36)	0.2549(27)	0.5633(27)	0.178(15)
C(16)	0.0693(36)	0.1743(27)	0.4799(26)	0.173(15)
C(17)	-0.0767(27)	0.2496(21)	0.5241(21)	0.124(11)
C(19)	0.2147(34)	0.3776(26)	0.5262(25)	0.162(15)
C(110)	0.0239(30)	0.4237(23)	0.5337(22)	0.131(12)
P(2)	0.2606(9)	0.3005(5)	0.0664(5)	0.115(4)
O(21)	0.1762(15)	0.2325(11)	0.0664(10)	0.086(5)
O(22)	0.2989(18)	0.2865(13)	-0.0118(13)	0.122(7)
C(28)	0.2566(26)	0.4058(19)	0.1166(19)	0.105(10)
C(21)	0.1312(50)	0.4874(38)	0.1978(38)	0.272(22)
C(22)	0.2081(38)	0.4285(28)	0.1978(29)	0.167(14)
C(23)	0.2842(47)	0.4859(36)	0.2820(34)	0.238(20)
C(24)	0.2198(33)	0.5499(25)	0.3288(23)	0.143(12)
C(25)	0.2493(53)	0.6177(36)	0.2998(37)	0.265(22)
C(26)	0.2066(46)	0.5721(35)	0.2042(34)	0.219(19)
C(27)	0.0919(38)	0.5076(31)	0.2793(31)	0.198(17)
C(29)	0.4064(50)	0.5313(37)	0.2965(37)	0.251(25)
C(210)	0.2542(51)	0.4370(39)	0.3279(39)	0.258(25)

Table AIII.6: Atomic coordinates and equivalent isotropic displacement parameters for **13**.

atom	x	y	z	U(eq)
P(3)	-0.5726(6)	0.1250(4)	-0.1339(4)	0.062(2)
O(31)	-0.6752(14)	0.1473(9)	-0.1062(9)	0.065(4)
O(32)	-0.5202(13)	0.0817(9)	-0.0992(9)	0.071(5)
C(38)	-0.5989(21)	0.0684(15)	-0.2454(14)	0.073(7)
C(31)	-0.5989(33)	0.2045(24)	-0.2630(25)	0.165(14)
C(32)	-0.6562(22)	0.1110(16)	-0.2879(15)	0.081(8)
C(33)	-0.6808(31)	0.0621(22)	-0.3870(20)	0.142(12)
C(34)	-0.6419(31)	0.1385(23)	-0.4013(22)	0.143(12)
C(35)	-0.5064(36)	0.1597(29)	-0.3772(27)	0.192(16)
C(36)	-0.4764(33)	0.2065(25)	-0.2777(25)	0.157(13)
C(37)	-0.6616(35)	0.2227(25)	-0.3245(25)	0.165(14)
C(39)	-0.6330(29	-0.0133(21)	-0.4309(21)	0.127(11)
C(310)	-0.8086(31)	0.0341(24)	-0.4194(23)	0.146(13)
P(4)	-0.2206(6)	0.3055(4)	0.1523(4)	0.080(2)
O(41)	-0.3296(14)	0.2347(10)	0.1050(10)	0.077(5)
O(42)	-0.1604(17)	0.3170(12)	0.2368(12)	0.115(7)
C(48)	-0.2256(23)	0.4137(17)	0.1792(16)	0.087(8)
C(41)	-0.2680(39)	0.3643(29)	0.0134(27)	0.192(16)
C(42)	-0.2942(29)	0.4097(23)	0.0989(22)	0.130(11)
C(43)	-0.3082(40)	0.5039(29)	0.1210(29)	0.226(19)
C(44)	-0.2974(31)	0.4991(23)	0.0399(24)	0.147(12)
C(45)	-0.1610(34)	0.5112(29)	0.0427(28)	0.181(16)
C(46)	-0.1419(43)	0.4269(33)	0.0362(34)	0.224(19)
C(47)	-0.3360(31)	0.3972(23)	-0.0357(22)	0.146(13)
C(49)	-0.2267(29)	0.5849(22)	0.1975(21)	0.126(11)
C(410)	-0.4325(35)	0.4972(25)	0.1114(25)	0.158(14)

Table AIII.6 contin.: Atomic coordinates and equivalent isotropic displacement parameters for **3**. U(eq) is defined as one third of the trace of the orthogonalized Uij tensor.

atom	x	y	z	U(eq)
P(5)	-0.1183(6)	0.1034(5)	-0.0469(4)	0.073(2)
O(51)	-0.2303(17)	0.1071(11)	-0.0366(10)	0.091(6)
O(52)	-0.0655(11)	0.0497(8)	-0.0216(7)	0.040(3)
C(58)	-0.1050(27)	0.0691(20)	-0.1522(19)	0.114(10)
C(51)	-0.0572(43)	0.2181(30)	-0.1532(31)	0.207(17)
C(52)	-0.1493(32)	0.1229(25)	-0.1882(24)	0.144(12)
C(53)	-0.1695(53)	0.0735(37)	-0.2876(32)	0.244(20)
C(54)	-0.1505(45)	0.1528(35)	-0.3001(33)	0.206(17)
C(55)	-0.0234(48)	0.1637(37)	-0.2808(37)	0.241(21)
C(56)	0.0502(50)	0.1983(41)	-0.1879(39)	0.271(23)
C(57)	-0.1224(59)	0.2410(41)	-0.2125(40)	0.304(26)
C(59)	-0.0950(51)	0.0144(39)	-0.3242(38)	0.257(25)
C(510)	-0.2953(54)	0.0519(40)	-0.3098(40)	0.270(27)
P(6)	-0.5840(5)	0.1347(5)	0.1290(4)	0.074(2)
O(61)	-0.5483(11)	0.0661(8)	0.0641(8)	0.046(4)
O(62)	-0.7049(17)	0.1148(11)	0.1285(10)	0.088(5)
C(68)	-0.4996(23)	0.1628(17)	0.2280(17)	0.090(8)
C(61)	-0.5305(60)	0.3103(37)	0.3139(41)	0.292(23)
C(62)	-0.5347(32)	0.2212(26)	0.3015(24)	0.145(12)
C(63)	-0.4644(46)	0.2386(35)	0.3930(31)	0.227(19)
C(64)	-0.4415(45)	0.3358(34)	0.4453(31)	0.205(17)
C(65)	-0.3333(50)	0.3508(42)	0.4062(41)	0.271(23)
C(66)	-0.4049(59)	0.3720(45)	0.3475(44)	0.298(26)
C(67)	-0.5497(49)	0.3544(39)	0.4117(40)	0.258(22)
C(69)	-0.3514(51)	0.2144(40)	0.3851(39)	0.265(26)
C(610)	-0.5658(47)	0.2152(36)	0.4282(35)	0.235(23)

Table AIII.6 contin.: Atomic coordinates and equivalent isotropic displacement parameters for **3**. U(eq) is defined as one third of the trace of the orthogonalized Uij tensor.

	Bond		Bond
Ca(1)-O(62)#1	2.29(2)	Ca(1)-O(11)	2.29(2)
Ca(1)-O(21)	2.34(2)	Ca(1)-O(52)	2.361(13)
Ca(1)-O(52)#2	2.366(12)	Ca(1)-O(3)	2.413(13)
Ca(1)-P(5)	3.434(8)	Ca(1)-P(5)#2	3.561(9)
Ca(1)-Ca(1)#2	3.670(8)	Ca(2)-O(51)	2.26(2)
Ca(2)-O(41)	2.29(2)	Ca(2)-O(32)	2.32(2)
Ca(2)-O(61)#3	2.371(13)	Ca(2)-O(61)	2.382(14)
Ca(2)-O(2)	2.414(13)	Ca(2)-P(6)	3.451(8)
Ca(2)-P(4)	3.550(8)	Ca(2)-P(6)#3	3.553(8)
Ca(2)-Ca(2)#3	3.635(8)	P(1)-O(11)	1.40(2)
P(1)-O(12)	1.49(2)	P(1)-C(18)	1.69(3)
C(18)-C(12)	1.57(3)	C(11)-C(12)	1.48(3)
C(11)-C(17)	1.54(4)	C(11)-C(16)	1.63(4)
C(12)-C(13)	1.62(4)	C(13)-C(110)	1.48(4)
C(13)-C(14)	1.50(4)	C(13)-C(19)	1.57(4)
C(14)-C(15)	1.59(4)	C(14)-C(17)	1.65(3)
C(15)-C(16)	1.48(4)	P(2)-O(21)	1.44(2)
P(2)-O(22)	1.50(2)	P(2)-C(28)	1.71(3)
C(28)-C(22)	1.59(5)	C(21)-C(27)	1.54(4)
C(21)-C(22)	1.58(4)	C(21)-C(26)	1.57(4)
C(22)-C(23)	1.47(4)	C(23)-C(29)	1.50(4)
C(23)-C(210)	1.51(4)	C(23)-C(24)	1.54(4)
C(24)-C(25)	1.55(4)	C(24)-C(27)	1.58(4)
C(25)-C(26)	1.52(4)	P(3)-O(32)	1.43(2)
P(3)-O(31)	1.50(2)	P(3)-C(38)	1.77(2)
C(38)-C(32)	1.55(3)	C(31)-C(32)	1.51(3)
C(31)-C(37)	1.51(4)	C(31)-C(36)	1.58(4)
C(32)-C(33)	1.57(3)	C(33)-C(34)	1.52(3)
C(33)-C(310)	1.53(3)	C(33)-C(39)	1.52(3)
C(34)-C(35)	1.62(4)	C(34)-C(37)	1.62(4)
C(35)-C(36)	1.58(4)	P(4)-O(41)	1.49(2)
P(4)-O(42)	1.56(2)	P(4)-C(48)	1.80(3)
C(48)-C(42)	1.59(4)	C(41)-C(42)	1.52(4)
C(41)-C(47)	1.57(4)	C(41)-C(46)	1.61(4)
C(42)-C(43)	1.62(4)	C(43)-C(44)	1.48(4)
C(43)-C(410)	1.52(4)	C(43)-C(49)	1.52(4)
C(44)-C(47)	1.63(3)	C(44)-C(45)	1.66(4)

Table AIII.7: Bond lengths [Å] for **13**.

	length		length
C(45)-C(46)	1.55(4)	P(5)-O(51)	1.45(2)
P(5)-O(52)	1.496(13)	P(5)-C(58)	1.78(3)
P(5)-Ca(1)#2	3.561(9)	O(52)-Ca(1)#2	2.366(12)
C(58)-C(52)	1.57(4)	C(51)-C(57)	1.55(4)
C(51)-C(56)	1.59(4)	C(51)-C(52)	1.64(4)
C(52)-C(53)	1.58(4)	C(53)-C(510)	1.50(4)
C(53)-C(54)	1.54(4)	C(53)-C(59)	1.54(4)
C(54)-C(55)	1.54(4)	C(54)-C(57)	1.59(4)
C(55)-C(56)	1.61(4)	P(6)-O(61)	1.465(14)
P(6)-O(62)	1.48(2)	P(6)-C(68)	1.79(3)
P(6)-Ca(2)#3	3.553(8)	O(61)-Ca(2)#3	2.371(13)
O(62)-Ca(1)#4	2.29(2)	C(68)-C(62)	1.47(4)
C(61)-C(62)	1.51(4)	C(61)-C(66)	1.58(4)
C(61)-C(67)	1.67(4)	C(62)-C(63)	1.67(4)
C(63)-C(64)	1.50(4)	C(63)-C(610)	1.56(4)
C(63)-C(69)	1.57(4)	C(64)-C(67)	1.59(4)
C(64)-C(65)	1.64(4)	C(65)-C(66)	1.56(4)

Table AIII.7 contin.: Bond lengths [Å] for **13**.

	Angle		Angle
O(62)#1-Ca(1)-O(11)	96.1(6)	O(62)#1-Ca(1)-O(21)	93.4(6)
O(11)-Ca(1)-O(21)	98.3(6)	O(62)#1-Ca(1)-O(52)	165.9(5)
O(11)-Ca(1)-O(52)	91.6(5)	O(21)-Ca(1)-O(52)	97.2(5)
O(62)#1-Ca(1)-O(52)#2	89.1(5)	O(11)-Ca(1)-O(52)#2	98.3(5)
O(21)-Ca(1)-O(52)#2	162.9(5)	O(52)-Ca(1)-O(52)#2	78.1(5)
O(62)#1-Ca(1)-O(3)	90.2(5)	O(11)-Ca(1)-O(3)	173.7(5)
O(21)-Ca(1)-O(3)	81.7(5)	O(52)-Ca(1)-O(3)	82.1(4)
O(52)#2-Ca(1)-O(3)	81.4(4)	O(62)#1-Ca(1)-P(5)	168.2(5)
O(11)-Ca(1)-P(5)	91.2(4)	O(21)-Ca(1)-P(5)	76.4(4)
O(52)-Ca(1)-P(5)	21.1(3)	O(52)#2-Ca(1)-P(5)	99.0(4)
O(3)-Ca(1)-P(5)	82.6(3)	O(62)#1-Ca(1)-P(5)#2	71.8(4)
O(11)-Ca(1)-P(5)#2	95.4(4)	O(21)-Ca(1)-P(5)#2	160.9(5)
O(52)-Ca(1)-P(5)#2	95.7(3)	O(52)#2-Ca(1)-P(5)#2	17.8(3)
O(3)-Ca(1)-P(5)#2	86.2(3)	P(5)-Ca(1)-P(5)#2	116.7(2)
O(62)#1-Ca(1)-Ca(1)#2	127.8(5)	O(11)-Ca(1)-Ca(1)#2	96.4(4)
O(21)-Ca(1)-Ca(1)#2	134.1(5)	O(52)-Ca(1)-Ca(1)#2	39.1(3)
O(52)#2-Ca(1)-Ca(1)#2	39.0(3)	O(3)-Ca(1)-Ca(1)#2	79.4(3)

Table AIII.8: Bond angles [°] for **13**.

	Angle		Angle
P(5)-Ca(1)-Ca(1)#2	60.1(2)	P(5)#2-Ca(1)-Ca(1)#2	56.7(2)
O(51)-Ca(2)-O(41)	88.0(6)	O(51)-Ca(2)-O(32)	101.1(6)
O(41)-Ca(2)-O(32)	102.9(5)	O(51)-Ca(2)-O(61)#3	98.4(6)
O(41)-Ca(2)-O(61)#3	165.2(5)	O(32)-Ca(2)-O(61)#3	89.0(5)
O(51)-Ca(2)-O(61)	172.8(5)	O(41)-Ca(2)-O(61)	91.7(5)
O(32)-Ca(2)-O(61)	86.0(5)	O(61)#3-Ca(2)-O(61)	80.3(5)
O(51)-Ca(2)-O(2)	91.7(6)	O(41)-Ca(2)-O(2)	85.5(5)
O(32)-Ca(2)-O(2)	164.8(5)	O(61)#3-Ca(2)-O(2)	81.0(4)
O(61)-Ca(2)-O(2)	81.1(4)	O(51)-Ca(2)-P(6)	159.5(5)
O(41)-Ca(2)-P(6)	71.8(4)	O(32)-Ca(2)-P(6)	87.5(4)
O(61)#3-Ca(2)-P(6)	100.3(4)	O(61)-Ca(2)-P(6)	20.1(3)
O(2)-Ca(2)-P(6)	83.1(3)	O(51)-Ca(2)-P(4)	73.5(5)
O(41)-Ca(2)-P(4)	16.2(4)	O(32)-Ca(2)-P(4)	112.1(4)
O(61)#3-Ca(2)-P(4)	158.4(4)	O(61)-Ca(2)-P(4)	105.2(4)
O(2)-Ca(2)-P(4)	79.2(3)	P(6)-Ca(2)-P(4)	86.0(2)
O(51)-Ca(2)-P(6)#3	81.6(5)	O(41)-Ca(2)-P(6)#3	165.5(4)
O(32)-Ca(2)-P(6)#3	89.0(4)	O(61)#3-Ca(2)-P(6)#3	17.2(3)
O(61)-Ca(2)-P(6)#3	97.4(3)	O(2)-Ca(2)-P(6)#3	84.7(3)
P(6)-Ca(2)-P(6)#3	117.5(2)	P(4)-Ca(2)-P(6)#3	149.8(2)
O(51)-Ca(2)-Ca(2)#3	138.2(5)	O(41)-Ca(2)-Ca(2)#3	130.5(5)
O(32)-Ca(2)-Ca(2)#3	86.7(4)	O(61)#3-Ca(2)-Ca(2)#3	40.2(3)
O(61)-Ca(2)-Ca(2)#3	40.0(3)	O(2)-Ca(2)-Ca(2)#3	78.3(3)
P(6)-Ca(2)-Ca(2)#3	60.1(2)	P(4)-Ca(2)-Ca(2)#3	141.1(2)
P(6)#3-Ca(2)-Ca(2)#3	57.4(2)	O(11)-P(1)-O(12)	121.4(9)
O(11)-P(1)-C(18)	117.9(12)	O(12)-P(1)-C(18)	113.8(11)
C(12)-C(11)-C(17)	106(3)	C(12)-C(11)-C(16)	116(3)
C(17)-C(11)-C(16)	103(3)	C(11)-C(12)-C(18)	108(3)
C(11)-C(12)-C(13)	103(3)	C(18)-C(12)-C(13)	117(3)
C(110)-C(13)-C(14)	98(3)	C(110)-C(13)-C(19)	123(4)
C(14)-C(13)-C(19)	107(4)	C(110)-C(13)-C(12)	108(3)
C(14)-C(13)-C(12)	98(3)	C(19)-C(13)-C(12)	117(3)
C(13)-C(14)-C(15)	109(3)	C(13)-C(14)-C(17)	111(3)
C(15)-C(14)-C(17)	93(3)	C(16)-C(15)-C(14)	111(3)
C(15)-C(16)-C(11)	94(3)	C(11)-C(17)-C(14)	86(3)
O(21)-P(2)-O(22)	121.3(11)	O(21)-P(2)-C(28)	120.5(13)
O(22)-P(2)-C(28)	106.0(14)	P(2)-O(21)-Ca(1)	151.9(11)
C(22)-C(28)-P(2)	112(2)	C(27)-C(21)-C(22)	101(4)

Table AIII.8 contin.: Bond angles [°] for **13**.

	Angle		Angle
C(22)-C(28)-P(2)	112(2)	C(27)-C(21)-C(22)	101(4)
C(27)-C(21)-C(26)	112(5)	C(22)-C(21)-C(26)	109(4)
C(23)-C(22)-C(21)	100(4)	C(23)-C(22)-C(28)	120(4)
C(21)-C(22)-C(28)	105(4)	C(22)-C(23)-C(29)	123(5)
C(22)-C(23)-C(210)	103(5)	C(29)-C(23)-C(210)	118(5)
C(22)-C(23)-C(24)	103(4)	C(29)-C(23)-C(24)	112(5)
C(210)-C(23)-C(24)	91(4)	C(23)-C(24)-C(25)	102(4)
C(23)-C(24)-C(27)	108(4)	C(25)-C(24)-C(27)	97(4)
C(26)-C(25)-C(24)	109(4)	C(25)-C(26)-C(21)	93(4)
C(21)-C(27)-C(24)	88(4)	O(32)-P(3)-O(31)	117.1(9)
O(32)-P(3)-C(38)	111.1(10)	O(31)-P(3)-C(38)	110.7(10)
P(3)-O(32)-Ca(2)	149.8(9)	C(32)-C(38)-P(3)	114(2)
C(32)-C(31)-C(37)	107(3)	C(32)-C(31)-C(36)	105(3)
C(37)-C(31)-C(36)	108(3)	C(31)-C(32)-C(38)	119(3)
C(31)-C(32)-C(33)	103(3)	C(38)-C(32)-C(33)	115(2)
C(34)-C(33)-C(310)	102(3)	C(34)-C(33)-C(39)	116(3)
C(310)-C(33)-C(39)	112(3)	C(34)-C(33)-C(32)	101(3)
C(310)-C(33)-C(32)	106(3)	C(39)-C(33)-C(32)	118(3)
C(33)-C(34)-C(35)	101(3)	C(33)-C(34)-C(37)	107(3)
C(35)-C(34)-C(37)	102(3)	C(36)-C(35)-C(34)	103(3)
C(35)-C(36)-C(31)	99(3)	C(31)-C(37)-C(34)	89(3)
O(41)-P(4)-O(42)	117.3(10)	O(41)-P(4)-C(48)	115.5(11)
O(42)-P(4)-C(48)	104.1(11)	O(41)-P(4)-Ca(2)	25.4(6)
O(42)-P(4)-Ca(2)	113.4(8)	C(48)-P(4)-Ca(2)	136.2(9)
P(4)-O(41)-Ca(2)	138.5(10)	C(42)-C(48)-P(4)	109(2)
C(42)-C(41)-C(47)	101(3)	C(42)-C(41)-C(46)	99(4)
C(47)-C(41)-C(46)	101(4)	C(41)-C(42)-C(48)	121(3)
C(41)-C(42)-C(43)	111(3)	C(48)-C(42)-C(43)	111(3)
C(44)-C(43)-C(410)	98(4)	C(44)-C(43)-C(49)	114(4)
C(410)-C(43)-C(49)	117(4)	C(44)-C(43)-C(42)	98(3)
C(410)-C(43)-C(42)	109(4)	C(49)-C(43)-C(42)	119(4)
C(43)-C(44)-C(47)	110(3)	C(43)-C(44)-C(45)	104(3)
C(47)-C(44)-C(45)	93(3)	C(46)-C(45)-C(44)	105(4)
C(45)-C(46)-C(41)	104(4)	C(41)-C(47)-C(44)	96(3)

Table AIII.8 contin.: Bond angles [°] for **13**.

	Angle		Angle
O(51)-P(5)-O(52)	119.5(9)	O(51)-P(5)-C(58)	113.4(13)
O(52)-P(5)-C(58)	104.9(12)	O(51)-P(5)-Ca(1)	136.5(7)
O(52)-P(5)-Ca(1)	34.6(5)	C(58)-P(5)-Ca(1)	108.5(11)
O(51)-P(5)-Ca(1)#2	102.6(7)	O(52)-P(5)-Ca(1)#2	28.9(5)
C(58)-P(5)-Ca(1)#2	93.3(11)	Ca(1)-P(5)-Ca(1)#2	63.3(2)
P(5)-O(51)-Ca(2)	158.9(11)	P(5)-O(52)-Ca(1)	124.3(7)
P(5)-O(52)-Ca(1)#2	133.3(8)	Ca(1)-O(52)-Ca(1)#2	101.9(5)
C(52)-C(58)-P(5)	113(2)	C(57)-C(51)-C(56)	106(5)
C(57)-C(51)-C(52)	95(4)	C(56)-C(51)-C(52)	106(4)
C(58)-C(52)-C(53)	110(3)	C(58)-C(52)-C(51)	112(3)
C(53)-C(52)-C(51)	106(4)	C(510)-C(53)-C(54)	94(5)
C(510)-C(53)-C(59)	129(6)	C(54)-C(53)-C(59)	116(5)
C(510)-C(53)-C(52)	98(4)	C(54)-C(53)-C(52)	99(4)
C(59)-C(53)-C(52)	116(5)	C(53)-C(54)-C(55)	88(4)
C(53)-C(54)-C(57)	111(5)	C(55)-C(54)-C(57)	86(4)
C(54)-C(55)-C(56)	123(5)	C(51)-C(56)-C(55)	88(4)
C(51)-C(57)-C(54)	101(4)	O(61)-P(6)-O(62)	117.2(9)
O(61)-P(6)-C(68)	106.2(11)	O(62)-P(6)-C(68)	110.7(12)
O(61)-P(6)-Ca(2)	34.0(5)	O(62)-P(6)-Ca(2)	144.8(7)
C(68)-P(6)-Ca(2)	100.1(9)	O(61)-P(6)-Ca(2)#3	28.5(5)
O(62)-P(6)-Ca(2)#3	92.5(7)	C(68)-P(6)-Ca(2)#3	104.8(9)
Ca(2)-P(6)-Ca(2)#3	62.5(2)	P(6)-O(61)-Ca(2)#3	134.3(8)
P(6)-O(61)-Ca(2)	125.9(8)	Ca(2)#3-O(61)-Ca(2)	99.7(5)
P(6)-O(62)-Ca(1)#4	145.9(10)	C(62)-C(68)-P(6)	114(2)
C(62)-C(61)-C(66)	111(5)	C(62)-C(61)-C(67)	97(4)
C(66)-C(61)-C(67)	91(5)	C(68)-C(62)-C(61)	117(4)
C(68)-C(62)-C(63)	114(3)	C(61)-C(62)-C(63)	106(4)
C(64)-C(63)-C(61)	95(4)	C(64)-C(63)-C(69)	111(5)
C(610)-C(63)-C(69)	134(5)	C(64)-C(63)-C(62)	100(4)
C(610)-C(63)-C(62)	100(4)	C(69)-C(63)-C(62)	112(4)
C(63)-C(64)-C(67)	105(4)	C(63)-C(64)-C(65)	90(4)
C(67)-C(64)-C(65)	116(5)	C(66)-C(65)-C(64)	90(4)
C(65)-C(66)-C(61)	110(6)	C(64)-C(67)-C(61)	92(4)

Table AIII.8 contin.: Bond angles [°] for **13**.

Symmetry transformations used to generate equivalent atoms:

#1 x+1, y, z #2 -x, -y, -z #3 -x-1, -y, -z, #4 x-1, y, z.

atom	U11	U22	U33	U23	U13	U12
Ca(1)	0.020(3)	0.056(3)	0.034(2)	0.005(2)	0.007(2)	0.002(2)
Ca(2)	0.017(3)	0.074(3)	0.062(3)	0.047(3)	0.005(2)	0.007(2)
P(1)	0.037(5)	0.124(6)	0.028(3)	0.018(3)	0.007(3)	0.043(4)
P(2)	0.168(9)	0.048(5)	0.110(6)	0.022(4)	0.085(6)	0.010(5)
P(3)	0.054(5)	0.103(5)	0.062(4)	0.062(4)	0.023(3)	0.035(4)
P(4)	0.086(6)	0.064(5)	0.084(5)	0.040(4)	0.005(4)	0.016(4)
P(5)	0.048(6)	0.129(6)	0.086(5)	0.081(5)	0.040(4)	0.032(4)
P(6)	0.021(5)	0.100(5)	0.045(4)	0.000(4)	-0.006(3)	0.009(4)

Table AIII.9: Anisotropic displacement parameters (Å x 10^3) for **13**. The anisotropic displacement factor exponent takes the form:
$-2\pi^2[h^2a^{*2}U11+...+2hka^*b^*U12]$

AIII.3 Complete bond lengths, bond angles, and thermal and positional parameters for **14**

	x	y	z	U(eq)
P(1)	0.5559(1)	0.2409(1)	0.1046(3)	0.023(1)
O(1)	0.5212(2)	0.2370(2)	0.2599(7)	0.031(2)
O(2)	0.6094(2)	0.2395(2)	0.1501(7)	0.025(2)
O(3)	0.5694(2)	0.2944(2)	0.0002(7)	0.034(2)
C(1)	0.3587(4)	0.1076(4)	-0.1535(12)	0.036(3)
C(2)	0.4193(4)	0.1350(4)	-0.2211(12)	0.036(3)
C(3)	0.4551(3)	0.1807(3)	-0.0837(10)	0.022(2)
C(4)	0.4083(3)	0.1678(3)	0.0493(11)	0.031(2)
C(5)	0.3871(4)	0.1098(3)	0.1302(11)	0.037(3)
C(6)	0.3501(4)	0.0679(4)	-0.0069(12)	0.040(3)
C(7)	0.3583(3)	0.1576(4)	-0.0610(12)	0.036(3)
C(8)	0.5101(3)	0.1831(3)	-0.0239(10)	0.022(2)
C(9)	0.4390(4)	0.0914(4)	-0.2555(13)	0.042(3)
C(10)	0.4243(4	0.1652(4)	-0.3855(11)	0.050(3)

Table AIII.10: Atomic coordinates and equivalent isotropic displacement parameters for **14**. U(eq) is defined as one third of the trace of the orthogonalized Uij tensor.

atom	length [Å]	atom	length [Å]
P(1)-O(2)	1.511(5)	P(1)-O(1)	1.534(6)
P(1)-O(3)	1.548(6)	P(1)-C(8)	1.762(8)
C(1)-C(7)	1.547(12)	C(3)-C(8)	1.532(10)
C(1)-C(6)	1.529(12)	C(4)-C(7)	1.521(12)
C(1)-C(2)	1.520(12)	C(4)-C(5)	1.521(11)
C(2)-C(10)	1.522(12)	C(4)-C(3)	1.555(11)
C(2)-C(9)	1.541(11)	C(6)-C(5)	1.538(12)
C(3)-C(2)	1.576(11)		

Table AIII.11: Bond lengths for **14** (Å), with estimated standard deviations in parentheses.

Atom	Angle	Atom	Angle
O(2)-P(1)-O(1)	11.2(3)	O(1)-P(1)-O(3)	110.8(3)
O(2)-P(1)-O(3)	111.9(3)	O(1)-P(1)-C(8)	106.4(3)
O(2)-P(1)-C(8)	112.2(3)	C(5)-C(4)-C(7)	102.6(7)
O(3)-P(1)-C(8)	104.0(4)	C(7)-C(4)-C(3)	100.8(7)
C(5)-C(4)-C(3)	111.7(7)	C(8)-C(3)-C(2)	117.1(6)
C(8)-C(3)-C(4)	117.1(7)	C(1)-C(2)-C(10)	111.0(8)
C(4)-C(3)-C(2)	101.3(6)	C(10)-C(2)-C(9)	106.3(8)
C(1)-C(2)-C(9)	112.9(7)	C(10)-C(2)-C(3)	109.6(7)
C(1)-C(2)-C(3)	102.7(7)	C(2)-C(1)-C(6)	111.6(8)
C(9)-C(2)-C(3)	114.4(7)	C(6)-C(1)-C(7)	100.1(8)
C(2)-C(1)-C(7)	102.8(7)	C(4)-C(5)-C(6)	102.8(7)
C(1)-C(6)-C(5)	102.9(7)	C(3)-C(8)-P(1)	117.3(5)
C(4)-C(7)-C(1)	92.7(7)		

Table AIII.12: Bond angles (°) for **14**, with estimated standard deviations in parentheses.

	U11	U22	U33	U23	U13	U12
P(1)	0.0163(14)	0.0173(14)	0.0364(14)	0.0006(12)	0.0003(12)	0.0080(11)
O(1)	0.024(3)	0.033(4)	0.035(4)	-0.012(3)	-0.007(3)	0.012(3)
O(2)	0.011(3)	0.026(3)	0.034(3)	0.005(3)	-0.004(3)	0.007(3)
O(3)	0.033(4)	0.014(3)	0.049(4)	0.001(3)	-0.005(3)	0.006(3)
C(1)	0.014(5)	0.034(6)	0.060(7)	-0.006(6)	-0.007(5)	0.012(5)
C(2)	0.021(6)	0.025(6)	0.057(7)	0.000(5)	0.001(5)	0.008(5)
C(3)	0.016(5)	0.018(5)	0.038(5)	-0.001(4)	-0.004(4)	0.014(4)
C(4)	0.019(5)	0.015(5)	0.050(6)	-0.001(5)	0.005(5)	0.001(4)
C(5)	0.023(5)	0.026(6)	0.050(6)	0.011(5)	0.007(5)	0.002(5)
C(6)	0.033(6)	0.023(6)	0.049(6)	0.010(5)	0.016(5)	0.002(5)
C(7)	0.015(5)	0.030(6)	0.065(7)	-0.007(5)	-0.008(5)	0.012(4)
C(8)	0.015(5)	0.017(5)	0.030(5)	0.004(4)	0.004(4)	0.005(4)
C(9)	0.032(6)	0.041(6)	0.058(7)	-0.013(6)	-0.013(5)	0.023(5)
C(10)	0.033(6)	0.046(7)	0.043(6)	0.005(5)	-0.006(5)	-0.001(5)

Table AIII.13: Anisotropic displacement parameters (A^2x10^3) for **14**. The anisotropic displacement factor exponent takes the form: $-2pi^2[h^2a^{*2}U11+...+ 2hk\ a^*b^*U12]$

Atom	x	y	z	U(eq)
H_{110}	0.5328	0.2523	0.3699	0.038
H_{130}	0.5920	0.3310	0.0570	0.041
H_1	0.4195(3)	0.1996(3)	0.1311(11)	0.037
H_2	0.4664(3)	0.2190(3)	-0.1317(10)	0.026
H_4	0.3286(4)	0.0897(4)	-0.2412(12)	0.044
$H_{5''}$	0.3633(4)	0.0408(4)	-0.0344(12)	0.048
$H_{5'}$	0.3094(4)	0.0462(4)	0.0267(12)	0.048
$H_{6'}$	0.3642(4)	0.1055(3)	0.2309(11)	0.045
$H_{6''}$	0.4193(4)	0.1040(3)	0.1607(11)	0.045
$H_{7''}$	0.3669(3)	0.1903(4)	-0.1343(12)	0.043
$H_{7'}$	0.3226(3)	0.1456(4)	0.0020(12)	0.043
$H_{8'}$	0.5320(3)	0.1837(3)	-0.1232(10)	0.026
$H_{8''}$	0.4993(3)	0.1473(3)	0.0370(10)	0.026
H_9	0.4087(10)	0.0583(11)	-0.3144(60)	0.062
$H_{9'}$	0.4472(22)	0.0788(17)	-0.1498(13)	0.062
$H_{9''}$	0.4736(14)	0.1093(8)	-0.3240(56)	0.062
H_{10}	0.4063(23)	0.1366(4)	-0.4739(17)	0.075
$H_{10'}$	0.4648(4)	0.1905(20)	-0.4122(38)	0.075
$H_{10''}$	0.4052(22)	0.1877(20)	-0.3764(25)	0.075

Table AIII.14: Hydrogen coordinates and isotropic displacement parameters for **14**.

AIII.4 Complete bond lengths, bond angles, and thermal and positional parameters for **22**

Atom	Length	Atom	Length
P(1)-C(8)	1.794(3)	C(1)-C(7)	1.532(5)
P(1)-C(11)	1.819(3)	C(2)-C(3)	1.584(5)
P(1)-C(12)	1.820(3)	C(2)-C(9)	1.518(5)
P(1)-C(13)	1.808(3)	C(2)-C(10)	1.533(5)
O(1)-C(11)	1.412(4)	C(3)-C(4)	1.524(5)
O(2)-C(12)	1.410(4)	C(3)-C(8)	1.542(4)
O(3)-C(13)	1.419(3)	C(4)-C(5)	1.543(5)
C(1)-C(2)	1.548(5)	C(4)-C(7)	1.539(5)
C(1)-C(6)	1.542(5)	C(5)-C(6)	1.542(5)

Table AIII.15: Bond lengths (Å) for **22**, with estimated standard deviations in parentheses.

Atom	Angle	Atom	Angle
C(8)-P(1)-C(13)	111.0(2)	C(9)-C(2)-C(1)	109.9(3)
C(13)-P(1)-C(11)	108.4(2)	C(4)-C(3)-C(2)	103.5(3)
C(13)-P(1)-C(12)	108.9(2)	C(4)-C(3)-C(8)	118.1(3)
C(8)-P(1)-C(11)	113.6(2)	C(8)-C(3)-C(2)	114.4(3)
C(8)-P(1)-C(12)	107.5(2)	C(3)-C(4)-C(5)	110.5(3)
C(11)-P(1)-C(12)	107.3(2)	C(3)-C(4)-C(7)	100.0(3)
C(7)-C(1)-C(2)	103.1(3)	C(7)-C(4)-C(5)	101.7(3)
C(7)-C(1)-C(6)	99.8(3)	C(6)-C(5)-C(4)	103.5(3)
C(6)-C(1)-C(2)	110.9(3)	C(1)-C(6)-C(5)	102.6(3)
C(9)-C(2)-C(10)	108.7(3)	C(1)-C(7)-C(4)	94.0(3)
C(10)-C(2)-C(1)	113.0(3)	C(3)-C(8)-P(1)	116.4(2)
C(10)-C(2)-C(3)	113.6(3)	O(1)-C(11)-P(1)	112.2(2)
C(1)-C(2)-C(3)	101.1(3)	O(2)-C(12)-P(1)	110.5(2)
C(9)-C(2)-C(3)	110.4(3)	O(3)-C(13)-P(1)	107.3(2)

Table AIII.16: Bond angles (°) for **22**, with estimated standard deviations in parentheses.

	x	y	z	U(eq)
Cl(1)	0.3994(1)	0.1965(1)	0.5127(1)	0.031(1)
P(1)	0.6361(1)	0.3016(1)	0.3463(1)	0.019(1)
O(1)	0.6909(1)	0.4503(3)	0.5367(2)	0.030(1)
O(2)	0.4773(1)	0.3555(3)	0.3144(2)	0.028(1)
O(3)	0.6801(2)	0.4669(3)	0.1701(2)	0.036(1)
C(1)	0.9296(2)	0.0676(5)	0.3554(3)	0.031(1)
C(2)	0.8468(2)	-0.0269(5)	0.3630(3)	0.027(1)
C(3)	0.7889(2)	0.1353(5)	0.3847(3)	0.025(1)
C(4)	0.8439(2)	0.2955(5)	0.3728(3)	0.032(1)
C(5)	0.8707(2)	0.3119(5)	0.2531(3)	0.041(1)
C(6)	0.9349(2)	0.1650(5)	0.2443(3)	0.040(1)
C(7)	0.9218(2)	0.2264(5)	0.4325(3)	0.039(1)
C(8)	0.7077(2)	0.1314(4)	0.3170(3)	0.020(1)
C(9)	0.8494(2)	-0.1520(5)	0.4609(3)	0.042(1)
C(10)	0.8224(2)	-0.1320(5)	0.2588(3)	0.038(1)
C(11)	0.6272(2)	0.3432(5)	0.4928(3)	0.025(1)
C(12)	0.5371(2)	0.2291(4)	0.2918(3)	0.025(1)
C(13)	0.6619(2)	0.5072(4)	0.2804(2)	0.023(1)

Table AIII.17: Atomic coordinates and equivalent isotropic displacement parameters for **22**. U(eq) is defined as one third of the trace of the orthogonalized Uij tensor.

	U11	U22	U33	U23	U13	U12
Cl(1)	0.0400(5)	0.0315(5)	0.0223(5)	-0.0023(4)	0.0077(4)	-0.0046(5)
P(1)	0.0203(4)	0.0217(5)	0.0141(4)	-0.0001(4)	0.0022(3)	-0.0007(4)
O(1)	0.0318(13)	0.0359(15)	0.0220(13)	-0.0075(12)	-0.0054(11)	0.0021(12)
O(2)	0.0228(12)	0.0296(13)	0.0305(13)	0.0063(12)	0.0041(10)	0.0008(11)
O(3)	0.058(2)	0.0289(15)	0.0210(13)	0.0055(12)	0.0140(12)	0.0089(13)
C(1)	0.021(2)	0.028(2)	0.043(2)	-0.001(2)	0.003(2)	0.006(2)
C(2)	0.028(2)	0.027(2)	0.027(2)	0.003(2)	0.002(2)	0.004(2)
C(3)	0.023(2)	0.030(2)	0.023(2)	-0.003(2)	0.0031(14)	0.004(2)
C(4)	0.026(2)	0.027(2)	0.046(2)	-0.003(2)	0.005(2)	0.003(2)
C(5)	0.032(2)	0.032(2)	0.057(3)	0.016(2)	0.007(2)	-0.009(2)
C(6)	0.034(2)	0.035(2)	0.052(3)	0.010(2)	0.016(2)	-0.003(2)
C(7)	0.027(2)	0.041(2)	0.047(2)	-0.008(2)	-0.005(2)	-0.003(2)
C(8)	0.026(2)	0.017(2)	0.018(2)	0.0003(14)	0.0035(14)	-0.0018(14)
C(9)	0.040(2)	0.042(3)	0.044(2)	0.016(2)	-0.001(2)	0.003(2)
C(10)	0.038(2)	0.030(2)	0.047(2)	-0.009(2)	0.005(2)	0.003(2)
C(11)	0.030(2)	0.029(2)	0.017(2)	-0.001(2)	0.0022(14)	0.002(2)
C(12)	0.026(2)	0.027(2)	0.021(2)	-0.002(2)	0.0030(14)	-0.006(2)
C(13)	0.033(2)	0.022(2)	0.013(2)	0.0010(15)	0.0021(14)	0.0017(15)

Table AIII.18: Anisotropic displacement parameters (A^2x10^3) for **22**. The anisotropic displacement factor exponent takes the form: $-2pi^2[h^2a^{*2}U11+...+2hka^*b^*U12]$.

Atom	x	y	z	U(eq)
H_{110}	0.6750(1)	0.5556(3)	0.5403(2)	0.045
H_{210}	0.4524(1)	0.3238(3)	0.3700(2)	0.041
H_{310}	0.6648(2)	0.5506(3)	0.1287(2)	0.053
H_1	0.9774(2)	-0.0097(5)	0.3742(3)	0.037
H_3	0.7754(2)	0.1292(5)	0.4641(3)	0.030
H_4	0.8223(2)	0.4074(5)	0.4041(3)	0.039
$H_{5''}$	0.8244(2)	0.2923(5)	0.1997(3)	0.049
$H_{5'}$	0.8944(2)	0.4298(5)	0.2397(3)	0.049
$H_{6''}$	0.9215(2)	0.0851(5)	0.1815(3)	0.048
$H_{6'}$	0.9896(2)	0.2155(5)	0.2358(3)	0.048
$H_{7''}$	0.9135(2)	0.1915(5)	0.5098(3)	0.047
$H_{7'}$	0.9678(2)	0.3100(5)	0.4291(3)	0.047
$H_{8''}$	0.6817(2)	0.0154(4)	0.3289(3)	0.024
$H_{8'}$	0.7196(2)	0.1389(4)	0.2379(3)	0.024
H_9	0.7957(2)	-0.2048(5)	0.4686(3)	0.063
H_9	0.8650(2)	-0.0862(5)	0.5281(3)	0.063
H_9	0.8892(2)	-0.2456(5)	0.4493(3)	0.063
H_{10}	0.8622(2)	-0.2258(5)	0.2478(3)	0.058
H_{10}	0.8205(2)	-0.0526(5)	0.1949(3)	0.058
H_{10}	0.7688(2)	-0.1849(5)	0.2670(3)	0.058
H_{11}	0.5747(2)	0.4021(5)	0.5047(3)	0.030
H_{11}	0.6275(2)	0.2289(5)	0.5327(3)	0.030
H_{12}	0.5389(2)	0.2115(4)	0.2112(3)	0.030
H_{12}	0.5231(2)	0.1145(4)	0.3257(3)	0.030
H_{12}	0.6158(2)	0.5909(4)	0.2816(2)	0.027
H_{13}	0.7095(2)	0.5621(4)	0.3194(2)	0.027

Table AIII.19: Hydrogen coordinates and isotropic displacement parameters for **22**.

AIII.5 Complete bond lengths, bond angles, and thermal and positional parameters for **30**

	x	y	z	U(eq)
U(1)	0.2500	0.2500	0.0000	0.058(1)
O(11)	0.3083(5)	0.3857(19)	0.0596(9)	0.071(5)
N(1)	0.2001(10)	0.3198(26)	0.0943(14)	0.071(6)
O(14)	0.2398(7)	0.2003(17)	0.1167(11)	0.086(6)
O(15)	0.1835(7)	0.3965(18)	0.0312(11)	0.082(5)
O(16)	0.1823(7)	0.3470(18)	0.1386(11)	0.093(5)
P(1)	0.1457(3)	0.5625(6)	0.8218(4)	0.066(2)
O(1)	0.3175(6)	0.0456(16)	0.0985(9)	0.073(5)
O(3)	0.1825(7)	0.7227(19)	0.8329(10)	0.097(5)
O(2)	0.0835(6)	0.6315(15)	0.8016(9)	0.068(4)
C(2)	0.0861(10)	0.7144(18)	0.8675(13)	0.072(6)
C(3)	0.2501(11)	0.7215(27)	0.8761(19)	0.135(11)
C(11)	0.4736(13)	0.4112(32)	0.3936(18)	0.097(8)
C(12)	0.4117(18)	0.3234(37)	0.3572(19)	0.133(12)
C(13)	0.4035(12)	0.2004(21)	0.2866(14)	0.082(8)
C(14)	0.4593(16)	0.2315(42)	0.2930(25)	0.151(14)
C(15)	0.5163(16)	0.1701(43)	0.3781(30)	0.207(23)
C(16)	0.5322(15)	0.2896(40)	0.4446(23)	0.172(16)
C(17)	0.4666(15)	0.4305(32)	0.3114(18)	0.126(11)
C(18)	0.3756(10)	0.0362(22)	0.2703(13)	0.072(7)
C(19)	0.4179(14)	0.2228(38)	0.4283(16)	0.141(13)
C(110)	0.3585(14)	0.4465(33)	0.3173(21)	0.171(16)

Table AIII.20: Atomic coordinates and equivalent isotropic displacement parameters for **30**. U(eq) is defined as one third of the trace of the orthogonalized Uij tensor.

Atom	Lenght	Atom	Lenght
U(1)-O(11)	1.668(14)	U(1)-O(11)#1	1.668(14)
U(1)-O(1)#1	2.345(14)	U(1)-O(1)	2.345(14)
U(1)-O(15)	2.51(2)	U(1)-O(15)#1	2.51(2)
U(1)-O(14)	2.52(2)	U(1)-O(14)#1	2.52(2)
U(1)-N(1)#1	2.94(2)	U(1)-N(1)	2.94(2)
N(1)-O(15)	1.21(2)	N(1)-O(16)	1.25(2)
N(1)-O(14)	1.30(2)	P(1)-O(1)#2	1.52(2)
P(1)-O(2)	1.557(13)	P(1)-O(3)	1.57(2)
P(1)-C(18)#2	1.74(2)	O(1)-P(1)#2	1.52(2)
O(3)-C(3)	1.45(2)	O(2)-C(2)	1.43(2)
C(11)-C(12)	1.52(4)	C(11)-C(17)	1.53(3)
C(11)-C(16)	1.58(4)	C(12)-C(110)	1.51(4)
C(12)-C(19)	1.54(3)	C(12)-C(13)	1.62(3)
C(13)-C(14)	1.44(3)	C(13)-C(18)	1.47(2)
C(14)-C(15)	1.50(4)	C(14)-C(17)	1.64(4)
C(15)-C(16)	1.47(4)	C(18)-P(1)#2	1.74(2)

Table AIII.21: Bond lengths (Å) and angles (°) for **30**.

Symmetry transformations used to generate equivalent atoms: #1 -x+1/2,-y+1/2,-z #2 -x+1/2, -y+1/2, -z+1

	Angle		Angle
O(11)-U(1)-O(11)#1	180.000(2)	O(11)-U(1)-O(1)#1	91.5(5)
O(11)#1-U(1)-O(1)#1	88.5(5)	O(11)-U(1)-O(1)	88.5(5)
O(11)#1-U(1)-O(1)	91.5(5)	O(1)#1-U(1)-O(1)	179.998(1)
O(11)-U(1)-O(15)	90.4(6)	O(11)#1-U(1)-O(15)	89.6(6)
O(1)#1-U(1)-O(15)	64.4(5)	O(1)-U(1)-O(15)	115.6(5)
O(11)-U(1)-O(15)#1	89.6(6)	O(11)#1-U(1)-O(15)#1	90.4(6)
O(1)#1-U(1)-O(15)#1	115.6(5)	O(1)-U(1)-O(15)#1	64.4(5)
O(15)-U(1)-O(15)#1	180.0	O(11)-U(1)-O(14)	92.2(6)
O(11)#1-U(1)-O(14)	87.8(6)	O(1)#1-U(1)-O(14)	114.5(5)

Table AIII.22: Bond lengths (Å) and angles (°) for **30**, with estimated standard deviations in parentheses.

	Angle		Angle
O(1)-U(1)-O(14)	65.5(5)	O(15)-U(1)-O(14)	50.2(5)
O(15)#1-U(1)-O(14)	129.8(5)	O(11)-U(1)-O(14)#1	87.8(6)
O(11)#1-U(1)-O(14)#1	92.2(6)	O(1)#1-U(1)-O(14)#1	65.5(5)
O(1)-U(1)-O(14)#1	114.5(5)	O(15)-U(1)-O(14)#1	129.8(5)
O(15)#1-U(1)-O(14)#1	50.2(5)	O(14)-U(1)-O(14)#1	179.998(1)
O(11)-U(1)-N(1)#1	89.1(6)	O(11)#1-U(1)-N(1)#1	90.9(6)
O(1)#1-U(1)-N(1)#1	91.6(6)	O(1)-U(1)-N(1)#1	88.4(6)
O(15)-U(1)-N(1)#1	156.0(5)	O(15)#1-U(1)-N(1)#1	24.1(5)
O(14)-U(1)-N(1)#1	153.9(5)	O(14)#1-U(1)-N(1)#1	26.1(5)
O(11)-U(1)-N(1)	90.9(6)	O(11)#1-U(1)-N(1)	89.1(6)
O(1)#1-U(1)-N(1)	88.4(6)	O(1)-U(1)-N(1)	91.6(6)
O(15)-U(1)-N(1)	24.0(5)	O(15)#1-U(1)-N(1)	155.9(5)
O(14)-U(1)-N(1)	26.1(5)	O(14)#1-U(1)-N(1)	153.9(5)
N(1)#1-U(1)-N(1)	180.000(1)	O(15)-N(1)-O(16)	125(2)
O(15)-N(1)-O(14)	116(2)	O(16)-N(1)-O(14)	119(2)
O(15)-N(1)-U(1)	57.8(11)	O(16)-N(1)-U(1)	176(2)
O(14)-N(1)-U(1)	58.6(12)	N(1)-O(14)-U(1)	95.3(14)
N(1)-O(15)-U(1)	98.1(14)	O(1)#2-P(1)-O(2)	112.5(8)
O(1)#2-P(1)-O(3)	112.6(9)	O(2)-P(1)-O(3)	102.4(8)
O(1)#2-P(1)-C(18)#2	114.0(9)	O(2)-P(1)-C(18)#2	106.7(10)
O(3)-P(1)-C(18)#2	107.8(9)	P(1)#2-O(1)-U(1)	161.3(8)
C(3)-O(3)-P(1)	122(2)	C(2)-O(2)-P(1)	119.4(12)
C(12)-C(11)-C(17)	99(2)	C(12)-C(11)-C(16)	112(2)
C(17)-C(11)-C(16)	100(3)	C(110)-C(12)-C(11)	110(3)
C(110)-C(12)-C(19)	112(3)	C(11)-C(12)-C(19)	110(3)
C(19)-C(12)-C(13)	110(2)	C(14)-C(13)-C(18)	123(2)
C(14)-C(13)-C(12)	103(2)	C(18)-C(13)-C(12)	122(2)
C(13)-C(14)-C(15)	109(3)	C(13)-C(14)-C(17)	100(2)
C(15)-C(14)-C(17)	100(2)	C(16)-C(15)-C(14)	109(3)
C(15)-C(16)-C(11)	102(3)	C(11)-C(17)-C(14)	93(2)
C(13)-C(18)-P(1)#2	117(2)		

Table AIII.22 contin.: Bond angles (°) for **30**, with estimated standard deviations in parentheses.

	U11	U22	U33	U23	U13	U12
U(1)	0.0698(7)	0.0284(5)	0.0741(8)	-0.0137(10)	0.0427(6)	-0.0059(10)
O(11)	0.023(7)	0.115(13)	0.072(10)	0.012(10)	0.026(7)	0.007(8)
N(1)	0.097(17)	0.071(14)	0.073(16)	-0.027(12)	0.067(16)	-0.011(13)
O(14)	0.108(12)	0.047(10)	0.099(13)	0.006(8)	0.061(11)	0.035(9)
O(15)	0.102(12)	0.054(9)	0.098(13)	0.007(9)	0.066(11)	0.000(8)
O(16)	0.114(13)	0.070(10)	0.116(14)	0.010(10)	0.081(12)	0.020(9)
P(1)	0.092(4)	0.030(3)	0.084(5)	-0.013(3)	0.058(4)	-0.010(3)
O(1)	0.078(10)	0.057(9)	0.066(11)	-0.024(9)	0.034(9)	0.009(8)
O(3)	0.123(12)	0.049(11)	0.119(12)	-0.026(10)	0.073(10)	-0.044(10)
O(2)	0.083(10)	0.046(8)	0.093(11)	0.005(8)	0.063(9)	0.009(7)
C(2)	0.110(15)	0.012(14)	0.099(16)	-0.008(10)	0.067(14)	0.011(9)
C(3)	0.089(17)	0.051(19)	0.233(31)	-0.025(19)	0.083(19)	-0.044(15)
C(11)	0.113(22)	0.070(18)	0.107(23)	-0.040(17)	0.068(19)	-0.040(17)
C(12)	0.236(38)	0.096(22)	0.094(23)	-0.042(18)	0.114(26)	-0.015(24)
C(13)	0.121(19)	0.037(15)	0.066(16)	-0.011(10)	0.047(15)	-0.041(12)
C(14)	0.132(25)	0.106(25)	0.242(40)	-0.114(31)	0.128(29)	-0.045(28)
C(15)	0.089(24)	0.134(31)	0.300(55)	-0.143(36)	0.071(32)	-0.024(24)
C(16)	0.126(25)	0.116(36)	0.176(34)	-0.051(28)	0.042(25)	-0.019(24)
C(17)	0.187(31)	0.077(20)	0.112(25)	-0.043(18)	0.092(24)	-0.065(20)
C(18)	0.101(17)	0.036(12)	0.074(16)	-0.013(11)	0.052(14)	-0.016(11)
C(19)	0.235(31)	0.121(28)	0.109(21)	-0.059(21)	0.128(23)	-0.096(26)
C(110)	0.192(32)	0.079(22)	0.199(37)	0.017(23)	0.097(29)	0.082(23)

Table AIII.23: Anisotropic displacement parameters ($A^2 x\ 10^3$) for **30**. The anisotropic displacement factor exponent takes the form: $2pi^2[h^2a^{*2}U11+...+ 2hka^*b^*U12]$

	x	y	z	U(eq)
H(2A)	0.0434(10)	0.7502(18)	0.8449(13)	0.108
H(2B)	0.1140(10)	0.8103(18)	0.8870(13)	0.108
H(2C)	0.1027(10)	0.6393(18)	0.9158(13)	0.108
H(3A)	0.2643(11)	0.8329(27)	0.8766(19)	0.203
H(3B)	0.2593(11)	0.6477(27)	0.8458(19)	0.203
H(3C)	0.2726(11)	0.6831(27)	0.9351(19)	0.203
H(11)	0.4798(13)	0.5165(32)	0.4239(18)	0.116
H(13)	0.3702(12)	0.2585(21)	0.2320(14)	0.098
H(14)	0.4566(16)	0.1965(42)	0.2424(25)	0.181
H(15A)	0.5071(16)	0.0616(43)	0.3908(30)	0.248
H(15B)	0.5526(16)	0.1576(43)	0.3769(30)	0.248
H(16A)	0.5723(15)	0.3476(40)	0.4679(23)	0.207
H(16B)	0.5356(15)	0.2355(40)	0.4922(23)	0.207
H(17A)	0.5048(15)	0.4775(32)	0.3213(18)	0.151
H(17B)	0.4283(15)	0.4932(32)	0.2664(18)	0.151
H(18A)	0.3374(10)	0.0453(22)	0.2674(13)	0.086
H(18B)	0.4063(10)	-0.0345(22)	0.3201(13)	0.086
H(19A)	0.4529(14)	0.1442(38)	0.4528(16)	0.211
H(19B)	0.3784(14)	0.1633(38)	0.4039(16)	0.211
H(19C)	0.4266(14)	0.2972(38)	0.4733(16)	0.211
H(11A)	0.3187(14)	0.3893(33)	0.2939(21)	0.257
H(11B)	0.3548(14)	0.5049(33)	0.2711(21)	0.257
H(11C)	0.3674(14)	0.5255(33)	0.3609(21)	0.257

Table III3.24: Hydrogen coordinates and isotropic displacement parameters for **30**.

Appendix IV

List of publications

The research described in this thesis is represented by the following publications:

1 W. Henderson, M.T. Leach, B.K. Nicholson, M. Sabat, *J. Chem. Dalton Trans.*, 1995, 2109.

2 W. Henderson, M.T. Leach, B.K. Nicholson, A. L. Wilkins, (the late) P.A.T. Hoye, *Polyhedron*, **17**, 3747-3752.

Appendix V

Compound	Method of identification	Literature values
phosphine	I.R υ_1 (P-H) 2320, υ_3 (P-H) 2325 cm^{-1}	2321, 2327[1] cm^{-1}
methane	I.R υ_3 (C-H) 3016, υ_2 (C-H) 1306 cm^{-1}	3020, 1306[2] cm^{-1}
	^1H NMR δ 0.21 (s)	δ 0.40[3]
acetylene	I.R υ_5 (C-H) 729 cm^{-1}	729[3] cm^{-1}
ethene	I.R υ_7 (C-H) 1889 cm^{-1}	1890[2] cm^{-1}
	^1H NMR δ 5.4 (s)	δ 5.28[3]
ethane	^1H NMR δ 0.86 (s)	δ 0.86[3]
cyclopentadiene	I.R υ_{26} (C-H) 663 cm^{-1}	663[4] cm^{-1}
	GCMS	
methylcyclo-pentadienes	GCMS	
benzene	I.R υ_{26} (C-H) 674 cm^{-1}	671[1], 673[5] cm^{-1}
	^1H NMR δ 7.35 (s)	δ 7.15[6]
	GCMS	
toluene	I.R υ_4 (C-H) 694 cm^{-1}	694[5] cm^{-1}
	^1H NMR δ 7.18 (m)	δ 7.01[6]
	GCMS	
xylenes	GCMS	
camphene	^1H NMR	reference 6
	GCMS	
bornylene	GCMS	
tricyclene	GCMS	

Table V.25: Identification of products from the I.R LPHP decomposition of phosphine **20**.

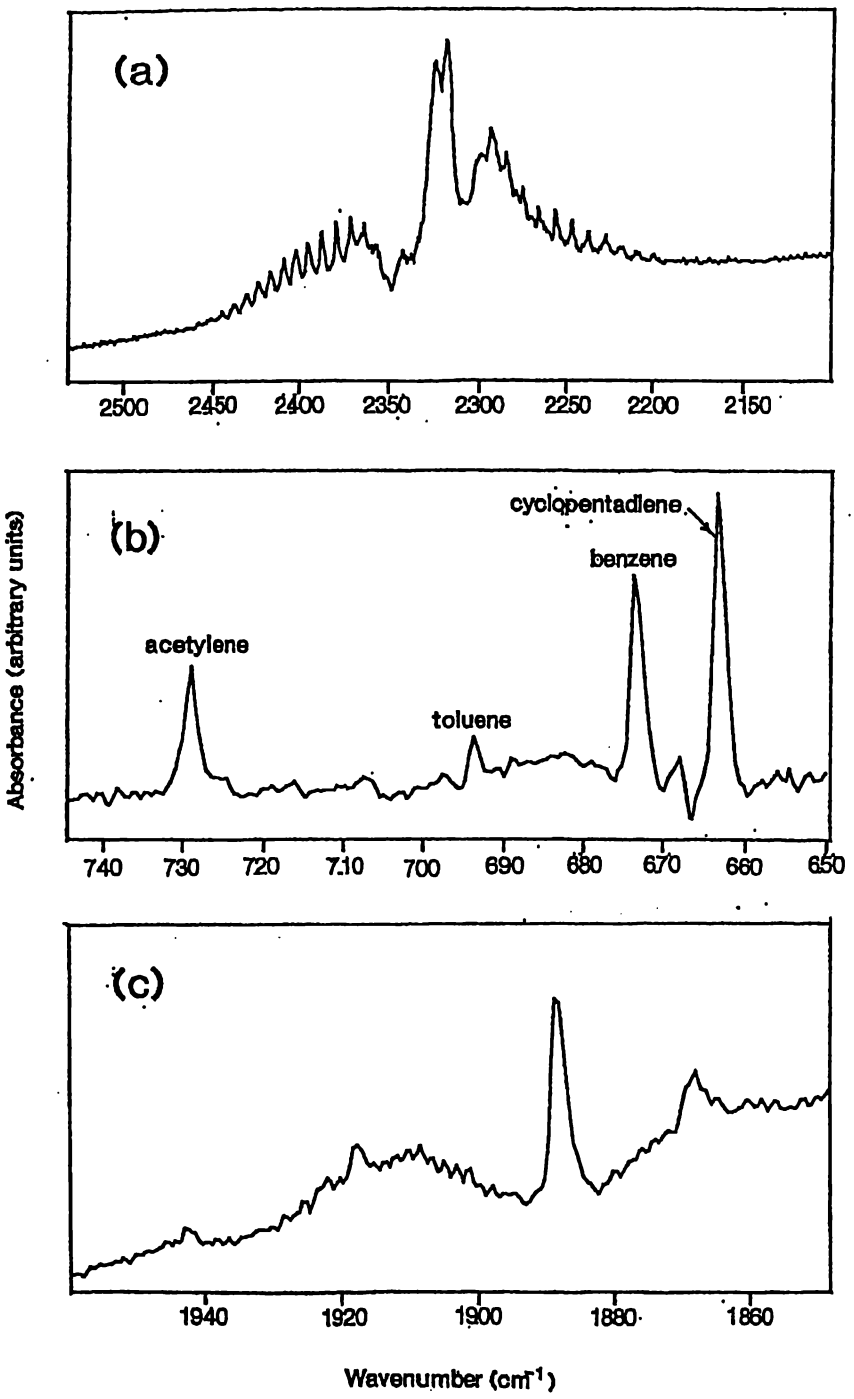

Figure V.1: I.R. spectra of products formed in the I.R HPLP decomposition of **20**. (a) I.R spectrum of phosphine, produced in the first step of the decomposition (b) I.R spectrum showing signals corresponding to cyclopentadiene, benzene, toluene and acetylene. (c) I.R spectrum of ethylene, with P and R branches. This signal, coupled with the stretch at 663 corresponding to cyclopentadiene [Figure 2 (b)], confirms the retro Diels-Alder decomposition pathway for camphene.

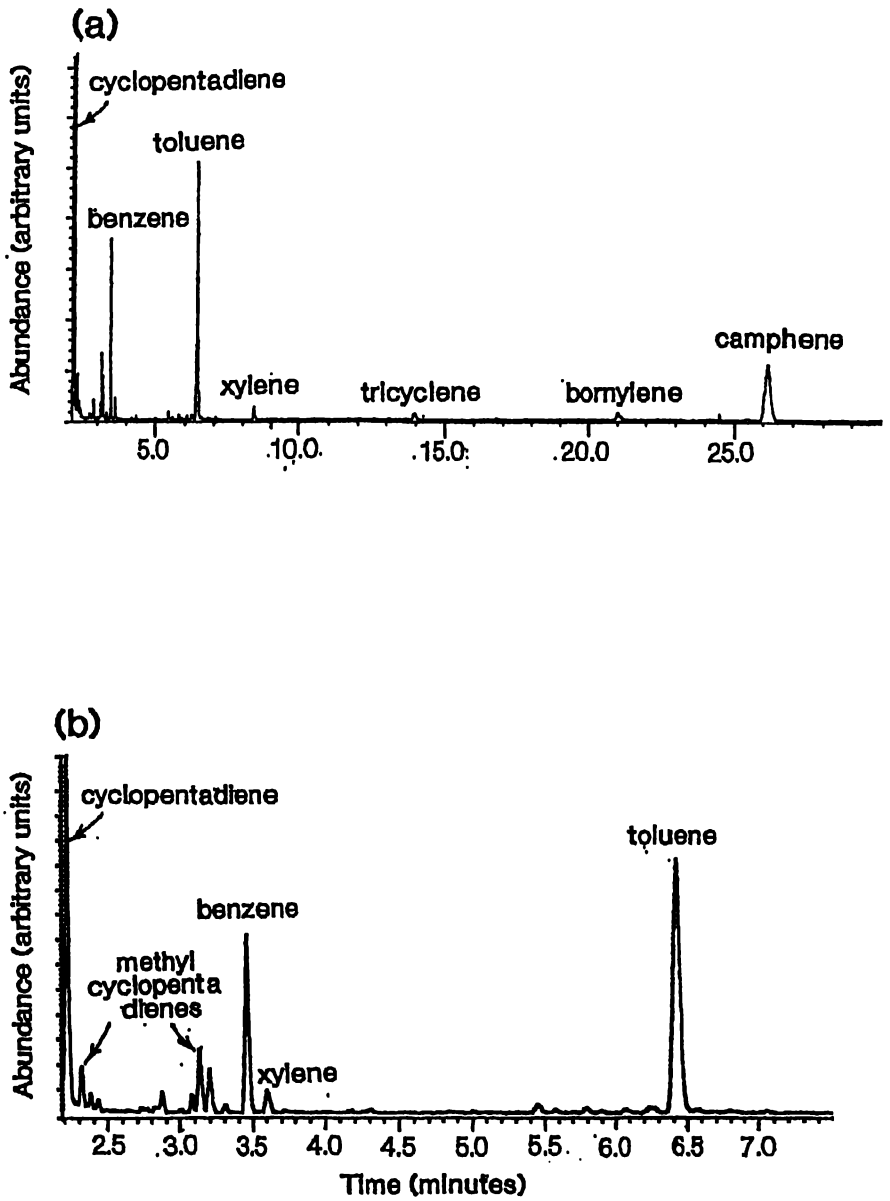

Figure V.2 (a) GCMS trace of semi-volatile products from the decomposition of 20. (b) shows an expanded view, showing peaks corresponding to methyl cyclopentadienes.

References

1 A. Balbacci, V. Malathy Devi, K. Narahari Rao, G. Tarrango, *J. Mol. Spectrosc* . 1980, **81**, 179.

2 G. Herzberg in *Molecular Spectra and Molecular Structure Vol II*, Van Nostrand Reinhold, 1945.

3 H. Freibolin in *Basic One and Two-Dimensional NMR Spectroscopy*, VCH Publishers 1991, Chapter 2.

4 E. Galinella, B. Fortunato, P. Mirone, *J. Mol. Spectrosc..*, 1967, **24**, 345.

5 C.J. Pouchert, *The Aldrich Library of FT-IR Spectra*, 1st Ed, Aldrich Chemical Company Press 1985.

6 C.J. Pouchert, *The Aldrich Library of NMR Spectra*, 2nd Ed, Aldrich Chemical Company Press 1983.